Deep sea seismic stratigraphy

Thesis

DEEP SEA SEISMIC STRATIGRAPHY

A thesis presented for the degree of

Doctor of Philosophy

by

Brian N. M. Biart

B.Sc. Hons. (Wales) July 1980

Author's number : HDJ 63208

Date of submission : 16 September 1985

Date of award : 15 May 1986

Department of Earth Sciences

Open University

September 1985

PAGE NUMBERING AS ORIGINAL

EX12

HIGHER DEGREES OFFICE

LIBRARY AUTHORISATION

STUDENT: BRIAN BIART SERIAL NO: .....

DEGREE: PH.D.

TITLE OF THESIS: DEEP SEA SEISMIC STRATIGRAPHY

.....

.....

I confirm that I am willing that my thesis be made available to readers and may be photocopied, subject tc the discretion of the Librarian.

21.4.87

Signed: ..... Date: .....

Abstract

Horizons responsible for the reflection of seismic waves within deep-sea sediments are shown to be less reliable for the purposes of correlation than their counter-parts in shallow margin sequences. Similar surfaces, such as abrupt lithological changes and unconformities, in the two different realms are not neccessarily produced by the same processes. It is the nature of these processes which control the chronostratigraphic significance of a reflector.

Thus reflectors may be correlated with reference to their genetic process. Horizons caused by time-restricted physical processes have enhanced chronostratigraphic significance.

In the deep-sea, layers in which the physical properties change slowly with depth (transition layers) are also important for reflector formation. In as much as these transitions can be affected by temperature, pressure and sediment geochemistry, as well as time, the equation of an horizon at two different localities does not neccessarily imply correlation in time (i.e. the horizon is not neccessarily a chronostratigraphic time line).

The two most important factors affecting impedance are the primary sedimentary geochemical composition and the nature of the grain to grain contacts within the sediment. Impedance increases with increasing grain density and increased rigidity of the sedimentary frame.

The inter-dependance of all sediment physical properties greatly complicates the study of the relationships between them. Modelling can be used to demonstrate the affects of variation of individual properties. Synthetic seismograms can be generated using either physical properties data measured from discrete samples or from wire-line data. While quality is a limiting factor to the performance of physical properties modelling, the latter is of value in that it enables modelling at many more localities than is possible with wire-line techniques alone.

Abrupt impedance contrasts that produce reflectors important in deep-sea seismic stratigraphy may be grouped into a) Compaction horizons produced by gradual increase in over-burden pressure, b) Cementation horizons produced by variation in diagenesis with depth c) Calcite compensation depth (CCD) controlled horizons characterised by marked variation in primary sedimentary content and d) Unconformities produced by bottom current action.

Contents

Abstract		i
Contents		iii
Figures		vi
Tables		ix
Plates		x
Acknowledgements		xi

CHAPTER ONE — Introduction

1.1	Introduction	1
1.2	What is a reflector?	3
1.3	A history of the study of deep sea seismic reflectors	5
	1.3.1 Early studies	5
	1.3.2 North American Basin	13
	1.3.3 The rest of the world	23
	i) West Africa	24
	ii) Eastern North Atlantic	24
	iii) Pacific	29
	1.3.4 Summary	30
1.4	Chronostratigraphy and seismic stratigraphy	32
1.5	Bottom simulating reflectors	41
	1.5.1 Clathrate	41
	1.5.2 Diagenetic fronts	46
	1.5.3 Summary	47

CHAPTER TWO — Factors affecting the velocity of seismic waves within deep sea sediments

	Symbols used in this chapter	xii
2.1	Theory	49
2.2	Porosity and Density	54
	2.2.1 Grain size	59
	2.2.2 Composition	59
2.3	Rigidity	62
2.4	Temperature	64
2.5	Pressure	66
2.6	Anisotropy	68

2.7 Water content 70
2.8 Rate and depth of deposition 71
2.9 Conclusions 72

CHAPTER THREE Synthetic seismogram modelling

3.1 Introduction to modelling 74
3.2 Description of modelling 76
3.2.1 Wavelet synthesis 76
3.2.2 Wire-line modelling 78
3.2.3 Physical property modelling 82
3.3 Problems of modelling in the deep sea 87
3.4 Equality of reflectors 91
3.5 Appraisal of modelling techniques 93
3.5.1 Comparison of corrected surface measurement and in situ measurement 93
3.5.2 Modelling at site 406 98
3.6 Theoretical modelling of horizon Beta 113

CHAPTER FOUR Reflectors of the North American Basin

4.1 Introduction 118
4.2 Site studies 119
4.2.1 Site 386 119
4.2.2 Site 387 127
4.2.3 Site 390 133
4.2.4 Site 391 135
4.2.5 Site 534 144

CHAPTER FIVE Reflectors of the eastern North Atlantic

5.1 Introduction 157
5.2 Site studies 159
5.2.1 Sites 403 and 404 159
5.2.2 Sites 406 and 405 176
5.2.3 Site 400 185
5.2.4 Site 402 188
5.2.5 Site 398 196
5.2.6 Site 416 204

CHAPTER SIX Case study: Physical properties modelling on Leg 93

6.1	Introduction	214
6.2	Site studies	214
	6.2.1 Site 603	214
	6.2.2 Site 604	233
	6.2.3 Site 605	239
	6.2.4 (Site 612)	251

CHAPTER SEVEN Summary of modelling results

7.1	Introduction	252
7.2	Summary of modelling	252
7.3	Sedimentology of reflectors	255
	7.3.1 Clay-to-claystone compaction horizon	255
	7.3.2 Cementation reflectors	258
	7.3.3 Calcite compensation depth reflectors	264
	7.3.4 Cretaceous and Jurassic reflectors	267
7.4	Correlation and deep sea reflectors	269

References 271

Figures

1.1	"A reflector" - the alignment of (shaded) loops	2
1.2	Fresnel zone of reflective return	2
1.3	'The lower horizon'	4
1.4	Major acoustic horizons in the N.A.B.	6
1.5	Horizons A and B	7
1.6	Deep reflectors over Rockall	26
1.7	Seismic stratigraphy in the Pacific Ocean	28
1.8	The problem caused by onlap in the deduction of subsidence	31
1.9	Lateral migration of an unconformity caused by the Western Boundary Undercurrent	34
1.10	Controls of sea-level change	34
1.11	P/T conditions required for hydrate formation	42
1.12	Relation between BSR's and isotherms	45
1.13	Distribution of identified BSR's	45
2.1	The effect of rigidity on velocity	51
2.2	Estimated porosity rebound versus depth	57
2.3	Empirical relations between porosity, density and velocity for various deep sea sediments	58a
2.4	Maximum overburden pressures and geothermal temperatures neccessary for diagenetic transformations	60
2.5a,b	Relation between velocity, pressure, grain size and saturation	67
2.6	Relations between elastic coefficients and wave velocities for transversely isotropic materials	67
2.7	Variation of velocity with depth and pressure	69a
3.1	Flow chart of computer programs	73
3.2a	Zero phase and minimum phase Butterworth wavelets	75
b	Amplitude and phase spectra of wavelets used in modelling	75
3.3a	Model of sea floor reflection, impedance profile of surficial sediments	77
b	Model of sea floor reflection, synthetic model	77
3.4	Comparison of 'primaries only' and 'all order multiples' models	80
3.5	Physical property cross plots	83
3.6	Velocity functions used to calculate velocity from porosity	85

3.7	Sound velocity in sea water versus depth	88
3.8	Comparison of properties measured in situ (by wire-line) and laboratory measurements, site 406	95
3.9	Wire-line model, site 406	99
3.10	Corrected model, site 406	100
3.11	Detail from wire-line logs at loop 11a, site 406	101A
3.12	Site survey profile IPOD76-2, site 406	102
3.13	Detail from wire-line logs at loop 15, site 406	106
3.14	Detail from wire-line logs at loops 16-17, site 406	108
3.15	Theoretical interbedded facies transition used to model horizon Beta	114
3.16	Results of theoretical modelling of horizon Beta	114
4.1	Location map of drill sites in the North American Basin.	117
4.2a	Glomar Challenger site survey profile and direct model, site 386	120
b	Lithostratigraphy and profile interpretation, site 386	120
4.3a	Depth plot of physical properties, site 386	122
b	Cross-plot, site 386	122
4.4a	Glomar Challenger site survey profile and direct model, site 387	125
b	Lithostratigraphy and profile interpretation, site 386	126
c	Depth plot of physical properties, site 387	128
4.5a	Glomar Challenger site survey profile and direct model, site 390	132
b	Lithostratigraphy and profile interpretation, site 390	132
4.6	Lithostratigraphy, site survey profile and direct model, site 391	134
4.7	Depth plot of physical properties, site 391	139
4.8	Depth plot of physical properties, site 534	148
4.9	Site survey profile and physical properties model, site 534	149
5.1	Location map of sites studied in chapter 5	156
5.2	Comparison of models, site 403	158
5.3	Models 1 and 5, site 403	161
5.4	Depth plot of physical properties, site 403	162
5.5	Site survey profile, site 403	164
5.6	Site survey profile, site 404	166

5.7	Direct model, site 404	168
5.8	Depth plot of physical properties, site 404	170
5.9	Direct model and reflection coefficient log, site 404	175
5.10	Sonic and density wire-line logs, site 406	177
5.11	Seismic profile IPOD76-2 between sites 405 and 406	178
5.12	Depth plot of physical properties, site 405	180
5.13	Depth plot of physical properties, site 406	183
5.14	Depth plot of physical properties, site 400	184
5.15	Seismic profile over site 402	187
5.16	Depth plot of physical properties, site 402	189
5.17	Comparison of models, site 402	190
5.18	Detail from sonic log, site 402	191
5.19	Chalk-to-limestone transition, site 402	193
5.20	Cross-plot of properties, site 398	197
5.21	Corrected model, site 398	199
5.22	Depth plot of physical properties, site 398	201
5.23	Acoustic stratigraphy, silica content and sediment rythms, site 398	203
5.24	Composite model, site 416	205
5.25	Acoustic stratigraphy, site 416	206
5.26	Depth plot of physical properties, site 416	207
5.27	Correlation between lithology and seismic stratigraphy, site 416	209
6.1	Location of drill sites, Leg 93	215
6.2	Site survey profile and seismic stratigraphy, site 603	217
6.3	Depth plot of physical properties, site 603	219
6.4	Physical properties' model, site 603	220
6.5	Interpretation of horizon X, site 603	228
6.6	Seimic profile USGS no.25 between sites 604 and 605	232
6.7	Depth plot of physical properties, site 604	234
6.8	Physical properties' model, site 604	236
6.9	Depth plot of physical properties, site 605	240
6.10	Physical properties' model, site 605	241
6.11	Physical properties' model, site 612	250a
7.1	Idealised physical properties variation over a clay-to-claystone transition horizon	256
7.2	Silica diagenesis	260
7.3	Idealised physical properties variation over a cementation horizon	256

7.4 Diagram to show the variation of impedance through time for two sediments of similar initial structure but different composition 263
7.5 Early shape of the North Atlantic Ocean 266

Tables

1.1 Age of horizon Beta 19
1.2 Age of unconformities in the North Atlantic 22
2.1 Percentage increase in length and volume of calcite between 20 - 200°C 65
2.2 Bulk moduli of calcite 69
3.1 Correlation of well-log and core depth, site 406 94
3.2 Physical properties of lithologies used for theoretical modelling of horizon Beta 115

4.1 Comparison of travel times to reflectors, site 391 136
4.2 Lithology and sub-units relevent to horizon M, site 391 137
4.3 Variation in carbonate below horizon C, site 391 142
4.4 Correlation of reflectors, site 534 146
4.5 Comparison of wire-line and physical property velocity functions, site 534 146
4.6a Age of horizon C, site 534 152
b Depth of horizon C, site 534 152
5.1 Correlation of reflectors, site 403 160
5.2 Velocity function, site 404 169
5.3 Correlation of reflectors and stratigraphy, site 400 182
5.4a,b Velocity anisotropy, site 402 194
5.5 Correlation of reflectors, site 398 194
5.6 Comparison of velocity functions, site 416 210
5.7 Correlation of lithostratigraphic units with travel time, sit 416 210
6.1 Correlation of reflectors, site 603 222
6.2 The age of horizon Beta 222
6.3 Comparison of modelled interval transit times, site 604 235
6.4 Comparison of semblance data from sites 604 and 605 237

Plates

6.1	The late Glomar Challenger	213
6.2	Scientific crew, Leg 93	213
6.3	Detail from plate 6.2 showing lepisheres in vughs and veins. Fabric clearly distinct from the overlying unit.	224
6.4	Scanning electron micrograph of radiolarian claystone, litho-unit 2, 603B-16R-6 80-81cm. Broken surface shows motteling due to formation of opal-CT.	224
6.5	Scanning electron micrograph of silt-rich claystone, litho-unit 1D, 603B-15R-2 80-81cm. Broken surface showing typical claystone ultra-fabric.	224
6.6	detail from plate 6.2 showing a lepishere filled vugh.	224

Acknowledgements

The completion of this work has been aided by very many people. In particular my thanks go to:

My supervisor, Sandra Smith, whose patience and guidance have prevented too many tangential goose chases and for such prompt reviewing of these pages as and when they emerged.

All concerned at the Deep Sea drilling Project on both sides of the Atlantic and throughout the fifteen years of its life. In particular, Joe Cann, who enabled my own participation in the Project and Jan van Hinte and Sherwood 'Woody' Wise, who were friends and co-chiefs on the cruise.

All members of the Earth Science department who made my time at Milton Keynes so enjoyable. Dave Wright, for his tutorial role in my computing career, deserves special mention, as does Helen Boxall, for her help in matters cartographic. Also Steve Daniels, for graphics, Dai Rees, for EMACS, Richard Austin ("Yes, the DEC is very friendly"), the staff of A.C.S. (my second home on campus) and the Gods of Computing at Cambridge, whom I have yet to meet.

The Open University Higher Degrees Office and the Petrogenesis Research Group for funding most of the work, the National Science Foundation of America (and not forgetting the Traffic Violations Enforcement Dept. of New York) for a happy and eventful three weeks States-side and Alan Soulsby and E.C.L. for their help at the end.

My parents, Elaine and Douglas, for their loving support and tolerance always and Sally, who, so kindly removed all unneccessary commas and things.

CHAPTER ONE

Seismic stratigraphy in the deep sea

1.1 Introduction

This thesis presents a study of the sediment column found in the deep ocean basins. There is a large body of data collected over the 23+ years of deep ocean profiling and the 15 years of the Deep Sea Drilling Project. The regional studies have been reliant on the various reflection stratigraphies for extending one dimensional well data to derive a three dimensional interpretation. The complimentary tasks of linking reflecting horizons with their lithological cause and the identification of lithological units on seismic profiles have been the keystones of this work. The construction of synthetic seismograms represents a rigorous method for performing the two tasks and the equally important problem of stating the error bounds on such analysis. A number of synthetic seismogram studies have been made at DSDP sites, but they number fewer than ten of the 77 cruises published. Several of these studies have not been used for interpretation but rather for confirmation of the lithostratigraphy or else are not compared directly at all. These studies employed data collected with petro-physical logging techniques and I have also used these data where they are available. Logging is restricted by the controls of cost and operational problems involved in logging open holes through the drillstring. Time also may prevent collection of these in situ data, as logging is the last operation to be performed at a site. Physical properties of the core are measured routinely and offer a much wider data-base. This study attempts to

Fig. 1.1 Diagram to show how a reflector is formed from the alignment of shaded loops

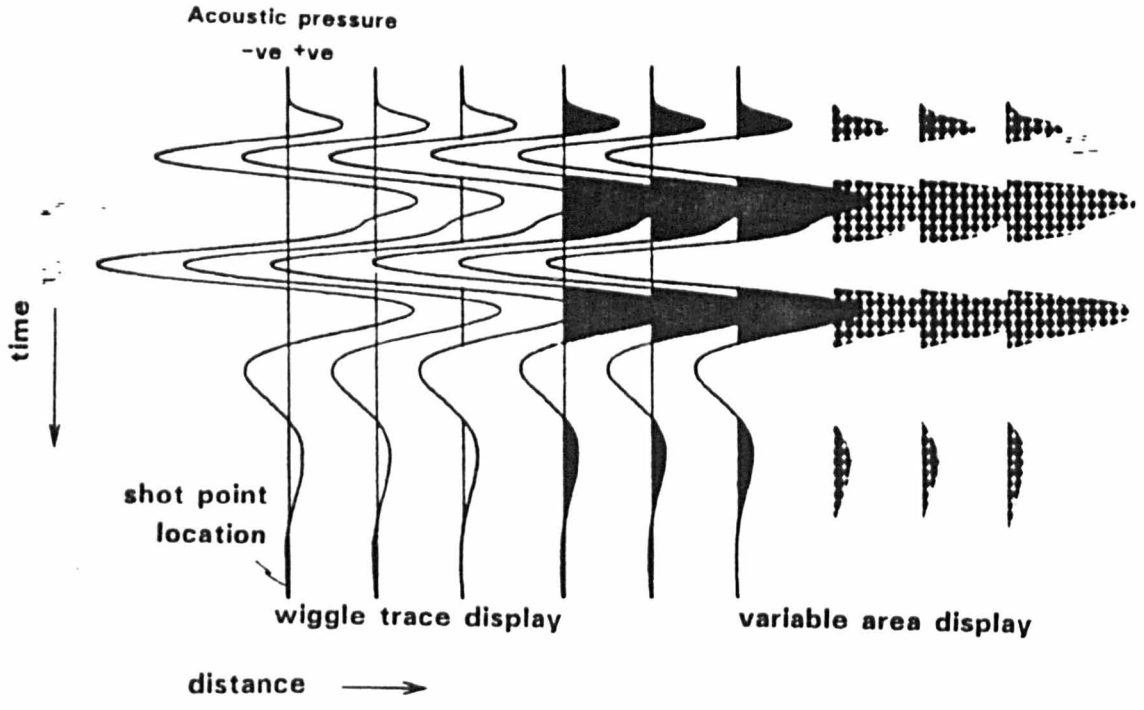

Fig. 1.2 Diagram to show how the area of the first Fresnel zone varies with depth and wavelength

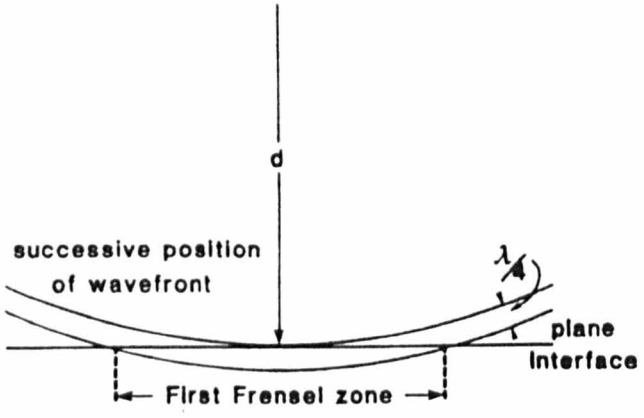

for spherical waves, $\text{Area} = \left[\left(d + \frac{\lambda}{4}\right)^2 - d^2\right]\pi$

if $\lambda/4 = 12\text{m}$ and $d = 3\text{km}$: Area $= 227000\,\text{m}^2$

cross sectional area of core $= 0.0137\,\text{m}^2$

find a method by which physical property data can be utilised to perform the previously stated tasks of correlation in an objective way. It is not intended as a definitive answer to the problems stated above but does show how existing data can be used more fully and by identifying deficiences suggests how improvements in data acquisition may be to the benefit of future studies.

Chapter two reviews the sedimentary factors controlling the properties of deep sea sediments and chapter three details how I have used such data to model seismic reflections. Subsequent chapters present the results of my modelling and summarise the causes of reflectors in the deep sea realm. I have restricted the area of my own study to the basins of the North Atlantic, but before adopting this restriction I will review the work that has been carried out in the study of seismic stratigraphy in the deep sea.

1.2 What is a reflector?

A reflector is a phenomenon which occurs on seismograms. Seismograms are graphical representations of the variation in amplitude of acoustic pressure as recorded against time (vertical axis) for different points on the earth's surface (horizontal axis). The method of display varies in detail, but principally peaks are represented by more black area (shading) than the intervening troughs. The near horizontal alignment of these peaks (and troughs) then forms an image which at first sight resembles a continuous line, a reflector (fig. 1.1).

The energy received over a given time interval is the sum of energy reflected from a surface within the sedimentary sequence. The surface

Fig. 1.3 "The lower horizon"

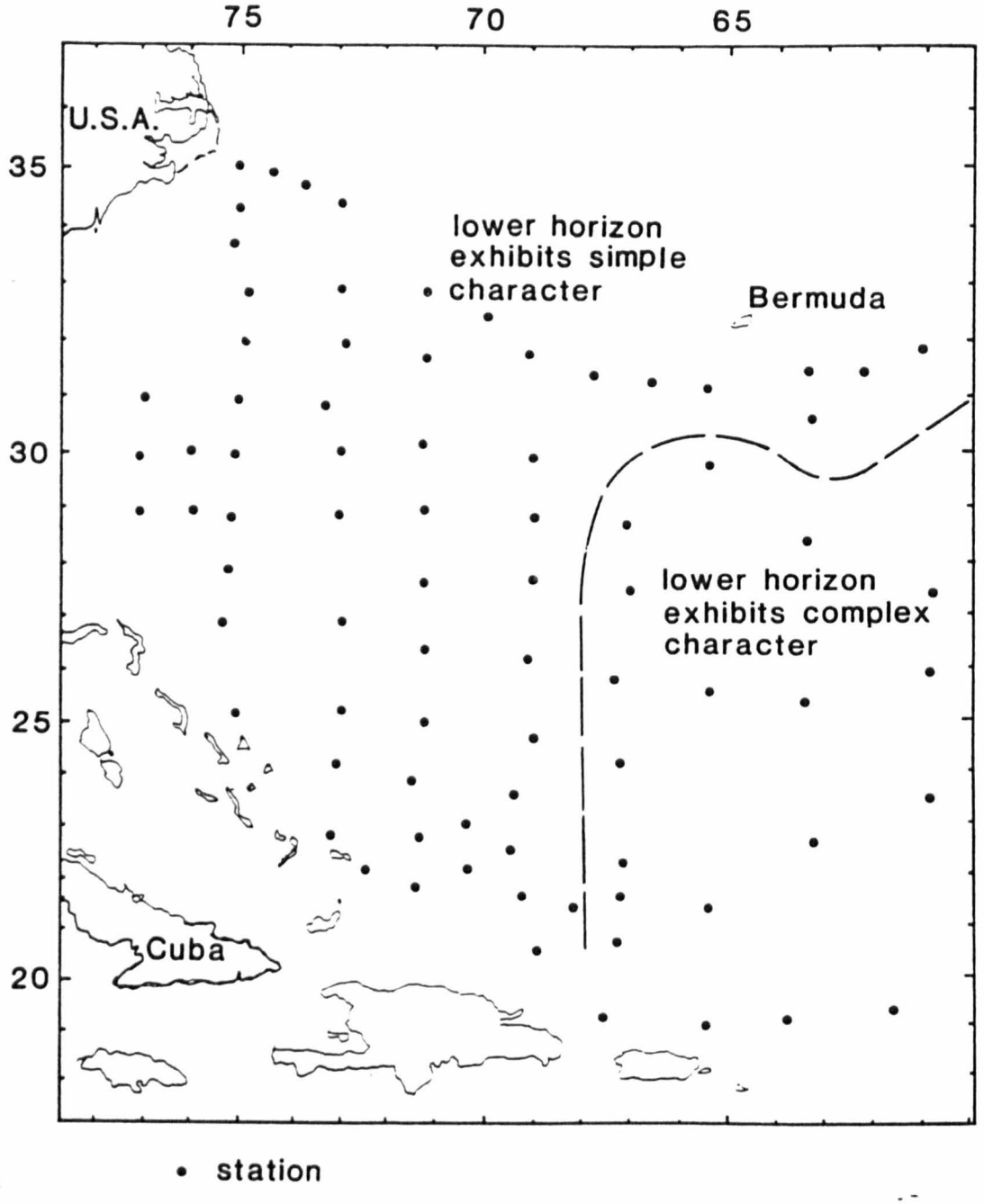

(after Hersey & Ewing, 1959)

is the Fresnel zone of constructive interference (fig. 1.2). In this way, the information obtained by measuring acoustic pressure at any given time interval represents an average of the various energies reflected from this zone. The size of the Fresnel zone is responsible for lateral resolution and is itself dependent on the frequency of imaging. We are fortunate in the pelagic environment because we may assume that a space-average model for the Fresnel zone can be constructed by extrapolation of the one-dimensional data from a bore-hole. Elsewhere, lateral variation of sediments mean that such extrapolation of lithology is unlikely to represent accurately the body of rock being surveyed.

1.3 A history of the study of deep sea seismic reflectors

1.3.1 Early studies

Early studies of deep sea seismic stratigraphy were restricted to investigations of the velocity structure by seismic refraction, wide-angle reflection (Ewing & Ewing, 1959) and normal incidence reflection (Hersey & Ewing,1949). Various seismic refraction measurements showed a very widespread velocity layering below the ocean floor (Raitt,1956; Gaskell, Hill and Swallow, 1958; Ewing and Ewing, 1959). Hersey & Ewing (1949) performed a discontinuous study and found at least one reflector at all their stations, which was interpreted as an extensive sub-bottom surface due to the systematic variation in its two-way travel time below the sea-floor. Many stations showed a second (deeper) reflection, again inferred to be continuous as a result of its gradual variation in lag-time following the first reflector. Each station could be classified according to the exact shape of this second reflection, permitting a sub-crop map of variation over the inferred surface to be produced (fig. 1.3),

Fig. 1.4 Major acoustic horizons in the North American Basin

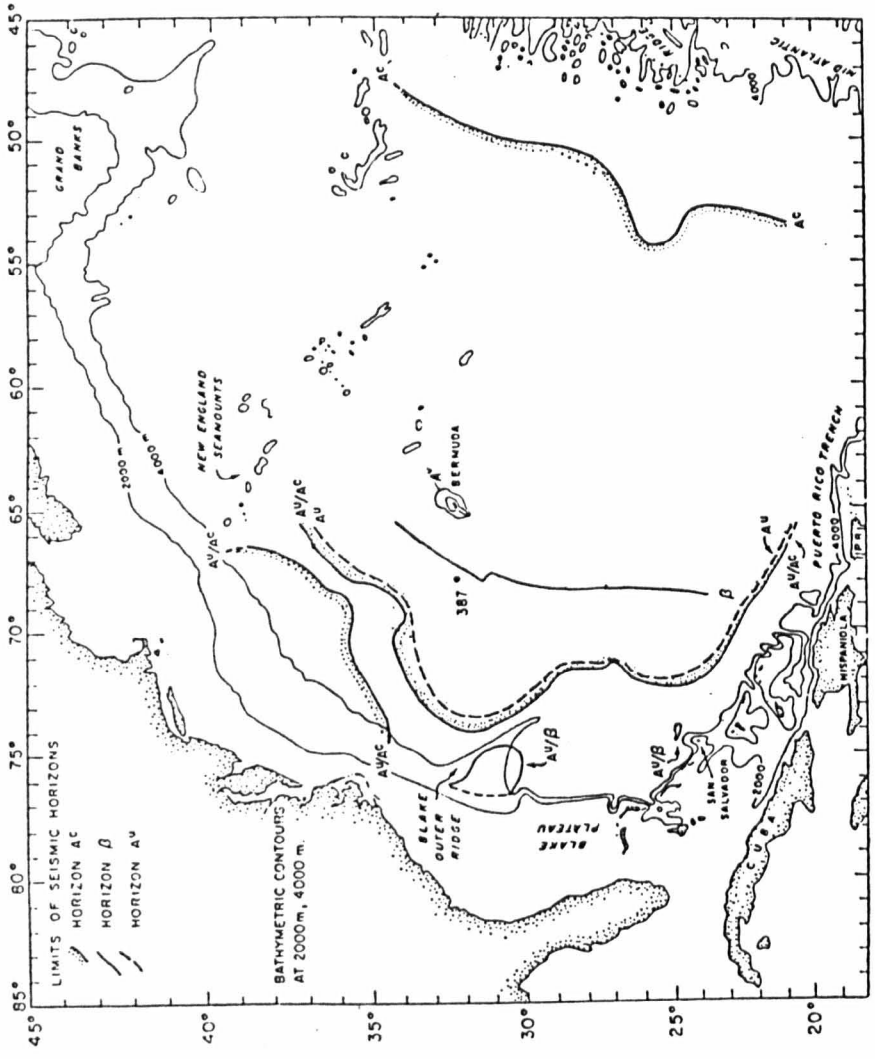

(after Tucholke, 1981)

Fig. 1.5 "Horizons A and B"

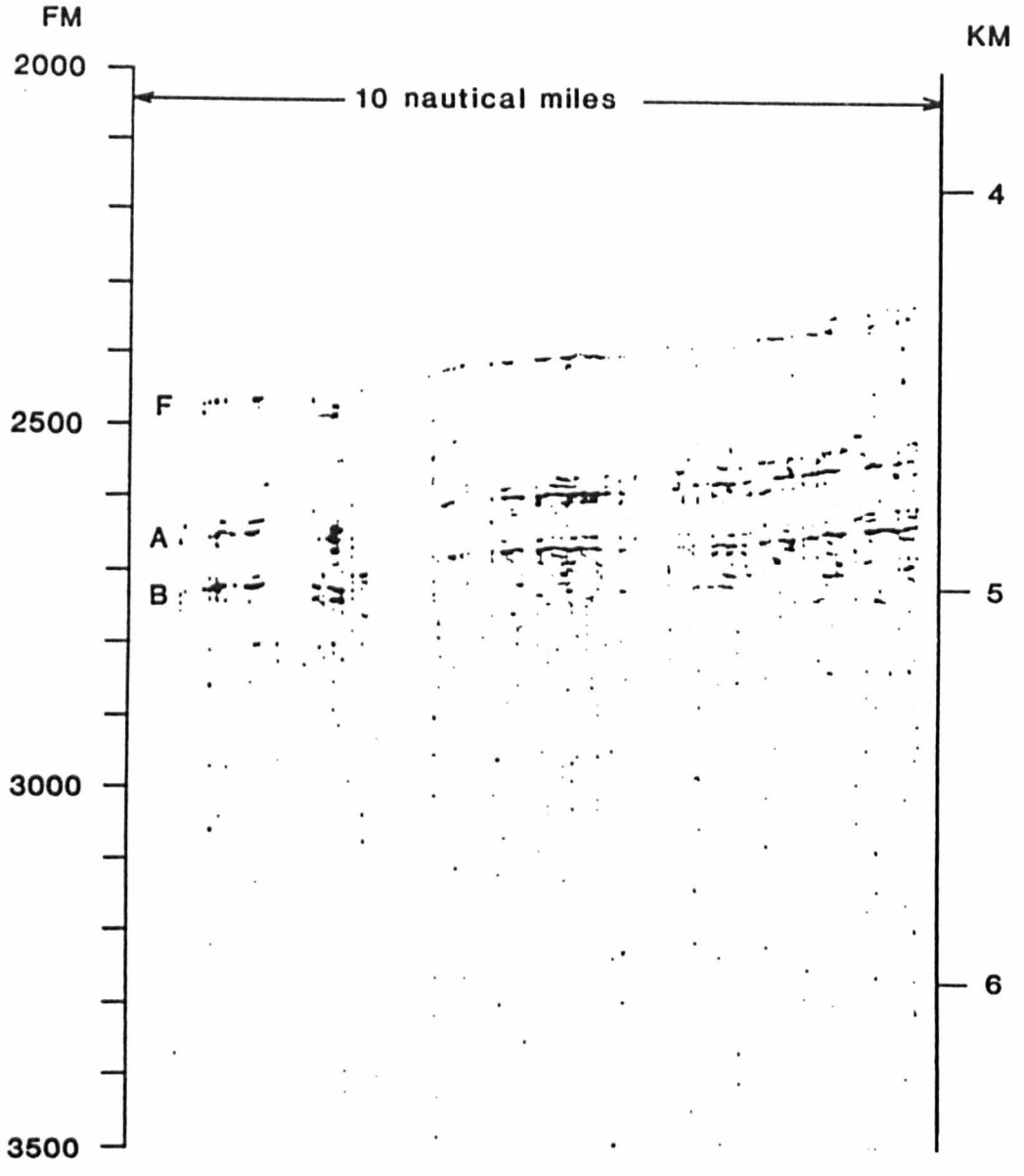

Sample record made with the gas exploder source in the Caribbean Sea near the south end of the *SH*-24 traverse. Note bubble pulse pattern in all reflected signals, indicating smooth interfaces. *F* indicates the floor of the ocean; *A* and *B* indicate strong reflectors in the sediment.

(after Ewing & Ewing, 1962a)

which compares favourably with with a sub-crop map of (the much later defined) horizon Beta (fig. 1.4).

North of Bermuda, Officer (1955) interpreted a continuous reflector as an unspecified discontinuity within otherwise homogeneous material.

The earliest continuous work began with the development of a deep sea profiling system by Ewing and Tirey (1961). Working in the Gulf of Mexico they found '...many reflectors ... showing horizontal layering above and gently dipping beds somewhat deeper.' The importance of this work was that the reflectors could be traced and shown to be continuous (within the limits of resolution).

With continued development of the profiling system the stratification became clearer. Using an airgun sound source Ewing and Ewing (1962) found a marked stratification in the sediments on continental rises which they attributed to a high percentage of turbidites. In the Puerto Rico Trough they found two sub-surface reflectors, which they labelled A and B (fig. 1.5). Horizon B was the acoustic basement and interpreted to be basement levelling sediments. Despite success in the Gulf of Mexico with correlating reflectors with the layering deduced from the refraction measurements (Ewing and Ewing, 1962), they were unable to do similarly with 'reflector A', which they attributed to an insufficient velocity contrast (Ewing and Ewing, 1962).

Reflector 'A' was shown to be characteristic of basin sediments in both the North and South Atlantic, being smoother than either the sea-floor or (assumed) igneous basement (Ewing and Ewing, 1963; Ewing, Ludwig and Ewing, 1964). Windisch et al. (1968) mention that:

'... two major reflecting horizons analogous to A and B

cover extensive areas of the Eastern and Southern Atlantic, the Caribbean and the Pacific. It had been postulated that these are stratigraphically related to horizons A and B in the NW Atlantic. If so, then those reflectors analogous to horizon B in other oceans could represent broad areas that were once covered by shallow sea.'

This interpretation of the origin of deep sea reflectors was in marked contrast to that of Ewing et al. (1966) and Rona and Clay (1967), who saw them as ancient abyssal plains. The morphology of such reflectors showed that deep sea sedimentation was not simply a 'rain from heaven', but included sub-marine erosion and reworking by turbidity (and other) currents. The fact that the reflectors were horizontal was taken to indicate that they formed after tectonic activity, in the form of sea-floor spreading, had ceased (Ewing and Ewing, 1962). This interpretation implied much greater rates of spreading than are observed today, because the oceans were supposed to have opened fully prior to the deposition of sediments and the formation of reflectors within them.

The reflectivity of these horizons was interpreted as being caused by an abrupt change in sedimentation from slowly deposited pelagic sediments, which constitute the acoustically transparent layers, to rapidly deposited turbidites caused by a process similar to that which formed the modern abyssal plains (i.e. a glacially-controlled lowering of sea-level, Ewing and Ewing, 1965a).

Turbidites were implied by the fact that on some particularly well resolved records reflector 'A' appears as a complex of closely spaced individual reflectors, similar to reflections from turbidites on modern abyssal plains (Ewing and Ewing, 1965b).

Horizon A was not claimed to be a single continuous bed, but it seemed to be at about the same stratigraphic horizon everywhere, suggesting that it could be used for stratigraphic correlation (Ewing et al., 1966; Windisch et al., 1968).

Like its origin, the exact age of horizon A was also unknown: it was traced to the western edge of the Hatteras Abyssal Plain (North American Basin), where it was found to crop out on the sea-floor. Dredge and piston-core samples from this locality recovered fine grained limestone and red clay of Upper Cretaceous age (Ewing et al., 1966).

When the Deep Sea Drilling Project (DSDP) began in 1968, one of its first objectives was to identify exactly the causes of these reflectors. The earliest cruises (Legs 1-3) showed that horizon A correlated with a hard Eocene chert horizon which was sufficiently indurated to halt drilling efforts. Leg 4 showed that the real picture was more complex: when cored at sites 23 and 24 (and 27) horizon A turned out to be due to a series of uncemented middle Eocene turbidites (Bader, Gerard et al., 1970). Leg 11 added to the problem by penetrating a layer labelled A which proved to be an unconformity of upper Tertiary on Cretaceous.

Reflectors similar to horizons A and B were identified in the western Pacific Ocean and labelled horizons Alpha, A', Beta and B' (Ewing, Saito, Ewing & Burckl, 1966) and another in the Caribbean, labelled horizon A" (Ewing, Talwani & Ewing, 1965). Synchronism between horizon A and horizon A" was confirmed by drilling, and also with the original reflector in the South Atlantic:

> 'On the basis of reflectivity, shape, and areal extent, the horizon labelled A is judged to have the same

characteristics as that designated A by Ewing and Ewing [1962] in the North Atlantic, except that it is more conformable in the South Atlantic than in the North Atlantic.' (Ewing, Ludwig and Ewing, 1964.)

The correlation of horizon A' with reflectors A and A" was not assured although an age of 46 Ma based on sedimentation rate matched the Eocene ages in the Atlantic (Ewing, Windisch and Ewing, 1970; Ewing, Saito, Ewing and Burckle, 1966). The fact that such a correlation was unfounded was inherent in the observation of Heezen et al. (1973) that the layer overlying horizon A' in the Pacific was not a single depositional event but was diachronous. A difference in character between A' in the north-west Pacific and at the more southerly site 199 suggested different processes were responsible.

Ewing, Windisch and Ewing (1970) recognised that the precise sedimentary process was not important for reflector formation, but rather it was the fact that they were anomalously siliceous. Matteson and Pessagno (1971) suggested that horizons A and A" were related to increased volcanism during the Eocene, which increased the supply of silica. Horizon A' was suggested to have been brought to the surface in Cuba by Quaternary tectonism as the Universidad Formation which contains a 10-15 m siliceous limestone (Matteson & Pessagno, 1971).

Tucholke (1979) notes that: ' The evolution of reflector terminology in the N. Atlantic, S. Atlantic and Pacific oceans has been based primarily on correlations of acoustic stratigraphy; that is on the acoustic stratigraphic position and homotaxial[1] nature of the

---

[1]**HOMOTAXIAL**: coincidence in order of organic succession but not necessarily in time, similarity in geological age, while not necessarily strict contemporaneity.

reflectors.'

The early supposition that deep sea reflectors could be traced worldwide was fuelled by the encouraging prospect for correlative study and by the poorly formulated origin of ocean basins and the sedimentary fill.

The matching by character can only be as reliable and accurate as the profiling system. The value of pioneering work done with early versions of the system is not to be understated as it allowed large scale study of the morphology of the ocean basins. Nevertheless, the validity of the correlation should only have been assessed within the limits of the technique used to draw it. The eye-ball matching of reflectors by oceanographers was in part prone to the pitfalls of geologists interpreting a time-section as they would a cross-section.

With continuing study more horizons were recognised to be regionally significant (Windisch et al., 1968; Rona & Clay, 1967). There was a tendency for these horizons to be defined locally for the purposes of a particular study, which led to confusion over their naming:

> 'Partly because of improved record quality and partly because of expanding worldwide data acquisition, the nomenclature applied to prominent seismic horizons has undergone a somewhat tortuous development.'
>
> (Tucholke and Mountain, 1979).

The regional extent of reflectors became more restricted with increased resolution. The finer detail not only revealed more subtle variations in reflector character, but also the complexity of the geological history regarding any one basin. The inertia of terminology resulted in redefinition of reflectors that were previously supposed

to be uniform on a global scale. While many of the world's deep basins were under-going reconnaisance and detailed investigation, the study in the North American Basin, (NAB), held a prominent position in the development of seismic stratigraphy of deep sea basins.

1.3.2 North American Basin

This prominence is explicable in terms of the Basin's proximity to a number of interested oceanographic institutions and to the fact that the study of its development throughout the Mesozoic and Caenozoic had important ramifications both for Atlantic margins and, more generally, for all passive margins.

A number of post horizon A reflectors have been recognised in this basin, including horizons X, M, M2, Y and T. They are of limited areal extent and varying importance.

Horizon M was named by Sheridan, Golovchenko and Ewing (1974) and was thought to be a calcarenitic turbidite. It is distinctive in part of the Blake-Bahama Basin, where it represents the top of a packet of closely spaced reflections (Bryan et al., 1979). Drilling at site 391 had shown it to correspond to the top of a Middle Miocene debris flow unit of relatively indurated chalk overlain by unconsolidated chalky oozes and hemipelagic muds (Benson et al., 1978; Sheridan, Pastouret & Mosditchian, 1978). Bryan et al. (1979) agree in principle with this correlation but admit to picking horizon M slightly higher on the basis of their sonobuoy data, which showed a much greater velocity contrast 20 km northeast of the site. These turbidites were derived from the slope to the west and can be seen to thin eastwards and eventually lap against a prominent reflector to the east, horizon X. At site 391 horizon M is the uppermost of a sequence of three

reflectors.

Ewing and Ewing (1964) found a reflector above horizon A forming the ancient core of the Blake Outer Ridge and named it horizon X. Horizon X cannot be discerned beneath the crest of the Ridge because of the high reflectivity of another horizon termed horizon Y (Markl, Bryan and Ewing, 1970). (Horizon Y is discussed in the section on Bottom Simulating Refectors.) Shipley and Watkins (1978) showed that horizon X was not a continuous reflection but a series of reflections, none of which were continuous, thus making strict reflector correlation impossible. On the basis of amplitude and reflection configuration they suggested that the seaward termination of reflector X might be a facies transition from seaward prograding continental rise sediments to abyssal plain turbidites, which agrees in essence with Sheridan et al (1974) and Bryan, Markl and Sheridan (1979) who correlate horizon X with the base of the Middle Miocene debris flow, the top of which correlates with horizon M. Benson, Sheridan et al. (1978) found what appeared to be Horizon X correlated with an increase in the stiffness of Miocene hemipelagic clays. The same horizon is found at site 603 and labelled horizon M2 (van Hinte, Wise et al., in prep; chapter 6, this study). This shows one of the problems of correlation and the pitfalls of homotaxial comparison.

Shipley and Watkins (1978) attempted a definition of Horizon A:

> 'Horizon A is defined to be the first strong reflector encountered on CDP reflection profile in the vicinity of DSDP hole 105 ... commonly it is one of a group of three or four reflections below a fairly transparent zone.'

While Bryan et al. (1979) note that horizon A is 'a prominent reflection typically preceeded by another strong event. Benson,

Sheridan et al. (1978) attribute horizon A to velocity inversion (site 391), but since this is caused by a prominent unconformity it is not likely to persist as an inversion.

Early multi-channel work was concerned with velocity analysis and confirmed refraction data on the grosser velocity layering of deep sea sediments (Savit et al., 1974). The first multi-channel investigation of the seismic stratigraphy of the North American Basin was by Dillon and Sheridan (1976). They still considered horizon A as a single entity but observed that horizon A was a moderately stratified sequence containing very discontinuous irregular reflectors, which are the source of many diffractions. These they explain as small scale channel fills in proximal turbidites of Tertiary age.

By 1977 horizon A was recognised as the previously hypothesised complex of reflectors, each member of which correlates with a particular lithological formation. The youngest, horizon Av, is a late Oligocene volcaniclastic turbidite produced as a result of weathering of volcanics on Bermuda; consequently, it is of limited areal extent (fig. 1.4). Its reflectivity is due to the coarse grain size of the turbidites, their bed thickness and their sharp top, the latter due to sub-aerial erosion. These characteristics decline with increased distance from the Bermuda pedestal. Deposition ended abruptly in the late Oligocene (Tucholke, 1979).

Horizon At is produced by a series of siliceous turbidites of middle Upper Eocene, which appear as an acoustically laminated facies first identified under the Greater Antilles Outer Ridge by Tucholke & Ewing (1974). They occur west of Bermuda, being derived from the North American continental slope and can be seen to offlap onto the Bermuda

rise indicating that Bermuda was undergoing uplift at this time. This causes horizon At to be diachronous at its western limit (Tucholke and Mountain, 1979). McCave (1979) notes that the individual turbidites are seldom more than one metre thick. Their reflectivity can, therefore, be attributed to a combined change in impedance. Horizon At and Av are largely coeval (Ewing et al., 1969).

Horizon Ac is a chert-bearing turbidite sequence containing cherts of upper Lower- to lower Middle Eocene age. It is normally the most reflective layer in the horizon A complex (Tucholke, 1981) and the most widespread being found over most of the NAB from 20°N to 40°N and 52°-55°W to the continental slope (Tucholke,1979). Tucholke (1979) states that:

> 'The strong reflectivity of horizon Ac clearly results from the large impedance contrast created by cherts in the sedimentary section.'

The correctness of this statement will be discussed later (chapter 6) with reference to the modelling of horizon Ac. Briefly, thin chert beds are not sufficient on their own to produce a reflection. The important thing is the widespread event, that changes the grosser composition of the sediments and facilitates chert formation. That event must ultimately be held to be the clear cause of horizon Ac. Ewing et al. (1970) point out the significance of the 'markedly siliceous sequence'. It correlates with siliceous turbidites where horizon At is present and in horizons rich in siliceous debris within pelagic sediments elsewhere. The cherts have a more limited stratigraphic range well within the silica rich units. The reason for this is not known definitely. Tucholke (1979) gives a number of reasons and notes that all layers are 20% enriched in carbonate. 'Lancelot (1973) discussed mechanisms for chert formation in clayey calcareous sediments and pointed out that the increased permeability of

carbonate-rich sediments may be important in the mobilisation and reprecipitation of biogenic silica to form chert.' Tucholke concludes that while this is important the controlling factor must be temporally restricted, such as high surface productivity as suggested by Matteson & Pessagno (1971).

The correlation found on Leg 11 of DSDP of horizon A with an unconformity was found at several more drilling sites on the lower continental slope (sites 99A, 4, 101, 391, 106, 105, 534, 533, 603, 605). All have erosional hiatuses ending in the middle to late Miocene. The extent of the erosion varies, but is most extensive close to the continental slope of Eocene times, where it bites into pre-horizon Beta sediments (Windisch et al., 1968; fig. 1.4). Horizon Au represents the impedance contrast across an angular unconformity eroded by enhanced bottom current circulation. The areal distribution of horizon Au clearly suggests that the unconformity was eroded by a southerly flowing, westward intensified abyssal boundary current, probably a precursor to the modern Western Boundary Undercurrent. The cause of this intensification is uncertain. One possibility is that currents gradually intensified during Late Paleogene time in response to climatic cooling and caused erosion for a period of some 15-20 Ma. Alternatively cold water from the Norwegian-Greenland Sea flooded the North American Basin following the subsidence of the Greenland-Iceland-Faroe Ridge in the late Oligocene, causing much more rapid erosion over a period of a few million years. (Talwani, Udintsev, 1976; Tucholke and Mountain, 1979; Jones et al., 1970). A combination of these two is the most likely solution. During this event 200,000 km^3 of material were removed; which may compliment the high sedimentation rate in the South Atlantic at this time (Paull and Dillon, 1980).

A lower and separate reflector was identified by Ewing et al. (1970) and later named horizon A* by Ewing and Hollister (1972). It is correlated with a thin calcareous facies of late Maestrichtian age (Tucholke, 1977). It is most distinct under the central Bermuda Rise, but merges with horizon A(t?) as it is traced westward. Results of drilling at site 105 suggested its correlation with the transition from multicoloured to black clays and might be related to climatic cooling which began at this time (Ewing & Hollister, 1972; Tucholke & Mountain, 1979). Also during the late Paleocene the silica content of Atlantic deep sea sediments started to increase. Volcanic production also increased, which might have coincided with upwelling of cooler, nutrient-rich bottom water.

It is not as widespead as horizon Ac, although this is in places because it is too close vertically to be distinguished from the stronger (and shallower horizon Ac). Tucholke (1979) attributes a short lived lowering in the CCD towards the end of Maestrichtian times with causing the "depositional pulse" that produces horizon A*. Thus its extent will be limited to areas affected by this CCD fluctuation - those already above the CCD will have been unaffected, just as those deeper than its greatest limit were. For instance, it is only poorly developed east of Bermuda where the basin was that much deeper.

As noted above, horizon Beta was first recognised as a reflector between A' and B' in the Pacific ocean. A reflector at a similar acousti-stratigraphic position in the NAB was found and named similarly. It was drilled at sites 5, 101 and 105 (Ewing, Worzel et al, 1969; Hollister, Ewing et al., 1972). Horizon Beta crops out within the larger "Horizon A" outcrop area northeast of San Salvador, but is covered by non-calcareous sediments not resolved by the profiler (Tucholke, 1979).

Table 1.1 - The age of Horizon Beta

	Mountain '77	Benson et al '78 Bryan et al '79	Tucholke '80	Sheridan, Gradstein et al '82
Black Clays	Barremian	Aptian	Mid Cretaceous	
			(Beta': Lower Albian- (Upper Aptian)	
Limestones	Hauterivian	Neocomian	Neocomian	Barremian

Horizon Beta correlates with the impedance contrast between black carbonaceous shales and underlying white to greyish limestones. The age of the horizon was the subject of debate (see section 1.3).

Once again the agreement on definition was reached in spite of contrasting descriptions by various authors. Horizon Beta represents a distinct change in reflection characteristics from well layered below to weakly layered above (Dillon and Sheridan, 1976). Shipley and Watkins (1978) identified horizon Beta as a strong, laterally continuous and nearly planar reflection, sometimes the middle of three prominent reflections, or, more often, the top of an interval containing low amplitude reflections. In contrast, Bryan et al. (1979) considered horizon Beta 'rarely outstanding' [in the Blake-Bahama Basin] and often difficult to trace: a fact they attributed to the problems of seismic surveys in very deep water. Tucholke (1980) considered horizon Beta 'well defined'. Sheridan, Gradstein et al. (1983) divide it into horizon Beta of Mountain (1977) and a new horizon termed Beta' and thought to correlate with Aptian claystone overlying Barremian calcareous claystone (cf Benson, et al., 1978 in Table 1.1). This change in lithology can be interpreted as a rise in the CCD in an intermittently anoxic environment (Tucholke and Vogt, 1979). The reflector is generally smooth beneath the continental rise and the Hatteras Abyssal Plain, but under the western Bermuda Rise it drapes over the irregular basaltic basement. This is in part due to the younger age of basement here which has not been levelled by pre-horizon Beta sediments.

The contact between these lithofacies is often transitional with interbedding of the two ocurring over several metres to tens of metres. The impedance contrast creating horizon Beta is presumed

to be the shallowest high-velocity calcareous sediment within the zone of interbedding.

Deeper reflectors are recognised below horizon Beta but less is known of them owing to their greater depth, which limits their detection to multichannel surveys, and their smaller areal extent. Horizon B was identified as a smooth reflector above basaltic basement by Ewing & Ewing (1965) and was thought to have been penetrated at site 100 and found to be extrusive basalt. Tucholke (1979) thinks this is unlikely and would prefer a sedimentary origin. Benson et al. (1978) identify horizon C, which they correlate with the transition from red argillaceous limestones of lower Tithonian age to white limestones of upper Tithonian age. Bryan et al. (1979) add horizon D, which was postulated to be Callovian/Bathonian in age (160 Ma). Both these reflectors occur as 'prominent doublets'. Dillon and Sheridan (1976) named reflector T, which correlates with horizon D. Drilling at site 534 found horizon D to correlate with turbiditic limestones of Lower Oxfordian age interbedded with a dark green, maroon and black shale (Sheridan, Bates, Shipley and Crosby, 1983). Klitgord and Grow (1980) identified three sub-Beta horizons and labelled them J3, J2 and J1, which they predicted to be of Jurassic age. Tucholke and Mountain (1979) and Jansa et al. (1979) had already correlated J1 with horizon C of Sheridan et al. (1978). Sheridan, Bates et al. (1983) also name two more reflectors: horizon C' at the upper/lower Berriasian boundary and horizon D', an intra Kimmeridgian reflector.

By 1979 much was known about the distribution, lithological character and age of the various regional reflectors, which together describe the palaeo-environment. 'The reflectors (Ac, A*, Au, Beta) also appear to represent real impedance and lithologic changes rather than signal interference artefacts' (Tucholke, 1980). So it is not surprising

Table 1.2 - Vail et al's (1980) interpretation of regional reflectors

M	basal Middle Tortonian	9.8 Ma
X	basal Langhian	16.5 Ma
Au	basal Middle Chattian	29.0 Ma
Ac	basal Upper Ypresian	49.5 Ma
A*	basal Thanetian	60.0 Ma
Beta	basal Middle Aptian	112.0 Ma

that these have persistently produced reflections despite the different sound sources and filters used for imaging. However, the lack of precise correlation of impedance break and lithological break has still to be demonstrated. For instance, Tucholke (1980) referring to horizon Beta: 'The impedance contrast correlating with the reflector at each hole coincides with or lies within a few metres of the lithologic boundary between limestones or chalks and overlying dark green-grey to black claystones.' Greater confidence in such coincidences is required before they are used for correlation.

The names for horizon A and horizon Beta are too entrenched in the literature to be ignored, but now that their complexity is better understood the naming of horizons is becoming more systematic (e.g. J1-J3 in the Jurassic). Vail et al. (1980) attribute all reflectors to unconformities or their correlative conformities and labels them according to the age of the oldest strata above the unconformity. These assignations are given in Table 1.2; the actual numerical age will vary depending upon the time-scale used (see section 1.4).

1.3.4 - The rest of the world

The studies in the NAB show the sensitivity of reflectors to the changes in basin palaeo-ecology. These changes are caused by very wide-spread events, and, while the changes locally may be different, their coeval timing shows their genetic relationships and allows their use in correlation between basins, but only on a coarse scale. For instance the idea that erosion to form horizon Au by a southerly flowing boundary current compliments a high sedimentation rate in the South Atlantic.

West Africa - In this way, reflectors A, A* and Beta as well as deeper reflectors were interpreted off West Africa on Leg 41 (Lancelot and Siebold, 1971). Later studies on Leg 75 refer to regional reflectors but with a different nomenclature and no implication of a genetic relationship to those in the NAB. (Leg 75, Hay & Sibuet, site 530; Leg 50, Lancelot & Winterer, site 416; Leg 41, Lancelot & Siebold, 1977, site 370). Unconformities were labelled D1 and D2. D1, the older, was predicted to be Cenomanian from extrapolation of Saharan well data (somewhere between A* and Beta). D2 was interpreted to be Oligocene to early Miocene age (Hinz, Siebold & Wissman, 1974).

Subsequent study data identify a number of regional reflectors labelled Brown, Tan, Red, Olive, Blue and Yellow (Hinz et al., 1974). (A similar stratigraphy of 'colour' horizons is found in the initial report for Leg 47 further north, but results from the intention to avoid implied correlation of reflectors and should not be confused). Drilling at site 530 showed the following correlations: the Brown reflector is from within early Miocene turbidites, the Tan reflector is from late Middle Eocene, the Red reflector is produced by the unconformity between early Eocene and late Paleocene and the Olive reflector roughly correlates with the Barremian. The olive reflector was previously labelled D1 and now thought to be horizon Beta, and as in the NAB, to equate with a cessation in carbonate sedimentation (Lancelot & Winterer, 1980). The study of seismic stratigraphy off West Africa differs in two important ways from the work described in the NAB. Firstly, the sediments are dominated by terrestrial input and secondly they have undergone varying degrees of tectonic flexure which complicates their original spatial relationships.

Eastern North Atlantic - A profiling system similar to that of

Ewing & Tirey (1961) as well as the later developed Flexotir method were used in the the eastern North Atlantic in the late sixties on the Galicia Bank and over the Bay of Biscay (Jones, 1968; Casand, Fail & Montadert, 1968). A strong reflector beneath the Biscay abyssal plain was thought to have been caused by turbidite influx about the time of the Cretaceous/Tertiary boundary from comparison with the 'Horizon A' identified in other Atlantic basins (Jones & Funnell, 1968).

Further north, another horizon A-type reflector, reflector R, was identified underlying much of the northern N.Atlantic and Labrador Sea. It was comparable to horizon A in both (supposed) age and character. Just as horizon A was known to underlie the Blake-Bahama Outer Ridge, so reflector R could be seen gently dipping under the Feni Ridge in the Rockall Trough. It was tentatively correlated with a similar reflector in the Labrador Sea, reflector ?R (Jones et al., 1970). Laughton (1971) found a mid-sediment reflector in the Labrador Sea, probably reflector ?R, which drilling on Leg 12 showed to be Oligocene in age (Laughton, Berggren et al., 1972).

Five reflectors (including basement) were identified in the deep sediments of the Rockall Trough (Scrutton & Roberts, 1971). Reflectors 1 and 2 were intermittent, in contrast to reflectors 3 and 4 which could be followed across the Trough. Later Reflector 4 was correlated with reflector R and so became known as reflector R4 (Jones et al., 1970; Roberts, 1975). It is an unconformity on the basin margins which becomes progressively more conformable towards the centre of the basin. Roberts (1975) disagrees with the previous interpretation of Laughton, Berggren et al. (1972) and correlates horizon R4 with an unconformity between lower Eocene green clays and overlying chert-rich oozes.

Fig. 1.6 Reflectors over Rockall

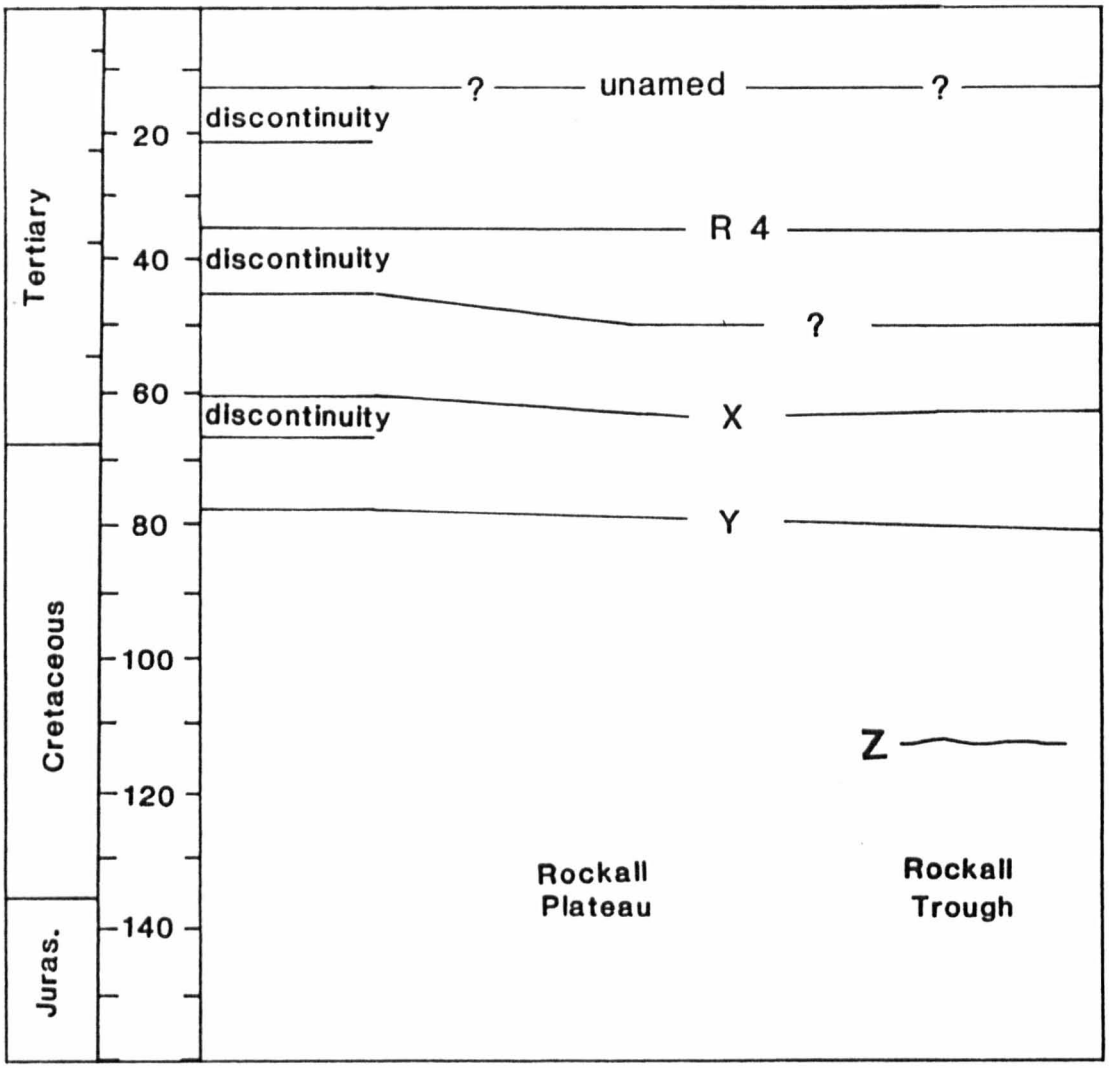

(after Roberts, 1975)

The margin studies of the eastern North Atlantic lend themselves readily to analysis by seismostratigraphic mapping of the inter-formational unconformities. Montadert et al. (1979) recognise a number of unconformities and four acoustic formations:

Formation 1: weakly layered (youngest)

Formation 2: several strong reflectors separated by finely layered strata

Formation 3: transparent or slightly layered

Formation 4: moderately to strongly layered

(Formation 5: basement)

The boundary between formations 1 and 2 post-dates the middle Eocene event which is marked by a sharp increase in silica content. It is dated as Late Eocene - Oligocene (reflector R4) (Montadert et al., 1979).

Roberts, Masson & Miles (1981) examine the history of the southern Rockall Trough with reference to four reflectors: R4, X, Y and Z (fig 1.6). Reflector R4 is traceable from the Bay of Biscay to the Rockall Plateau and confirms Middle Eocene to Oligocene age (Roberts, 1975; Montadert, Roberts et al., 1979; Roberts, Montadert & Searle, 1979). Reflector X is dated as mid-Paleocene (Kidd et al., in prep) and merges with horizon R towards Biscay. Reflector Y correlates with the unconformity between Maestrichtian and Late Paleocene at site 400A and a shorter mid-Paleocene hiatus at site 401 (Roberts et al., 1981). Reflector Z divides pre-Y sediments in the Rockall Trough. It is interpreted as a 'sequence of interbedded lava flows, sills and sediments that is probably equivalent to the late Paleocene interval observed at site 403 and 404', (Roberts et al., 1981) and is thought to be Cenomanian (Kidd & Hill, 1984).

Fig 1.7 Seismic stratigraphy in the Pacific Ocean

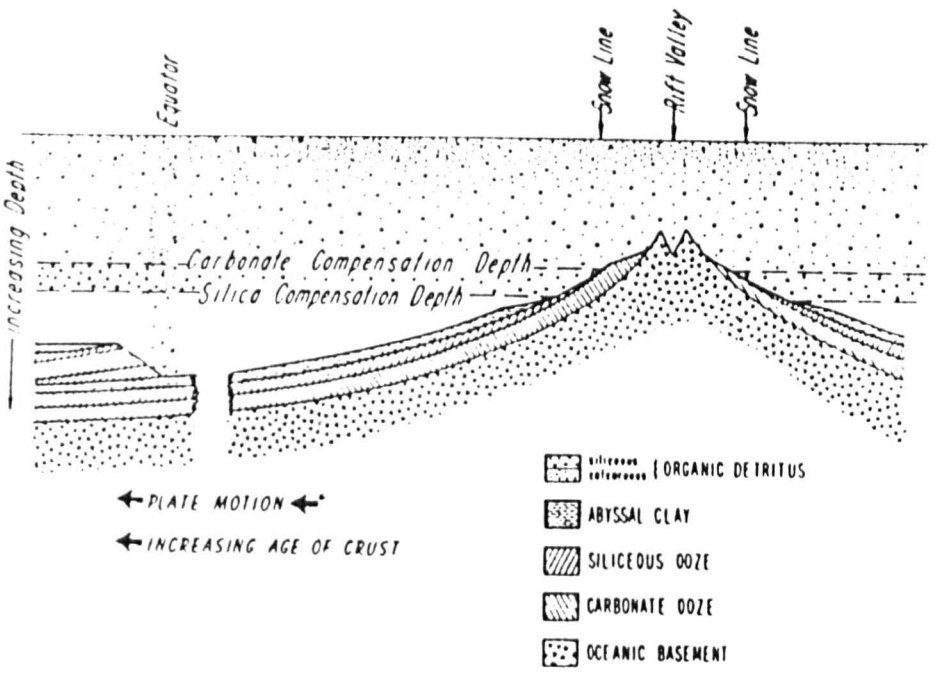

(after Heezen, et al., 1973)

Four unconformities were found by Leg 80 at sites 548, 549 and 550 off Rockall. They are middle Paleocene (horizon X), middle Oligocene (horizon R4), early Miocene and late Miocene.

In the Norwegian Sea a number of reflectors are named. They are sedimentary features related to the early opening of the Atlantic. Horizon TP (Top Paleocene) is correlated with the 'Ash Marker' horizon of that age found in the North Sea and horizon TL is thought to equate with the top of lavas in the Faeroes (Smythe, et al., 1983). Horizon K is a distinctive reflector possibly caused by the interface between dykes and lavas in oceanic crust (Talwani et al., 1984).

Pacific - The early work in the Pacific has already been outlined. The low (to negligible) terrestrial input over much of the Pacific basins and/or depocentres affords special conditions for reflector formation as compared to those described from the Atlantic Ocean. In particular, the seismic character of pelagic sediments can be seen more clearly.

Ewing et al. (1968) found five acoustic units:

5. upper transparent layer
4. upper opaque layer
3. lower transparent layer
2. lower opaque layer
1. basement

Heezen et al. (1973) outline the controls on pelagic deposition and propose a simple 'kinematic' model for the pelagic stratigraphy which compares favourably with recovered core material (fig. 1.7). They attribute the principal boundaries between the lithologic units with

providing the contrasts in acoustic impedance necessary to create major reflectors of regional extent.

Layer 5 was correlated with clay in the west and central Pacific, turbidites in the north and east and with unconsolidated ooze at the equator. Layer 4 was shown to correlate with chert-rich carbonates in the west. Layer 3 pinches out in the north and was thought to be Cretaceous clay. Layer 2 was thought to be another cherty carbonate unit of equatorial origin. Layer 1 equates with horizon B' of Ewing M. et al. (1966) where it is smooth (Heezen et al., 1973).

Other studies concentrate on the detailed relationship of fine scale reflectors to the variations in sediment producing them (see Chapter 2). Packham & van der Lingen (1972) showed how reflectors correlated with changes in the sediments brought about as a result of progressive diagenesis. Other workers have shown how climate can control the initial composition of sediments and so cause changes which produce reflectors (Berger & Mayer, 1978; Mayer, 1979). Embley & Johnson (1980) show that even these finer reflectors can be traced and shown to be regionally significant. They name three Miocene reflectors, R_0, R_1 and R_2, and show them to be diachronous.

1.3.3 Summary

The course of deep sea seismo-stratigraphic study shows a curious mix between equation of reflectors in different basins and the recognition of dissimilarities between them.

Horizons A and B were first found everywhere and thought to be the same. Drilling showed difference in composition and greater complexity of the individual reflectors was recognised. Increased resolution

Fig. 1.8 the problem caused by onlap in the deduction of subsidence

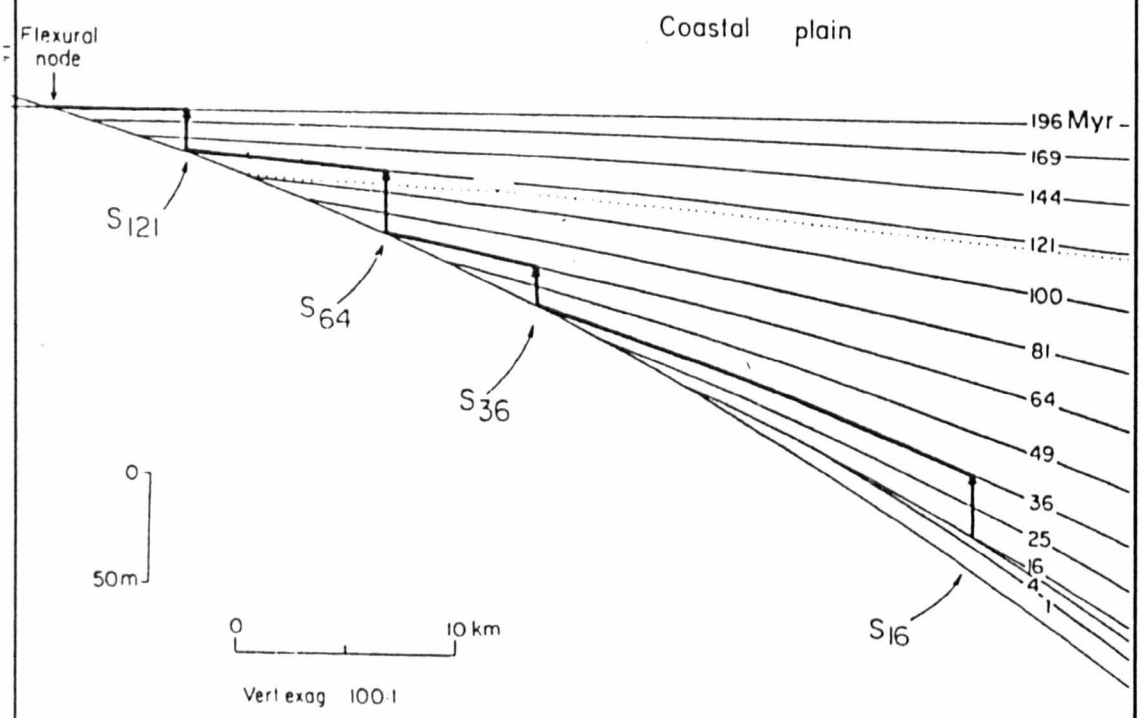

The heavy solid lines illustrate the procedure used by Vail et al., 1977, to estimate the vertical component of coastal onlap.

The dotted line illustrates the equilibrium shoreline where the rate of change of long-term sea level fall equals the subsidence rate.

The main problem is that Vail et al. determine sea level fall by measuring the vertical component of onlap in an overlying sequence directly to the lowest point of onlap in an overlying sequence. Because the record is largely removed by erosion during a sea level fall, the incremental method can not be used to measure onlap. The affects of tectonics during sea level fall are not satisfactorily accounted for.

Starting with the S_{16}, the lowest point of onlap in the sequence, the first increment of onlap is 28 m and the time interval is 16-32 Ma. The total onlap for the sequence is 94 m.

revealed more layers, which combined with drilling permitted a study of the ocean basins and their development.

However, it is interesting to note that the four-layer stratigraphies of Ewing et al. (1968) in the Pacific and of Montadert et al. (1979) in the eastern N.Atlantic are homotaxially identical. Ages and lithologies of horizons differ but the comparison remains.

1.4 Chronostratigraphy and Seismic Stratigraphy

The primary application of seismic profiling is to predict stratigraphy; that is, to infer the lithology and its age to within a known precision. Traditionally, this has been done by extrapolation of the stratigraphic column recovered at a borehole. The work of Vail et al (1977) endeavours to predict stratigraphy without the need of borehole calibration. To achieve this they first define seismic sequences and their associated seismic facies and then deduce a local curve of relative changes of sea level from the genetic relationship of these facies. Local sea level changes are deduced by summing the vertical component of coastal onlap and correcting for subsidence and compaction. A problem of this method is that these vertical components are measured between the highest point of onlap in an underlying sequence directly to the lowest point of onlap in an overlying sequence (fig. 1.8). Erosion during regression (offlap) prevents the incremental method from being used to measure this episode. Thus, the effects of tectonics during sea level fall are not satisfactorily accounted for (Watts, 1982). This also explains why early curves were characterised by rapid falls of sea-level, whereas more recent curves published in the light of such criticism are smoother.A further problem is suggested by models of the thermal subsidence of passive margins

(McKenzie, 1978; Watts, 1982), which predict that coastal onlap is a characteristic feature of such subsidence (i.e. onlap need not imply eustatic change). Failure to include this will lead to a static error in all calculations. Vail et al. (1977) calculate a global sea level curve from the modal average of three or more correlative regional cycles from different continents. 'The more continents represented, the greater the accuracy' (Vail et al., 1977). However, 'boundaries of most of the supercycles of Vail et al. (1977) appear to correlate with major tectonic events associated with the break up of Pangaea. Thus the supercycles identified by Vail et al. (1977) may be widespread because a number of widely separated continental margins are characterised by similar ages for the transition from fault controlled to flexural-controlled subsidence, but they are unlikely to be worldwide' (Watts et al., 1982). So Vail's method is useful as a quantitative comparison of the development of similar margins, but extrapolation globally is dangerous and more compilcated than originally suggested.

A seismic sequence is delineated by unconformities and their correlative conformities. These unconformities as described by Vail et al. (1977) are not necessarily correlative as single reflections, but are defined by terminations of reflections (Shipley and Watkins, 1978). The connection between sea level change and erosion had already been used to explain a eustatic lowering of sea level of the order of hundreds of metres which was suggested as the cause of physical and chemical changes caused by the worldwide hiatuses in Miocene marine sediments found on early DSDP cruises (Rona, 1973). Vail et al. (1980) state that 'the geological time significance of an unconformity is that all the rocks below the unconformity are older than the rocks above it' and that 'the conformable part of a sequence boundary is practically synchronous because the hiatus is not measurable' (Vail et

Fig. 1.9 lateral migration of an unconformity caused by the Western Undercurrent, (after Tucholke, 1981)

A Seafloor at arbitrary times T_0 and T_8

B Resulting depositional sequence

C Distribution in time and space of resulting hiatus.

Note the hiatus is diachronous.

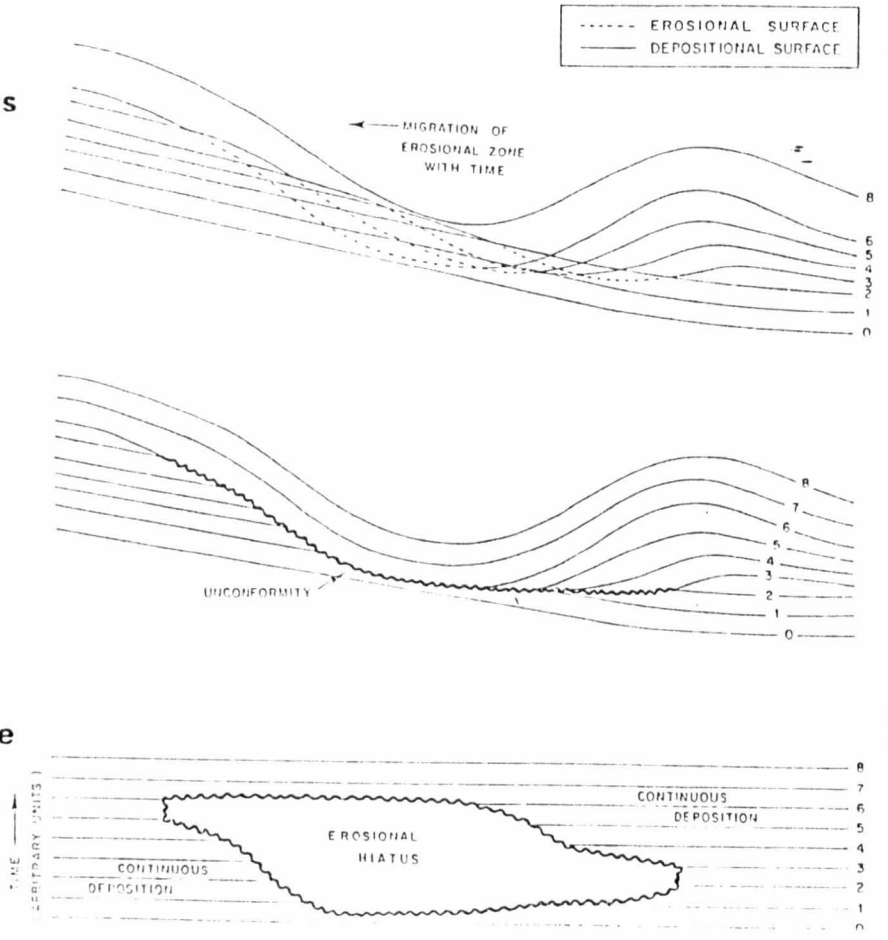

Fig. 1.10 Controls of sea level change

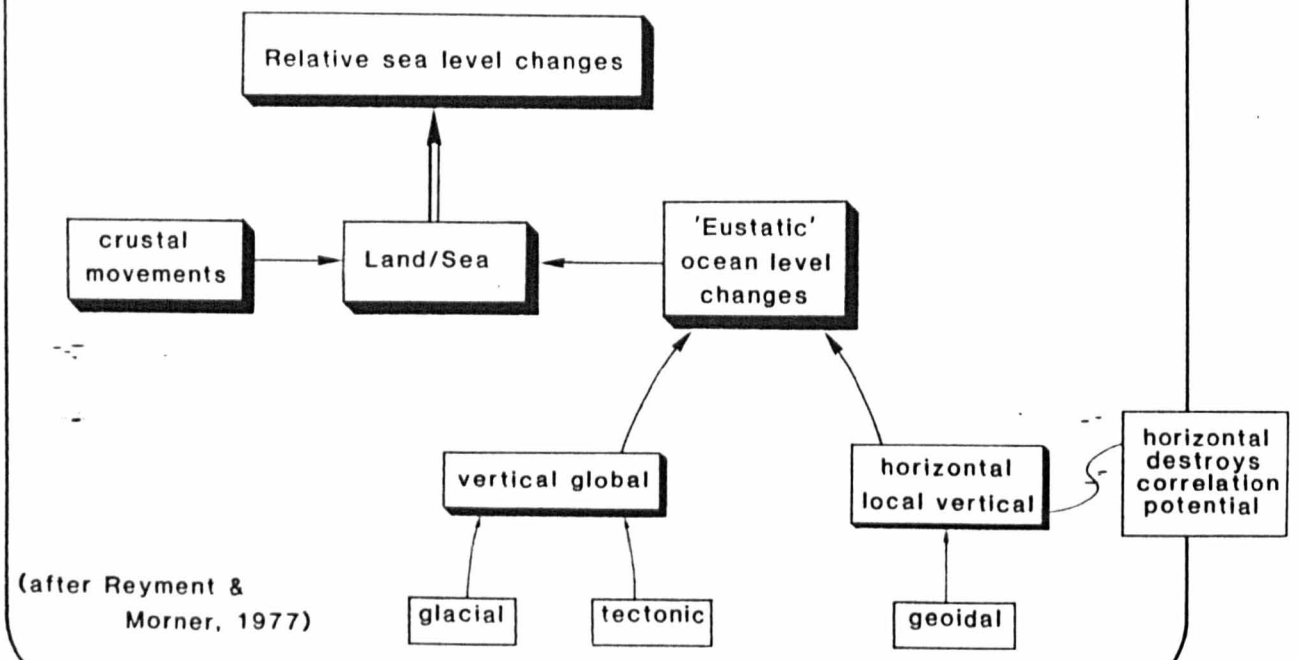

(after Reyment & Morner, 1977)

al, 1977). Obviously, their method hinges on the chronostratigraphic significance of seismic reflections and the correctness of the two assumptions.

Erosional truncation in the deep sea is a very different process when compared to that on the continental shelf. On the shelf, hiatuses are caused by shoreline movements and, in general, all transgressions onlap in the same direction. In the deep sea, erosional truncation can occur by current action of enhanced bottom-water circulation. One example is the Western Boundary Undercurrent in the western North American Basin. This current causes sedimentation on its flanks producing levees of the order of 3 km wavelength and 75 m high; lateral migration of the current partially erodes one flank-set producing a large-scale climbing ripple lamination pattern on seismic profiles. At any given point on a line parallel to the direction of migration (that is, perpendicular to flow) erosion by the current is followed by a resumption of deposition. This resumption occurs at different times along the line of migration, thereby countering Vail's assumption that all strata above an unconformity are younger than all those below it (Tucholke, 1980; fig. 1.9). The second assumption that refers to the measurability of a hiatus is a measure of the accuracy of the method: the problem of hiatus recognition is common to all forms of stratigraphic correlation.

Vail et al. (1977) have attempted to correct for tectonism and subsidence. The fact that eustatic sea level changes have occured is not in dispute, only the precise form of 'the curve' following overprinting by regional forces and the method of derivation of a global curve from regional curves. Morner (1976, 1980, 1981) and Reyment and Morner (1977) suggest that eustacy is a regional phenomenon. Sea level is affected by local changes and eustatic

changes (fig. 1.10). There are three types of eustatic change: glacial, tectonic and geoidal. (The geoid is the equipotential surface produced by the interaction of the gravitational and rotational potentials (Morner, 1981)). Morner draws attention to observed irregularities (deviations from a theoretical ellipsoid) over the Maldive Islands and Indonesia which amount to 180 m variation in sea level in 50-60 degrees of longitude. If such anomalies were to migrate then large regressions/transgressions might occur. Morner's argument (1981) relies on the size of these excursions in the geoid and their ability to change rapidly. He suggests that movements of the continents unbalance the earth's angular momentum causing the core to shift. This shift would then be expected to produce large anomalies (eustatic, but regional) which would migrate with subsequent shifts of the core producing simultaneously regressions and transgressions. He suggests the influence of the core/mantle boundary is supported by the similarity of the sea level curve and the palaeomagnetic reversals for the Holocene (Morner, 1980). Morner (1981) states that geoidal eustacy can have an amplitude of 200 m - sufficient to dominate any sea-level curve. More recently satellite altimetry has been used to investigate convection cells within the mantle (McKenzie, 1983). By removing the gravity anomalies due to crustal variation (mainly sea floor bathymetry) and filtering out variations with a wavelength of less than 300 km he arrives at a residual gravity anomaly map caused by variations in the mantle. His numerical model predicts that the change from bulge to trough caused by convection in the mantle is about 20 m over a distance of 2000 km. He does not find a signal caused by core/mantle irregularities. Thus Morner's geoid is dominated by sea floor bathymetry - itself related to tectonism. It is a possible source for further error but not of the type or scale that Morner suggests.

Leg 80 found a number of unconformities off Rockall, whose stratigraphic positions are remarkably close to worldwide unconformities. They have equivalents on many other margins and are correlated with seismic unconformities on the site survey profiles. Roberts et al. (1981) note that it is unlikely that sea-level fluctuations alone could produce the breaks almost simultaneously at shelf, slope and abyssal locations and suggest other mechanisms, such as changes in bottom-water circulation, and vertical fluctuations of the carbonate-compensation depth, may have a more direct influence. These mechanisms were probably linked by other agents, such as climatic cycles, regional tectonism, and the adjustment of plate positions that accompanied sea-floor spreading.

Ignoring the rate of sediment supply and tectonic effects, changes in relative sea level are important for producing unconformities. Such changes are measured relative to basement. The rate of thermal subsidence of passive margins decreases with time. If erosion (and non-deposition) is caused by a reduction in the water column then an unconformity is only formed where the rate of subsidence of basement is less than the rate of sea level change. Since margin subsidence is a function of the time since rifting, the size of the unconformity will change with age of the margin. Simply, young margins subside at a high rate, so only the sharpest changes in sea level cause an unconformity on these. Absolute sea level change (eustatic) must be the same everywhere. If an unconformity is seen on margins of different age, it must be due to sea level changes whose rate exceeds the rate of subsidence of the youngest margin. Similarly, the size of an unconformity will vary with the age of the margin (Thorne & Watts, 1984). Thorne & Watts (1984) calculate precise limits for the minimum duration of an unconformity for it to be identified on a seismic section. They assume the reflectors are time parallel and non-

deposition or erosion are the only causes of angular unconformity. For a 30 Ma unconformity this duration is 4 Ma for a margin that rifted 100 Ma ago. This figure increases with older margins and lowered seismic resolution, and is proportional to the sedimentation rate. (Resolution generally decreases with increasing water depth). Moreover, as the acoustic velocity increases, reflectors become less likely to result from individual structural changes, but from the interference pattern of several.

Angular relationships between seismic reflectors identified on passive margins may be formed by two differing mechanisms. The first of these is erosion or non-deposition of primary sedimentary surfaces that result in unconformities and paraconformities. These surfaces indicate a change (with time) of the sedimentary processes affecting a given point. A second mechanism is more an artefact of the seismic survey although it does witness important variations in sub-surface structure. The angularity results from the interference pattern of reflections from stratal surfaces and secondary diagenetic surfaces. These may include diagenetic surfaces (Thorne & Watts, 1984; Biart, in review) and clathrate horizons (horizon Y of Sheridan, Golovschenko & Ewing, 1974).

An important aspect of Vail et al.'s (1977) argument is their assertion that 'seismic reflections tend to parallel stratification surfaces, rather than the gross boundaries of lithologic units that may cut across stratification surfaces (Vail et al., 1977, p56). This is in contradiction to Fitch (1976), who states that 'Seismic continuity of a reflection is not an expression of the continuity of a geological unit. It is an expression of the continuity of two geological units, one following immediately on another; and at their contact is the interface at which the reflection is produced.' The

applicability of this technique to deep sea seismic stratigraphy has been questioned by Tucholke (1980). Horizon Beta is a regional reflector found in the western North American Basin (section 1.3.3). It represents the change from laminated carbonates (Neocomian) to grey shales (upper Lower Cretaceous): a boundary primarily controlled by a shoaling of the CCD. The boundary between the two lithologies will be found at different times for sea floors of different depth and, as the CCD is not a horizontal surface, it will vary with location (particularly with latitude as the CCD is likely to be depressed at the equator). Shipley and Watkins (1978) note that 'on a scale of kilometres, horizon Beta is more nearly horizontal than the underlying section, suggesting an unconformable relationship. Drilling results have not suggested any hiatus is associated with horizon Beta within the precision of dating and core recovery'. Yet horizon Beta is a real reflector. Van Hinte (pers. comm.) suggests that their disagreement stems from a difference in the resolution of the seismic profiles they are used to working with. He suggests that an horizon Beta-type reflector when viewed with the resolution that Vail is used to would merely appear as the lithostratigraphic boundary shown by amplitude variation of reflectors parallel to chronostratigraphic stratal surfaces.

Another difference in the deep sea realm that affects resolution is that Vail is used to reflectors at a depth of 2-4s (TWT) while most abyssal plains are found at depths in excess of 7s (TWT). This has effects on the precision of processing (velocity analysis is not as reliable for the deeper reflectors).

The question is examined further in the case example of the New Jersey Transect (Chapter 6). Unfortunately, in order to test this criticism in the deep sea environment we need to have a high resolution

profile between two continuously cored boreholes (over the relevant sequences) and preferably both wire-line logged, showing one such reflector. The early images of horizon A were considered to be due to a single surface, but greater resolution has revealed the complex character. Interpretation may yet benefit from improved resolution.

The Vail controversy is divisible into the two problems i) are reflectors chronostratigraphic and ii) can sea level changes be deduced accurately from onlap/offlap relations visible on profiles? Acceptance of the first being necessary before acceptance of the second.

The answer appears to boil down to resolution. All geological conclusions have an inherent error: dating is only to within half-a-stage, say, approximately one million years. The second assumption that refers to the measurability of a hiatus is a measure of the accuracy of the method: the problem of hiatus recognition is common to all forms of stratigraphic correlation. While it is unfair to expect another method to immediately provide better resolution the question still remains whether seismic reflections are strata-parallel or litho-parallel.

It is perhaps something of a compliment to Vail that he has provoked such eminent opposition. His original argument appears to be seriously flawed; the derivation of chronostratigraphy from a seismic section is not as straightforward as hoped. The combined criticism of Vail's ideas have lead to a ratification of the method which through greatly improved understanding of passive margins has permitted seismology to be developed as a predictive tool.

1.5 Bottom simulating reflectors

The term bottom simulating reflector or BSR was first used by Dillon et al. (1980) to describe cross-cutting reflections which mimicked the seafloor on profiles in the southern part of the North American Basin. The term is applied to any similar reflector whose form bears less relation to the sediments within which it occurs than to changes in seafloor depth. Generally, they are caused by impedance contrasts between layers whose variation in physical properties are depth dependent. They are divisible into two groups: those due to clathrates and those produced by diagenetic fronts.

1.5.1 Clathrate

Clathrate is a particular form of gas hydrate, a class of chemical substances which are collectively known as inclusion compounds. Inclusion compounds consist of a lattice of molecules of the host component within which the guest is trapped or 'included'. Clathrate consists of an expanded framework of host molecules with roughly spherical voids containing the guest such as methane. If the host is water then the term hydrate is used (Macleod, 1982).

The idea that hydrate could occur naturally within deep ocean sediments was first suggested by Stoll et al. (1971) following the discovery of large quantities of gas within sediments recovered on Leg 11 of DSDP (Ewing and Hollister, 1972). Markl, Bryan & Ewing (1970) found a strong reflector on the Blake-Bahama Outer Ridge, which in places obscured lower reflectors such as horizon X due to strong absorption. It parallels the sea-floor and is prominent only above 5.6 s (TWT). A 'complexity' of horizon Y was that it possessed a number of internal reflectors sub-parallel on the crest but increasingly

Fig. 1.11 Pressure/temperature conditions required for hydrate formation

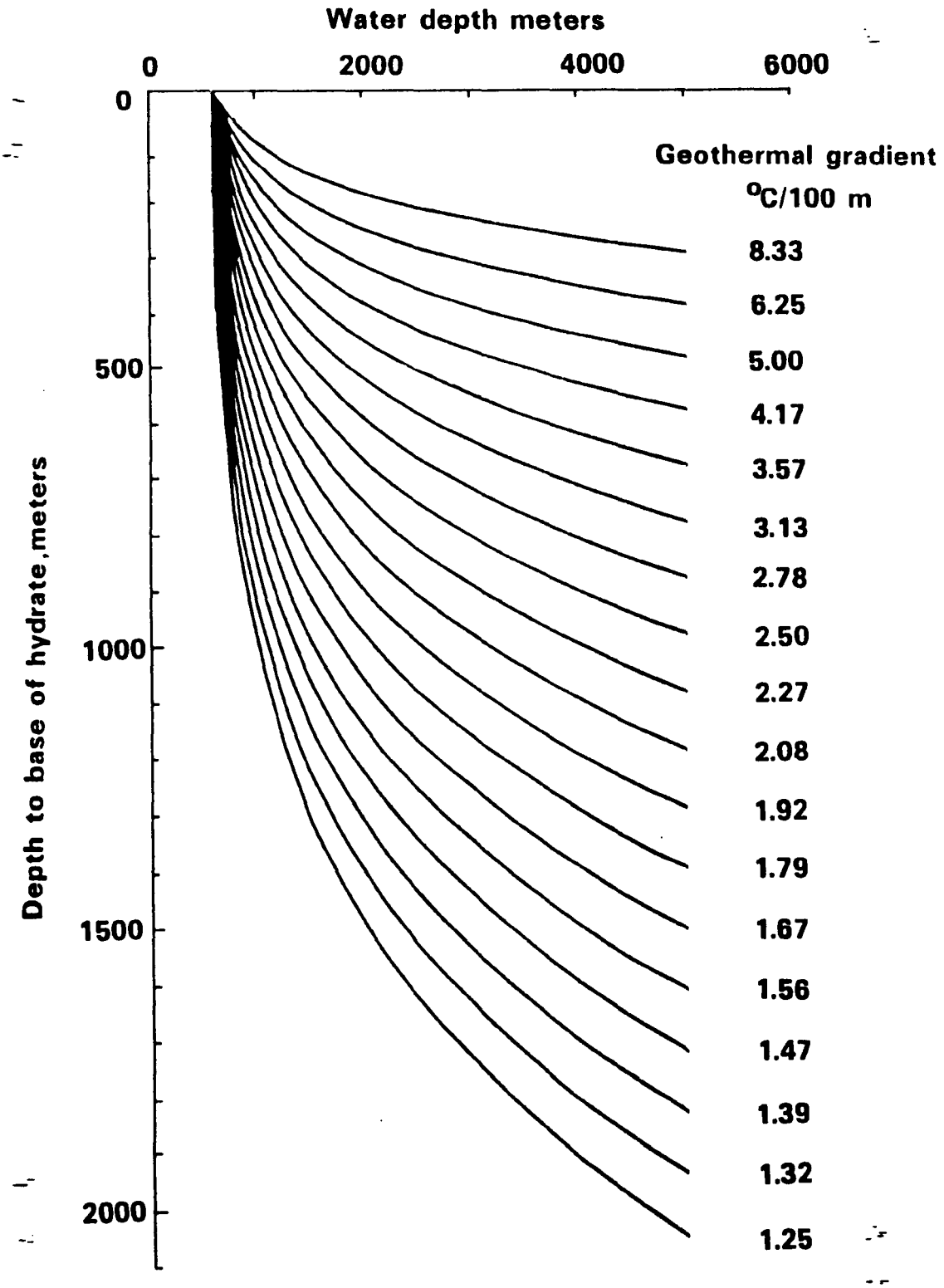

(after MacLeod, 1982)

oblique on the flanks. Some even appeared to cross horizon Y. Drill sites 102, 103 and 104 showed that the minor reflections are synchronous, whereas the 'arching' reflector Y proved to result from diagenesis, 'possibly associated with gas hydration' (Sheridan, Golovchenko & Ewing, 1974). (Methane hydrate contains five times the quantity of methane that would dissolve in the same volume of water.) High pressure and low temperature are required for the formation of gas hydrate and these requirements restrict the possibility of its natural occurrence to deep ocean bottom sediments and areas of thick permafrost. Large reserves of gas hydrate were known to occur in parts of Siberia (Chersky and Makogan, 1970). Despite the fact that necessary pressure/temperature conditions (fig. 1.11) are met over most of the deep sea floor, BSR's are far from common. They can only form where gas concentration exceeds that necessary to saturate pore water (Tucholke et al., 1977): therefore, structural control is important to the formation of clathrate-type BSR's. The first identification of a BSR in the deep sea was by Markl et al. (1970) on the Blake Bahama Outer Ridge and on the upper continental rise off New Jersey, where they found a regionally significant reflector, which occurs at a sub-bottom depth of roughly 0.6 s (two-way time) and which they named 'reflector Y' - the arching reflector. Markl et al. (1970) noted that these areas are structurally similar - both are broad anticlines striking parallel to the continental rise. Further importance of structure to hydrate formation is given by Katz (1981) with reference to BSR's on the south-east continental rise of North Island, New Zealand. A regional BSR occurs at 0.6 s-0.8 s (TWT) beneath much of the rise which is strongly deformed by Tertiary tectonism. However, reflections from major synclinal depressions are generally weaker or non-existent, suggesting that gas has migrated up-dip. The attitude of the BSR cutting across bedding-parallel reflections indicates that the ultimate trap is formed by the hydrate

layer itself (Katz, 1981). The implication is that free gas is trapped beneath BSR's - a possibility first suggested by Bryan (1974). Bryan (1974) used sonobuoy data to determine that BSR's were caused by layers of anomalously high velocity. This has been confirmed by laboratory measurements made on artificial methane hydrates formed within sand, which caused an increase in velocity from 1.8km/s to 2.26 km/s (Stoll and Bryan, 1979). This increase in velocity is explained by the increase in the frame bulk modulus (see Chapter 2) as a result of the cementation effect of hydrate crystallising at the interstices, so increasing the rigidity of the sediment.

Another physical property that is strongly affected by the presence of hydrate is thermal conductivity, which is markedly decreased. This is in contrast to saturated sand, whose thermal conductivity increases on freezing (Stoll and Bryan, 1979).

Tucholke et al. (1977) recognised three classes of BSR along the continental rise of the North American Basin, which were characterised by their differences in lateral continuity and amplitude. They are attributed to variation in the degree to which a solid hydrate layer is developed. Hydrate development is dependent on those factors which affect the stability of hydrate. These factors include composition of the gas, pressure, temperature and the salinity of pore water. The purity of the hydrate affects the velocity of sound transmission and hence the depth sub-bottom, in terms of two-way travel time, to the bottom of the layer. Purity also affects the limits of pressure and temperature at which hydrate is stable; in general, the greater the impurity of the host component the lower the temperature must be for stability to prevail, while the greater the impurity of the guest component, the higher (and, therefore, deeper/thicker) the temperature at which hydrate becomes unstable (Macleod, 1982). Pressure and

Fig. 1.12 Relation between BSR's, isotherms and water depth

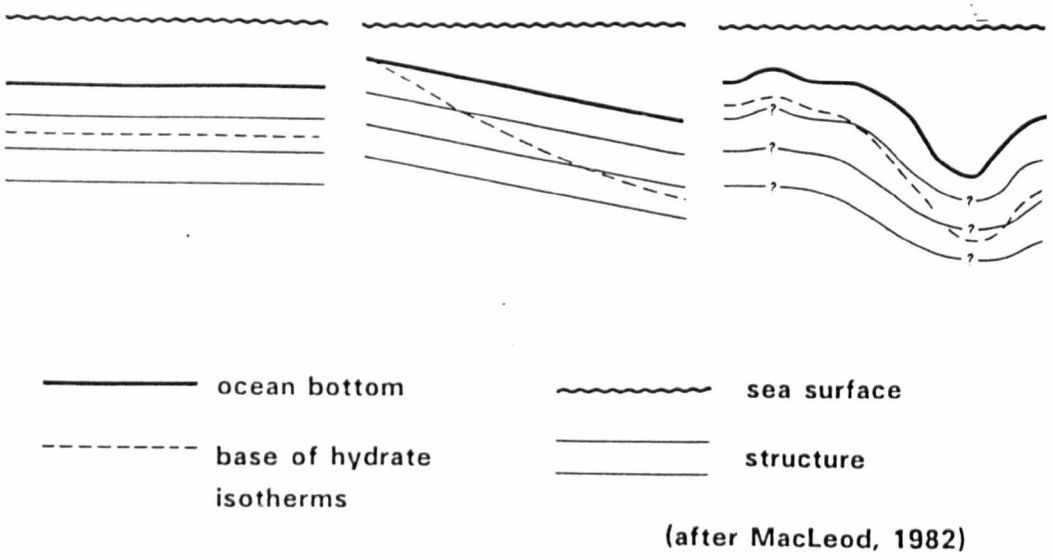

(after MacLeod, 1982)

Fig. 1.13 distribution of identified BSR's

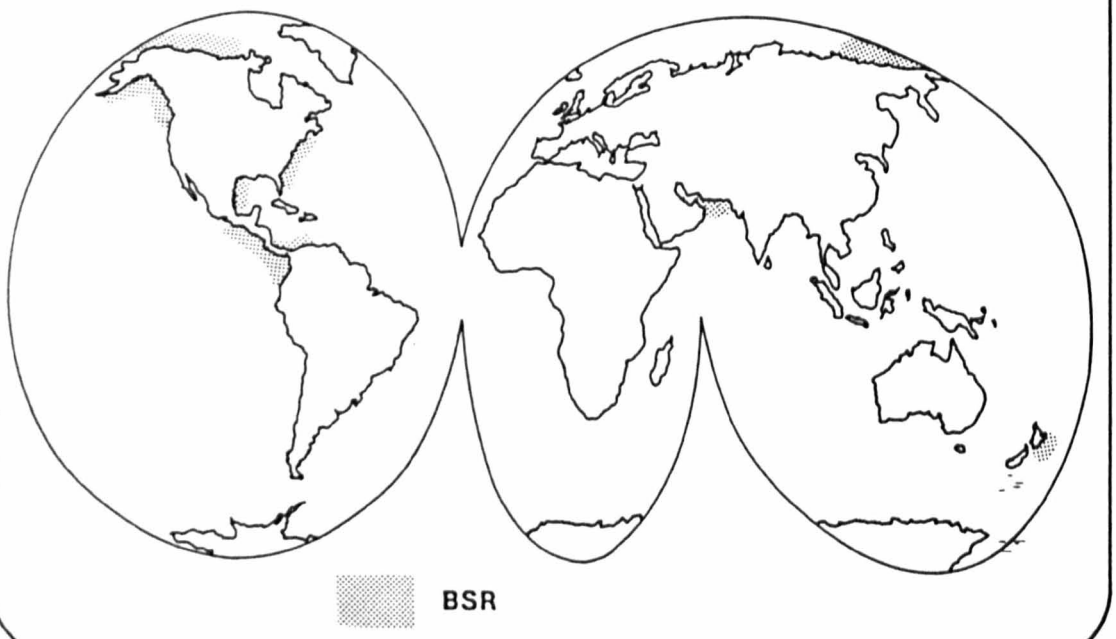

temperature are both depth dependent: temperature being the most important to the morphology of the reflector. If we ignore the variation in pressure, and given both an (almost) uniform bottom-water temperature and laterally constant geothermal gradient, then isotherms will all run parallel to the seafloor, that is, be 'bottom simulating'. In actual fact bottom-water temperature tends to decrease slightly with increased depth, thus the isothermal surface will be slightly deeper below the sea floor at greater seafloor depths. This means that BSR's do not perfectly simulate the sea floor above (fig. 1.12). Gas hydrate has been recovered off the west coast of Mexico during Leg 66 of DSDP (Moore, Watkins et al., 1979) and on the Blake Outer Ridge where cores recovered contained several ice-lenses of the order of 4-5 cm thick (Kvenvolden and McMenamin, 1981). Suspected occurrences have been suggested in several areas (fig. 1.13).

1.5.2 Diagenetic Fronts

Prior to hydrate recovery in DSDP cores, it was thought that the impedance contrast responsible for BSR's might be the result of diagenesis (i.e. unlithified overlying lithified sediments) (cf early postulates on the origin of horizon A, section 1.2). If the sediments are homogeneous then the chemical reactions responsible for the formation of cements might be controlled by conditions such as temperature, which being depth dependent themselves, might produce BSR's. Tucholke et al. (1977) suggested that siderite deposition might possibly be controlled by the vertical variability of gas state and gas solubility in the sediment column. If precipitation were not constant as the critical isotherm migrated up (with continuing deposition above) then relict 'fronts' would become stranded and so produce the necessary impedance contrast. Early drilling of reflector Y, mentioned above, found it correlated with a siderite

nodule-rich layer, the more attractive in light of the current hypothesis that horizon A was produced by a layer rich in chert nodules. The BSR character was presumed to be caused by isothermal control, but of what was open to debate (Ewing, Hollister, et al., 1972).

One confirmed diagenetic front BSR is beneath the Umnak Plateau in the Bering Sea (Scholl and Creager, 1973; Hein et al., 1978). The BSR occurs at a depth of 450 m-650 m and marks the upper surface where silicification is active. The transformation of opal-A to opal-CT and then to quartz is primarilly controlled by temperature and time. The BSR is thus thought to represent an isotherm.

1.5.3 Summary

Of the two types of bottom simulating reflector (BSR) discussed, differentiation is quite simple. The gas hydrate type clearly needs a specialised structural environment and their depth sub-bottom is a function of the actual sea-floor depth - temperature being the dominant variable. Unfortunately, temperature is also the primary factor affecting diagenesis, but the boundary should be more transitional. The single most important difference between the two types of BSR is their polarity. The gas hydrate type passes upwards from (probably) gas-bearing sediments, with consequently anomalously low impedance (approximately 50% reduction compared to non-hydrate bearing sediment) to hydrate cemented/saturated sediment with consequently anomalously higher impedance (approximately 30% increase) giving an overall reflection coefficient of about 0.4 and negative polarity. The diagenetic type, on the other hand, passes upward from high impedance silicified sediments to low impedance silica-bearing sediments - a positive reflection coefficient, but of smaller

amplitude.

Symbols used in Chapter Two

V_p Compressional wave velocity;

V_w of pore water

V_m of sediment matrix

V_s Shear wave velocity;

V_{sh} horizontally polarised

V_{sv} vertically polarised

K Bulk modulus; β compressibility;

K_s of sediment β_s of sediment

K_w of pore water β_w of pore water

K_f of frame β_f of frame

μ Rigidity modulus

ρ Density;

ρ_s wet bulk density

ρ_m grain density

ρ_w pore water density

ϕ Fractional porosity

a,b,c Crystallographic axes

P Pressure

P_h hydrostatic

P_e effective

CHAPTER TWO

Factors affecting the velocity of seismic waves within deep-sea sediments.

2.1 Theory

Seismology is based on the theory of elasticity. Elastic properties of substances are characterised by elastic moduli which specify the relationship between stress and strain for that substance. Stress may be compressive or shearing depending on the direction of force with respect to the affected body. Strains are deformations which produce restoring forces opposed to the stress. Hooke's Law relates stress and strain:

stress = k . strain where k is the elastic modulus

If the stress applied to an elastic medium is released suddenly the condition of strain propagates within the medium as an elastic wave. A sound pulse is an acceleration of particles of a medium according to the elastic rebound of the propagating medium (Boyce, 1976). There are three types of seismic wave:

1. Compressional - displacement of particles parallel to propagation
2. Shearing - displacement of particles perpendicular to propagation
3. Surface - propagate along a free surface

The fundamental equation for the velocity of a compressional wave in a perfectly elastic medium is:

$$V_p = \left(\frac{\kappa + 4/3\,\mu}{\rho}\right)^{1/2} \qquad (1)$$

$$\text{if } \mu = 0 \Rightarrow V_p = (\beta\rho)^{-1/2} \qquad (1a)$$

The parameters of compressibility (β) and density (ρ) vary with composition, sediment fabric and the conditions under which measurements are made. Subsequent sections describe the findings of authors working with real samples which reveal something of the empirical relationships governing the velocity of seismic waves. If the effects of attenuation are to be included then a viscoelastic model must be employed (Hamilton, 1971). Attenuation has not been considered in this work. The elastic models described relate the individual properties of the constituents (including the material filling the pore-space) in order to predict the properties of the aggregate. The most comprehensive theory for wave propagation in fluid-saturated porous media by Biot (1956) predicts two kinds of dilatational waves, often referred to as fast and slow respectively, and a shear wave. The fast dilatational wave and shear waves propagate mainly in the solid constituent but modified by the fluid whereas the slow wave propagates primarily in the fluid and is subject to the presence of the solid (Chandler, 1981; Attenborough, 1982). Hamilton (1971) is only concerned with unlithified sediments. The models become less applicble with increasing diagenesis. As the grain-to-grain contacts become cemented the primary path for sound conduction by-passes the pore-water and porosity only remains important for its control of overall density. Strictly, porosity only includes that volume with open connection to 'the outer surface' (Attenborough, 1982), in practice the route to a free surface may be excessively tortuous for much of the absolute porosity as to render its contribution negligible and effective porosity is reduced. Porosity is important in unlithified sediments because it controls the influence of pore-water on the fast wave.

The general approach is to consider the properties of the individual

Fig. 2.1 The effect of rigidity on velocity

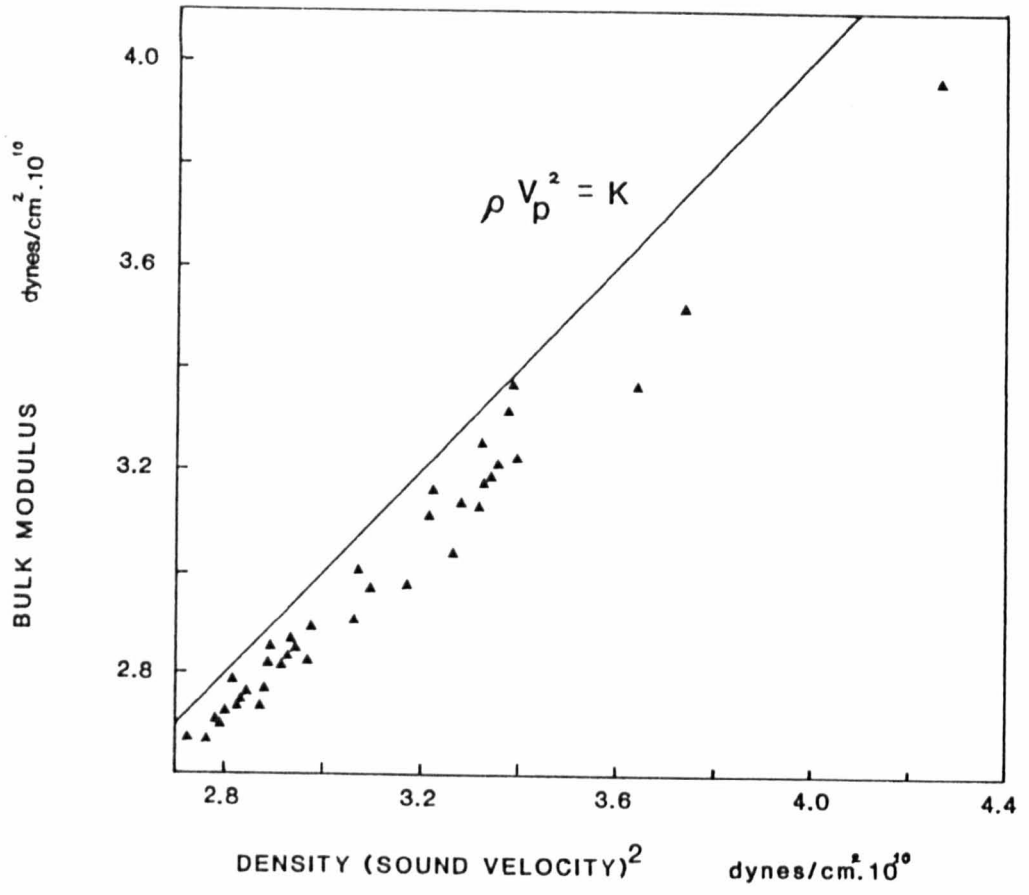

(after Hamilton, 1971)

constituents and combine these to derive an expression for the properties of the whole sediment. Wood (1941) derived an equation for the aggregate compressibility of emulsions and suspensions:

$$\beta_{sw} = \phi\beta_w + (1-\phi)\beta_s \quad (2)$$

$$K_{sw} = K_w K_s / [\phi(K_s - K_w) + K_w] \quad (2a)$$

$$\rho = \phi\rho_w + (1-\phi)\rho_s \quad (3)$$

combining (2) and (3)

$$V_p = \left[\left\{\phi\beta_w + (1-\phi)\beta_s\right\}.\left\{\phi\rho_w + (1-\phi)\rho_s\right\}\right]^{-1/2} \quad (4)$$

(after Wood, 1941)

Urick (1947) confirmed Wood's equation using a suspension of kaolinite in water (a deflocculent was necessary to avoid complication from the particles surface activity). The assumption that sediments can be modelled as liquids is obviously an over simplification. The interaction between grains imparts a strength to the aggregate, which affects the compressibility (fig. 2.1). The excess is due to dynamic rigidity of the sediment and is represented by μ in eq(1). It is related to the structure of the sedimentary framework and not to the rigidity of the constituents. Its computation relies on knowing both V_p and V_s.

Wyllie et al. (1956) developed an equation applying to rock with rigidity:

$$\frac{1}{V_p} = \frac{\phi}{V_w} + \frac{(1-\phi)}{V_m} \quad (5)$$

Nafe & Drake (1963) derived an equation applying to rock with varying degrees of rigidity, which is controlled by the value of n:

$$V_p^2 = \phi V_w^2\left\{1 + \left(\frac{\rho_w}{\rho_{sw}}\right)(1-\phi)\right\}\frac{\rho_s}{\rho_w}(1-\phi)^n . V_s^2 \quad (6)$$

V_m and n must be empirically determined. They show the interaction between paramenters, but do not allow complete forward modelling. Using experimentally determined values for V_p and V_s, Hamilton (1971) computed the system bulk modulus, K .

$$K = \rho \left(V_p^2 - \tfrac{4}{3} V_s^2 \right) \qquad (7)$$

In all cases the true bulk modulus was greater than the agregate bulk modulus, eq(2a), due to the incompressibility of the sediment structure. Thus

$$K = K_{sw} + K_f \qquad (8)$$

The behaviour of minerals and pore-water in sediments is affected by pressure. Gassman (1951) considered the transmission of sound through closely packed spheres and recognised three components of pressure:

1. Hydrostatic pressure, P_h, acting on the pore water
2. " " " " " grains
3. Effective (intergranular) pressure, P_e, acting on the frame.

These three pressures acting on the sediment result in three components of compressibility (the inverse of the bulk modulus).

$$K = K_s \frac{K_f + Q}{K_s + Q} \qquad \text{where} \quad Q = \frac{K_w (K_s - K_f)}{\phi (K_s - K_f)} \qquad (9)$$

$$K_f = \frac{K[\phi (K_s - K_w) + K_w] - K_s K_w}{\phi (K_s - K_w) + K_w (K/K_s - 1)} \qquad (10)$$

To derive the system bulk modulus, , one has to find the four parameters, , , and . It is usually assumed that the pore-water and the bottom-water have the same salinity and thus the same compressibility. The compressibility of the aggregate is an average of the compressibilities of the constituent minerals as calculated using the Voigt-Reuss-Hill method. Voigt takes the simple arithmetic mean weighted according to the fractional volume of each component and Reuss take the harmonic mean weighted similarly. Hill (1963) showed the true value lies halfway between:

$$\text{Voigt :} \quad K_V = V_1 K_1 + V_2 K_2 + \ldots \qquad (11a)$$

$$\text{Reuss :} \quad K_R = V_1/K_1 + V_2/K_2 + \ldots \qquad (11b)$$

$$\text{Hill :} \quad K_S = \tfrac{1}{2} \left(K_V + K_R \right) \qquad (11c)$$

(after Hill, 1963)

The remaining parameters of porosity and the frame bulk modulus must

be determined experimentally. Porosity is determined gravimetrically or by mercury porosimeter. The derivation of the frame bulk modulus is best performed from the epirical relation with porosity (on which it is dependent)(Hamilton, 1971). Laughton (1957) measured frame compressibility directly by drained static compression tests, but noted that the artificial conditions of laboratory measurement would lead to inaccuracies when the resulting values were used to calculate velocities in real sediments. Hamilton (1971) avoids this problem by deriving from measurement of compressional and shear wave velocities and density. The disadvantage of this method is that it does not allow predictive modelling of any given sediment, although Hamilton does present data for a variety of sediment types. (The theoretical derivation of wet bulk density is simply the arithmetic mean of the sediment components weighted according to their fractional volume.)

The accuracy of theoretically derived (compressional) wave velocity relies on the diagenetic state of the sediment. Other properties which also vary with diagenesis may be used as an index to determine the 'strength' of the sediment, but no absolute route exists.

2.2 Porosity and Density

It is impossible to separate porosity from particle size in any attempt to predict the cause of velocity variation (Buchan et al., 1972). However, Brandt et al. (1960) recognise porosity as 'the most important factor affecting velocity.' Wyllie et al. (1956) confirms this stating the relation:

$$\frac{1}{V_p} = \frac{\phi}{V_w} + \frac{(1-\phi)}{V_m} \qquad (12)$$

Deep-sea sediments are divisible into calcareous and non-calcareous.

These two groups differ widely in physical character and in their response to external forces.

Non-calcareous sediments consist of siliceous oozes, clays and turbidites. The comparative rapidity of sand- and siltstone deposition means that the properties of porosity and density are largely controlled by the packing of the grains. Frazer (1935) calculated the minimum porosity for a packing of uniform spheres as 45%. This is reduced for mixed grain size.

In pelitic sediments the strong affinity between clay and water leads to the development of a negative charge on the surface of the clay particle. (This is due to the presence of sea water which is a strong electrolyte.) The negative charge on the plate surface induces a positive charge at the plate edges; this induced dipole force causes a honeycomb to be formed, which is responsible for high sediment shear strength despite its low density. Compaction to 10-20 Å inter-particle distance overcomes the repulsion and a strong cohesive force results in the plates being tightly packed (Buchan et al., 1972). This change corresponds to the clay-to-claystone transition seen in homogeneous sequences such as the Blake Ridge formation of the North American Basin. Aoyagi & Kazama (1980) recognise three porosity zones in argillaceous sediments.

1.	porosity > 30%	shallow burial	viscous rock
2.	" 30-10%	late compaction	plastic rock
3.	" < 10%	deep burial	elastic rock

They tie these zones to their seven diagenetic mineral zones (see section 2.2, fig. 2.4).

There are two stages in the long term reduction of porosity in calcareous sediments (Schlanger & Douglas, 1974). The first is the

early dewatering stage which occurs in the upper 200 m within which half the porosity reduction takes place over 10 Ma by gravitational compaction; porosity is reduced from 80% to 60%. After this comes the cementation stage. Below 200 m over a period of tens of Ma porosity is reduced from 60% to 40%.

Carbonate sediments are composed of biogenic remains, of which foraminiferal remains, by virtue of their size, are dominant. The tests themselves have a porosity of 80%, which together with spherical packing can give an initial porosity of 90%. Pelagic forms often account for over 99% of the sediment supply. Benthic forms are more preservable because of their thicker walls and fewer pores. During the ooze-chalk-limestone transition, thin walled forms are lost, especially porous rotalines and miliolids. There is a concomitant increase in the number of broken tests which also increases angularity. Diagenesis proceeds with dissolution of less stable forms (planktonic forms may be reduced to 2% of their initial proportion) and collapse of weakened tests. The volume of dissolved calcite is approximately equal to the amount precipitated in the form of interstitial cement, calcite over-growths and infilling within remaining tests. Particles of the order of 1 micron diameter such as nannofossils are important in pelagic carbonate diagenesis because they are easily dissolved. Precipitation favours larger particles of the order of 10 microns diameter such as discoaster remains. This process proceeds because it achieves a lower free energy for the system (Adelseck et al., 1973). Coccoliths are generally far better preserved in samples containing high amounts of clay, zeolite, volcanic ash or siliceous microfossils than in pure carbonate ooze (Burky et al., 1971).

Velocity increases with progressive cementation at grain-to-grain

Fig. 2.2 Estimated porosity rebound versus depth

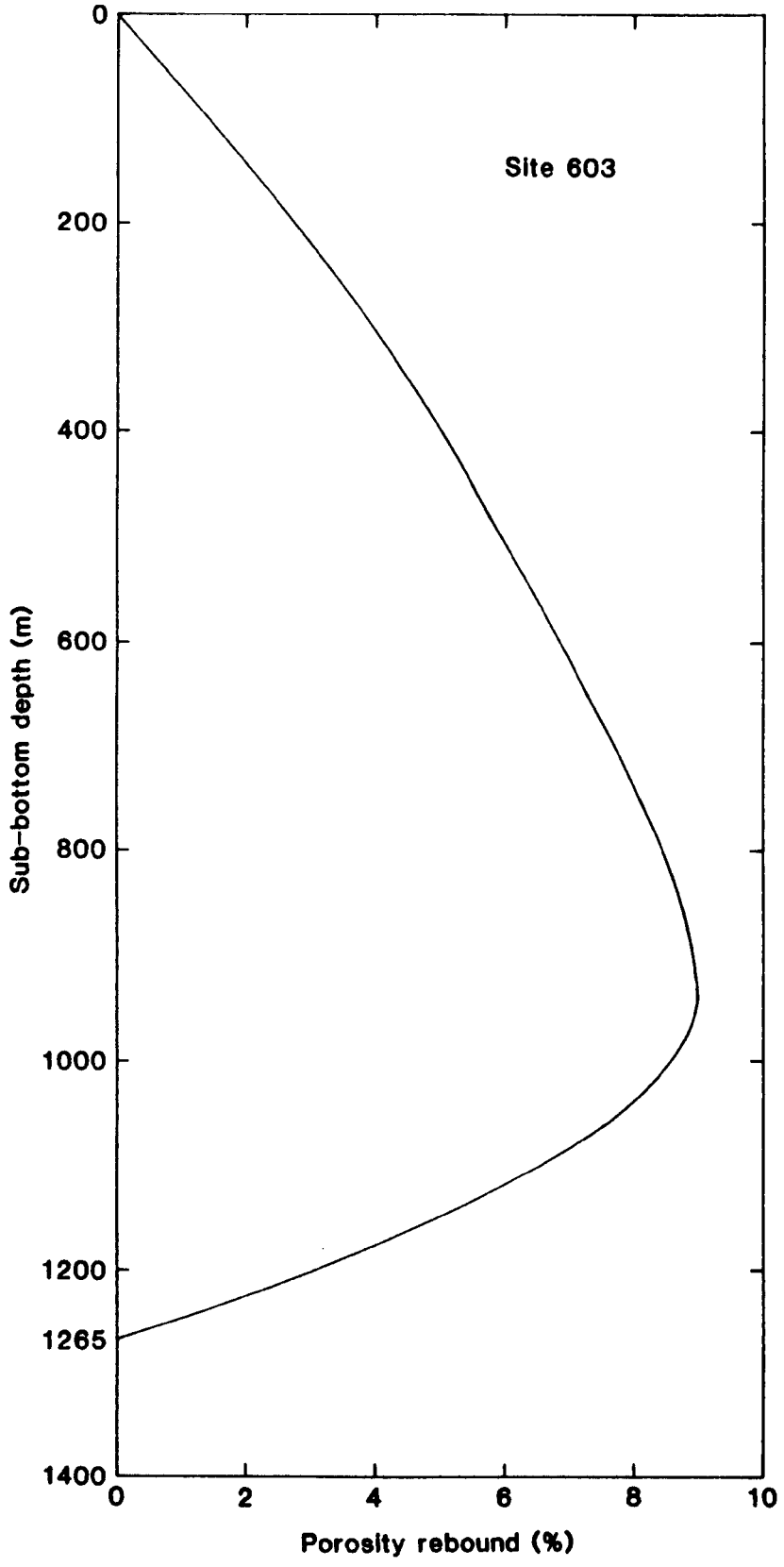

contacts. Once the rock is consolidated, velocity is dependent on porosity (Gregory, 1977). Porosity is a measure of the relative importance of the lattice of connected particles in determining the stiffness, and of the kind and number of particle contacts (Nafe & Drake, 1957). However, finer sands have higher porosity and more numerous grain-to-grain contacts. Thus rigidity will increase with increasing porosity (Hamilton, 1971). Porosity is lowered by improved packing, which also increases rigidity and so also compressional wave velocity (Hardin & Richart, 1963; Horn et al., 1968).

Cementation lowers permeability which reduces pore fluid mobility and the previous 'free' system of Brandt (1955, 1960) approaches Gassman's (1955) 'closed' system. Johnson and Plona (1982) have demonstrated that the slow wave is present only when the water-saturated medium is somewhat consolidated such as by cementation or by external pressure.

Heat is thought to increase the number of microcracks, giving a small increase in porosity. Thermal expansion will lower density (see section 2.4).

The porosity of unlithified (calcareous and terrigenous) sediment as measured under laboratory conditions must be corrected for in situ pressure. The reduction in pressure as core samples are removed from overburden pressure allows porosity to increase, or rebound (Hamilton, 1976). Porosity rebound increases with sub-bottom depth. Shipley (1983) observes that lithified sediments undergo no such relaxation and suggests the curve of porosity rebound falls steeply over the depth interval in which lithification is taking place (fig. 2.2).

Several authors give empirical relations between porosity, density

Fig. 2.3 Empirical relations between porosity, density and velocity for deep-sea sediments

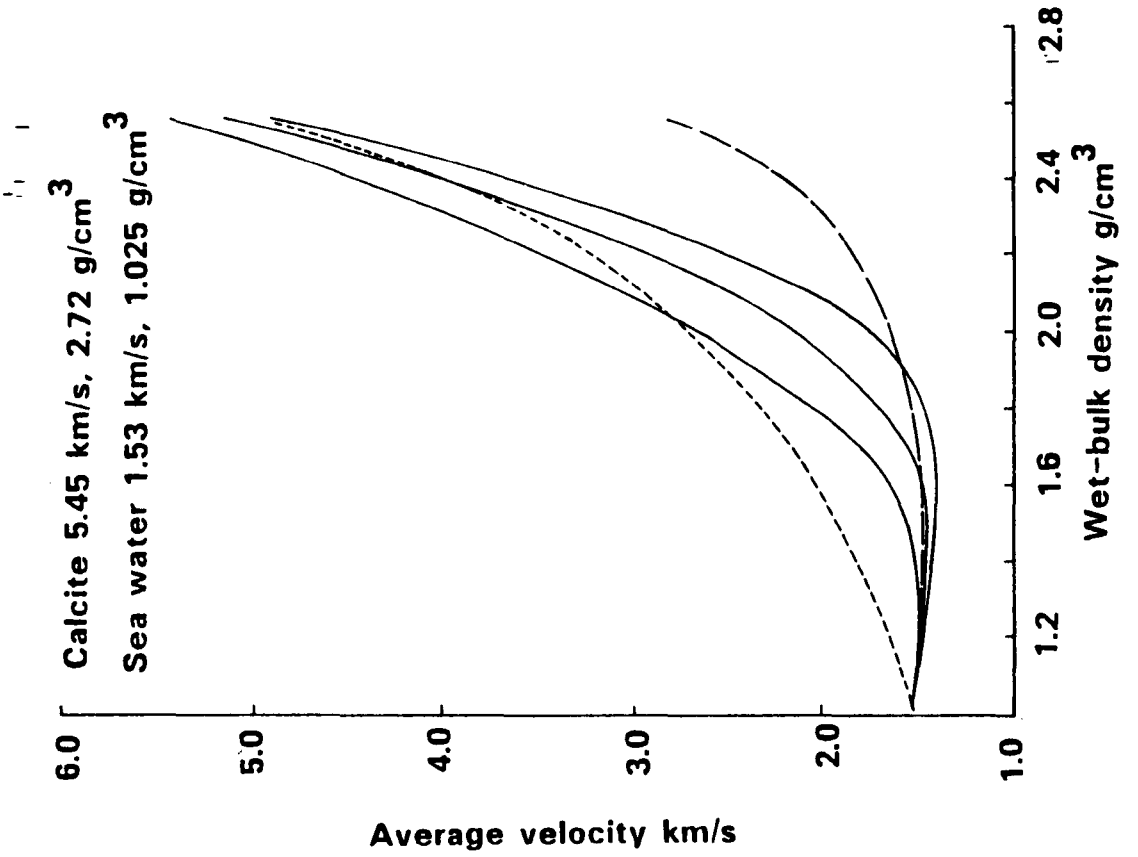

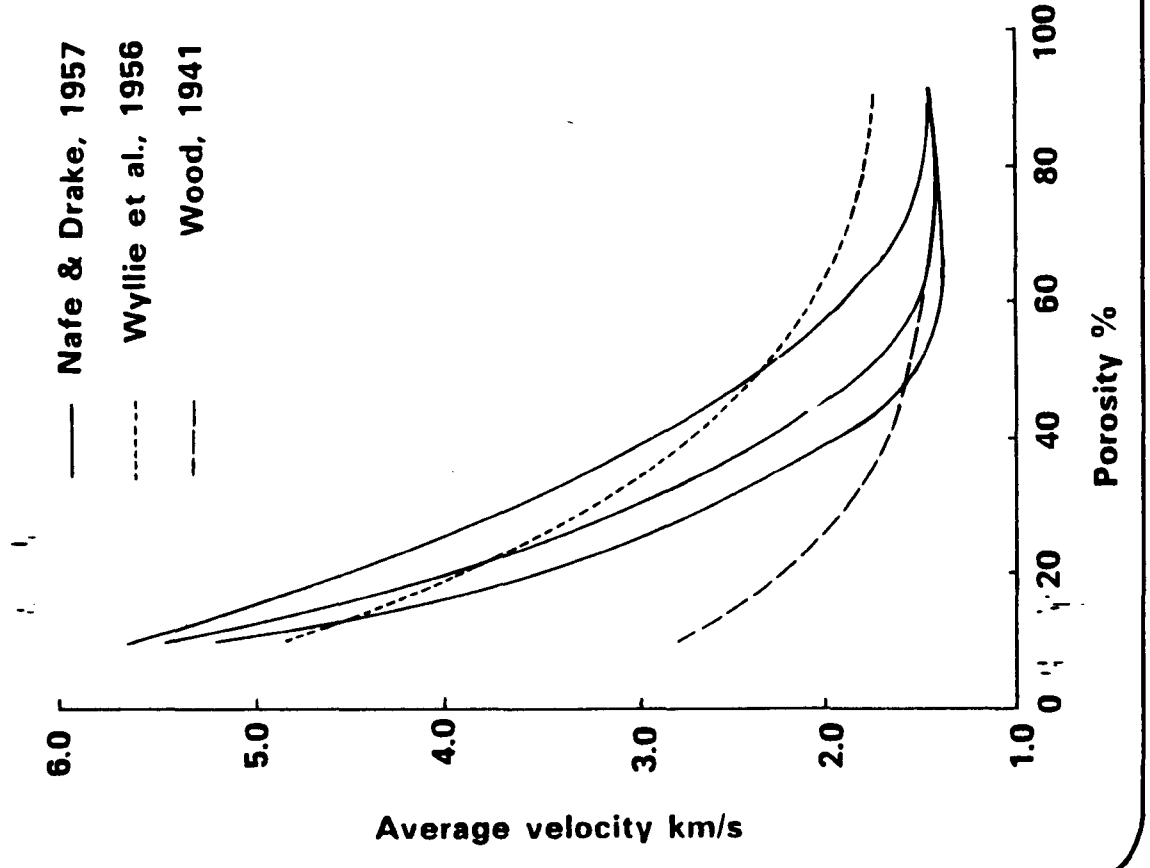

and velocity for various sediment types; fig 2.3, Buchan et al. (1972), Boyce (1984), Hamilton (1977).

2.2.1 Grain size - The most important factor in the variability of acoustic data is that of particle size. As mean particle size increases, so too does attenuation and velocity (Buchan et al., 1972). Hamilton (1956) established a positive correlation between velocity and median grain size. However, there is a danger in using mean particle diameter as a criterion of velocity, because of the large range in grain density between solid sand grains and near-hollow, sand sized foram tests (Morton, 1975). Grain size correlates with the shear strength of sediment, although this may be a reflection of angularity, which increases with decreasing grain size (Hamilton 1971). Hamilton (1956a) found grain size decreases with increasing sorting for a given mean grain size (Horn et al., 1968).

2.2.2 Composition - Studies of factors affecting velocity is hindered by the vast diversity of possible sediments. Some general conclusions can be made. Horn et al. (1968) found that coarser sediments, especially turbidites, have higher velocities than deep-sea muds. A large part of the strength of a marine sediment is related to the quantity of clay minerals present and the composition of the interstitial waters. Below 5 microns particles are surface active and capable of long range interaction without physical contact. Interaction of mineral particles either by frictional contact in the case of coarse sediments or by electrochemical forces in clays , gives a frame structure to the medium. As a result bulk modulus increases and shear modulus is non-zero. When fine particles fall to the bottom they are apt to stick to the grain where they first alight and be held there by inter-molecular forces to form a three-dimensional honeycomb structure (see section 2.2). In addition, clay particles adhere to

Fig. 2.4 Maximum overburden pressures and geothermal temperatures necessary for diagenetic transformations

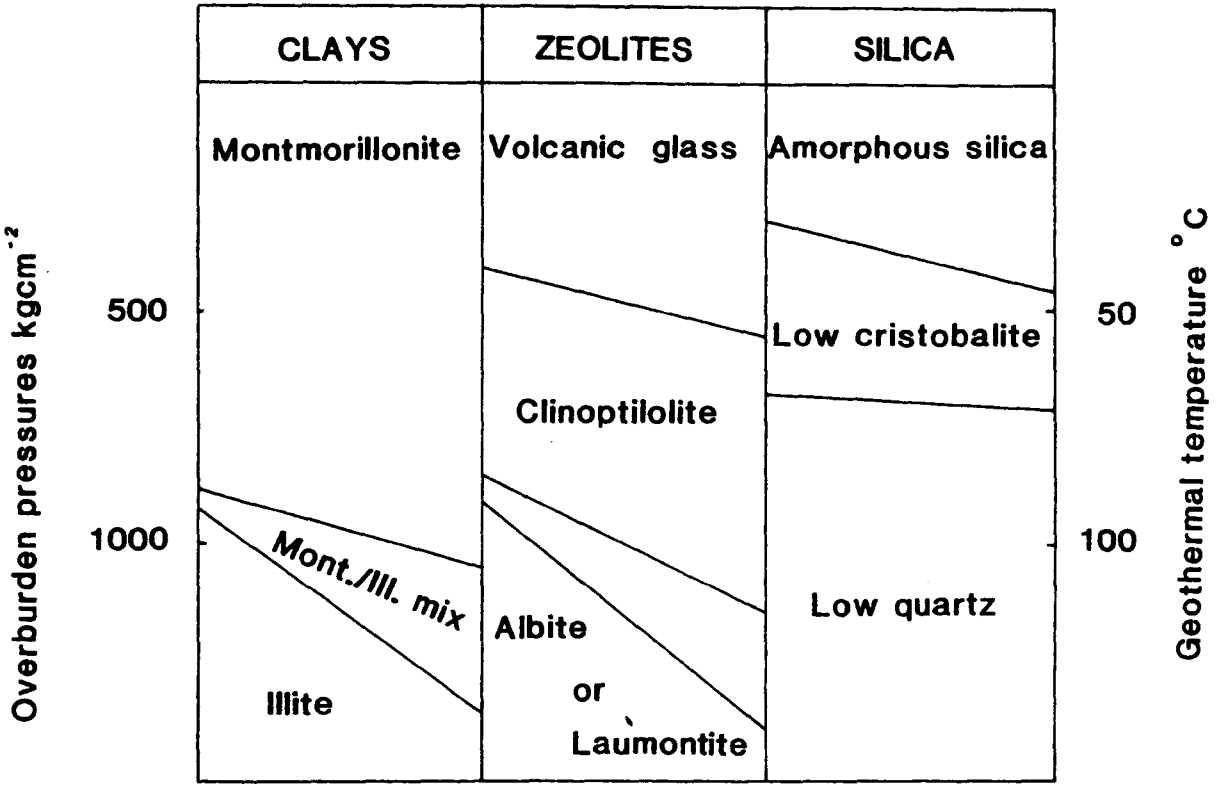

(after Aoyagi, 1978)

make flocs when in an electrolyte (Hamilton, 1956b). Becking (1959) confirms that many sediments are made up of compound particles. Shear strength of upper (inorganic) sediments is due to alteration of clay minerals. The increase of pressure and temperature with burial is responsible for further mineralogical transformations which can be used to delineate seven mineral assemblage zones (Aoyagi & Kazama, 1980; fig. 2.4).

Not until the presence of a coarse fraction starts to break up the honeycomb structure and form its own supporting frame is there any increase in velocity with decreasing porosity. The point at which this occurs is about 50% by volume and corresponds to a sudden decrease in porosity with increasing median diameter. Grim (1962) supports the theory of the effects of adsorbed water as a contributor to cohesion and notes the large capacity of montmorillonite for holding water, which increases the minerals shear strength. This also varies with the composition (salinity) of the pore water with which it must be in ionic equilibrium. The honeycomb floc structure is easy to break down by compression to the simpler honeycomb arrangement. Platey minerals are responsible for increasing the porosity due to their bridging effect (Hamilton, 1956). For example, Frazer (1935) achieved a porosity of 92% with a sample of crushed mica. Below 400 microns no correlation exists between particle size and composition (Becking, 1959).

A number of workers have observed that velocity increases with increasing carbonate content (Laughton, 1954; Sutton, 1957; Schreiber, 1968). Mayer (1979) found that samples of deep-sea oozes with high carbonate values are dominated by low density spiny siliceous microfossils. Horn et al. (1968) contend that no relation exists between percentage carbonate and velocity. Buchan et al. (1972)

suggest that the contradiction may be due to the difficulty of separating grain size effects (which are so closely related to composition).

In calcareous sediments the magnesium carbonate content affects the solubility of the test and hence increases the preservation potential: high magnesian calcite tests possess a high diagenetic potential which will result in the layer being lithified sooner (i.e. give rise to a rigidity contrast with respect to adjacent horizons). Magnesium carbonate content is affected by species supply (in turn due to salinity and temperature of surface waters), (Schlanger & Douglas, 1974).

Schreiber (1968) examining velocity/density and velocity/particle diameter relationships, attributed deviations from the empirical line to three factors: 1) poor sorting causes both anomalously high and low values of velocity depending on the mode distribution of grain sizes, 2) the biogenic component, whether foraminifera- or radiolarian-rich, cause anomalously low porosities compared with equivalent clastic sediments (due to their secondary porosity) and 3) gels caused by authigenic weathering in volcaniclastic sediments and/or by contained zeolites, montmorillonite or clinoptilolite. Velocity is either increased or decreased according to the rigidity they give to the sediment.

2.3 Rigidity

Velocity changes can best be understood by supposing the particles of the sediment to form a structure which in part supports the stresses during the transmission of an elastic wave and which plays an

increasingly important part as the compaction becomes more advanced (Laughton, 1957). Cementation further increases rigidity and therefore velocity.

In saturated sediments, dynamic rigidity and static shear strength are related to the same factors of sediment structure and the complex parameters restricting relative inter-particle movements under shear stresses. Thus rigidity is related to 1) sliding and rolling friction between grains, 2) the number of inter-grain contacts (governed by grain size and packing; packing in turn reflects porosity for a given grain size) and 3) the extent of interlocking between grains (governed by packing and grain angularity). Rigidity is inversely related to porosity.

Shumway (1960) suggested that the effective rigidity is also increased by physical contact between grains, particularly sand and large silt size particles. He proposed that the effective rigidity should be a function of the volume fraction occupied by the sand size particles:

$$V^2 = \frac{\kappa_{sw} + b(1-\phi)\mu}{\rho_{sw}} \qquad (13)$$

where b = constant

According to Hamilton (1971) the best empirical index for rigidity is $\rho . V_p^2$ in the abyssal plain environment, while clay content is better in the abyssal hill environment. Rigidity has a positive correlation with percentage volume of clay, illite and chlorite (Moore, 1964). These relationships are explicable in terms of facies that such minerals characterise and their implicit rate of deposition. Morton (1975) contends that facies is the only independent variable affecting rigidity. As noted in section 2.2.2 the amount of adsorbed water has an effect on the rigidity of some minerals.

Morton (1975) stated that rigidity is the most important factor controlling velocity in high carbonate sediments. The shape of the particles is of primary importance for determining the rigidity. Angular fragments should produce extremely rigid sediments, while spherical tests will reduce rigidity. In angular sands rigidity is probably less a function of grain size and more dependent on the packing of the particles.

Shear strength of upper sediments is due to alteration of clay minerals (Buchan et al., 1972). Rigidity accounts for 1-2% of the compressional wave velocity of upper sediments (Hamilton, 1971). Dynamic rigidity decreases by 15% with the addition of as little as 1-4% moisture, with no additional decrease with greater saturation (Hardin & Richart, 1963). This has important consequences in gas saturated layers such as are found beneath gas hydrates, and for the abruptness of the clay-to-claystone transition.

2.4 Temperature

Temperature increases with increased depth below the sea-floor. The gradient varies with heat-flow and the thermal conductivity of the sediments. In situ temperature is measured most accurately with the von Herzen temperature probe. Temperature gradients of 0.05°C/m and 0.09°C/m were measured at sites 206 and 210 respectively.

Velocity of pore water varies with compressibility which is influenced by both pressure and temperature (Gregory, 1977). Both bulk and rigidity moduli decrease with increasing temperature. For instance an increase in temperature from 0°C to 100°C causes a 0.4% reduction in the compressibility of quartz (equivalent to a reduction

Table 2.1 - Increase in length and volume between 20-200°C

	Aragonite %	Calcite %	Quartz %
parallel to c-axis	0.58	0.096	0.18
volume	1.00	0.285	0.78

(after Birch, 1966).

Table 2.2 - Bulk moduli of calcite

parallel to c-axis	1.75 $mbars^{-1}$
perpendicular to c-axis	1.13 $mbars^{-1}$
perpendicular to c-axis	4.03 $mbars^{-1}$

(after Birch, 1961, quoted in Carlson et al, 1984)

in velocity of 6%). Pore-water compressibility varies more than crystals, so temperature has a greater effect on unconsolidated sediments which have minimal structural rigidity.

Differential expansion of different minerals along different axes may result in structural damage, which can substantially reduce the acoustic velocity of rocks (see table 2.1).

2.5 Pressure

Velocity is affected by the effective overburden pressure, P_e:

$$P_e = P_C - P_i \qquad (14)$$

where P_C = total overburden pressure

P_i = formation fluid pressure

Where P_e increases, velocity increases (Gregory, 1977).

Work by Brandt (1955), Fatt(1958) and Banthia et al. (1965) suggests a more accurate analysis is of the form:

$$P_e = P_C - n \cdot P_i \qquad (15)$$

where n = coefficient of deformation = $\dfrac{\beta_{sw} - \beta_f}{\beta_{sw}}$

Velocity increases with increasing pressure as microcracks or grain-to-grain contacts are closed. However, velocity is less affected by microcracks than by strains developed due to static stress because a considerable amount of acoustic energy may by-pass many cracks, particularly those cracks orientated parallel to the direction of propagation (Ide, 1936). Kuster & Toksoz (1974) investigated the shape of oblate spheroidal inclusions on the velocity of P and S waves. Using aspect ratios as low as 10^{-4} the effects of cracks are modelled. 'It is found that the concentrations, shapes and properties

Fig. 2.5 a,b Relation between velocity, pressure, grain size and saturation

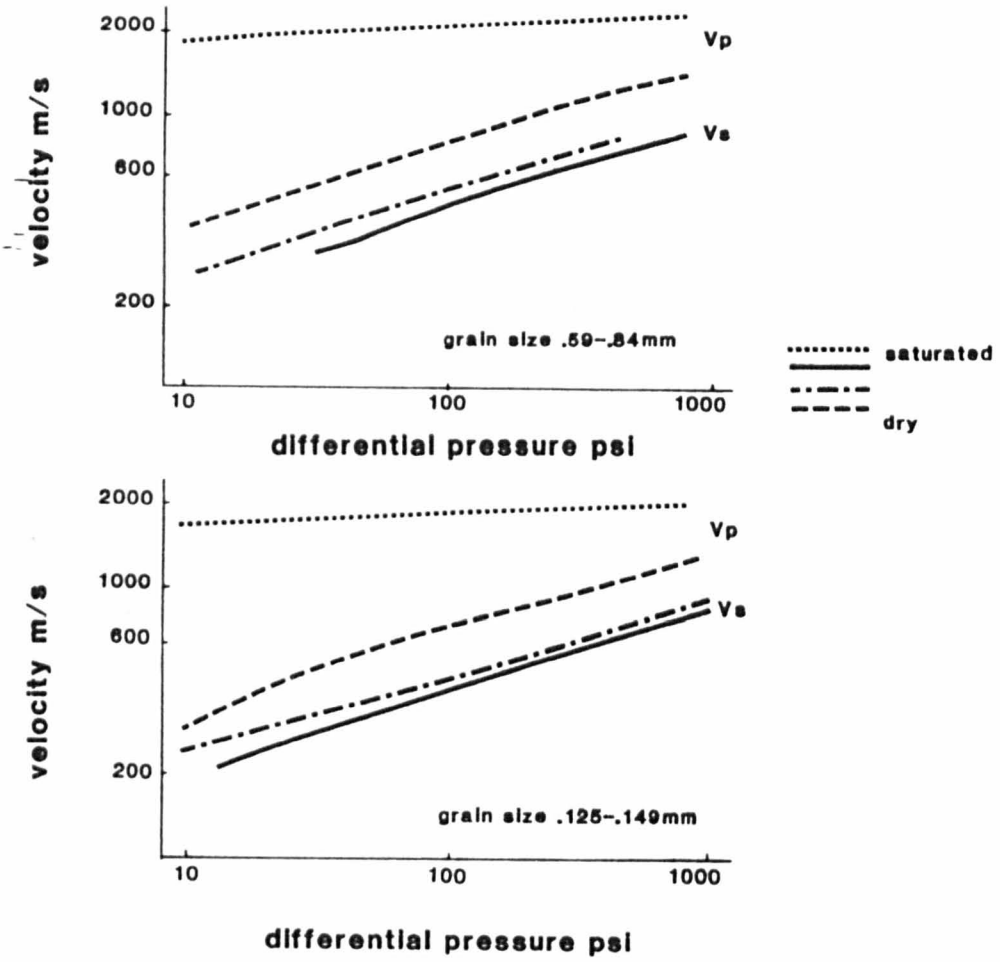

(after Hamilton, 1971)

Fig. 2.6 Elastic coefficients and wave velocities in transversely isotropic materials

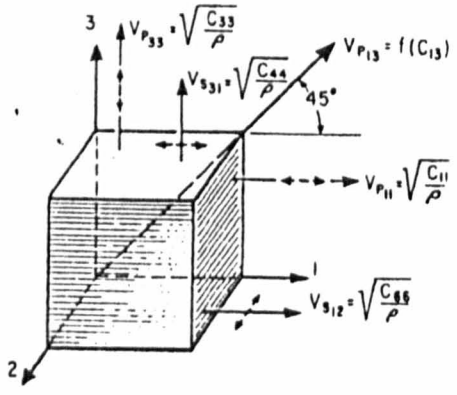

(after Podio, 1968)

of the inclusions are important parameters.' In crystalline rocks they found flatter inclusions have a greater effect, e.g. at low concentration (0.01%) thin inclusions could decrease velocities in the composite medium by up to 10%.

As mentioned in section 2.4 compressibility of fluid varies with pressure. Boyce (1976) notes that the effect of pressure on sediment properties is dominated by the response of pore-water to the adiabatic pressure gradient. This is because water's low density and elasticity cause a much larger change in its properties than in the solid phase of the sediment. However, such a variation does not vary linearly with respect to porosity variation (see figs 2.5a and 2.5b). Of course once the sediment is lithified pore water plays no part in the transmission of sound and only the minor change in density need be considered. (Sound velocity increases with depth in sea water, see fig. 3.6.)

2.6 Anisotropy

Anisotropy in crystalline rocks is due to anisotropy in minerals (the minerals being aligned) and to microcracks (Birch, 1961). Layered sediments may be considered to be transversely isotropic, that is, there are five independent elastic stiffnesses which characterise any given sediment (fig. 2.6; Gregory, 1977). Marine sediments under overburden pressure develop elastic anisotropy which can lead to errors in wide-angle reflection profiling. Velocity has an angular dependence which is faster parallel to bedding.

The failure of anisotropy to decrease with increasing confining pressure suggests that it is not produced by the alignment of cracks.

Fig. 2.7 Variation of velocity with depth and pressure

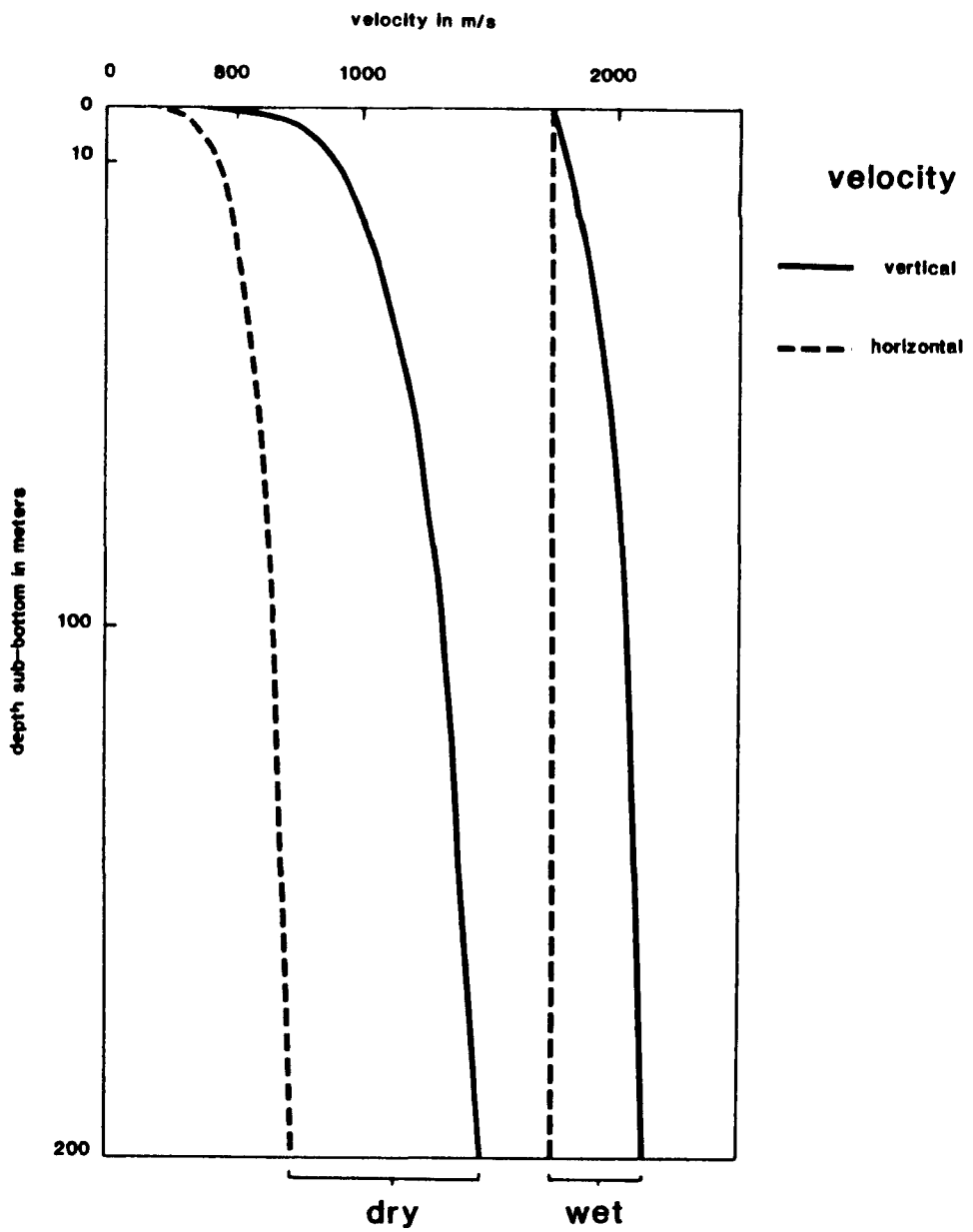

(after Gassman, 1951)

In calcareous sediments it may be explained by the elastic properties of calcite which vary with respect to crystallographic axis (see Table 2.2). An alignment of c axes perpendicular to bedding would produce the observed velocity distributions. Such a fabric might arise due to 1) an alignment of microfossils by compaction, particularly discoasters, 2) epitaxial growth of aligned forms during diagenesis and 3) recrystallisation of calcite parallel to pressure (Bachman, 1979; Carlson & Christensen, 1979). Pressure enhances anisotropy, particularly in bedded sediments. Processes which disturb this ordering will affect the degree of anisotropy. Bioturbation of laminated carbonates removes the anisotropy present in laminated layers of the Blake-Bahama formation (NAB) (Biart & Johns, in prep.).

When the sediment column is layered on a scale much finer than the wavelength of seismic waves, the waves average the physical properties of the layers and act as if they were travelling in a single transversely isotropic solid (Levin, 1979).

2.7 Water content

Saturation increases compressional wave velocity becauses it increases the system bulk modulus, but lowers shear wave velocity by lowering the rigidity of the frame because the inter-particle friction is reduced as a result of the increase in pore fluid pressure (see figs 2.4, 2.5a and 2.5b).

Compressional wave velocity varies non-linearly with brine saturation. Velocity remains almost constant from 0% to 85% saturation. Further saturation increases abruptly and appreciably to the 100% saturation velocity (Domenico, 1976) (see fig. 2.7). Domenico

also showed by comparison of thoeretical curves with figure 2.7 that the best model was the one in which acoustic coupling between fluid and frame was unity (i.e. the closed system of Gassman, 1951). Shear wave velocity decreases moderately and uniformly with increasing saturation.

2.8 Rate and depth of deposition

A rapid rate of deposition leads to low value for sediment rigidity. For instance rigidity of deltaic sediments is approximately zero in its upper parts. The slower rate found in deep-sea environments gives a non-zero value. Rigidity increases with age because post-depositional changes have time to occur. This is shown by the relative lack of porosity reduction with overburden pressure in slowly deposited sediments. Such sediments have a characteristically high rigidity (Hamilton, 1970). Very slow deposition rates allow chemical alteration to occur, which give the (inorganic) top sediments fairly high shear strengths and hence high velocity (Buchan et al., 1972; see section 2.2.2). Rate of deposition is characteristic of the environment. Consequently, it will correlate with other environmental characteristics such as sediment composition (see section 2.3). Faster deposition lessens the effect of incipient cementation near the water-sediment interface (Moore, 1964).

Mean grain size decreases at deeper depositional sites, primarily because of dissolution and fragmentation of calcareous microfossils and mechanical sorting (of terrigenous material). This in turn results in the sediments formed in deeper water having lower sound velocities and less shear strength. The physical properties of calcareous ooze are not significantly affected by any reprecipitation or cementation

that may occur soon after deposition (Johnson et al., 1977).

2.9 Conclusions

The problem is complicated by the inter-dependence of variables which mask the true (and valuable) relationships between the independent variables.

Most authors seem biassed in favour of the importance of their own specialist field in the determination of velocity and density. Brandt et al. (1960) see porosity as 'the most important factor affecting velocity', while Horton et al. (1968) believed grain size to be the most important acoustical factor. This is confirmed by many empirical results. Morton (1965) considers rigidity to be the most important factor, a view shared by Horton (1975) for the case of carbonate sediments.

The methods of study are too varied to allow reliable extrapolation of results between the studies and the areas studied tend to be too narrow. In short, there is a lack of wholly objective analysis covering all deep-sea sediments: clastic and carbonates and from soft sediments to hard rock.

'Perhaps the most important result is the observation that none of these properties [bulk density, porosity, and sonic velocity] change uniformly with sub-bottom depth' (Davies & Edgar, 1974).

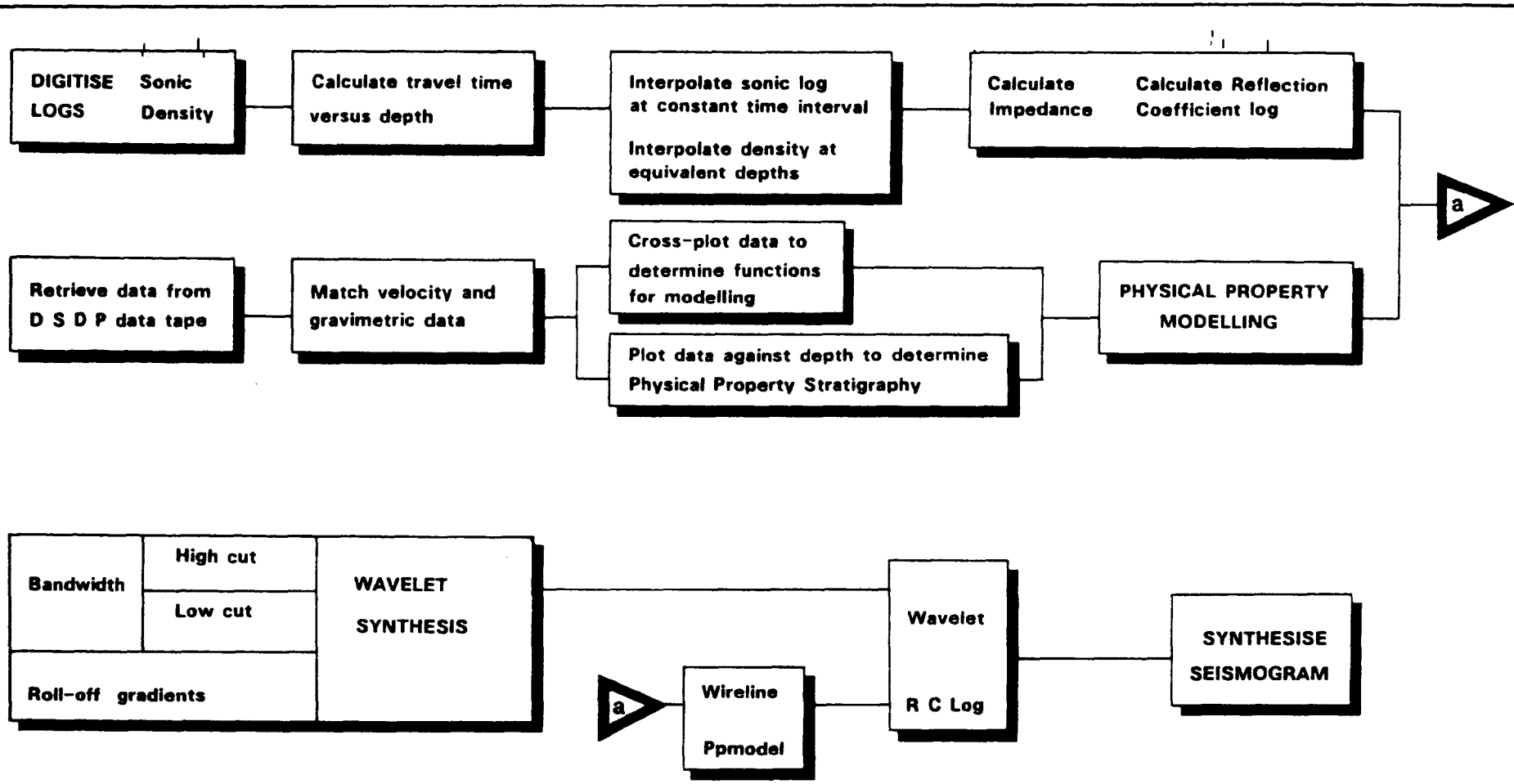

Fig. 3.1 Flow chart of computer programs

CHAPTER THREE

Synthetic seismogram modelling

3.1 Introduction to modelling

The reflection of seismic waves from within sediments was modelled by convolution of a band limited source wavelet with the impulse response of the sediments (Fig. 3.1). Modelling assumes normal incidence of a plane-wave. In the deep sea this assumption is justified for the case of single channel studies. The detail available from such a survey can only be improved to a limited extent by processing of the recorded data. Multichannel surveys using a streamer containing many separate receivers can achieve greater resolution. These streamers may be many hundreds of metres long, so the separation between source and reciever is no-longer negligible and is different for each channel. Sophisticated processing is required to retrieve the true seismic signal from the data. Correction for the effects of dipping strata are also possible.

The models could have been constructed by a method analogous to that of real seismograms. This might have included calculation of the effects of spherical spreading and non-normal incidence for those rays received by large offset hydrophones situated towards the end of the streamer. The individual arrivals might have been corrected for move-out, summed (stacked) and filtered to simulate the processing of the original survey. For the purposes of this study it was assumed the processing company had achieved their aim of producing a seismic section 'as if' it were the result of a normally incident plane-wave

Fig. 3.2a Zero phase and minimum phase Butterworth wavelets

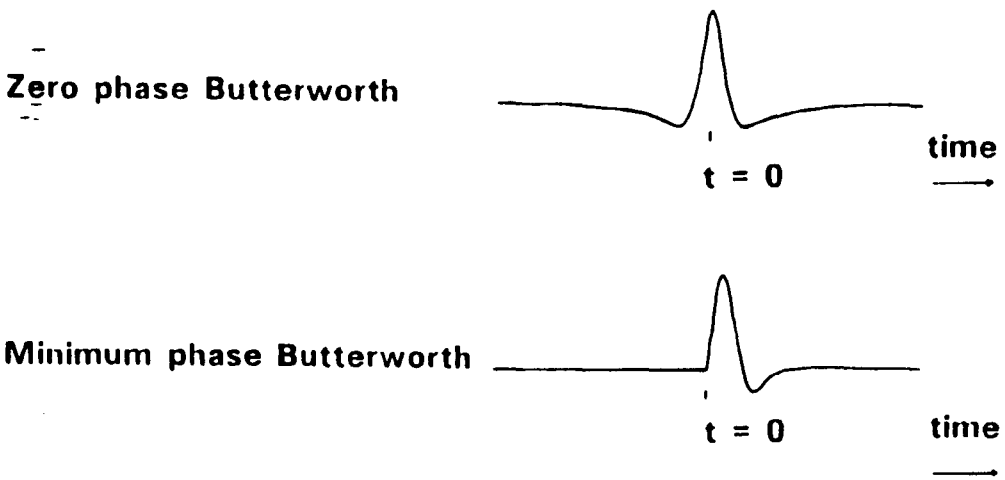

Fig. 3.2b Amplitude and phase spectra of wavelets used in modelling

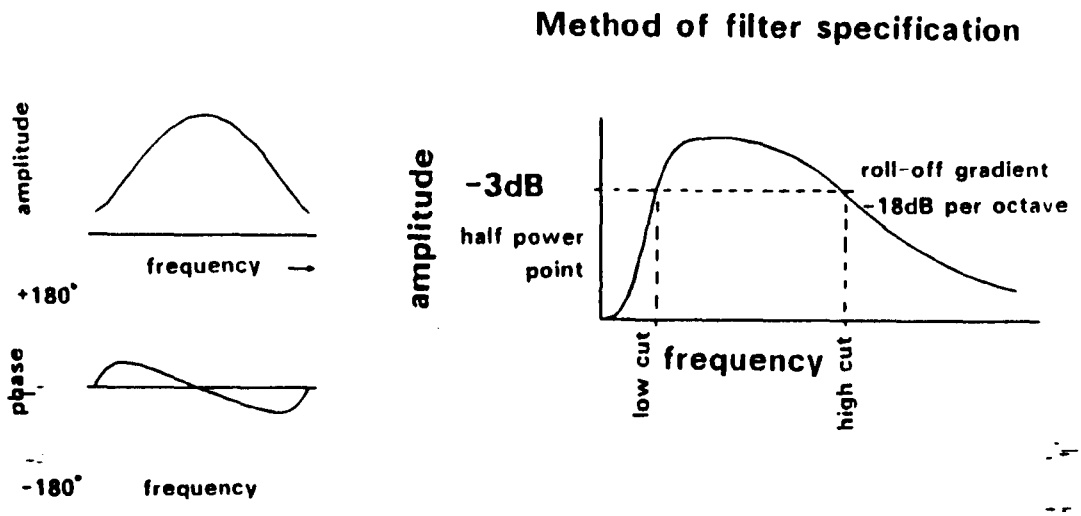

Minimum phase and Zero phase spectra

with no transmission loss. So it seemed reasonable (and more reliable) to model for comparison with their target signal.

3.2 Description of modelling

A seismogram trace is a time series recording the relative acoustic pressure at a given point on the earth's surface as it changes with time. Seismogram synthesis attempts to predict the response of the Earth to the passage of an acoustic disturbance. Modelling may be divided into the synthesis of such an input wavelet and the construction of the impulse reponse of the sediments, the so-called 'Earth filter'. Both these must be time series if their product is also to be one (fig. 3.2).

3.2.1 Wavelet synthesis - All real signals have a finite beginning and an energy envelope which is a maximum as near to this beginning as the frequency content will permit. Such minimum delay waveforms are also termed minimum phase (Silvia & Robinson, 1979; fig. 3.2a). The synthetic wavelet is the impulse response to a given band-limiting filter. A Butterworth filter was used, which gives a good approximation to a minimum delay wavelet. The quadrature functions for each wavelet are computed in the frequency domain initially, and transformed using a Fast Fourier Transform (FFT) routine to obtain the real part of the wavelet in the time domain. A corresponding zero-phase wavelet can also be constructed by taking the FFT of the amplitude spectrum alone (i.e. the phase spectrum is zero). Such a wavelet is used to model land surveys produced by the vibroseis cross correlation technique, and for comparison with other modelling which only use zero phase wave input.

Fig. 3.3a Model of sea floor reflection

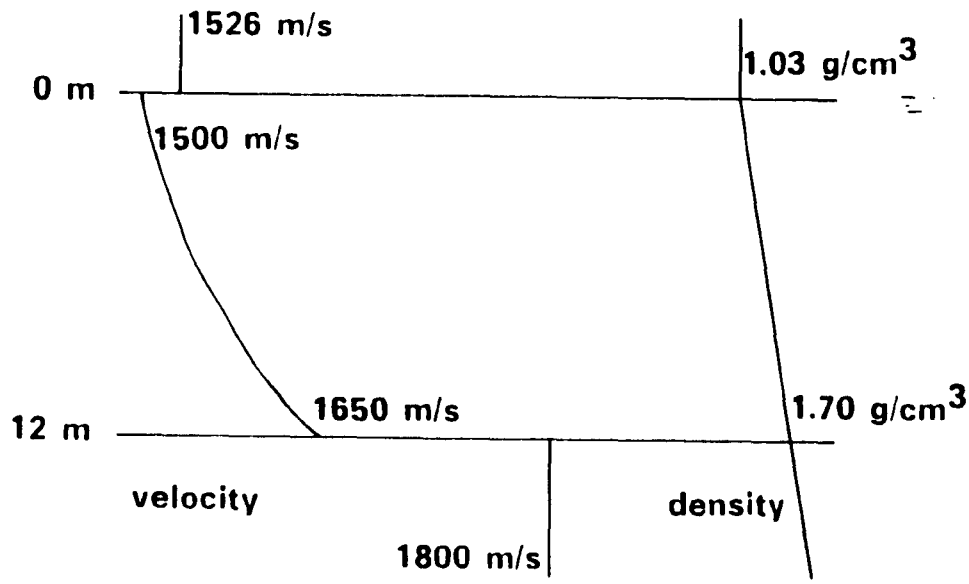

Upper sediment properties for Tufts Abyssal Plain

Fig. 3.3b Model of sea floor reflection, synthetic model

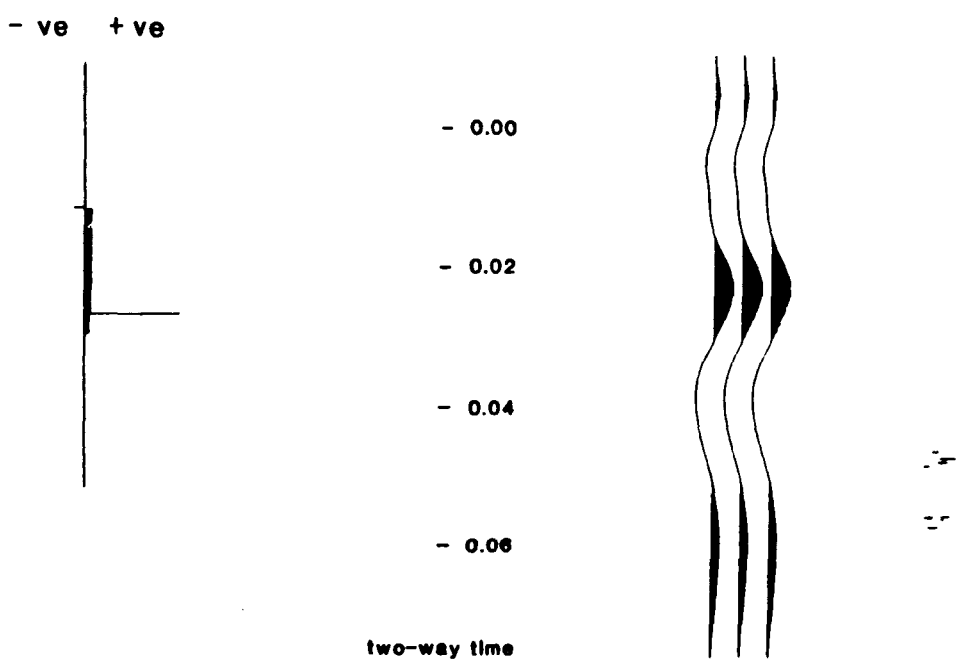

In terms of vertical resolution the high- and low-cut frequencies are the most important characteristics of a wavelet. They are varied to match those used in the processing of the profile to be modelled. The roll-off gradients are also important, particularly the high cut, and were adjusted to match the wavelet to the sea-bed reflection (fig. 3.2). This presumes that the sea-bed reflection is a simple step rise in acoustic impedance and, being much stronger than any near surface reflectors, its shape is that of the far field source wavelet. This is a simplification, but comparison of a more realistic model after Chapman et al. (1983) with the single spike shows the error is negligible (fig. 3.3). An interactive routine is used to examine the effects of variations of the synthesis parameters to be examined and compared. This is the routine WAVSYN and is described in Biart (1985).

The wavelet is represented in the computer as a time series representing the relative amplitude of acoustic pressure at equally spaced points in time. A time interval of one millisecond (.001 s) was used. This represents a Nyquist frequency of 500 Hz (or one sample every metre assuming a sonic velocity of 2 km/s).

3.2.2 Wire-line modelling - When acoustic energy is transmitted across the boundary between two media of different elastic properties a stress will result from the different compressibilities of the media (compressibility is the inverse of the bulk modulus). The propagation of the resultant strain through the first medium is termed the **reflected wave**. We may represent the acoustic character of the sediments by the variation of acoustic impedance with increasing depth. Acoustic impedance for a given substance is given by:

$$z_i = \rho_i \cdot v_i \qquad (3.1)$$

where z_i is impedance, ρ_i is density and v_i is velocity.

Petrophysical logs of interval transit time (Bore-hole compensated sonic log, BHC) and density (Formation density compensated, FDC) digitised at equivalent points equally spaced in depth would allow us to calculate a depth series for impedance. In order that we may carry out modelling in the time-domain we need to calculate impedance as a time series. By integrating the interval transit time of the sonic log, we may obtain the one way travel time to any depth. Interpolation, using cubic splines, is then carried out on the transit time series to produce a series of depths spaced at a constant transit time of half a millisecond (.0005 s). Doubling the integrated transit time then gives the two-way travel time to each depth (and a series with a sampling frequency of 500 Hz). The velocity and density depth series are interpolated, again by cubic splines at these depths. A time series of acoustic impedance is obtained by multiplying these velocity and density series (see Biart, 1985, for a description of the routine NNAG9).

The reflection coefficient, R, of a boundary between two media is given by the equation:

$$R = \frac{z_1 - z_0}{z_1 + z_0} \qquad (3.2)$$

From the impedance time series we can easily calculate the reflectivity time series. This is the acoustic impulse response of the sediments (ignoring multiples and transmission loss) or reflection coefficient log, RC log. Sea-bed multiples are not a problem in the deep sea, only intra-bed multiples need to be considered and these are usually of low amplitude. It might be closer to reality to take account of transmission loss and then equalise the trace, since the synthesised seismograms are intended to be compared with seismograms that have been trace equalised for display. The extra effort is no guarantee of improved results and only makes later interpretation more

Fig. 3.4 Comparison of 'Primaries only' and 'All order multiples' models

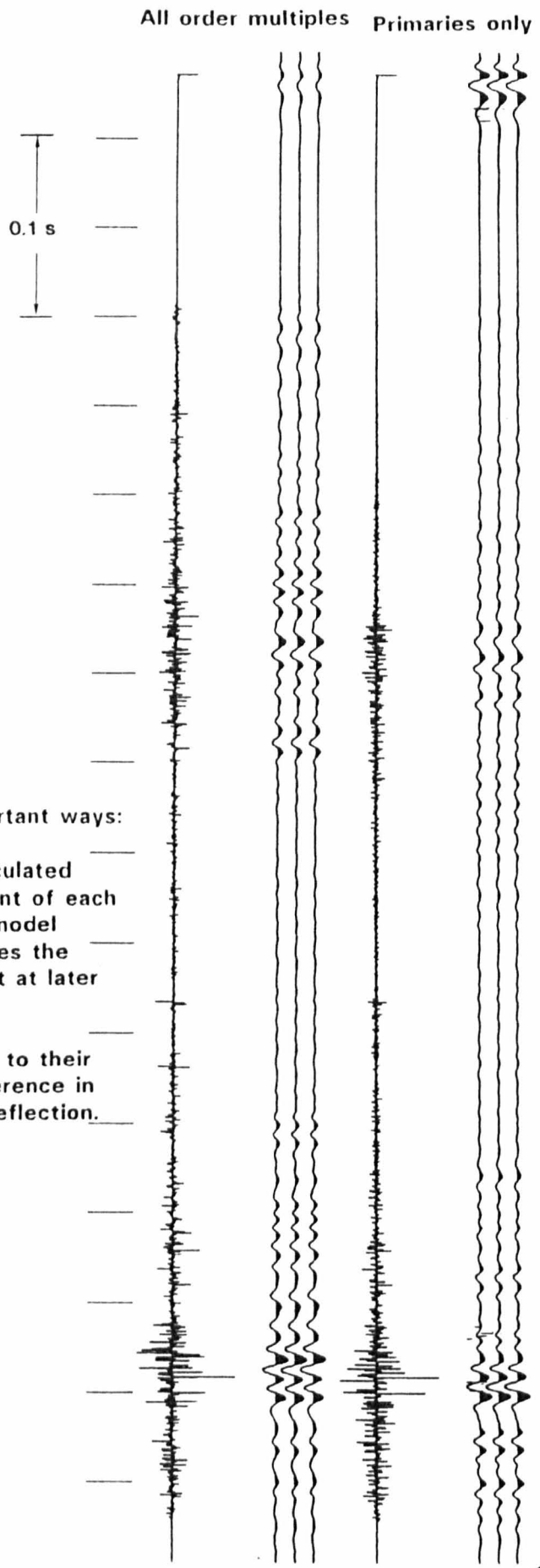

N.B.

The seismograms differ in two important ways:

1. The 'primaries only' model is calculated directly from the reflection coefficient of each 'boundary'. The 'all order multiples' model includes transmission loss. This causes the multiple energy to be more dominant at later arrivals.

2. The traces have been normalised to their maximum amplitude. Notice the difference in apparent amplitude of the sea bed reflection.

difficult. The effect of multiples was explored by comparing synthetic seismograms constructed using two RC logs, one containing primary reflections and the other containing all order multiples. The latter series is calculated by considering a two dimensional finite element grid consisting of the up- and down-going elements of wave energy for each layer of .0005 s transit time thickness. This routine calculates all order multiples from the RC log of primary reflections. (See Biart, 1985, for a description of routine MULT3; also, fig. 3.4). Transmission loss degrades the information in the lower parts of the sedimentary sequence, and for this reason intra-bed multiples are more important at later arrival times as the total reflected energy is less. Predictive deconvolution carried out during processing should remove multiples.

No single-bit DSDP holes are cased; the only casing used is that suspended beneath re-entry cones. The top of the hole drilled within unconsolidated sediments relies on the presence of the rotating drill-string and constant flushing with sea-water to keep it open. When a hole is logged, the drill string is raised as far as possible, but some portion must remain to support the hole. This may be up to 500 metres. Only the gamma-ray log can operate within the 'cased' section. For this reason, no-wireline data is available for modelling over this unlogged interval. This is important because without the sonic log the interval transit time between the sea-bed and the top of logging cannot be calculated. Consequently, any model produced from wire-line data has to be positioned on the time section by estimating the top-most interval velocity. The simplest algorithm is to assume that the first reading of the sonic log is the same as the overlying sediments. This probably over-estimates the top velocity. Alternatively, an average value from physical property measurement may be used. (See parameters of the wire-line modelling routine NNAG9 in

Biart, 1985). A more sophisticated method is to approximate the velocity function. Houtz (1973) investigated fitting higher order polynomials to sonobuoy data, but concluded that the improvement was negligible considering the accuracy of the data upon which it was based. Even though velocity inversions cannot be incorporated, the accuracy of reflectors' depths calculated from arrival times was about 15m. Houtz (1973) gives several velocity functions for various parts of the world's oceans and assumes they are of the form

$$V = a + b.t \qquad (3.3)$$

where V is instantaneous velocity

t is one-way travel time

a,b are coefficients

We may obtain two-way travel time to a given depth by integration with respect to t:

$$h = a.t + (b.t^2)/ 2 \qquad (3.4)$$

(See HOUTZ4, Biart, 1985).

3.2.3 Physical property modelling - The physical property measurements made aboard ship constitute an alternative data set for the construction of an RC log. If modelling is to be applied widely it must be use possible to use it alone, without the aid of wire-line data, which is only available at a minority of sites. Owing to the factors of pressure and temperature changes, and disturbance by drilling, the properties measured at surface cannot be used directly to describe the **in situ** properties. Another important difference is that the measurements are all made at discrete points rather than the more continuous data of wireline techniques. For these reasons, modelling with physical property data is less precise; the velocity and density measurements can be used to produce an impedance log directly with breaks taken between samples, but this contains too much noise to permit modelling. High frequency random noise caused by poor

Fig. 3.5 Physical property cross-plots

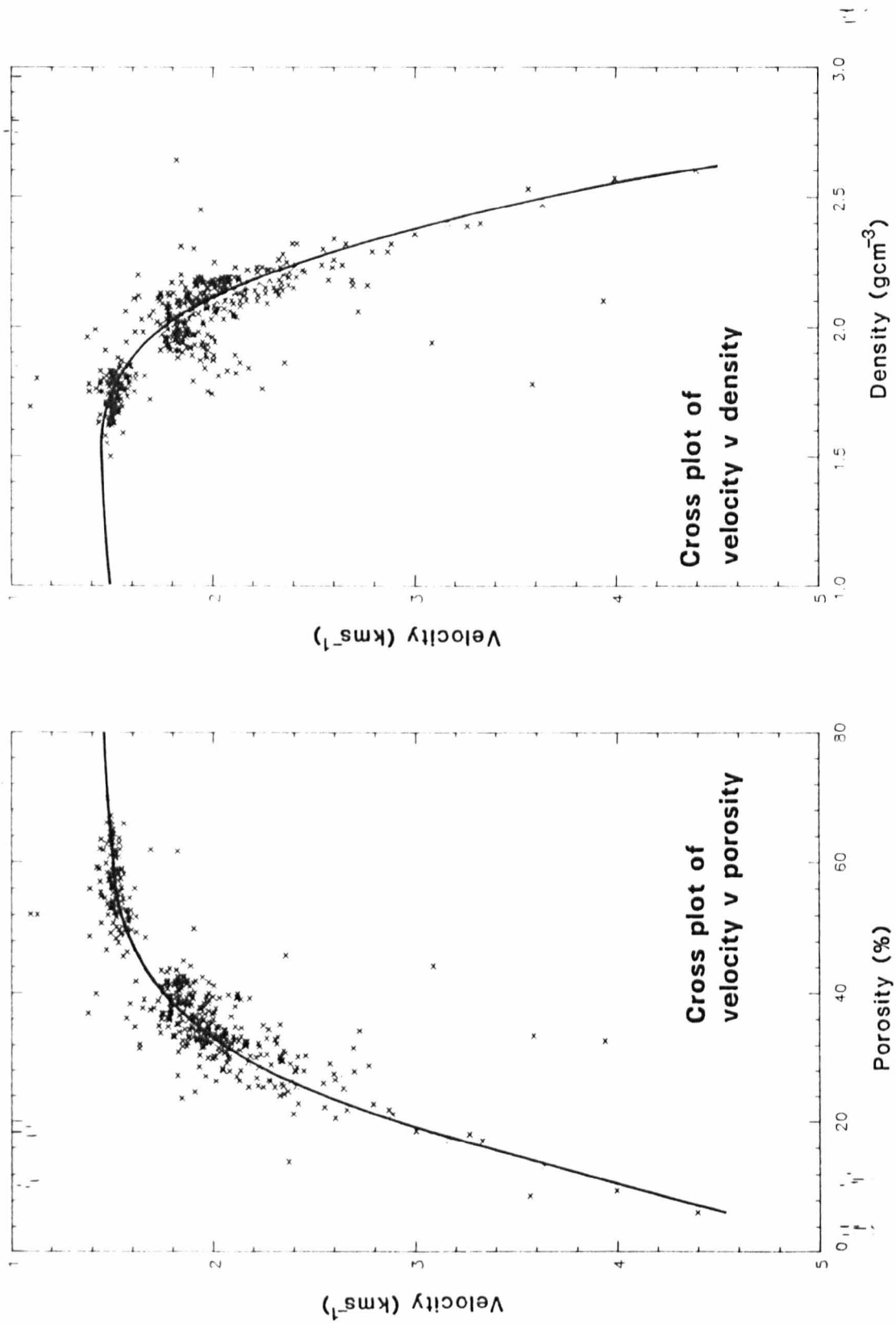

data quality degrades the final model but is removed by the filtering property of subsequent convolution. More important with respect to the frequency content is noise that is spatially biassed. This biassing results from the systematic sampling. Samples are taken at most once per section but usually once per core or less frequently. Minor lithologies tend to be measured more often than their proportion warrants. Further, the unrecovered material is likely to differ markedly from the recovered section: in ignoring this fact the averaged properties will err in a systematic way - overestimating velocity and thus compressing the time scale for further modelling. So minor lithologies are favoured, while those lithologies which fail to be recovered are accounted for inadequately.

'Breaks' in the physical properties were picked from graphs of each parameter measured against depth (depth-plots). To construct a model we need to calculate the polarity and amplitude of each break, and by means of a velocity function, calculate the two-way travel time to each break.

In general two models have been constructed based on the method of Shipley (1983) which allows an estimate of both the velocity function and the reflection coefficient at each break. Cross-plots of porosity versus vertical velocity and density versus vertical velocity are used to establish empirical functions relating these parameters at a particular site (fig. 3.5). Porosity is then corrected for rebound using the curve of Hamilton (1976) extrapolated in the manner of Shipley (1983) (fig. 2.2). The point of zero porosity rebound, corresponding to fully lithified sediment, will vary with each site. Velocity is calculated from corrected porosity and then this derived velocity is used to calculate a value for **in situ** density. The individual functions used to calculate velocity and density are

Fig. 3.6b Velocity functions used to calculate velocity from porosity

Cubic

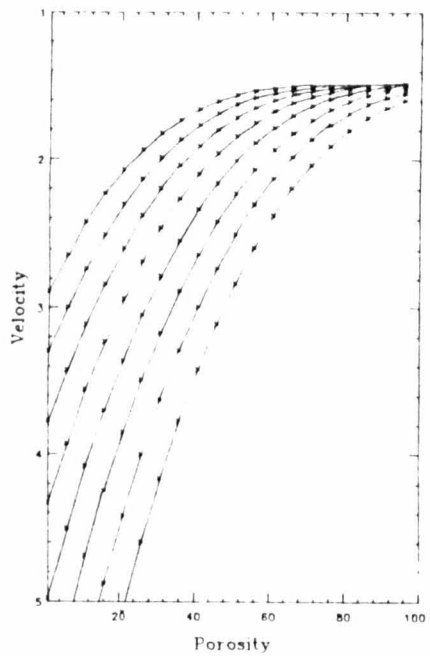

Quadratic

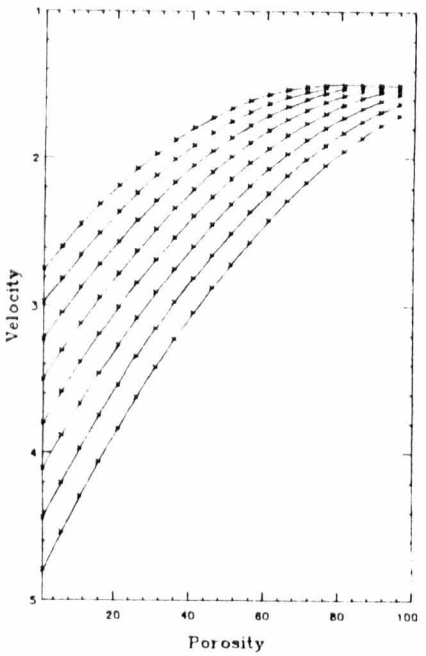

Quartic

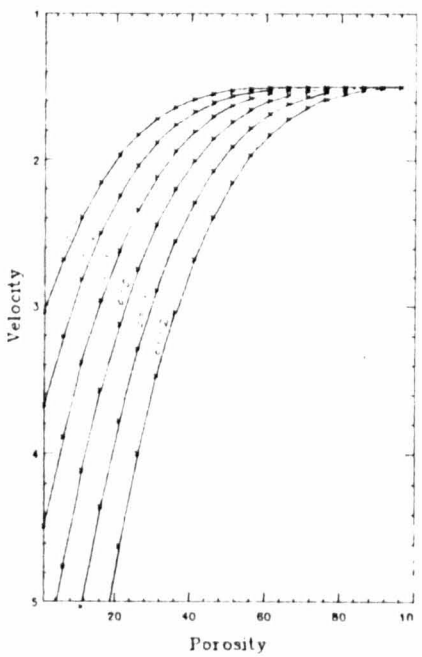

Quintic

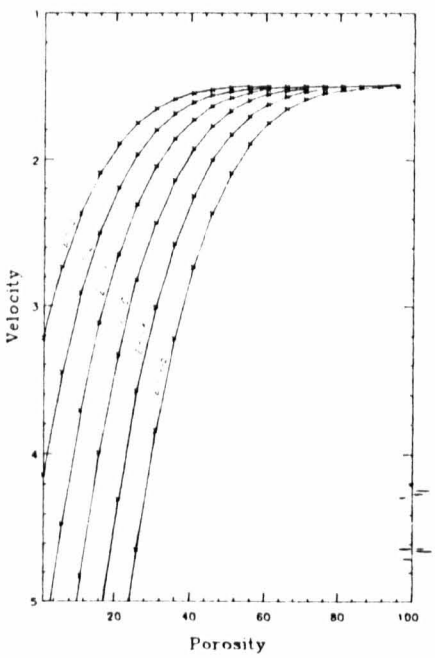

derived from cross-plots of porosity/velocity and velocity/density. Either a least-squares fit from the cross-plotted data is used (fig. 3.5) or,where the data are more scattered, the cross-plot is compared to a series of curves (fig. 3.6). The values of velocity and density are then averaged for each unit. A reflection coefficient for each boundary and two-way travel time is calculated from these averaged values. Shipley (1983) used the stratigraphy from the site report: generally, the number of layers produced in this way is insufficient for modelling. Litho-stratigraphic boundaries coincide with a physical property break and for this reason the physical property stratigraphy can be used alone. This approach assumes that the recovered section is an unbiassed sample of the whole column. As mentioned above it is quite possible that the unrecovered portion was lost just because it was different. Shipley (1983) suggests all unrecovered material may be assumed to have been argillaceous and lost by washing during drilling. This assumption is obviously an 'end-member' in the set of possible lithological columns, but as such gives an estimate of the maximum error in the method. The second model is calculated assuming that the unrecovered material is mud. The unrecovered part of each interval is assigned the velocity and density of argillaceous material calculated by cross-plotting with regard to lithology and calculating a relative value for the 'argillaceous' portion. The properties are then averaged over the whole interval and multiplied to give a mud-corrected acoustic impedance. In general, the transit time for a given layer is increased, and the reflection coefficients between layers are increased (low recovery sections being more affected by the correction). The latter model is termed the 'corrected physical properties model' and the former the 'direct physical properties model'. This terminology is should not be taken to imply a difference in accuracy.

Biart, 1985, presents a description and listing of routines used to perform physical properties modelling. These include:

DSDPFT - obtains raw data from DSDP data-bank for a particular site

PAIRVD - pairs velocity and density data for samples from similar depth, including data from several holes at the same site

XPLTDSDP- produces cross-plots of Velocity v Porosity and Velocity v Density for estimation of velocity and density functions to be used in subsequent modelling

PLOTDSDP- produces a plot of the different properties measured at one site. The physical property stratigraphy is drawn from this diagram.

SHIPLEY - constructs two reflection coefficient logs from physical property data averaged over the physical property stratigraphy. The models differ in the properties assumed for the unrecovered material.

SSM6 - produces a synthetic seismogram from wavelet data (input) and reflection coefficient logs (models).

3.3 Problems of modelling in the deep sea

The most obvious measurement datum for the comparison of core material and seismic records is the sea-bed, or sediment-water interface. However, the location of this surface is not simple on either the depth or time scales.

The most accurate measurement of travel-time to the sea-bed is given with the 3.5 kHz echo-sounder or Precision Depth Recorder, PDR. This

Fig. 3.7 Sound velocity in sea water versus depth

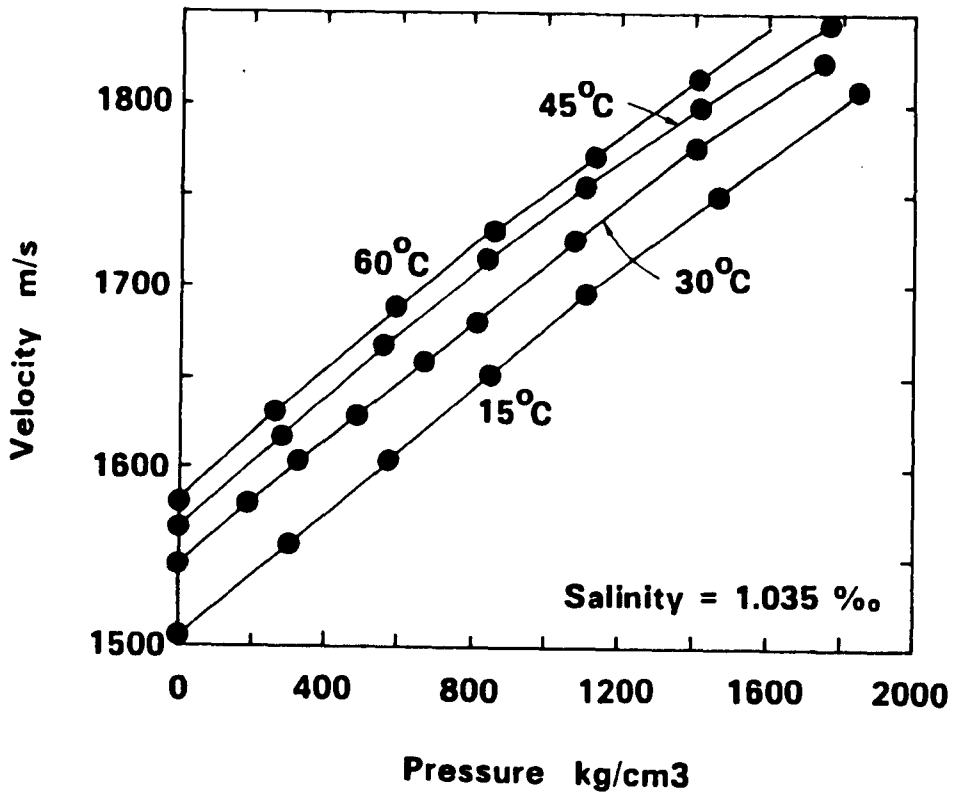

(after Carnevale and Litovitz, 1955)

accurately locates the shortest distance from the sea-surface to the sea-bed in seconds of travel-time (it assumes a horizontal sea-floor). During drilling the Glomar Challenger is seldom vertically above the site and may be off-set up to half a mile, but usually allowance is made during calculation of water depth. Conversion to depth is by means of a tabulated velocity function which is different for different regions throughout the world. Velocity of sound in water varies with salinity, temperature and pressure (Clarke, 1966; fig. 3.7). Thus the conversion to depth is only as accurate as the function used, which is itself an average of a number of measurements over a region (this function will also vary with the passage of ocean current storms.)

Matching the PDR travel time to seabed with the seismic record is not trivial. First, they can be easily mislocated - oceanic navigation is only reliable to within 100 metres (assuming satelite navigation). More importantly, the frequencies of acoustic imaging produce reflections from different apparent surfaces. The wavelength of a 3.5 kHz signal is 60 cm, while that of a 12-45 Hz signal filtered seismic source is 50 m. This difference of two orders of magnitude means that their respective rise-times will vary by about .060 s (TWT) assuming a velocity of 1.5 km/s.

The accurate measurement of depth by the drill string and/or wire-line is also open to error. The drill string is not necessarily vertical; a two degree deviation over 4.5 km amounts to a 2.7 m error. It should also hang in a catenary which further increases the error. For the purposes of drilling the weight on the cutting-bit is varied. This is achieved by telescoping the splined sections of the bottom-hole assembly, BHA. These sections may vary in length by more than 10 metres, although the actual amount should have been taken into

account when calculating the drill-string length. If the telescoping mechanism is damaged its length may not be accounted for correctly.

Another measure of the sea-bed depth is the depth at which it is 'felt' by the drill-string. This may be either a resistance to the weight of the BHA by surficial sediments or the level of sediment within a partially filled core. The 'bottom felt' criterion is tricky to operate as the top few metres of sediment (?10+ m) may return an acoustic reflection, but offer no resistance to the 200,000 lbs weight of the BHA. The first core taken is intended to be half-empty to show precisely where the sea-bed occurs relative to the drill-string. However, this method relies on penetrating sufficiently indurated sediment to plug the core-catcher and prevent loss of soupy sediment during the considerable journey to the surface. Wire-line measurement of the mud-line is invariably through the casing and only the gamma-ray log can be used. Frequently logging, which starts at the bottom of the hole, is stopped at the bottom of the 'casing' so that no direct measurement is possible.

The next most obvious datum for correlation is basement, although it is reached rather infrequently. Igneous basement returns a strong seismic signal, can be seen in the cores and is easily felt aboard ship due to the increase in drilling vibration it causes. Errors in sub-bottom depth can occur if the hole is not drilled vertically although the dip of the drill-string can be measured and correction made. Deviations in excess of 50 metres are quite possible in deep holes.

Obviously, it would be useful to make reliable correlations at both the sea-bed and basement as we would then have firm ties at each end of the sediment column. Although the precise velocity function between

these two data would remain uncertain, it would be better constrained.

An illustration of these problems can be found in the operations report for site 534 in the western North Atlantic:

"The bit stopped at a total depth of 5992.5 m rather than the previously established 6011.5 m - this was 19 m shallower than before re-entry. The most likely explanation is that a combination of changes in ship positioning relative to the cone and the bending of the pipe in the deep current changed the distance from the ship to the bottom of the hole.

"... sub-bottom depth and total depth are calculated based on the accumulation of drilled and cored intervals. Presumably these drilled and cored intervals were each in error, one more than the other, if the ship movements and the currents were moving the pipe in the water in some unknown way.

"As a result of this depth discrepancy, the depth error, which can be assigned to the recorded depth of a cored interval is +/- 2 per cent. This order of uncertainty in depth of core samples will affect the calculations based on intervals, such as sedimentation rates and seismic interval velocities."

3.4 Equality of reflectors

In order to study seismic stratigraphy we need to understand the methodology by which it is carried out and the purpose for which it is intended. Seismic surveying is a widely used tool for remotely determining the structure of the sub-surface and the interpreted profiles closely resemble the cross-sections of structural geology. Effort is required to remember the subtle implications of the time-section convention for display and the physics by which seismic

waves reveal the subsurface structure. The latter is essential to the correct interpretation of the profile. The deep sea offers an environment in which the processes affecting seismic stratigraphy are simpler and changes in them spatially less frequent. The correlation of individual reflectors with a particular sub-bottom depth is a fundamental problem. However, the value of reflectors lies in their ability to be traced laterally and so permit extrapolation of interpretation onto a regional scale.

In order to do this we should clarify how we equate reflectors. First we pre-suppose that a reflector is identifiable at two different localities. If these identifications are to be equated then they should possess at least one of three qualities:

1. be of the same age
2. be a product of the same sedimentary mechanism
3. be continuous between the two sites.

All of these deserve further qualification.

Age - Age is determined by palaeontology, magnetic stratigraphy or, more rarely, radio-isotopic dating. These methods have their own limits of resolution and palaeontology, the most common, is dependent on the sediments being fossiliferous. If reflectors are to be used to infer stratigraphy, it is necessary to decide whether a reflector is of precisely the same age everywhere (a time line) or whether it can be allowed to be diachronous within specified limits, such as the resolution of dating. (This question has already been addressed in part in section 1.3.)

Sedimentary mechanism - The contrast in acoustic impedance responsible for producing a reflection is the result of changes in the sedimentary fabric, which in turn is characteristic of the sedimentary history. In general, a reflector need not be limited to the strict

definition of Fitch (1976; see section 1.3) but may also be produced by the variation of the same parameter in a variety of different sediments, such as a pronounced porosity reduction. The term 'sedimentary mechanism' also covers those reflectors whose existence is due to the same event or process. If this is an unconformity it may be diachronous as explained earlier and, because it is produced by the impedance contrast between different suites of lithologies, it may change polarity laterally, yet still be considered a single reflector.

Continuity - Continuity is dependent on the resolution of the profiling system and ideally should be found in all surveys regardless of the number of channels and the frequency. However, some important reflectors are characterised by an increase in amplitude as other reflectors cross them, for example BSR's.

It is interesting to note that continuity is the most obvious criterion when present as proof of equality between localities, but it relies on profiles existing between localities. The other criteria permit equality to be established even if continuity is known to be broken. For example the sub-crop of horizon Beta is divided in two by the unconformity that produces horizon A^u (fig. 1.6).

3.5 Appraisal of modelling techniques

No correction is applied to wire-line data, which is taken to represent the **in situ** properties. In contrast the physical property model assumes that measurements made at the surface can be corrected to **in situ** conditions. This assumption has been tested at site 406.

Table 3.1 - Correlation of well-log and core depth, site 406.

depth sub-btm	Well log data Vel	n	Den	n	Phys props Vel	Den	n	depth sub-datum
461-480	2.174	58	1.90	157	2.033	1.96	3	3430-3449
480-518	2.096	117	1.88	294	2.044	1.97	7	3449-3487
518-546	2.075	99	1.87	204	2.077	1.99	6	3487-3515
546-556	2.097	49	1.83	62	2.118	2.01	3	3515-3525
556-603	1.910	222	1.73	282	2.214	2.07	2	3525-3572
603-620	1.890	110	1.70	96	2.142	2.03	6	3572-3589
620-625	2.049	22	1.67	25	2.127	2.02	2	3589-3594
625-635	2.147	49	1.81	44	2.138	2.02	3	3594-3604
635-643	2.311	42	1.90	41	2.086	1.99	3	3604-3612
643-670	2.396	173	1.95	150	2.400	2.16	5	3612-3636
670-679	2.532	47	2.011	57	2.456	2.19	3	3636-3648
679-694	2.813	109	2.12	116	2.641	2.28	5	3648-3663
694-711	2.651	157	2.11	153	2.716	2.31	6	3663-3680
711-727	2.663	130	2.11	112	3.015	2.44	4	3680-3696
727-733	3.057	21	2.21	39	2.983	2.43	3	3696-3702
733-755	2.849	155	2.21	147	2.983	2.43	1	3702-3724
755-765	2.884	51	2.23	66	2.620	2.27	4	3724-3734
765-784	2.288	128	2.01	150	2.294	2.10	5	3734-3753
784-803	1.975	115	1.92	121	2.297	2.11	4	3753-3772

* Based on an assumed sea-floor depth of 2890m below mean sea-level.
* n = the no. of data for interval from which mean value is calculated.

(Subsequent study shows an even closer fit if a depth of 2901m is used).

Fig. 3.8 Comparison of properties measured in situ (by wire-line) and laboratory measurements, site 406

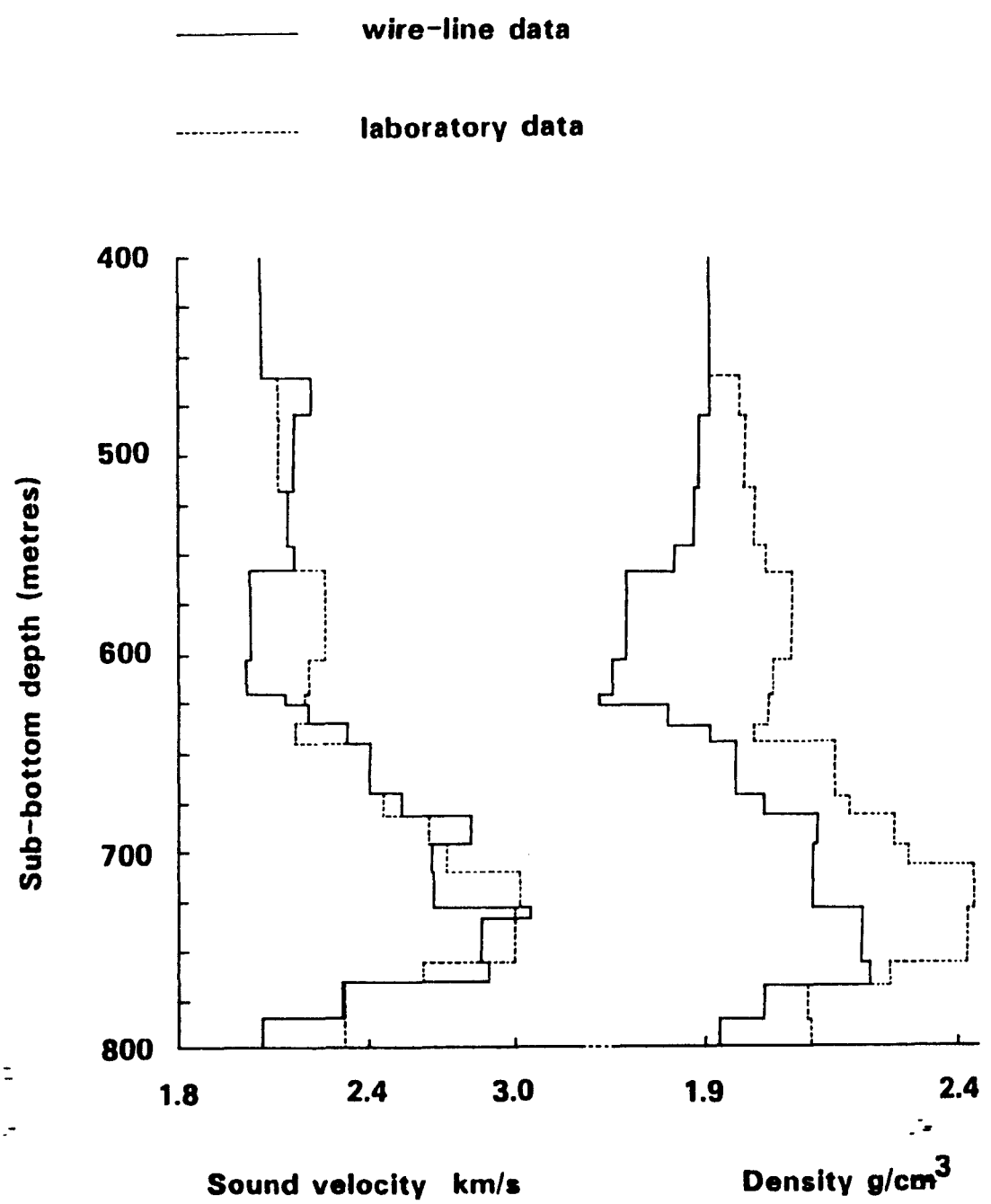

3.5.1 Comparison of corrected surface measurement and in situ measurement.

Site 406 on the Rockall Plateau provides a suitable case study at which to test the above assumption, as wire-line data recovered at the site is of the highest quality, and the physical properties have been well sampled over the continuously cored interval between 450 m and 800 m (total depth).

The number of data available from the two methods of measurement is in strong contrast: the well logs are very finely digitised, producing about 4000 datum points for bulk density and transit time, while only 80 measurements are available from laboratory measurement. (No information is available on the stacking velocities used in processing the profile which would serve as an additional comparison.)

The mean velocities and densities are calculated by averaging the measurements between two depths which bound a given unit. For the wire-line each measurement is weighted according to the depth below the preceeding measurement. This weighting filters cycle-skipping noise as well as compensating for series which are not regularly sampled in depth. They are listed in table 3.1 and displayed in figure 3.8.

A seafloor depth of 2969 metres was used in modelling the well-log data. This depth is the mean of the two elevations-above-permanent-datum given on the sonic and density logs (BHC datum=-3027 m, and FDC datum=-2911 m). However, when compared with the physical properties data a large discrepancy with the sub-bottom depths was revealed. The comparison was repeated assuming a seabed depth of 2901 metres with much improved results.

The velocity data is surprisingly similar between the two methods. The largest discepancy is between 556 m and 620 m which coincides with litho unit 3, which comprised diatomaceous nannofossil and calcareous chalk and calcareous diatomite. Core recovery for this interval is very poor (only 15% between 556 m and 608 m), so the error could be because of insufficient physical property data to accurately characterise the **in situ** properties, or the hole conditions degraded the performance of the logging tools.

The density data is not as closely related. The values run roughly parallel (again with discrepancy between 556 m and 620 m) but the corrected laboratory data considerably overestimate all values.

When cross-plotted the velocity and density data are too scattered to allow a simple quadratic function to describe their inter-relationship adequately (c.f. fig. 3.5). Clearly the velocity versus porosity function was good enough. This supports the comment by Mayer (1979) that density is more important for impedance variation than velocity, because it is more variable. However, the consistency of the error means that only the absolute value of impedance is overestimated. The difference between values used to calculate a reflection coefficient log is of more or less the correct magnitude (a different density/ velocity function would also give better results.) Also, the small error in the velocity data (including its correction) means that the transit times between breaks is fairly accurate. This is important for reconstructing the velocity function which ultimately is responsible for spacing the individual reflection events.

3.5.2 Modelling at site 406

The validity of the assumptions involved in constructing the

Fig. 3.9 Wire-line model, site 406

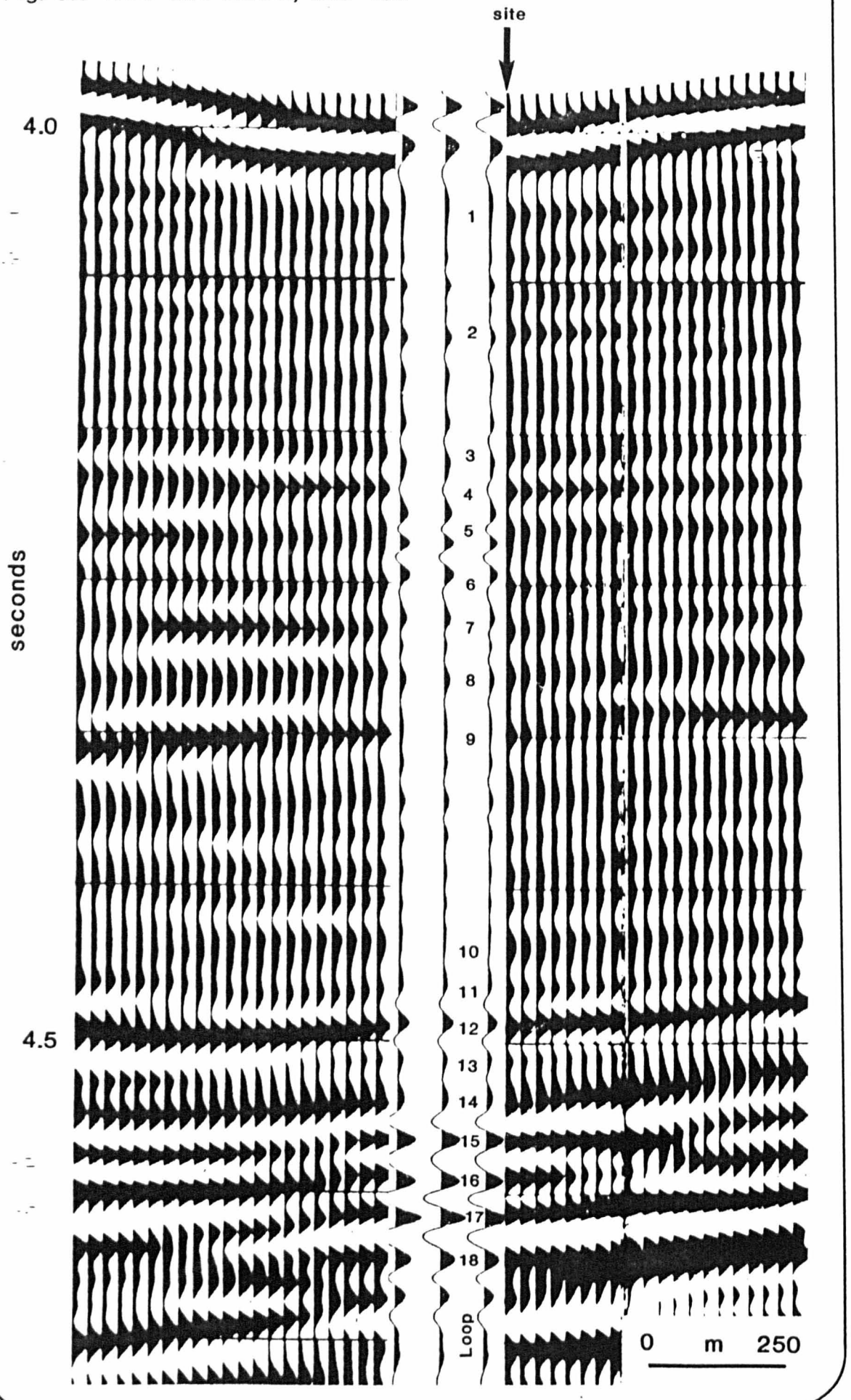

Fig. 3.10 Corrected model, site 406

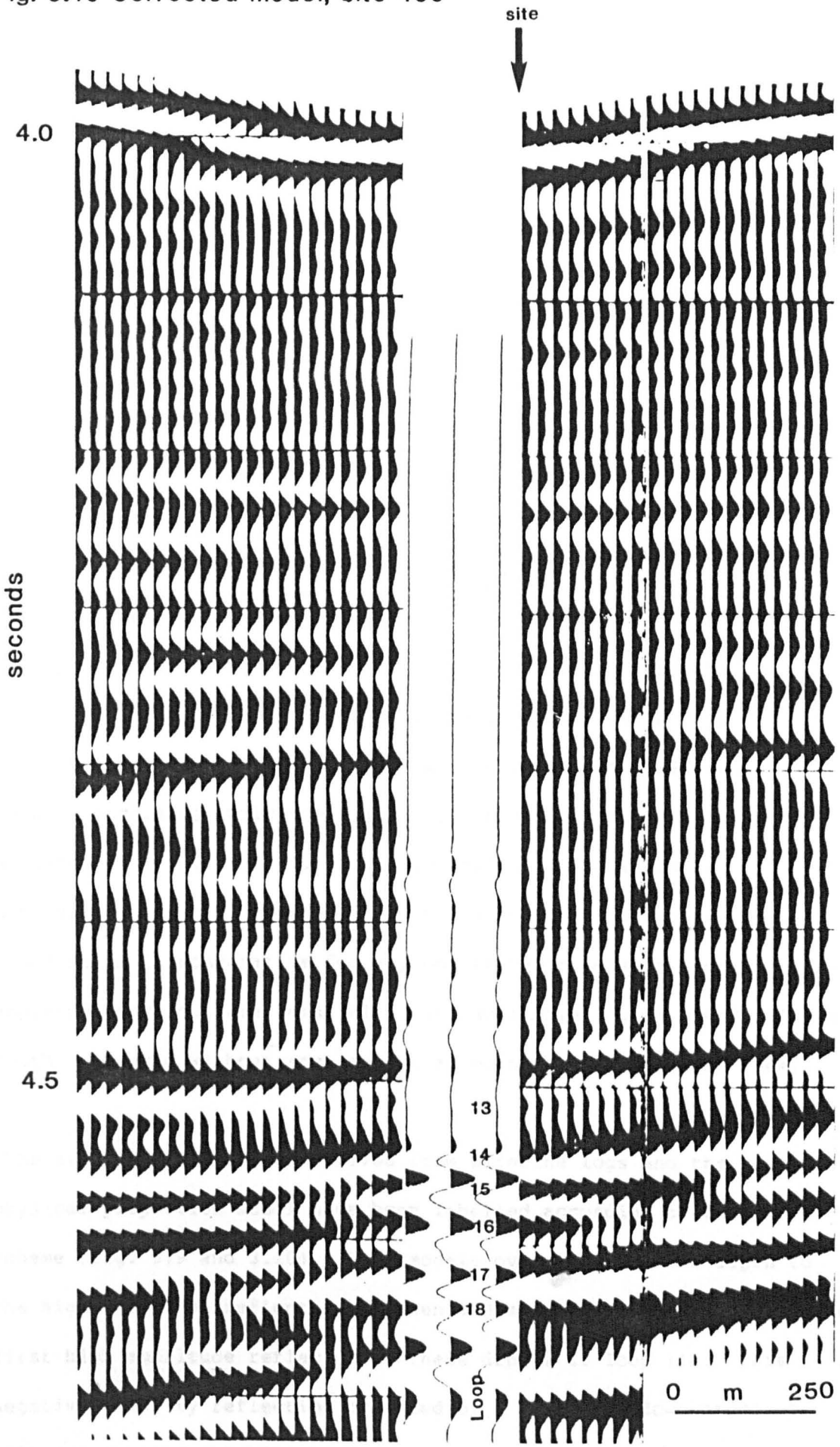

reflection coefficient time series will ultimately govern whether or not the model is a good one. For this reason the performance of the two schemes has been studied at site 406 for which high quality data is available.

Three models were constructed, one from the wire-line data, and two from the physical properties data. The same wavelet input has been used for models from the same site. The corrected physical properties model is the most accurate as discussed in section 3.5.1 and will be compared with the wire-line model.

The seismic section is composed of traces with the variable area, wiggle trace display system. Horizontal alignment of black peaks or white troughs constitute 'reflectors'. Each excursion from the zero line of each trace, whether positive or negative is termed a LOOP. Thus loops may be either black or white according to their polarity. For convenience, the loops are numbered from the sea-bed downwards (arabic numerals). Only the black loops above a given (subjective) amplitude threshold are numbered. Succeeding white loops are given the same value with the letter 'a' to denote inverted polarity. Amplitude description is comparative for any one trace or seismic section. True amplitude sections are, generally, not available. 'Low', 'medium' and 'high' are used without any particular bounds to distinguish them.

The synthetic seismogram derived from wireline logs and the corrected physical properties model have been labelled according to the above scheme (fig. 3.9 and 3.10). Both models over-estimate the depth to the high amplitude reflectors between 450 m and 800 m sub-bottom. The first high amplitude reflector at these depths is loop 11a. This is a negative polarity reflection produced by a decrease (downwards) of bulk density and velocity at 3459 m logging depth. The change on the

Fig. 3.11 Detail from wire-line logs at loop 11a, site 406

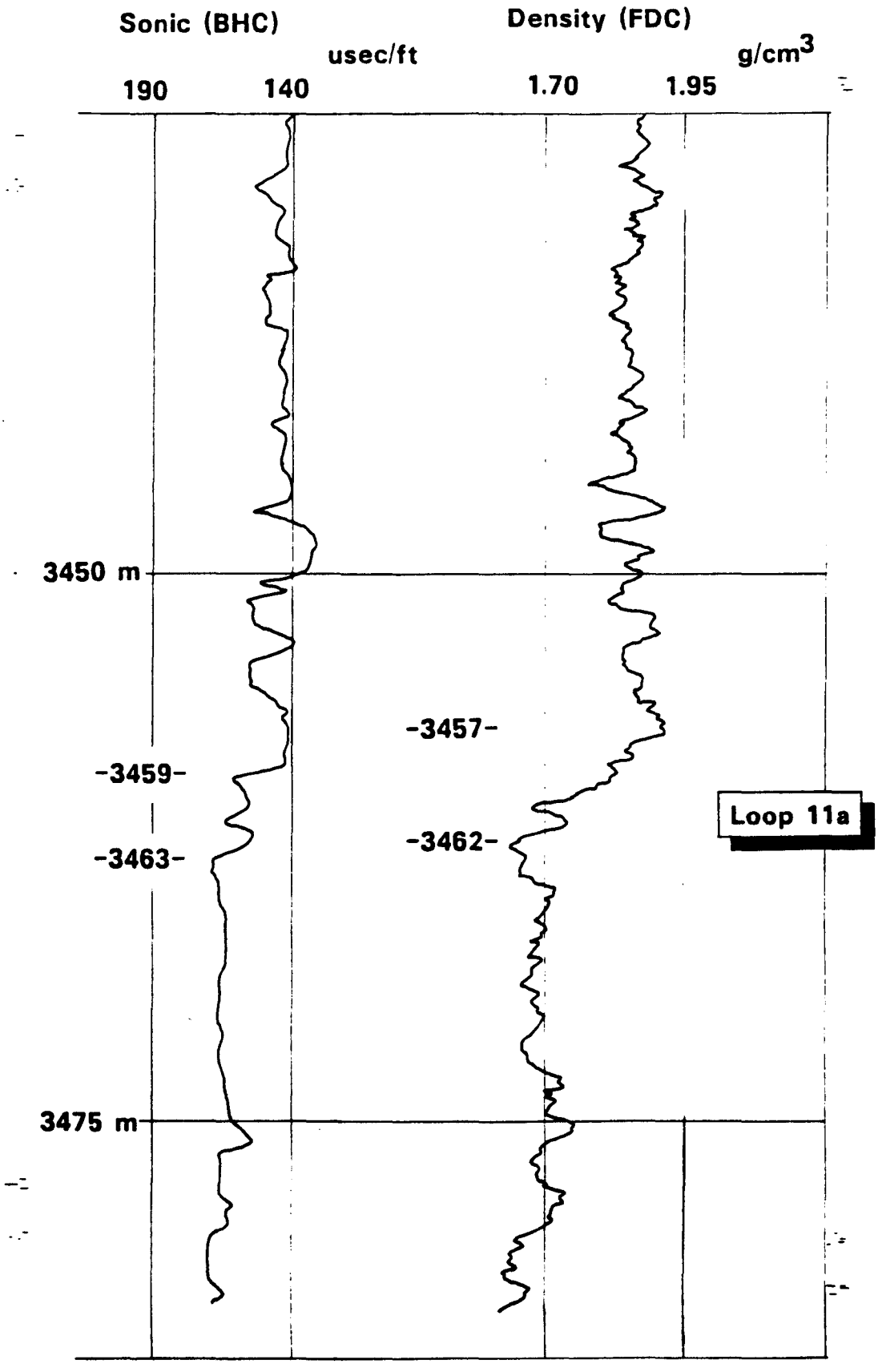

Fig. 3.12 Site survey profile IPOD76-2, site 406

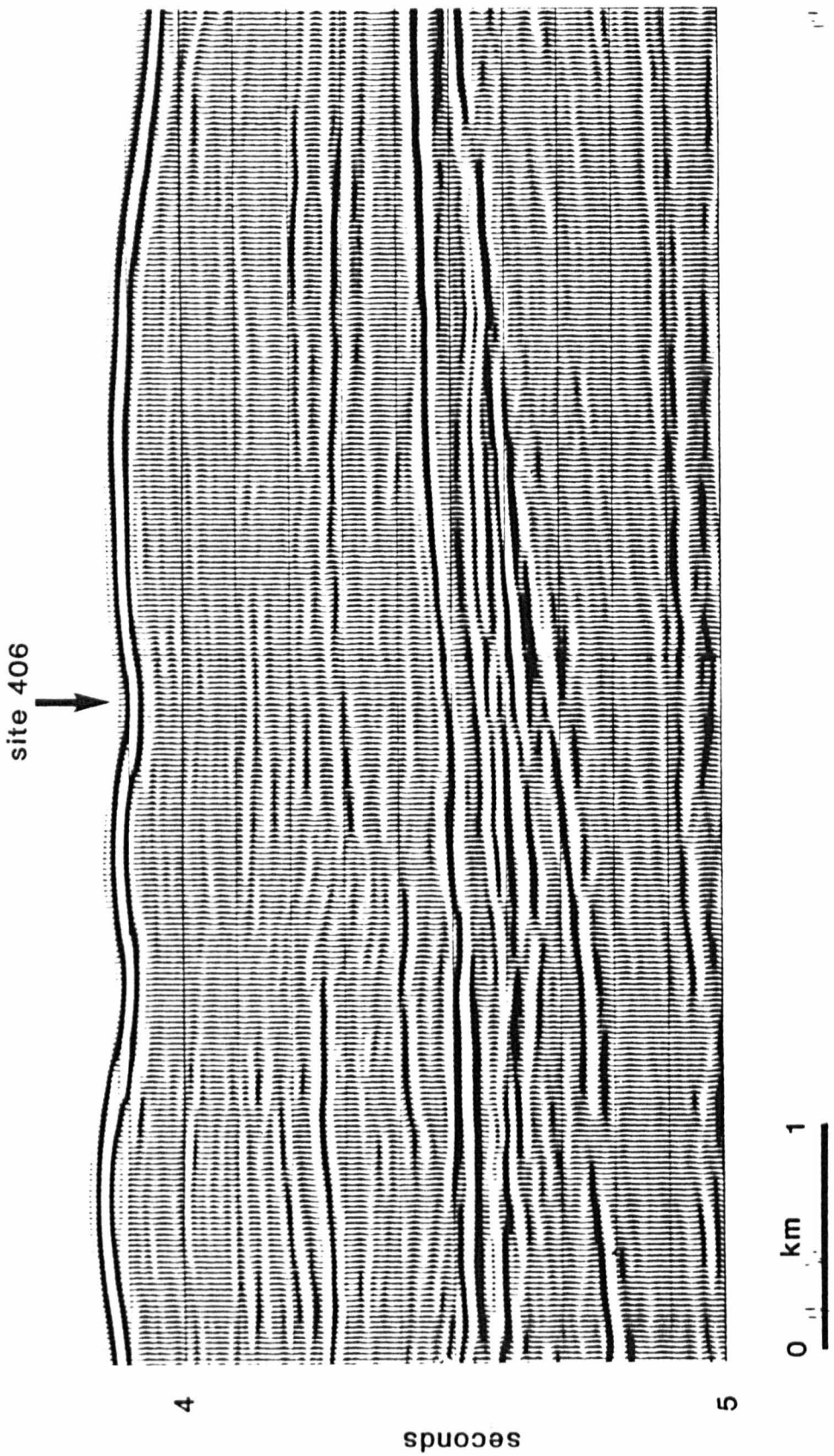

sonic log is most abrupt at 3459 m with a further negative break at 3463 m. The blocked nature of the sonic log indicates interbedding of different lithologies (see fig. 3.11). The change in bulk density is much more gradual, occurring between 3457 m and 3462 m. It is possible that the logging depths on sonic (BHC) and density (FDC) are not exact - the FDC depth being some two metres shallower. The interbedding is also seen on the curve (fig. 3.11) (this curve shows the correction for mud cake and hole rugosity, which in turn are related to porosity variation.) There is also a large peak (1 metre at apex) on the natural gamma log. Using the revised sea-bed depth of 2901 m from the previous study, the equivalent sub-bottom depth is 558-573 m. The revised DSB gives a better match between the models and is used in subsequent calculations.

Loop 11a of the wire-line synthetic matches a surface dividing on-lapping reflectors above and sub-parallel reflections below, i.e. an unconformity (fig. 3.12). The closest lithological boundary is at 557.5 m between unit 2 and unit 3 (406-24-1/406-24-2). It is interesting to note that core 23 is interpreted as a transitional facies between the two units exhibiting interbeds of siliceous chalk within the nannofossil chalk of unit 2. Unit 3 is diatom-, nanno- and calcareous chalk. Biostratigraphically, core 24 is NN4 and NN5 (nanno-zones) except for the bottom 18cms which is NN1. There is a tentative unconformity marked on the initial core desciptions, page 203, and, on page 229 of the initial report, 549 m is shown as the middle Miocene /lower Miocene boundary (N8-9 above N1-6 i.e. no N7: foram zones).

The physical properties model is in error at this horizon (11a). The very low core recovery provides insufficient data for the algorithm. The values of sonic velocity and density for the preceeding layer have

to be extrapolated downwards: the interbedded formation at the base of unit 2 probably contributes a minor amount of positive reflected energy to loop 11 above. The mud correction (in theory) should compensate for this. The actual correction assumes the unrecovered portion to have a velocity and density 13% lower than the recovered material. The in situ measurements (wireline) show that velocities in unit 3 are 18% lower than unit 2. Thus most of the 'corrected' density values are slightly too high.

The apparent match of loops 11-12 on the physical properties model is only good fortune: the higher interval velocity calculated by the model reduces the spacing (in time) of the 556 m and 643 m events such that the reversed polarity reflection of the model is 180 degrees out of phase with that of the section (i.e. white against white looks like a match), (fig. 3.10).

Loops 12 and 12a are trailing energy from loop 11a. Loop 13 is of low amplitude and is related to an increase in the 'roughness' of the acoustic impedance log below 3485 m (ca. 584 m sub-bottom). This roughness is similar to that attributed to interbedding at the base of unit 2. No further comment can be made as low recovery prevents accurate physical property modelling.

Loop 14 is caused by a (downward) increase in the acoustic impedance between 3511 m and 3514 m (density log) and 3512 m - 3513 m (sonic log), (there is no disparity between log depths.) A further rise at 3522-24m (density) and 3519-23 (sonic) add to the main event. Using the adjusted DSB (2901m) gives a correlation at 611 m and at 621 m sub-bottom.

The base of unit 3 is at 617.5 m where calcareous diatomite overlies

Fig. 3.13 Detail from wire-line logs at loop 15, site 406

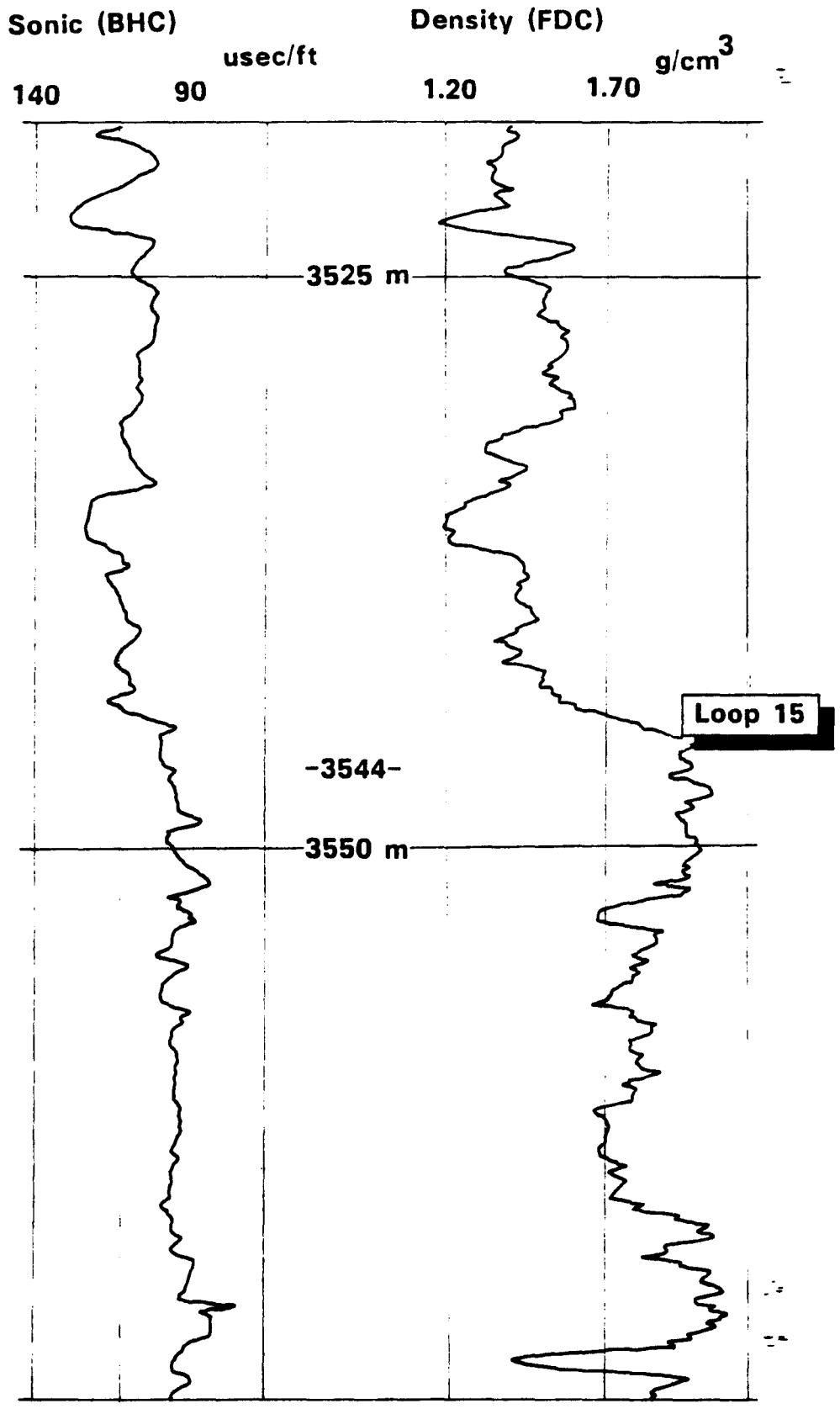

calcareous chalk and siliceous chalk. Kagami (1979) does not note any diagenetic change in the silica state until much lower (ca. 710 m), but this lithological unit boundary would appear to represent an important change in sedimentology (either primary or diagenetic). Physical property breaks were drawn at 620 m, 625 m and 635 m. These were made in an attempt to model the interbedding, which from the physical properties data appears to have a (spatial) wavelength on the order of 10 m (although this may be an artefact of sampling). The uppermost event (620 m) is most closely related to the lithological boundary (unit 3/ unit 4). No hiatus or unconformity is detected at this level. The poor data quality, which affects physical property modelling of loop 13, also affects the shape of loop 14.

Loop 14a corresponds to a small reduction in impedance at 3534 m (sonic) or 633 m sub-bottom. As explained, much of the energy may be attributed to the tail of earlier reflections. The polarity suggests that this minor horizon equates with the interbedded horizon at 635 m. This is the top of a siliceous calcareous chalk within unit 4A, and about 2.5 m thick although low recovery means that this is a minimum thickness (core 32).

Loop 15 correlates with a rise in impedance between 3546 m and 3551 m (density log) and 3544 m (sonic log), which gives 645 m sub-bottom (fig. 3.13). Again, this is within subunit 4A, which comprises interbedded calcareous ansd siliceous chalks. The sonic log shows one rise and remains fairly constant thereafter, while the density log shows more variation (fig. 3.13). Density rises to 2.1 g/cm^3 at 3550 m and then drops to 2.0 g/cm^3 some 7 m lower. Rigidity is affected by particle roughness and cementation (amongst other things): generally, siliceous tests are rougher; variation in chemical composition may cause enhanced diagenesis. The constancy of velocity

Fig. 3.14 Detail from wire-line logs at loops 16-17, site 406

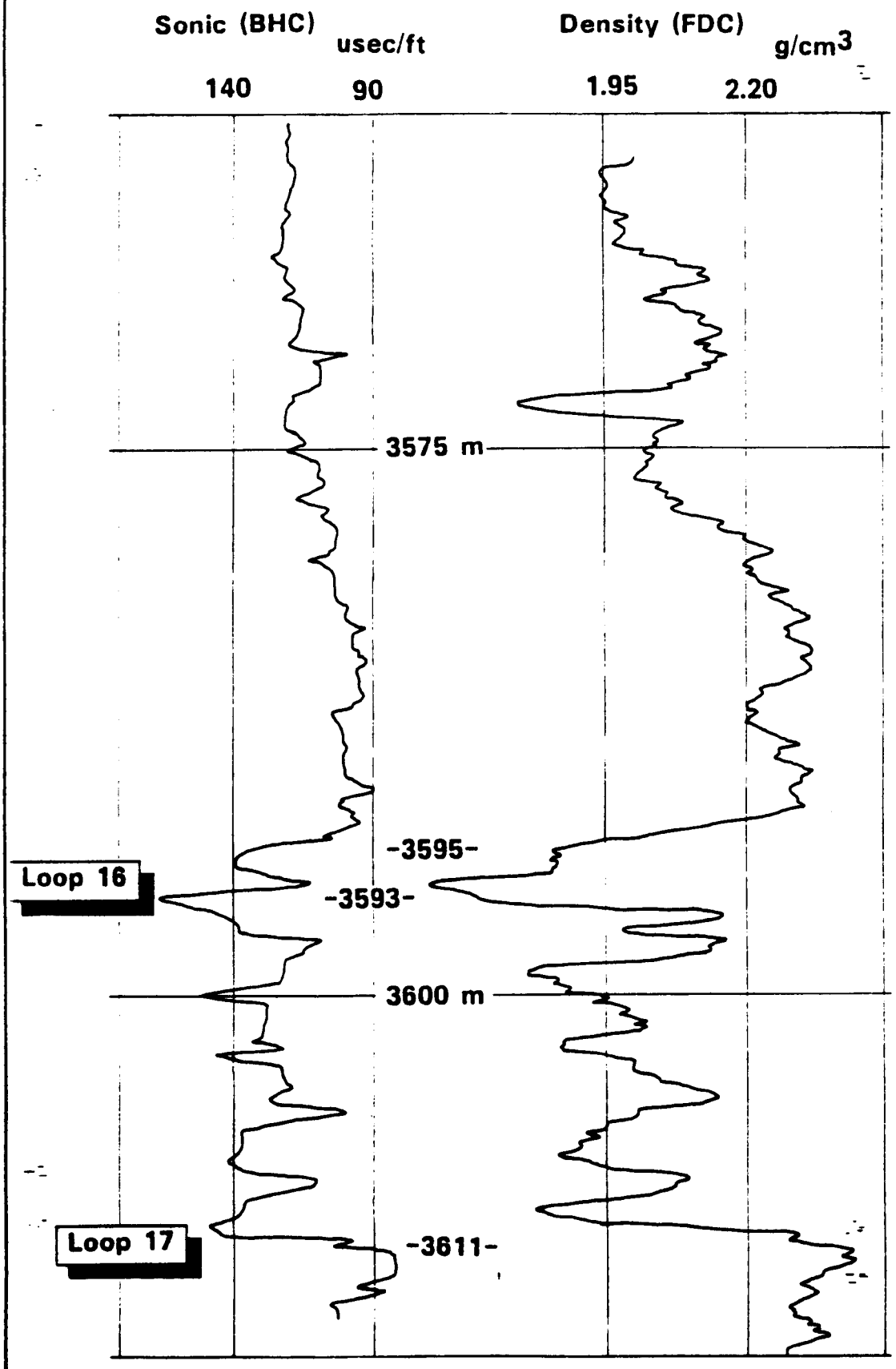

indicates that minor reductions in density, caused by increases in silica content, are matched by increases in rigidity and consequently velocity.

Comparison of the logs with the plots of physical properties variation suggests an equivalence of this horizon with 643 m. This is the depth at which porosity falls sharply, so it is possibly a diagenetic horizon within the interbedded unit. Such a change might be expected to cause a lithological unit boundary to be defined, but experience at site 605 shows this need not be the case. However, the fact remains that there is sufficient physical change to produce a reflection. Opal-CT is not recorded as occurring until lower in the section (Kagami, 1979, coarse fraction study only). Elsewhere, site 612, such a porosity change was related to the mobilisation of silica as it changed mineral phase in response to diagenesis (Wilkens, pers. comm.). Diatoms are present at this level - the first chert layer recovered is only 20 m lower. There is a strong inference of an horizon A^C-type of reflector. However, the age of the diatom layer is Middle Oligocene. The cherts here are all middle Oligocene and form above the unconformity with Upper Eocene (see below). Horizon A^C is a middle Eocene reflector.

Loop 16 equates with a general increase in acoustic impedance between 3566 m and 3581 m (density log) and 3566 m and 3584 m (sonic), 665-680 m sub-bottom (fig. 3.14). The physical property model attributes loop 16 to a number of positive polarity events between 670 m and 685 m. There is an unconformity between Oligocene and Upper Eocene at 679 m sub-bottom. The seismic profile is not easy to interpret accurately between 0.6 s and 0.8 s sub-bottom owing to the number of high amplitude reflections which return from a generally thinning sequence (fig. 3.9, 3.10, 3.13). Truncation of individual

reflectors can be due to either erosion or lateral changes in the interference pattern. However, loop 16 at site 406 does appear to be on a surface of truncation, which itself onlaps 1500 m up dip. Lithologically, this is the top of unit 4 (670 m), which is characterised by slumped interbeds of foraminiferal nannofossil chalk. Possibly, the slumping is what is visible on the seismic profile, which might be expected to be more confused.

Loop 16a is produced by a large drop in acoustic impedance between 3592-3596 m (FDC) and 3593-3595 m (BHC) (fig. 3.14), which is eqivalent to 693 m sub-bottom. Good recovery on core 38 (689-698.5 m) allows excellent correlation of cores and logs - 693 m equates with the appearance (downwards) of diatom mudstone and calcareous chalk with porcellanite (see page 247, initial report). The match between the physical properties model and the profile is not as close as the preceeding loops. This can be explained by the mud correction algorithm which is less accurate for the diatomaceous sediments than the calcareous. This depth, 689 m, is recognised as the top of a layer of amorphous silica. This represents something of a diagenetic inversion and is explicable in terms of a variation in the saturation of bottom water with respect to silica: high saturation causing precipitation of opal-CT, while a lower saturation allows siliceous organisms to flourish enriching the sediment in amorphous silica (Latouche and Maillet, 1979).

Loop 17 is produced by the positive impedance jump at the base of this diatom-rich formation, at 3611 m (sonic and density logs) (fig. 3.14) or 711 m sub-bottom. This is in the middle of core 40, which exhibits a chert based diatom rich unit overlying a dolomitic limestone. Kagami (1979) recognises the appearance of opal-CT at this depth from examination of the coarse fraction, while Latouche and

Maillet (1979) recognise this as the top of the opal-CT layer - there being no changes in the state of silica below this depth. This is the top of subunit 4C. Porosity is now much reduced - we are below the chalk to limestone transition. The age is Upper Eocene.

Loops 17a and 18 are not related to particular discontinuities in the acoustic impedance, but are explicable in terms of tail-end energy of higher reflectors. Their two-way travel time (on the profile) can, however, be given a correlative depth (in meters):

Loop 17a - 3633 m - 732 m

Loop 18 - 3646 m - 745 m

They are both within subunit 4C, which is homogeneous marly limestone and shows signs of having slumped. Cores 43 and 44 show very poor recovery (736.5-755.5 m). The physical properties above and below this interval are different so a break is valid, but probably only one and not with an amplitude of the order of those modelled at 733 m and 755 m. Nevertheless, loops 17a and 18 do match the seismic profile surprisingly well.

Loop 18a is correlated with a decrease in acoustic impedance which occurs at 3664 m (sonic), while on the density log the biggest drop is at 3659 m, but continues to fall unevenly down to 3680 m. The delineation of a break at 3664 m is supported by gamma and caliper logs: it is equivalent to 763 m, which is the boundary between unit 4 and unit 5, marly limestone (slumped) overlying marly chalk with calcareous claystone (note the diagenetic inversion). This depth, 765 m, is also an unconformity between Middle and Lower Eocene. The seismic section exhibits a surface with onlapping reflectors above, which could be chosen either at loop 18a or loop 19. The unconformity is obviously of negative polarity which favours loop 18a.

Loops 19 and 19a are tail end energy from the unconformity above.

The flatness of loop 20 is partly due to insufficient data (as we have now reached total depth) and partly that a slight rise in density (3695 m or 794 m sub-bottom) cancels the tail of higher reflections. It is only a minor impedance change, but the wireline model compares reasonably well with the section. Data is insufficient to allow the physical property model to work - loop 20 is purely energy from above. The density rise is due to a minor change from marly nannofossil chalk to marly calcareous chalk (both with calcareous claystone).

The two modelling schemes have permitted detailed correlation to be made between core material and seismic section. There is no doubt about the correlation - this in itself is unusual. The site has provided an invaluable test hole at which to examine the performance of the physical property modelling scheme. Despite obvious errors in some of the assumptions necessary to the working of the algorithm (e.g. the density correction) it appears to be robust enough to work well given closely spaced physical property data from continuously cored intervals. It can be improved following the first run as obvious non-alignments can be corrected; porosity does not always break in the same direction as the more important parameters of velocity and density, nor are the actual breaks necessarily of the correct magnitude. However, the timing is the most important factor for accurate modelling as demonstrated by the phase/polarity problem at loop 12 and this is not changed. The overall accuracy is very encouraging, but caution is still necessary before accepting a particular model. All reflectors whether black or white loops have proved to be due to lithological variation - but not necessarily particularly marked. That is to say that minor changes such as porosity reduction or a change in carbonate content appear perfectly

adequate for the formation of reflectors.

Outstanding in this respect is the correlation of opal-CT occurrence with units of high impedance. It is not clear from studies at the site whether this is a product of diagenesis or a primary sedimentary feature. Latouche and Maillet, 1979, attribute all occurrence of opal-CT to direct precipitation from super-saturated pore/bottom water. They do not consider the possibility that opal-CT can form from the diagenesis of biogenous silica en route to becoming porcellanite/chert. The high silica periods that characterise the Eocene throughout most of the world's oceans are shown to be important in the Oligocene as well at this site. Also unusual is the way in which opal-CT and amorphous silica alternate. At other sites it is common for only one change to be seen. This considerably complicates the reflector story and may explain why horizon A^c is not singularly well developed in the eastern North Atlantic. The change in mineralogical assemblage clearly shows the importance of bottom circulation to the cessation of opal-CT formation/precipitation: underlining the palaeo-environmental significance of horizon A^c. If circulation may vary at a sub-basinwide level horizon A^c may be diachronous but it is not clear how much and whether such change is discernable within the resolution of palaeontology.

3.6 Theoretical modelling of horizon Beta

Horizon Beta is produced by the shoaling of the CCD between Barremian and Hauterivian times, which caused a change in sedimentation from carbonates to black claystones. Where this event was rapid the boundary produced is sharp and the corresponding reflection coefficient clear and large. Often the final shoaling is heralded by a transitional facies comprising interbeds of the two lithologies, with

Fig. 3.15 Theoretical interbedded facies transition used to model horizon Beta

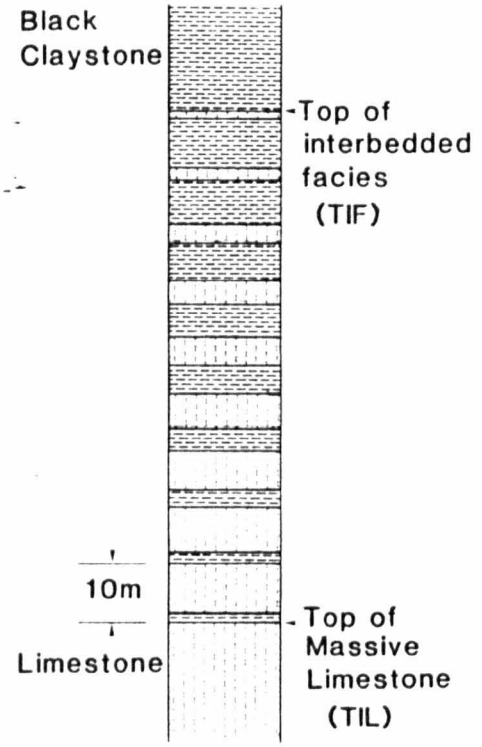

Fig. 3.16 Results of theoretical modelling of horizon Beta

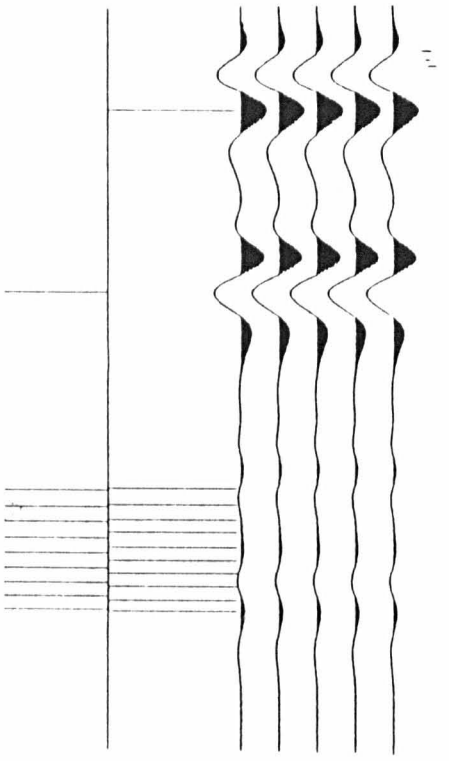

15–50 Hz

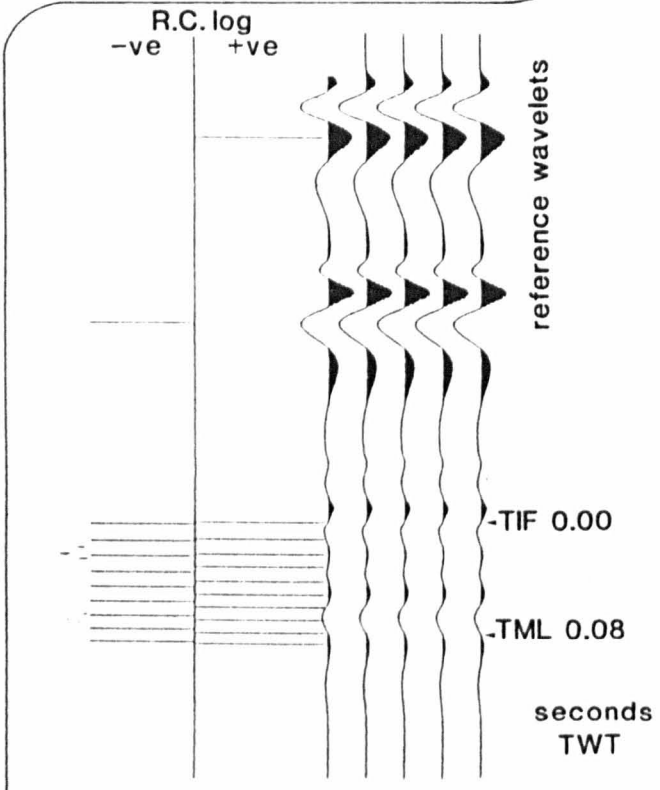

12–40 Hz

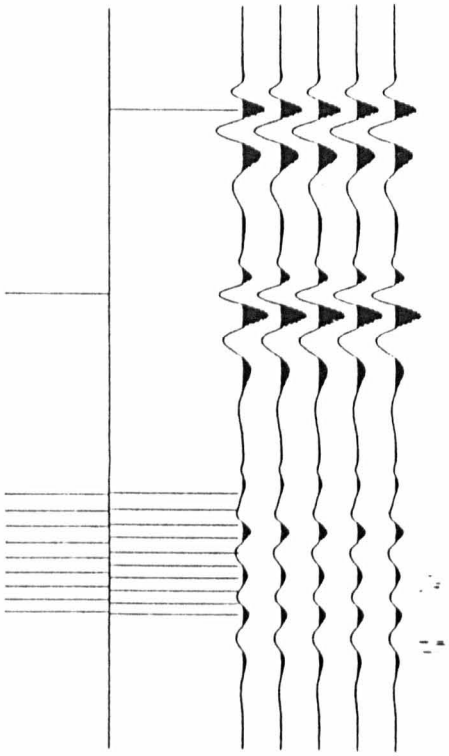

15–45 Hz

the claystones becoming dominant upwards. We may model this by constructing an idealised lithological column and using assumed velocities and densities for the two lithologies (fig 3.15 and table 3.2). We shall assume the transitional facies to extend over 100 metres.

Table 3.2 - Physical properties of lithologies used for theoretical modelling of horizon Beta

	Velocity	Density
Black clays	2.33 km/s	1.92 g/cc
Limestones	3.28	2.19

For convenience all boundaries are assumed to have the same reflection coefficient, although the polarity alternates. The two-way transit time for each bed is used to construct a time series, a RC log. Two additional coefficients are added with the same magnitude as the claystone/limestone boundary but with sufficient separation to prevent interference with the theoretical model. Their purpose is to show the form of the different input wavelets and serve as a comparison of the magnitude of the two types of horizon Beta. The resulting RC log was then convolved with three different input waveforms. The effect of peg-leg multiples has not been investigated. The results are shown in fig. 3.16.

The amplitude of reflection is an order of magnitude lower than for a similar impedance which occurs only once. The interbedded transitional facies mutes the reflection from the massive limestone and produces a reflection of similar magnitude of its own making. This combined reflection is clearly frequency dependent: the lower the dominant frequency the less the reflection. This means that with increased

resolution the first reflection becomes more important, but interpretation of the largest loop must be drawn within the tansitional facies. In contrast early surveys performed with a narrower band-width would be expected to detect only the reflection from the massive limestone. (N.B. This study is on a finer scale than the physical properties modelling scheme is usually run at.)

Fig 4.1 Location map for sites studied

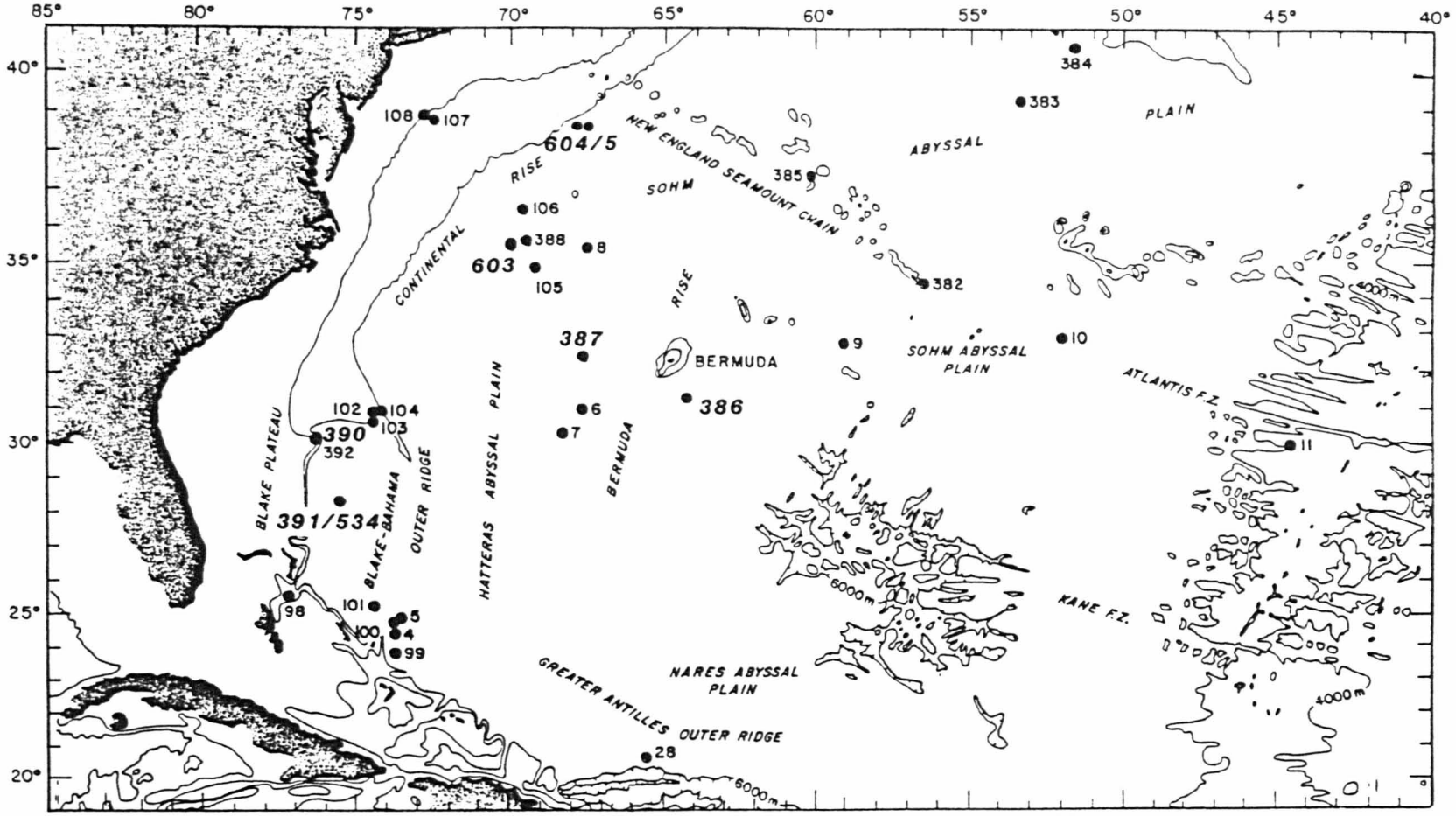

CHAPTER FOUR

Reflectors of the North American Basin

4.1 Introduction

In this chapter I present the results of lithological interpretation of seismic reflectors based upon my own synthetic seismogram modelling. I have concentrated on those reflectors which have been shown to be of regional extent over the North American Basin by previous authors (see chapter one). For the purposes of this study the interpretation and tracing has been accepted as correct although the quality of data used to perform this task is no better than that used for this work.

Over thirty-five sites have been investigated by drilling throughout the basin (fig. 4.1) but I have performed physical property modelling at only eight of these (five in this chapter). The suitability of a given site for the purposes of modelling depend primarily on the quality of physical properties data collected. By and large the early sites were cored too discontinuously or the measurements from recovered core made too infrequently to allow accurate modelling (the modelling scheme will work with any amount of data, but will produce misleading results with poor quality data.) Not all holes are particularly deep (eg sites 388, 107, 383 or 389) and others have insufficient seismic stratigraphic correlation (i.e. the regional reflectors have not been traced to a particular locality), (eg sites 10, 98, 390 and 392.)

The answer to the question of what caused the regional reflectors was one of the initial objectives of the DSDP. The early work showed something of the complexity, but insufficient detail prevented a full understanding. Legs 43 and 44 were designed specifically to answer the regional reflector problem. The paper of Tucholke (1977) is a good summary of the 'state of the art' following these two cruises. I have not carried out modelling at any earlier sites.

In general, all modelling of synthetic seismograms presented in this chapter have been produced using the schemes outlined in chapter three. The **direct** model is based on the physical properties of the recovered core, while the **corrected** model uses the same data but assumes it is a biassed sample of the **in situ** properties and makes allowance for this fact. The **wire-line** models use data obtained by down-hole logging.

The performance of these models is judged by comparison with the site survey seismic profiles. For presentation, these seismograms have been cut along the trace nearest to the site locality and the model inserted. Each model consists of several identical traces to emphasise the lateral alignment of black and white loops which constitute reflectors.

4.2 Site studies

4.2.1 Site 386

Site 386 is situated on the Bermuda Rise and is the most easterly site included in this regional group (fig. 4.1). Sedimentation in the vicinity of site 386 is controlled by basement structure. The

Fig. 4.2a Glomar Challenger site survey profile and direct model, site 386

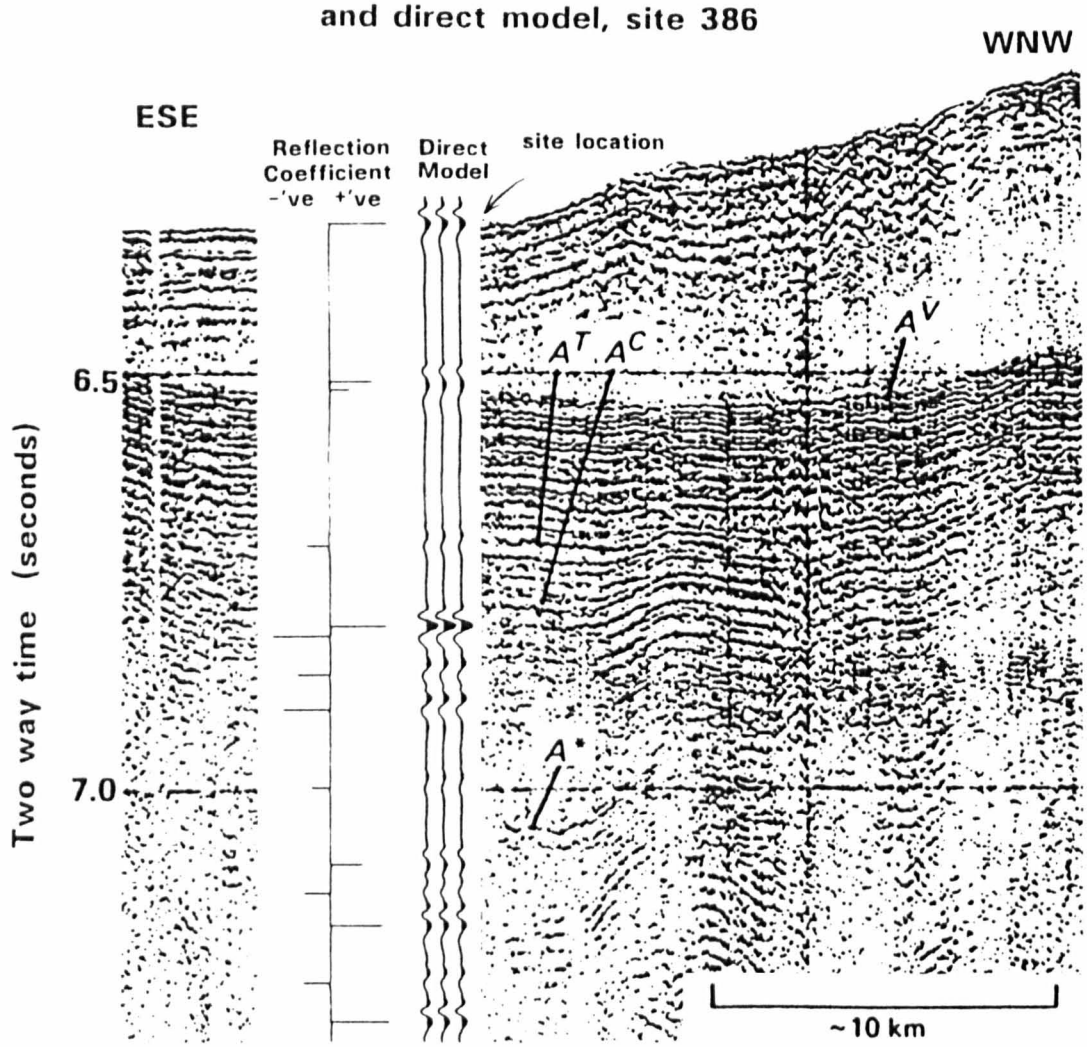

Fig. 4.2b Lithostratigraphy and profile interpretation, site 386

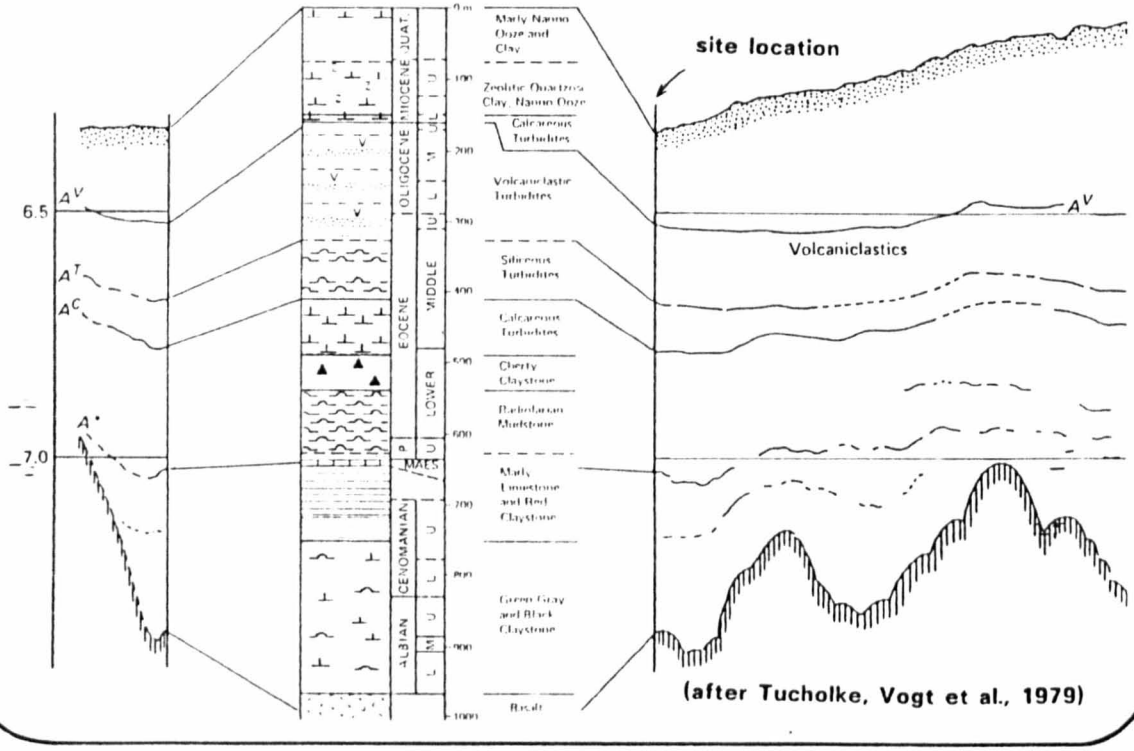

thickness varying with the troughs and highs of basement. Regional reflectors Au, At, Ac and A* are identified at the site and are best developed in the basement troughs. The lowest of these is A* and was thought to correlate with the transition from multicoloured clays into underlying Cretaceous black clays at site 105 (Ewing & Hollister, 1972). Precise lithologic seismic correlation is made difficult by the pronounced lateral variability of the reflectors (fig. 4.2a). It is also difficult to pick reflectors from the records because the low frequency needed to gain penetration produces a profile with reverberations at each reflector.

The uppermost reflector, horizon Av, is correctly interpreted by the site chapter. Data quality is poor for this part of the hole and the velocity function of the corrected model is underestimated (there is only data between 54 m and 61 m, which is extrapolated to cover 0-170 m, horizon Av.) It is interesting to note that this depth is close to the clay-to-claystone transition level, where sediment rigidity increases, enhancing sonic velocity. If the implied velocity of 1.73 km/s is used to correct the physical property model over the upper interval, then the corrected model matches basement closely (0.01 s difference). The velocities in general match those of the site chapter (fig. 4.2b). The velocity down to 400 m of the corrected model hovers around 1.65-1.55 km/s which is significantly lower than the 1.74 km/s used above. The velocities used in the site chapter all add up nicely, but the interpretation of the profile is not obvious. Although the velocities appear to work, they are inconsistent with the shape of the velocity function from physical property data and are calculated to match the assumed basement. In particular, the subunit 4B calcareous turbidites have been given a velocity of 1.91 km/s by the site chapter. If the true velocity is somewhere nearer 2.5 km/s then the transit time for the unit (400-550 m, say) would change from

Fig. 4.3A – Depth plot of physical properties, Site 386

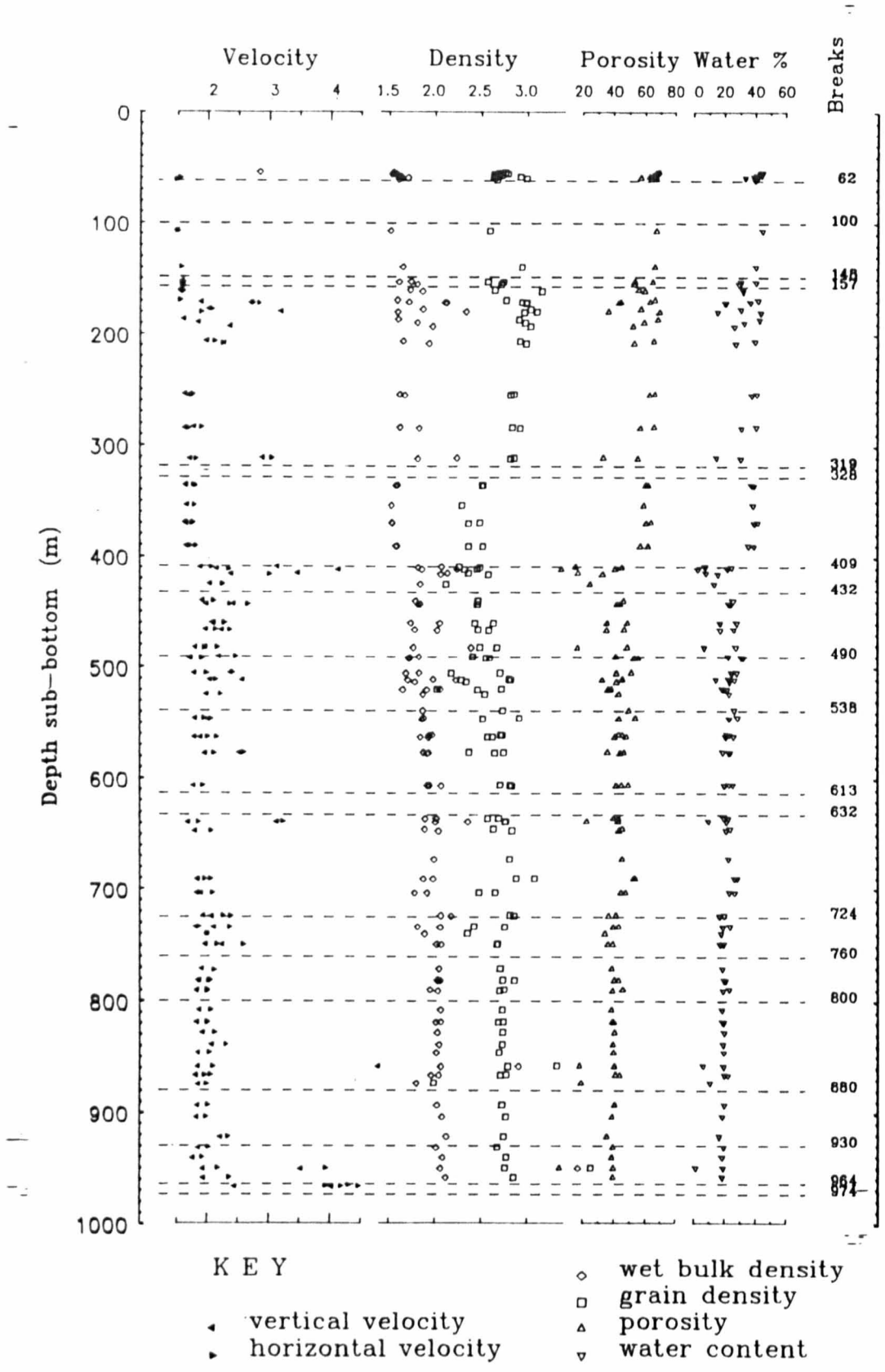

.105 s to .080 s, i.e. basement would be .025 s TWT higher. Such an error would improve the fit of the corrected model with the interpretation given by the site chapter. The size of the reflection coefficient of my models corresponding to horizon Av is much less than might be expected from the character seen from the site survey profile which shows such a marked change from transparent to strongly stratified. Whereas, that modelled for horizon Ac is much larger than is apparent from the very vague horizon Ac. The latter difference may be explained in terms of the low amount of transmitted energy penetrating horizon Av.

The depth plot of physical properties shows that horizon Av is a product of variation in the sonic velocity and grain density data rather than the porosity data alone (fig. 4.3a). This would explain the deficiency of the models because the scheme is based on porosity variation.

Horizon At is a negative polarity event, which is best explained by the plots of wet bulk- and grain density (fig. 4.3a) and represents the vague boundary between volcaniclastic turbidites and siliceous turbidites.

Horizon Ac correlates with the large reflection coefficient modelled at 408 m and is due to the largest physical property break most clearly shown by porosity. Other properties agree with the interesting exception of grain density, which shows little change. This would ordinarily be a sign of diagenesis: a change in the frame structure of the sediment causing enhanced acoustic transmission without any difference in composition. However, this depth, 408 m, coincides with the boundary between sub-unit 4A, siliceous turbidites, and sub-unit 4B, calcareous turbidites. There is no significant

difference in the carbonate content of these two sub-units, which explains the constancy of the grain density data (sub-unit 4B has twice as much organic carbon). Von Rad and Rosch (1974) describes the diagenesis of silica in terms of opal-CT formation to produce porcellanites. It is not clear, however, just where the diagenetic front occurs. It is above 495 m where the presence of cherty claystones indicates an advanced state of diagenesis. From its lithological classification, horizon Ac would appear to be poorly named, since it correlates with the top of calcareous turbidites and is overlain by siliceous turbidites (Tucholke, Vogt, et al., 1979). The upper unit is very rich in siliceous fossils which are most common at the base of each turbidite sequence. Some layers are so rich that they may be called 'spicule sands' (site chapter). The underlying calcareous turbidites have no biogenic silica debris, but do contain 7%, by volume, disordered cristobalite that is "derived from alteration of biogenic opal" (site chapter). This is another way of describing the intermediate opal-CT mineral phase between biogenous opal and chert. The proportion is as high as 19% in some samples, which is ample to explain the contrast in impedance.

In terms of the physical properties, horizon A* is the least distinct horizon (fig. 4.2a). The data quality is not good and there are deeper reflectors of equal character. The site chapter correlates horizon A* with a 2-3 m thick limestone of Maestrichtian age which is too thin to give a reflection. The break recognised at 724 m (fig. 4.3a) is larger and gives a stronger reflection, but the correlation is uncertain.

My physical property model has not worked particularly well over the upper sediments and the site chapter appears to have done a more reasonable job. If basement does occur 0.2 s TWT shallower then the

Fig. 4.4a Glomar Challenger site survey profile and direct model, site 387

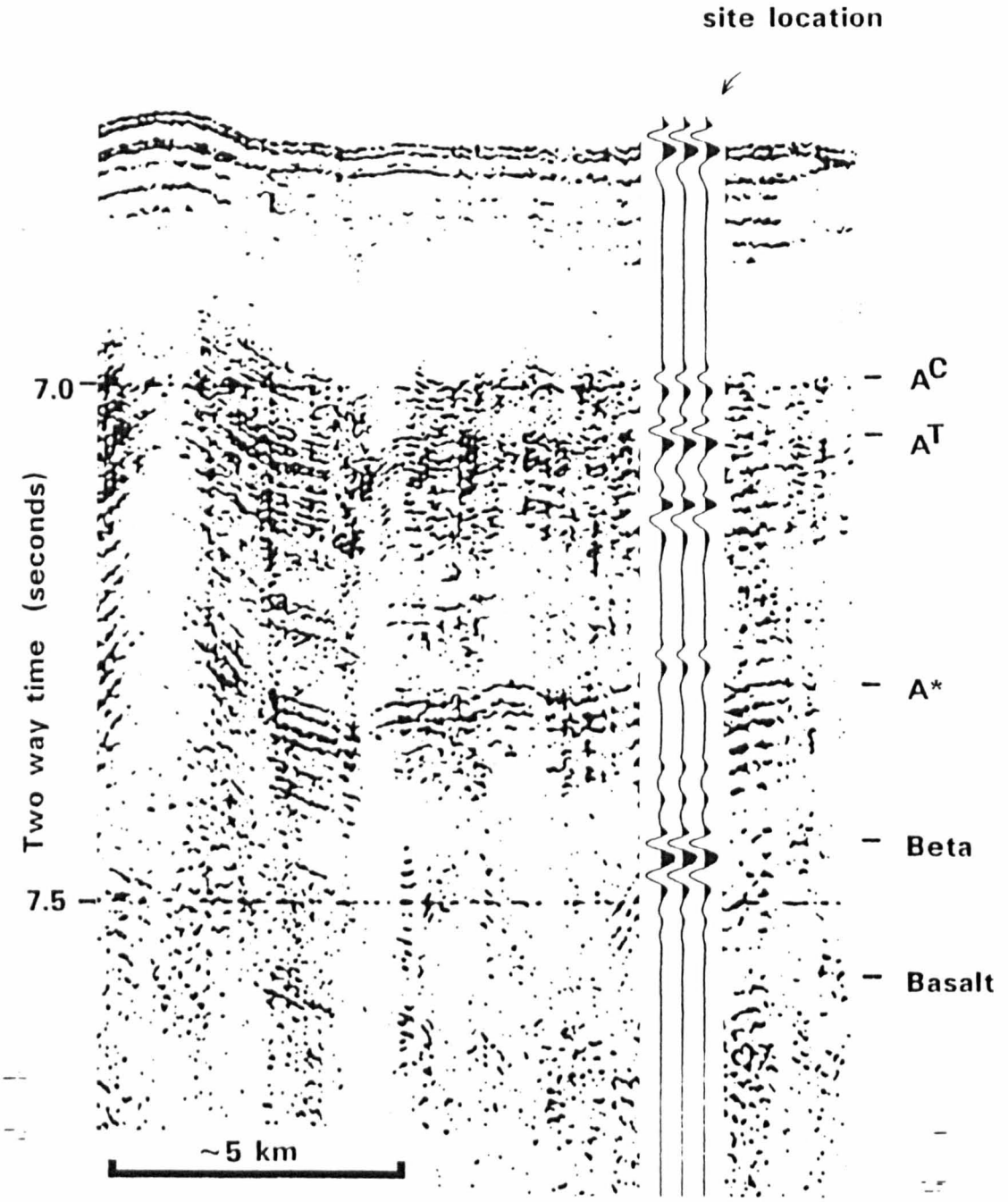

Fig. 4.4b Correlation between seismic profile and drilling results,

site 387

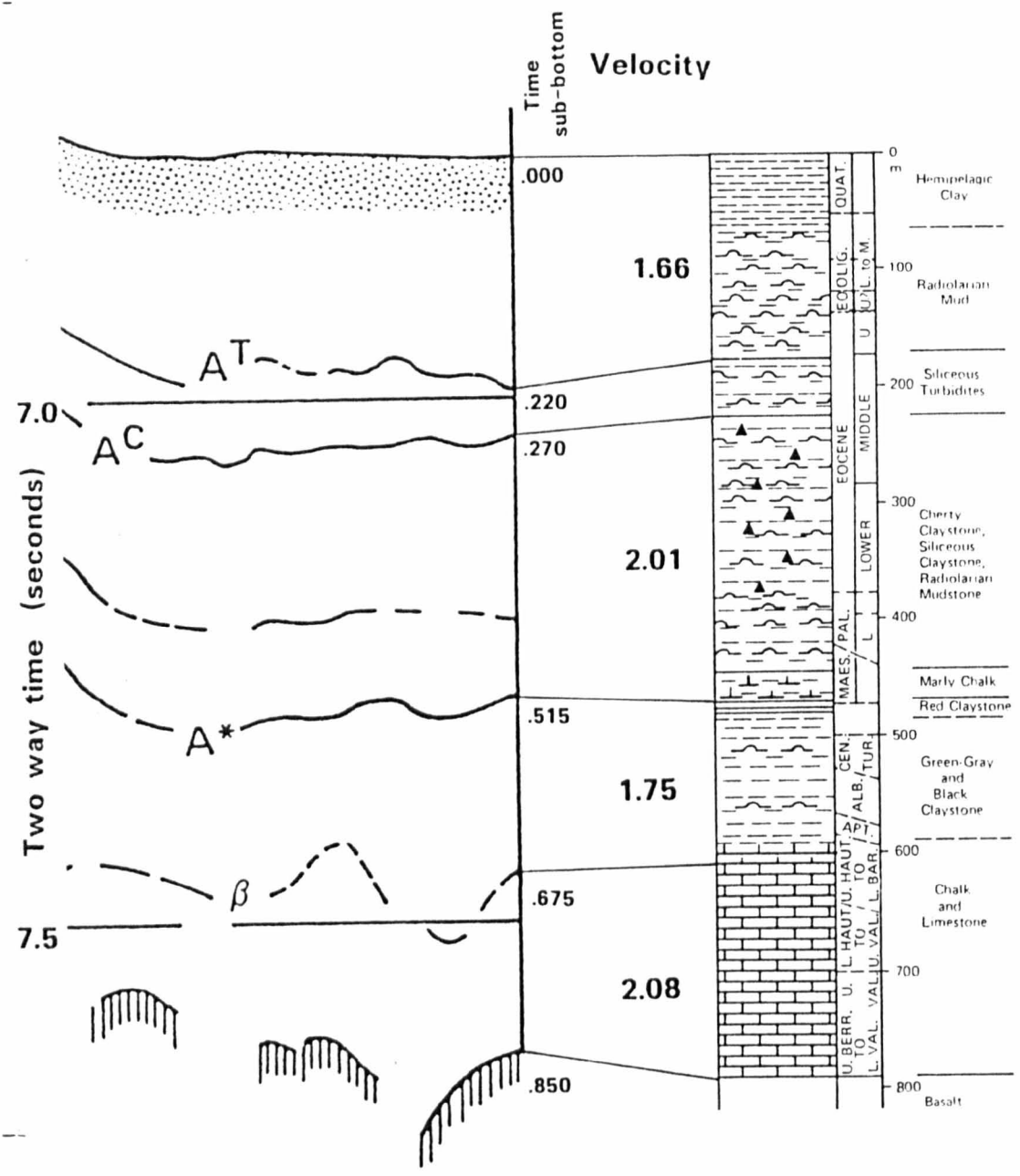

(after Tucholke, Vogt et al., 1979)

implied velocities improve the performance of the physical property model. The variety of amplitudes of reflections modelled and their differing expressions on the physical property depth plots are interesting. These show that reflectors can be caused by a number of processes.

4.2.2 Site 387

Site 387 is situated on the Bermuda Rise in line with the very distal end of the New Jersey transect (fig. 4.1). The interpretation of Tucholke in the site chapter has been used for comparison (fig. 4.4b). My direct model gives good ties with all the interpretations of the site chapter, but disagrees with the time to basement. This might suggest the whole model is wrong as basement is usually one of the more obvious reflections. An average of the two physical property models gives a good time to basement, but disagrees with the interpretation of some of the reflectors. The interval transit time calculated from the correlation between horizon Beta and basement yields an interval velocity lower than the laboratory data; normally measurements made at the surface are lower. The interpretation of the site chapter notes: 'Acoustic basement... is also poorly defined; it is very irregular, exhibiting apparent crest-to-trough amplitudes in excess of 0.2 s (nominally 200 m).' If a high interval velocity is used then the site chapter matches the direct model. However, the basement may have been misinterpreted such that either the arrival is shallower or true basement was not reached.

I correlate horizon At with 175 m by my direct model (fig. 4.4a) which agrees with the site chapter. Tucholke and Vogt (1979) suggest that it might be due to a shallower impedance contrast but dismiss the

Fig. 4.4C -- Depth plot of physical properties, Site 387

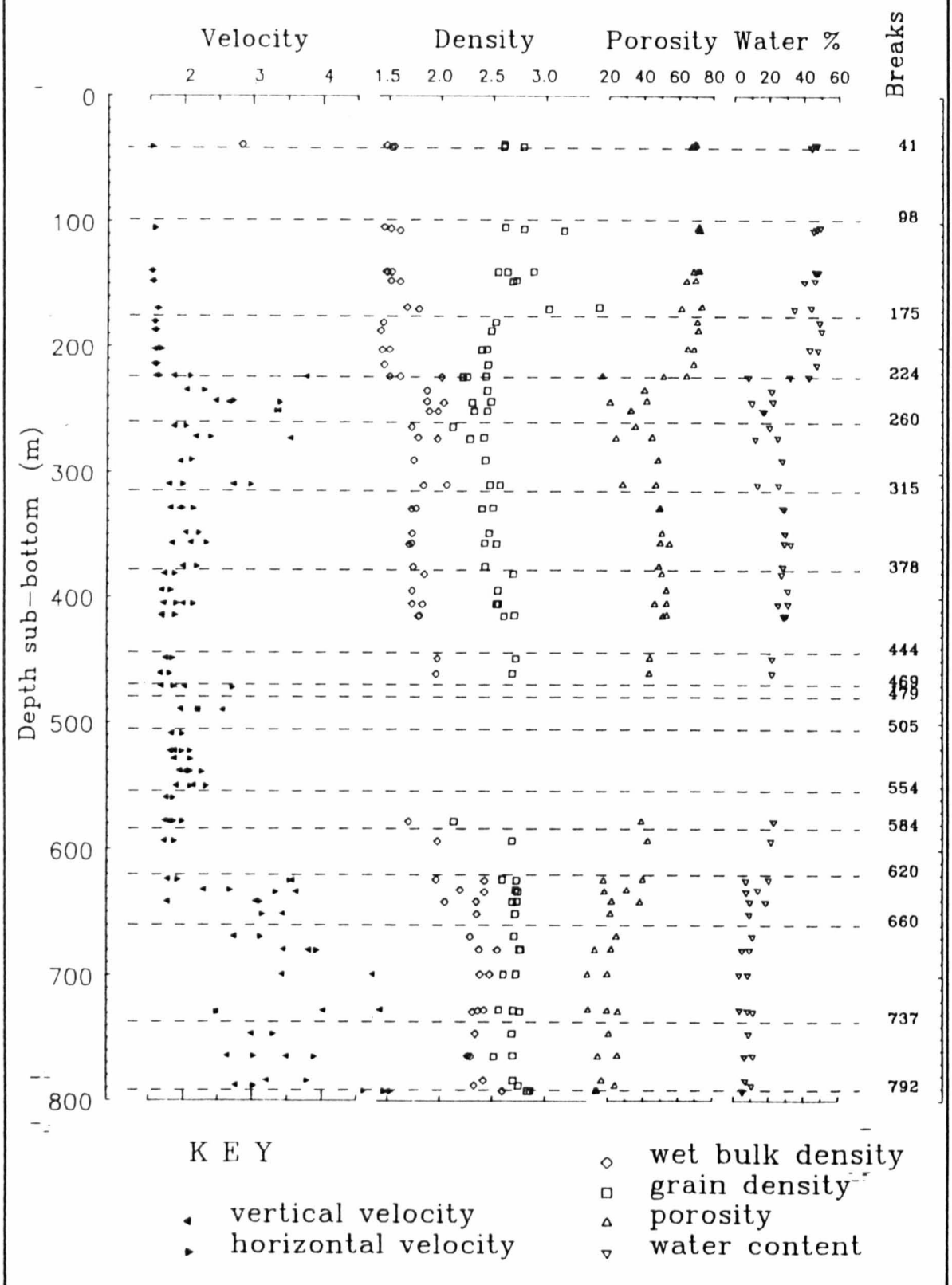

possibility on the grounds of unlikely interval velocities needed. From the seismic profile horizon At can be seen to be the top of a thick, acoustically layered sequence, which also includes horizon Ac. The physical properties break that distinguishes horizon At is best shown by the change in character of the plotted properties (fig. 4.4c). These change from variable above the horizon to much more ordered and clustered below. This depth is roughly correct for the rapid change in shear strength seen at other sites (eg those of Leg 93, see chapter 7), where compaction causes a disproportionate increase in rigidity when compared to the amount of water loss. At other sites this depth is the clay-to-claystone transition. The variability of the data from the interval above is explicable in terms of the damage caused to sediment structure by coring, handling and measurement. It may correlate with compositional change as implied by the assignation of the name horizon At, but no such differences were described for this interval and the interpretation of the site chapter was based on a depth estimated by assuming velocity.

Horizon Ac correlates with 224 m by my direct model and according to the site chapter. The physical property break is clear (fig. 4.4c): porosity decreases rapidly, velocity increases rapidly although both are transitional, wet bulk density jumps, but grain density shows no change. This compares exactly with site 386. The low porosity continues to about 310 m depth and correlates closely with the layered unit below horizon Ac. Lithologically, this is the depth at which silica diagenesis starts and it is within unit 3 which comprises siliceous turbidites.

The unnamed reflector at 0.435 s TWT (fig. 4.4a) is between 380-390 m which agrees with the site chapter (which gives 390 m). Tucholke, Vogt et al. (1979) note that this is 'near the top of the chert-free

siliceous claystones in the lower part of lithologic sub-unit 3B. The physical properties break is shown by a decrease in velocity (fig. 4.4c), (lower anisotropy) and increased grain density. Wet bulk density does not change much. This is interesting; it is an anti-Ac reflector. The physical properties indicate an increase in carbonate and loss of silica and a concomitant decrease in the degree of lithification. So it appears that the reflector is the top of the chert-free siliceous claystones.

Horizon A* is correlated to 455 m by my direct model. This is Maestrichtian marly chalk, the middle of unit 4. The site chapter locates horizon A* at the base of unit 4 at the negative impedance contrast with unit 5. However, it also notes that if correlation is drawn at the top of unit 4, not only are inferred interval velocities more reasonable but the correlation matches that at site 386 (the top is not properly known due to poor core recovery between 420-440 m.) The thickness of unit 4 (441-469 m) is on the limit of resolution of the seismic method and to choose between the three possible alternatives is beyond the accuracy of the physical property modelling with the available data. It is worth noting that CHN analysis (organic geochemistry) notes two cores with anomalously high carbonate content (Tucholke, Vogt, et al., 1979). These are between 460 m and 470 m or from the middle to the base of unit 4. Unit 4 shows higher density, but no difference in velocity compared to higher formations and reduced porosity. The interval of high carbonate content gives increased velocity also found in unit 5, but unfortunately physical property data from unit 5 is restricted to velocity which prevents accurate modelling. It is possible that horizon A* correlates with 440 m, the middle of unit 4.

The CHN data also show the abrupt boundary between carbonate-poor

Cretaceous black claystones and carbonate-rich Neocomian chalks and limestones, 594 m. My direct model places horizon Beta at 615 m. The site chapter notes: 'The exact sub-bottom depth at which the major acoustic impedance contrast occurs is somewhat problematical. The problem is complicated by discontinuous coring at the level of the reflector and by the relatively low and biassed recovery.' The first chalks encountered were at 593 m. The site chapter locates horizon Beta at 624 m (or above up to 610 m). This problem is similar to situations discussed at sites 391 and 534 (and 386), (see sections 4.2.4-5).

The main differences across the horizon Beta contrast are a porosity reduction which causes elevated velocities and strong anisotropy (anisotropy is taken to be the difference between horizontal and vertical compressional velocity, and may be seen by the separation of velocity symbols on the physical properties depth plot, fig. 4.4c.) The velocity data is highly variable which is explained by the variation in lithology of marls and limestone interbeds which comprise the Blake-Bahama formation. Wet bulk density increases slightly, but no change is seen in the grain density, although no data exists from the overlying unit 6 (fig. 4.4c).

The interval between basement and horizon Beta is assigned an interval velocity of 2.08 km/s (by the site chapter) which is well below all measurements from recovered core. The site chapter argues that recovery is very biassed and only the most indurated limestones are available for measurement. The low velocity is necessary because it is assumed that the basalt in the last core was basement. The site chapter does mention that the petrographic evidence suggests that the basalt cored was a sill. So it seems quite plausible that the three metres of basalt are not the same basement producing the reflection at

Fig. 4.5a Correlation of site survey profile,
direct model and lithology, site 390

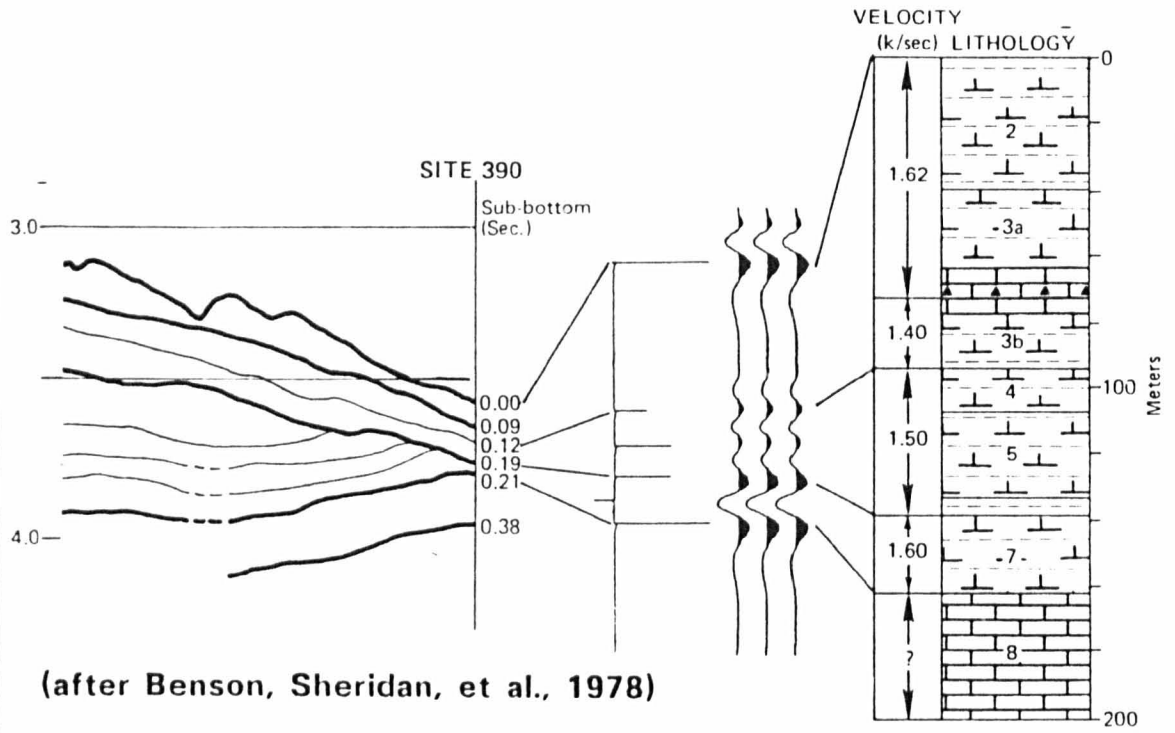

(after Benson, Sheridan, et al., 1978)

Fig. 4.5b Seismic profile made by DV **Glomar Challenger**
across sites 389 and 390

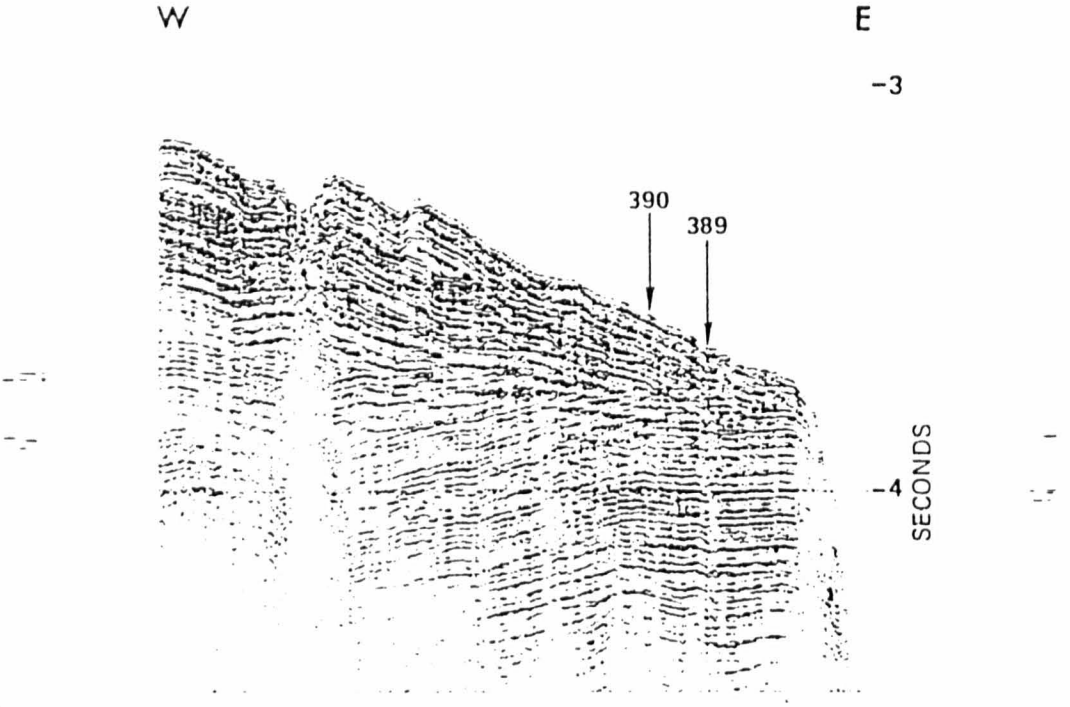

0.850 s (TWT), which removes the need for a low velocity for the unit and indicates that my direct model is probably correct.

4.2.3 Site 390

Site 390 was drilled on the edge of the Blake Plateau (fig. 4.1) and is much shallower than other sites studied in this chapter (sea-floor depth is 2660 m). The drilled section penetrates a number of reflectors between 0.0-0.2 s TWT sub-bottom. These give good expressions on the physical property plot, which allow modelling of this stratigraphy. My direct model compares fairly well with the interpretation given in the site chapter. The seismic section from which the reflectors have been identified is not good (fig. 4.5b). Although, the site chapter agrees with the direct model it uses unrealistic interval velocities of 1.40 km/s to model the Paleocene nannofossil ooze.

'The reflector at 0.09 s TWT is correlated with reflector 1 of Ewing et al. (1966) and the reflector 0.19 s is reflector 4' (Benson, Sheridan, et al., 1978). The site chapter correlates 0.09 s reflector with tan cherty limestones that are interbedded with the lower Eocene and upper Paleocene nannofossil oozes which agrees with my model. Its character is similar to that of horizon Ac in the abyssal plains. The site chapter says reflector 2 is weak compared with reflector 1 which disagrees with my model. Nevertheless, our time-to-depth correlations agree.

No physical property break is modelled at 0.19 s TWT despite being noted to be a strong reflector.

The close spacing of the reflectors is on the limit of resolution for

Fig. 4.6 Correlation of lithology, corrected model and site survey profile, site 391

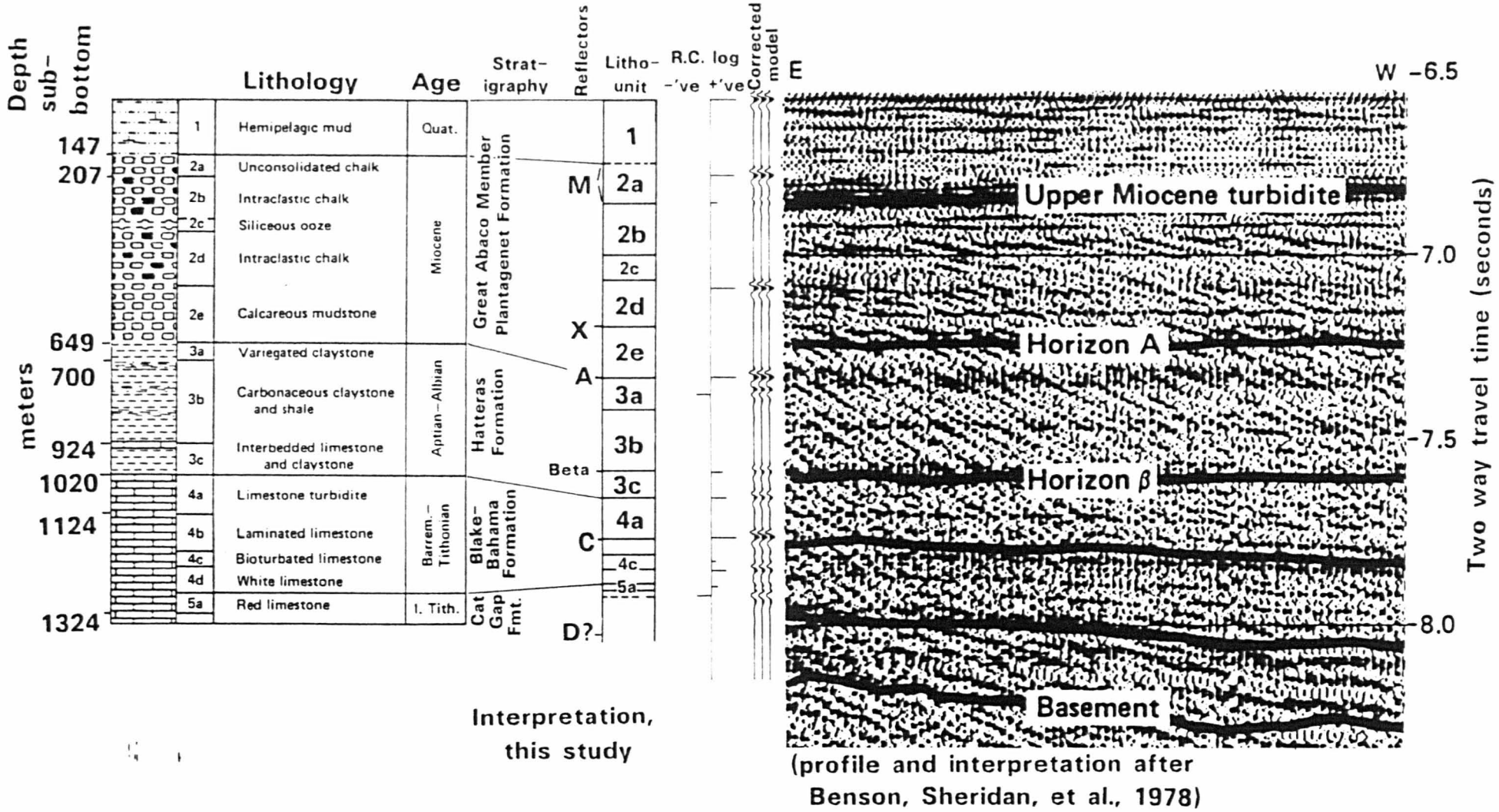

the estimated frequency (the same waveform as used at site 603 was re-used.) The wavelet used is a simple one with one large positive peak. The seismic section has an input wavelet with considerable reverberation, so the chance of accurately recognising reflectors spaced 0.02 s TWT apart is somewhat optimistic.

This site is much shallower than the other sites studied and shows the contrast in sedimentation between the continental slope and the abyssal plains. The reflectors are more numerous, but, as a result of the complex history, they are not as regionally significant.

4.2.4 Site 391

Site 391 is in the Blake-Bahama Basin near to site 534 with a lithological succession that typifies sedimentation in the North American Basin (fig. 4.1). The top 649 m comprise gravity flow deposits of the Great Abaco Member of the Blake Ridge Formation. The thin Bermuda Rise Formation has been removed by erosion (fig. 4.6). The second unit comprises multi-coloured claystones of the Plantagenet Formation. Black claystones between 725 m and 991 m make up the underlying Hatteras Formation. At the bottom of the hole (1412 m) is the reddish nannofossil claystone of the Cat Gap Formation. Drilled in four holes, the last, 391C, was a record-breaking, single bit hole reaching over 1400 metres below the sea-floor, but failing to reach basement.

The site is important in the history of reflector studies because, at one site, it penetrated a number of important horizons. These are horizons M, A, Beta and C. Horizon X was not identified at the site at the time of drilling.

Table 4.1 - Comparison of travel time to refletors, site 391.

Horizon	Two-way travel time			
	as given in text[1]	as measured from fig.[1]	Models[2] Direct	Corrected
- M	.21	.28	.28	.30
A	.59	.65	.75	.80
Beta	.97	1.01	1.08	1.14
C	1.14	1.20	1.18	1.23
(D not reached)	1.32	1.40	-	-
Basement	1.44	1.56	-	-
Total depth	1.23		1.37	1.45

[1] Benson, Sheridan, et al, 1978.

[2] this study.

Table 4.2 - Lithological unit relevant to horizon M, site 391.

Depth	Litho-unit	Description
0 m		
	1	silty clay with nannofossil ooze beds
147 m		
	2A	Chalk, without clasts
207 m		
	2B	Intraclastic chalk with soft angular clasts of soft siliceous ooze (turbidites and gravity flows)

No logging was carried out at this site, so only the physical property modelling is available for interpretation. Only five cores were recovered from the top 300 metres, where it may be better to use a Houtz-type velocity function derived from sonobuoy data. Therefore, the precise velocity function for the upper parts of the hole is uncertain. The TWT to 400 m given by the two physical property models does not agree with sonobuoy data from the site survey (Bryan, Markl & Sheridan, 1980):

Direct model	.474 s	implying a velocity of 1.69 km/s
Corrected model	.493 s	----------"---------- 1.62 km/s
Sonobuoy data	.464 s	----------"---------- 1.72 km/s

Correlation of the physical properties' models is hindered by a contradiction in the site chapter. The travel-times to reflectors given do not match their labelled figure (see table 4.1, fig. 4.6). There are thus two sets of possible correlations and the times taken from the figure have been used here. Neither model agrees with the travel time to total depth given in the site chapter, although the direct model, which appears to be more accurate, agrees that horizon D was not reached (fig. 4.6). The problem of the velocity function will be discussed with horizon Au.

The shallowest named reflector is horizon M. The site chapter makes the correlation at 207 m, the boundary between subunits 2A and 2B. The line drawn on the figure is at .28 s (TWT) and indeed corresponds to 207 m using the velocity function of the direct model (fig. 4.6). However, a much stronger reflection is modelled at .21 s (TWT), the depth labelled on the diagram as horizon M and correlates with the boundary between unit 1 and 2. The lithologies of the units/subunits are given in table 4.2.

Fig. 4.7 – Depth plot of physical properties, Site 391

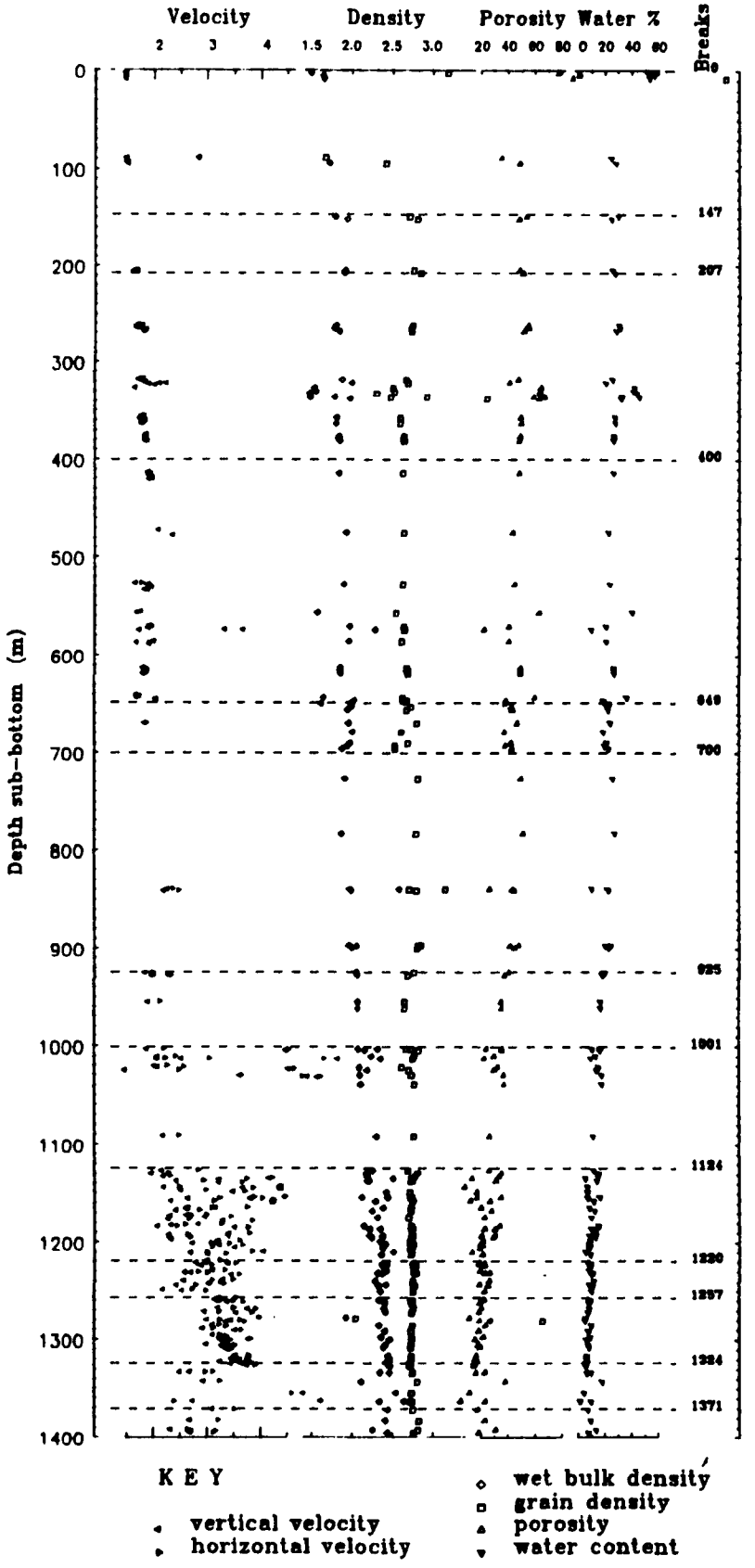

A consequence of this time/depth correlation is that the interval velocity down to 207 m is 1.478 km/s, which seems rather low although it does agree with sonobuoy data (Houtz, 1978).

Horizon A as drawn in the site chapter occurs at 649 m sub-bottom and .59 s (TWT). This is not confirmed by my modelling. At this depth there is an unconformity between Early Miocene interbedded chalk-without-clasts, mudstone and chalk-with-clasts and Lower Cretaceous claystone. The direct model gives a TWT to this depth of .748 s, which matches well with a broad reflector immediately beneath the one labelled A in the site chapter. There is no doubt from the lithostratigraphy and chronostratigraphy that this is an unconformity that elsewhere causes horizon Au. However, the seismic profile is not clear due to the effects of spatial aliasing and the thick interpretation line (fig. 4.6). Unit 2 exhibits variable lithology and would be expected to yield several good reflectors, not dissimilar from those present between horizons M and A. The direct model only divides the unit at one depth, at 400 m, within subunit 2D (fig. 4.7). This physical property break correlates with a strong narrow reflector at .48 s (TWT). The implied interval velocity between horizons M and A is 1.77 km/s, which agrees with sonobuoy data (Houtz, 1978). Therefore, modelling indicates that the interpretation of horizon A should be made 0.1 s lower.

Only a few physical property data are available from between 700 m and 900 m, so there may be some error in the transit time for this interval (fig. 4.7) (lower parts of the models may 'arrive' up to .015 s sooner.)

Horizon Beta is interpreted to have been caused by an abrupt raising of the CCD. At site 391 this event appears to be spread over about

75 m of sediment. Throughout this interval, limestone and black claystone are interbedded although the proportion of carbonate sediment steadily increases with age. According to the site chapter, horizon Beta probably correlates with the base of this 75 m thick transition zone, at 1020 m, the top of lithological unit 4. This correlates with a travel time of 1.09 s by my direct model. A physical property break has been drawn at 1001 m mainly because the interval immediately above was wash-cored making it appear a prominent break. The site chapter interprets horizon Beta at .97 s which is equivalent to 886 m by the direct model. This confusing state of affairs may be explained by considering the acoustic character of the interbedded unit (see section 3.6). What appears to be happening at site 391 is that the site chapter makes a firm correlation between the horizon Beta reflector and the top of Unit 4, when in fact the reflector really corresponds to approximately the top of sub-unit 3C and the seismic expression of Unit 4 comes 0.08 s lower. The exact correlation of the horizon Beta-type reflector will vary with the band-width of the seismic profile.

True horizon Beta would therefore come a little below 1.05 s (TWT) which corresponds to 1001 m by my direct model. The low amplitude reflections modelled are very similar to a theoretical model of horizon Beta (see section 3.6) in which the limestone facies of Lower Barremian/Upper Valanginian age are divided by a transitional 'interbedded' facies. The fact that subunit 3C contains a few thick limestones enhances the reflection from this unit, causing it to overshadow true horizon Beta. If this is true then such a miscorrelation may easily have been drawn elsewhere.

Horizon C is a strong reflector ocurring at 1.20 s (TWT). The site

Table 4.3 - Variation in carbonate content below horizon C, site 391.

Unit	Average carbonate content (wt%)
4C	64
4D	79
5A	45

chapter draws the correlation at the litho-unit 4/5 boundary, 1330 m. The implied interval velocity of the site chapter is 3.646 km/s and is justified if horizon C really correlates with 1330 m. My physical properties models all agree that horizon Beta is higher, 924/1001 m, and consequently correlate the strong reflector that is horizon C with 1124 m. This depth is the sub-unit boundary between 4A and 4B, grey limestone turbidites above bioturbated white limestone with dark grey stringers. This lithological boundary is very marked: subunit 4A is sandy and silty and very poorly consolidated. The average core recovery for the subunit is 22%, dropping to only 0.3% for the bottom two cores: 391C-22 and -23. In contrast, unit 4B is a competent limestone interbedded with calcareous claystone. Core 391C-24 achieved 89% recovery and the average for the subunit is 62%. The limestones of subunit 4B are generally much paler than those above which underlines the physical contrast. So it seems quite reasonable to expect a strong reflector from this interface.

Total depth was reached at 1412 m, which means that 288 m of sediment were drilled below my horizon C. If the interpretation lines of figure 4.6 are used and compared with the direct model, then the model clearly confirms the interpretation of the site chapter that total depth was reached above horizon D, and basement is up to 300 m below horizon D (which I predict at 1700-1800 m.) This sequence of sediments is well lithified and consequently has high velocities. Their reflections are squeezed together and interfere to give the layered seismic facies/character between horizons C and D (fig. 4.6). In particular, the top of subunit 4D gives a good reflection. It is described as having greenish shale partings with the suggestion that there is more clay than the overlying subunit 4C. The colour, though, is significantly whiter, which generally is associated with higher velocities. The carbonate content corresponds with this observation

(see table 4.3).

There are several serious problems with interpreting the site-survey profile at site 391 which are typical of seismic stratigraphic studies in the deep sea:

1. Quality of the profile is poor. Some reflectors appear as dipping foresets due to spatial aliasing of the display. The section available is insufficient to permit my own interpretation, which would be useful for the recognition of unconformities. Also, the most important horizons, the main reflectors, are covered by thick interpretation lines on the sections available to me.
2. The travel time to these reflectors as given by the labels of the diagram are different when compared to the times measured from the diagram. It seems likely that the section shown is different from that used to perform the interpretation.
3. The physical properties data is of poor quality in the surficial sediments and for the interval between 700 m and 900 m sub-bottom. The consequence of this is that the velocity function is difficult to calculate. Any errors affect all lower horizons so errors increase down the hole.
4. Basement was not reached, which further impedes modelling of the velocity function.

4.2.5 Site 534

Site 534 was drilled only 22 km from site 391 with a prime objective to reach basement that had not been reached at site 391. Also of importance were the strong reflectors seen below horizon Beta. No attempt was made to recover the top 536 m of sediment as it was not expected to differ much from site 391. Obviously this effects the modelling of this interval.

As mentioned in chapter 3, the modelling scheme used in this study was developed from the technique of Shipley (1983). The latter work concerned the interpretation of seismic data at this site. Shipley (1983) assumes the correlation of horizon Au based on sonobuoy data is correct and then proceeds to model the deeper reflectors. 'The Eocene-Maestrichtian unconformity at 723.5 m is correlated with horizon A. This correlation and the depth at which basalt was first encountered at 1639 m are two end points in the seismic modelling' (Shipley, 1983). The accuracy of this initial correlation should be viewed in the light of the number of horizons close (vertically) to horizon Au that are likely to produce strong reflections (fig. 4.8).

A first approximation for the upper interval can be gained by assuming the same stratigraphy as at site 391. However, the column is thicker at site 534 - vis. horizon A is at 649 m at site 391 and at 724 m at site 534, 0.614 s against 0.724 s.

The direct model predicts velocities for the upper sediments which agree with the sonobuoy data of Houtz (1973). The interpretation given in the site chapter is probably wrong for the reasons cited by Shipley (1983). Model 2 of Shipley (1983) gives a good tie to basement and has been constructed with considerable attention to lithological variation. The top sediment velocities are taken from site 391:

Shipley, model 2	0-546 m	.566 s
Direct model, this study	0-546 m	.616 s

However, Shipley's error at horizon Au is about the same as the direct model:

time on section	.711 s
Shipley, 1983	.698 s

Table 4.4 - Correlation of reflectors at site 534

horizon	TWT[1]	drill string depth		
	(s)	site report[2]	Shipley, 1983	this study
M	.222			ca. 200
X	.511			ca. 434
A	.711			660
Beta'	.889	892	892	ca. 870
Beta	.933	975	948	950
C'	1.148	1251	1204	1202
C	1.185	1343	1270	1268
D'	1.244	1433	1343	1345
D	1.333	1555	1555	1549
Basement	1.437	1638	1638	1638

[1] from point C of figure 7, Shipley, 1983.
[2] also Sheridan, Gradstein, et al, 1982.

Table 4.5 - Comparison of wire-line and physical property models, site 534.

	Interval	Travel time	Velocity
sonic log	536 - 717 m	.128 s (TWT)	2.83 km/s
direct model	545 - 714 m	.124 s (TWT)	2.73 km/s

This represents a 3% error or .005 s on the transit time of the interval modelled. In view of the data quality this is not significant.

Direct model .726 s

I have tried an alternative derivation of the velocity function without attempting to fit the upper sediments explicitly. Instead, the correlation with basement is assumed to be correct and the location of the reflecting horizons made relative to this datum. The lack of data for the top 536 m means that the sea-bed reflection has not been modelled. The data recovered at site 391 has been used to attempt a model for the upper sediments, but no great accuracy is expected (nor found) in view of the difference in thickness of pre-horizon A sediments at the two sites.

It should be noted that the use of basement depth is hampered by two factors:

1. topography of basement - profiles are not directly over the location of the site (Shipley, 1983)
2. errors in measurement of drill string length (see section 3.4).

A number of important regional reflectors were penetrated at site 534 including Jurassic sediments and basement for the first time. Horizon Beta', C' and D' were defined for the first time at this site (Sheridan, Gradstein, et al., 1982), (see table 4.4).

As in section 3.5, one check of the physical property model is to compare it with the velocity function measured by the sonic velocity log, the integrated transit time. Only the top section of hole 534A was logged successfully with the sonic tool, between 536 m and 717 m. This may be compared to the interval 545 - 714 m of the direct model (see table 4.5).

Fig. 4.8 – Depth plot of physical properties, Site 534

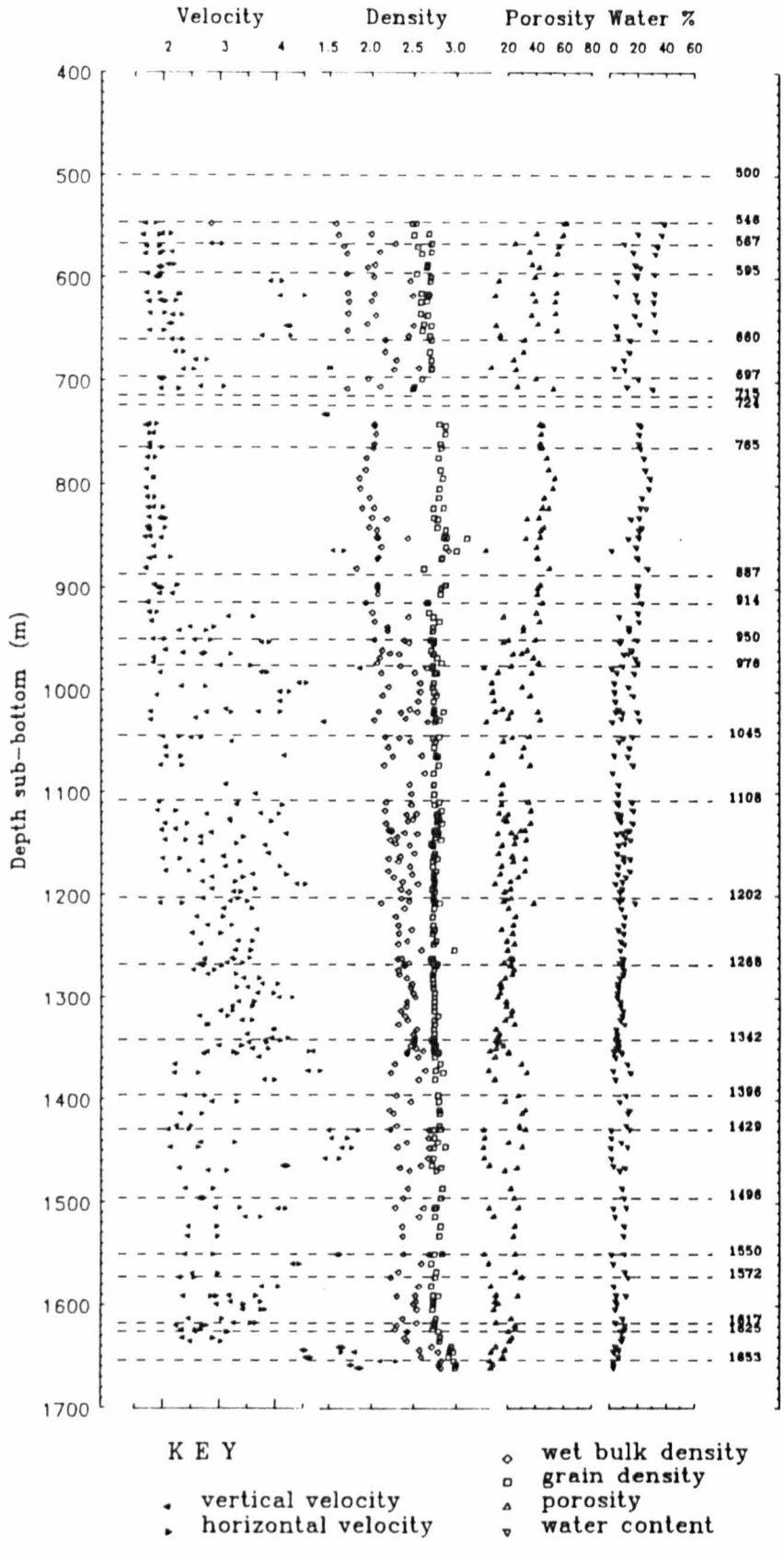

Fig 4.9 Correlation of site survey profile, Site 534

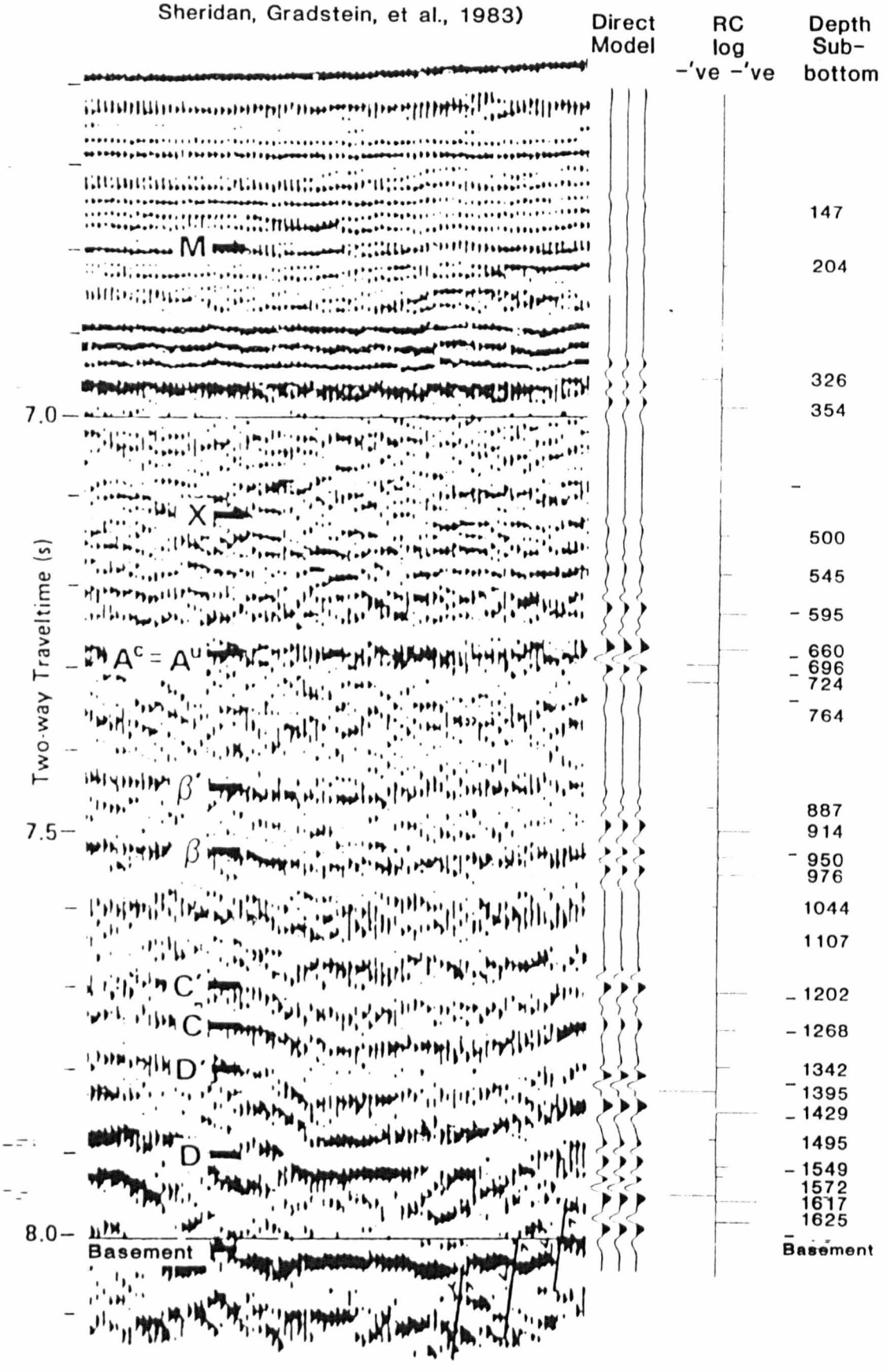

Using the direct model tied at horizon Au (724 m and .712 s, TWT) the following correlations can be drawn, which largely agree with the correlations made by Shipley (1983) (fig. 4.9).

Horizon Au is preceeded by one strong reflection at 595 m. The models of Shipley (1983) also show one such precursor; the subunit boundary between 2B and 2C chalk turbidites above interbedded calcareous gravity flows and green claystones. Both are divisions of the Great Abaco Member. The size of the physical property break is caused by a large rise in velocity and density due to a large reduction in mean porosity. This is because of the first occurrence of well lithified limestones (ie low porosity). As such it is likely to be a strong reflector, depending, of course, on the thickness of the limestones. The subunit boundary between 2C and 2D at 660 m shows a similar physical property signature (fig. 4.10) despite the lithological similarity between subunits 2B and 2D which might be expected to result in reversed polarity. The strong positive break is due to a further marked decrease in porosity. This physical property break most closely correlates with the black loop that is labelled horizon Au (fig. 4.9,4.10). At 696 m there is the unconformity between the Miocene Great Abaco Member and the Eocene Bermuda Rise formation. The latter is siliceous, but with no significant development of opal-CT cement. The physical properties break is strongly negative because of reduced velocity and density (and higher porosity). This break is important as the white loop succeeding the black loop labelled horizon Au and for providing a tail which destructively interferes with energy from 724 m. The unconformity at 696 m is generally accepted to be the cause of horizon Au elsewhere, but its polarity at site 534 shows it to correlate just below the reflector labelled horizon Au. The lowest horizon affecting horizon Au is the unconformable boundary between litho-unit 3, the Bermuda Rise Formation and litho-unit 4a, the

Plantagenet Formation.

Horizon Beta' is approximately 870 m sub-bottom by the direct model. This disagrees slightly with the site chapter and Shipley (1983), who suggest it is at 892 m. The site chapter names horizon Beta' for the first time and defines it to be the unconformity between Aptian and Albian. The depth 870 m occurs towards the base of litho-subunit 4b. It is not a particularly strong reflector and does not correlate with any marked physical property break. Shipley (1983) notes that the doublet is created by the spacing and the sum of the slight positive impedance contrast between subunits 4B and 4C (intra Hatteras Formation) and the slight negative impedance contrast between 4C and 4D (also intra Hatteras). The doublet is not laterally persistant. If the initial interpretation is wrong, then we should be careful that we do not confuse the name of a reflector with its proposed correlation. The name "Beta'" must remain with the reflector interpreted from the seismic profiles. If the unconformity does show a seismic expression then this ought to bear a different label.

Horizon Beta is only slightly stronger as a reflection than the preceeding loop labelled horizon Beta'. It is correlated with 950 m at the top of calcareous sediments within the upper Barremian. The character of this reflector is similar to that found at site 391 and to the theoretical study described in section 3.6. It is interesting to note that the direct model agrees with Shipley (1983) but that the site chapter draws the correlation 25 m lower at the top of the massive limestones that characterise subunit 5a.

Horizon C' is correlated with the subunit boundary 5B/5C at 1202 m of early Valanginian age. Shipley (1983) notes that it also seems to represent a transition from a sheet drape deposit below to a more

Table 4.6a - Comparison of the age of horizon C at site 391 and 534.

	Site 391		Site 534	
	Depth	Age	Depth	Age
site chapter	1330	Upper-Lower Tith.	1342	Lower Berriasian/ Tithonian
Model	1124	Lower Barrem./ Upper Valang.	1289	Upper/ Lower Berriasian
Shipley, 1983	not available		1270	Upper Berriasian

Table 4.6b - Interpretation of horizon C at sites 391 and 534

	Site 391			Site 534		
	Age	Depth	TWT	Age	Depth	TWT
Site report	top L.Tith Lst.	1330	1.14	top Tith.	1342	1.17
Direct model	L.Barr-U.Valan	1124	1.20	U.Berr	1268	1.19
Shipley, 1983				U.Berr	1270	1.19

ponded basin fill deposit above but that the sedimentology of subunits 5B and 5C are similar and do not indicate this expected facies change. The transition from drape to fill is probably due to the initiation of current activity. Subunit 5A has a greater sand content which may be evidence of transport in the sediments.

Horizon C is the marked change from laminated chalks to rather pure bioturbated limestones, litho-unit 5C/5D at 1268 m in the upper Berriasian. It is dated from sites 99, 100, 105 and 391 as Tithonian and caused by a down-section change to more argillaceous (red) claystone (table 4.6a). The site chapters agree but could easily be wrong as the interpretation at site 534 has been made on the assumption that the interpretation at site 391 was correct. Shipley (1983) and my direct model agree to within 20 m, which supports my earlier interpretation at site 391 within the limits of resolution.

Horizon D' correlates with a reversed polarity wavelet from 5D/6A at 1342 m in the Tithonian. This is the position at which there is a 20 m transition to significantly more mudstones.

Between D' and D - one more reflection correlates with 6A2/6B at 1429 m; Kimmeridgian, at the top of high velocity, low porosity limestones.

Horizon D correlates with the marked increase in limestone abundance in 7B at 1549 m, early Oxfordian.

Site 534 represents a case study in the application of modelling techniques to the interpretation of seismic profiles. Considerable modelling has been carried out by members of the shipboard party and by myself. All interpretations differ in details which should not be

ignored.

In particular the choice of seismic section and the location of the site on it compared with a given model varies with the author. The site chapter compares with seismic profiles MC88 and MC89 and uses the interpretations from site 391 to 'colour' their judgement. For example the site chapter positions site 534 on the edge of a small basement high. Shipley interprets the same section and places site 534 in the adjacent low. The difference is considerable when you consider that basement differs by .1 s (TWT) between these possibilities (equivalent to 150 m difference at 3.0 km/s). If the physical properties data is well defined for the lower part of the site , such an error must be taken up in the upper layers where the effect of varying TWT by .1 s has a more marked effect on the implied interval velocity. Data used in this study positions site 534 on the opposite side of the basement low, where interpretation is further hampered by lost quality at the depth of horizon A.

The short section of sonic log available suggests that modelling of horizon A by this study is correct. However, it also agrees with Shipley's model. The problem remains as to where this bit of synthesised seismogram fits into the complete section.

Comparisons are still possible with site 391 some 25 km away. There is no record of the Bermuda Rise formation at site 391, and, therefore, no horizon Ac. Horizon Beta was equated with 924 m, the top of unit 3C which is a transitional facies between the claystones of the Hatteras formation and the carbonates of the Blake-Bahama formation. The boundary between these two formations at site 534 is much less gradual. It starts (downwards) with a thick chalk limestone unit absent at site 391C. The claystone returns after 5 m and remains

important if not dominant throughout much of the Blake-Bahama succession. Thus units 4D and 5A of site 534, which are Aptian/ Barremian/Hauterivian in age are lithologically similar to unit 3C of site 391 (Aptian/L. Barremian/U.Valanginian). The positioning of horizon Beta at the top of 3C at site 391 is consistent with drawing it at the 4D/5A boundary (950 m) as per Shipley. So it seems the modelling scheme works well at site 391 but no better at site 534 where, theoretically, the achievement of hitting basement should have considerably refined the modelling. This study also illustrates the variability of stratigraphic division from cruise to cruise. Formation boundaries may easily be transitional when related to facies migration making the 'line' difficult to draw particularly when different teams of sedimentologists are responsible.

Horizon C at site 391 is at 1124 m, the 4A/4B boundary, consistent with the higher correlation of horizon Beta. It has a lower Barremian/ upper Valanginian age. Shipley places horizon C at 1270 m at site 391 and my own model goes even lower. The correlation of horizon C was changed at site 391 following the work of Bryan et al. (1980). The change was from middle Tithonian to top Tithonian (see table 4.6b).

- o O o -

Conclusions on the performance of the schemes for seismogram synthesis and the results of these modelling studies are discussed in chapter seven.

Fig. 5.1 Location map of DSDP sites
in the eastern North Atlantic

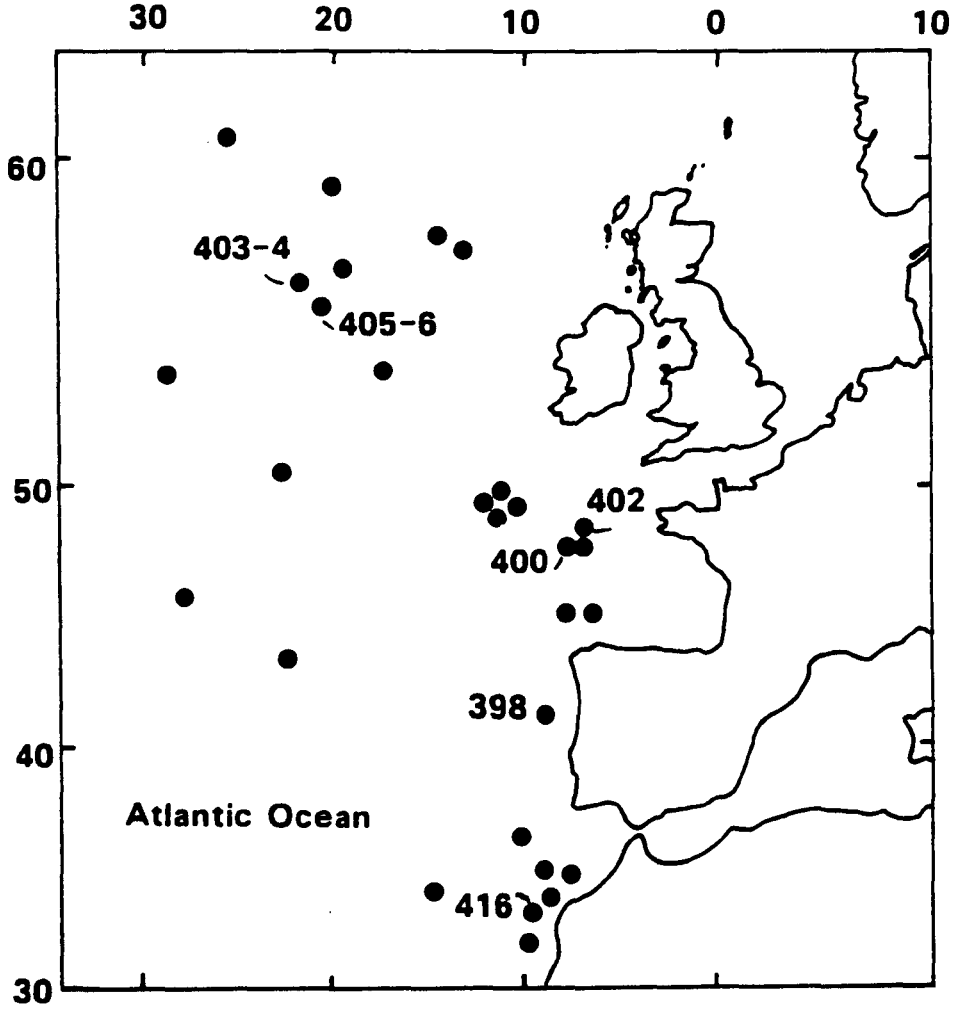

CHAPTER FIVE

Reflectors of the eastern North Atlantic

5.1 Introduction

The study of reflectors in the North American Basin (N.A.B.) has been described in chapters one and four. The same methods of analysis are relevant to reflector studies in other oceanic basins such as the eastern North Atlantic (E.N.A.). I have suggested (section 3.4) that the nomenclature of seismic stratigraphy should be considered synonymous with the palaeoceano-graphic events that bring about the stratigraphy. If this is so, then we may expect similar stratigraphy in the eastern North Atlantic. Although the study of seismic stratigraphy in the E.N.A. developed in parallel with the work in the N.A.B. the nomenclature has not developed in the same way (to some extent, workers have positively avoided drawing correlations.) Nevertheless, seismic stratigraphy has been useful for understanding basin development.

The same schemes for modelling and interpretation of seismic reflectors will be used to study the seismic stratigraphy at 8 sites in the basin (fig. 5.1). The success of modelling varies with the quality of data and a number of limitations to the modelling scheme came to light. These will be discussed in chapter 7 along with conclusions on the nature of reflecting horizons. As in chapter four the number of sites is limited by the availability of data. Only sites on Legs 41 through 77 could be considered; earlier legs provide insufficient physical properties data as a result of spot coring or

Fig 5.2 Comparison of models, Site 403

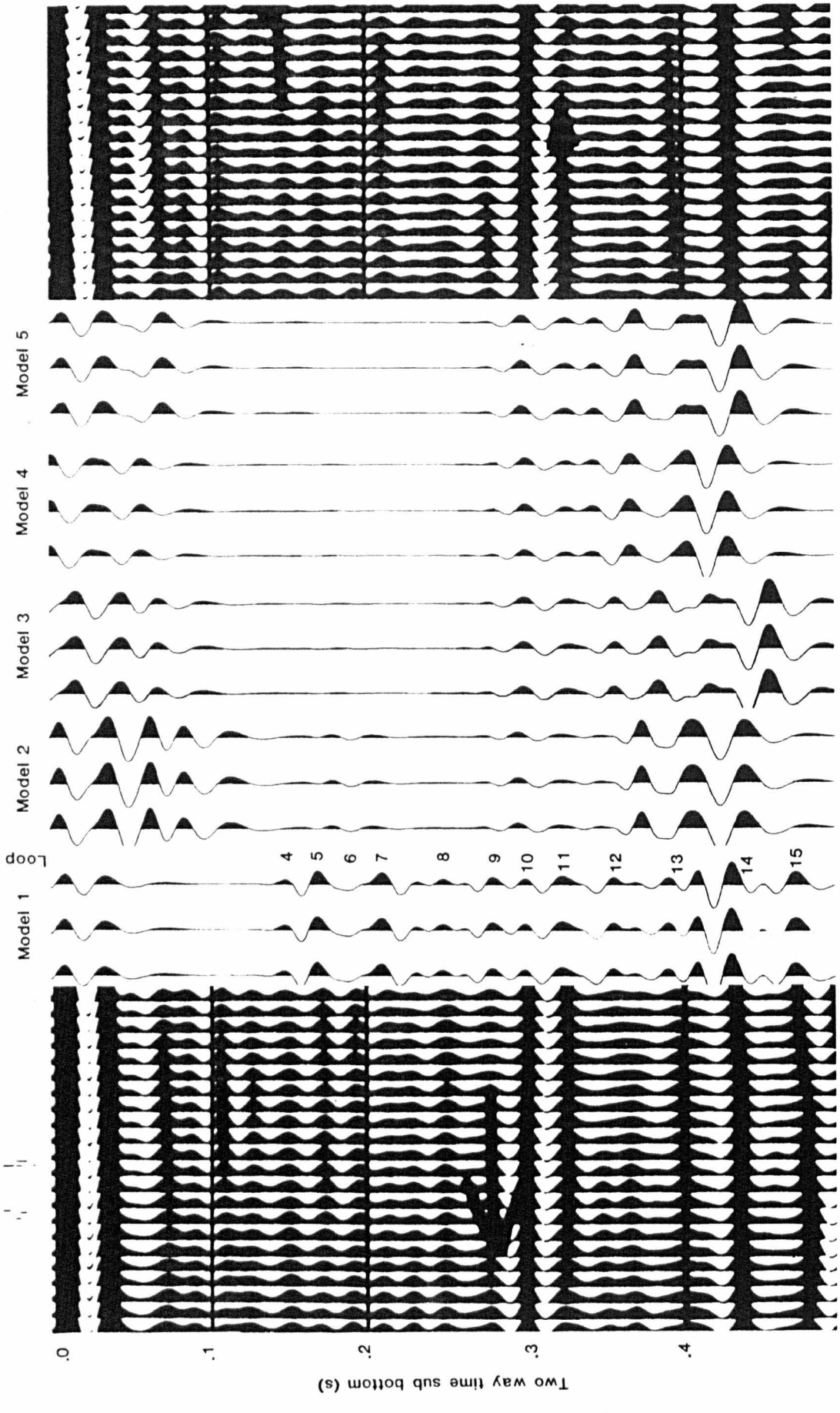

widely spaced sampling and data from later studies of the eastern North Atlantic, which include Legs 79, 80, 81 and 94, could not be obtained. The Norwegian Sea is not included in this study.

5.2 Site studies

The sites will be described in geographic order starting with the most northerly (fig. 5.1).

5.2.1 Sites 403 and 404

Site 403 is situated on the south west margin of the Rockall Plateau. The succession comprises biogenous pelagic sediments with shallow marine tuffs and arkosic sands below 250 m. The hole bottomed in early Eocene-late Paleocene at 489 m. An unconformity between upper Oligocene and upper Miocene was found at 223 m and another between Oligocene and middle Eocene at 232 m. The hole was logged between 125 m and 440 m, while physical property data are only available down to 390 m due to poor recovery from below this depth. I compared a number of modelling methods at this site because physical property data alone was too sparse and wire-line data lacked any information on density (fig. 5.2):

1. A wire-line model based on two sonic velocity logs. No density log was obtained at the site.

2 & 3. Direct and corrected physical property models.

4. Combined model using reflection coefficients from the corrected model and a velocity function from the velocity analysis carried out during processing of the profile.

5. Combined model as 4. but using the velocity function measured by the sonic log.

The complicated form of the source wavelet means that the last loop of each model lacks the interference of later horizons. Therefore, these last loops should not be compared with the profile. The wire-

Table 5.1 Correlation of travel time to depth, site 403.

Reflector	Loop	Travel time (ms)	Depth		
			Model 1	Model 5	Site chapter*
	4	134	125		
	5	157	144		
	6	179	161		
	7	200	175		
	8	237	214		
	9	266	243	230/250	
1	10	288	264	262	ca.260
	11	312	290	(262)	
	12	349	320	333	
2A	13	385	353/370	356/374	ca.365
	14	419	(398)	387/ ?	
2B?	15	458	ca.425		460
2		520	not penetrated		

* Montadert, Roberts, et al, 1979.
(Bracketed depths denote tail-end energy responsible for reflection)

N.B. The site chapter cites reflector 2A at 490 ms sub-bottom, but a figure in the same chapter shows reflector at 528 ms. A estimate for the velocity at this depth would be in excess of 2 km/s. An error of 38 ms at 2 km/s is equivalent to an error in depth of 38 m.
Similarly, reflector 1 is shown at 275 ms and not 300 ms.

Fig. 5.3 Physical properties' models, site 403

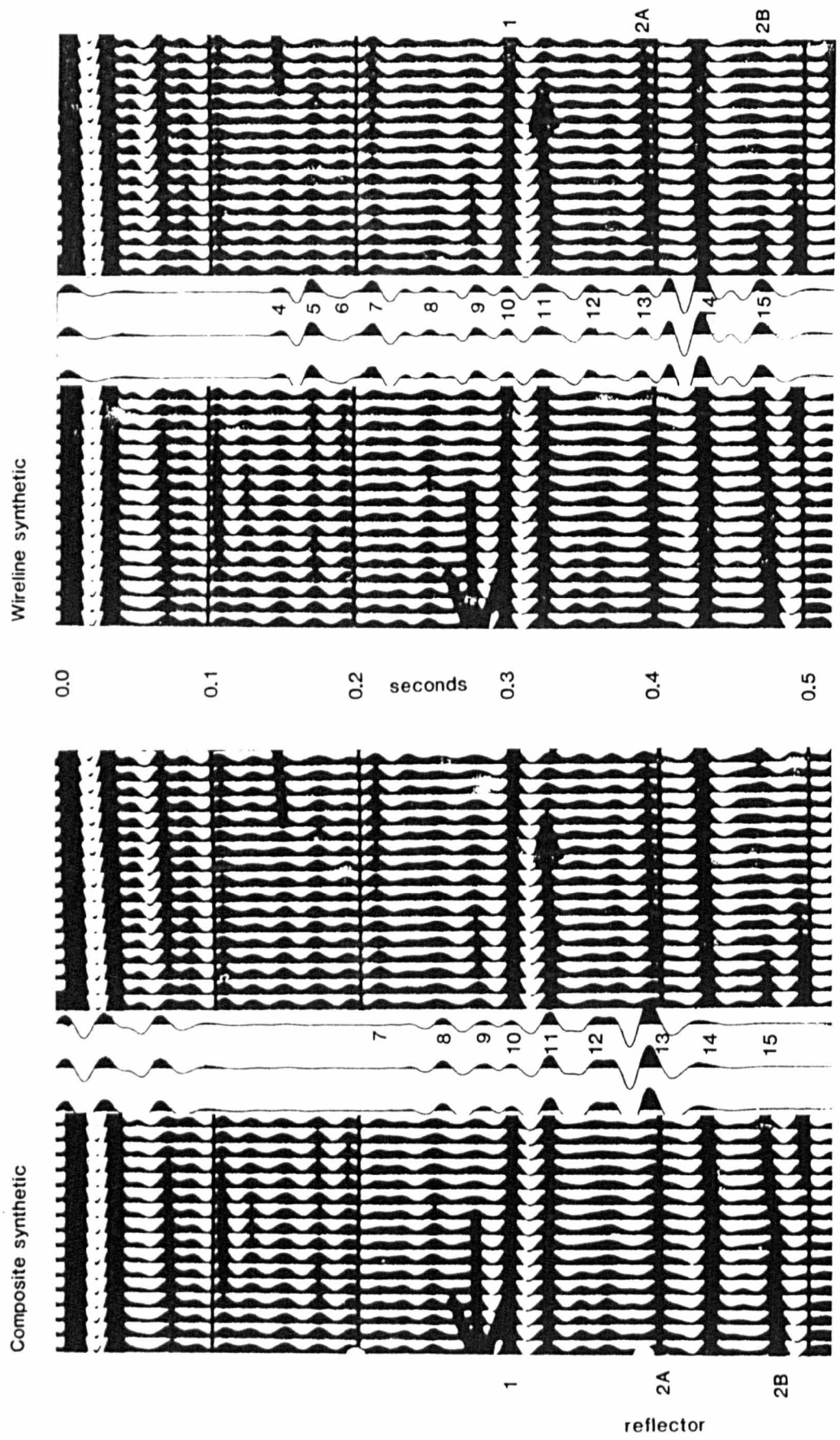

Fig. 5.4 - Depth plot of physical properties, Site 403

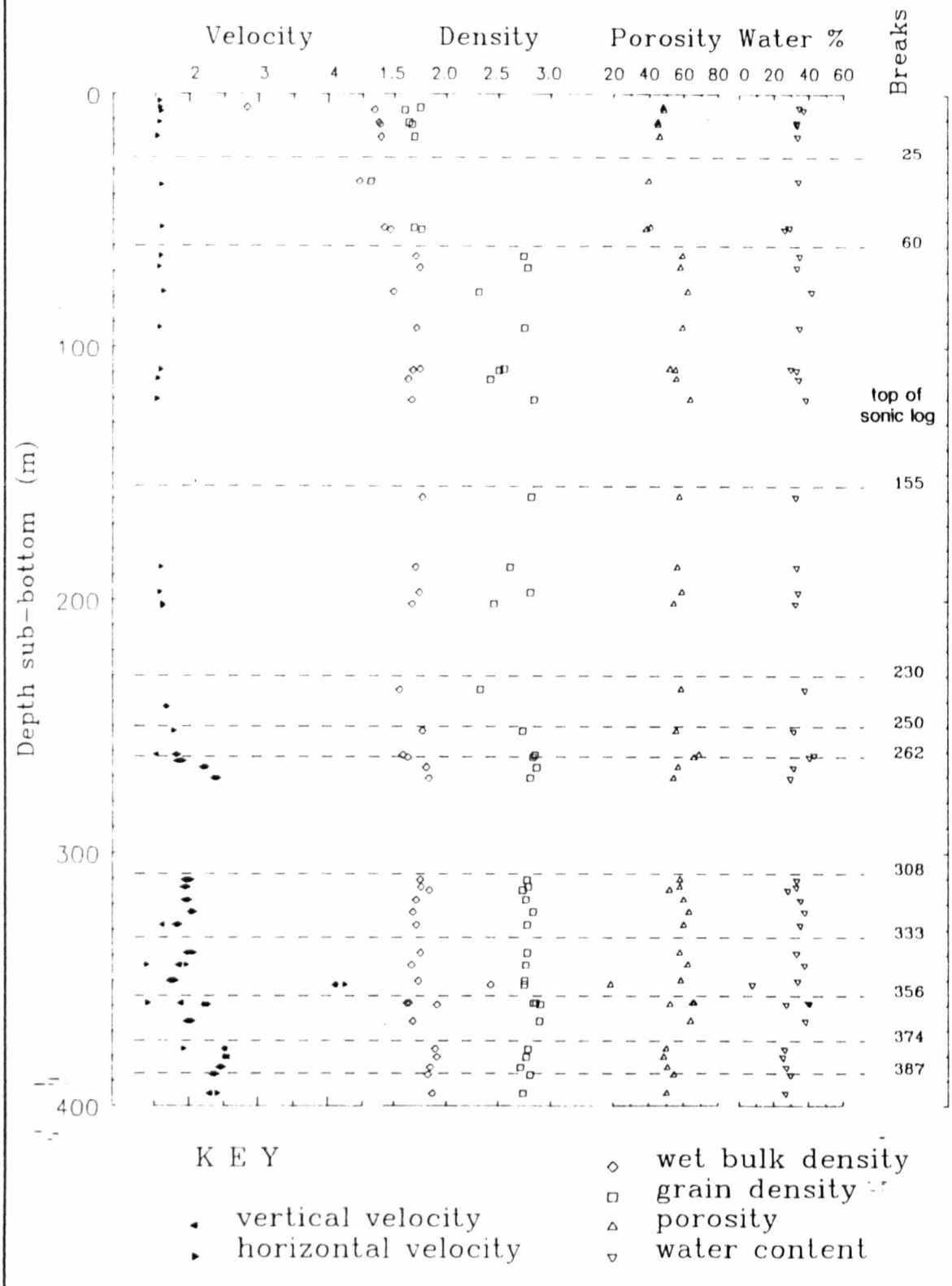

line model is known to yield the most accurate velocity function (see section 3.5) but does not give a very good model at site 403, which may be explained by the lack of density data. The physical property models require closer sampling if they are to give reliable models. The velocity function used to construct model four has only two layers yet is very similar to the other models. The fifth model agrees reasonably with the profile.

The site chapter identifies three reflectors which are used for correlation with nearby site 404. The depth to travel-time correlations of the site chapter compare closely with those obtained using my wire-line model (table 5.1). There is a discrepancy in the site chapter concerning the travel times to reflectors 1 and 2B. The text gives travel times of about 300 ms and 490 ms respectively, but these do not match the horizons shown in the summary figure. A further problem is that because the reflectors are dipping and the hole was drilled ca. 1800 m off section, the pattern of reflection is not expected to give a perfect match. The black and white loops of the profile were numbered as per section 3.5 and interpretation based on models 1 and 5 (see table 5.1 and fig. 5.3).

Two physical property breaks were identified at 20 m and 65 m and correlate with reflections immediately succeeding the sea-bed reflection (fig. 5.4). The break seen at 65 m is marked by a large rise in porosity from around 40% to 60%. Litho-unit 1 is sub-divided at about 45 m based on the change from calcareous mud (subunit 1A) to nannofossil ooze. It is not clear why porosity should show this increase, although it may correlate with the proportion or preservation of foraminifera and the secondary porosity caused by their tests. This horizon is close to the Miocene-Pliocene boundary. Subunit 1B is further divided:

Fig. 5.5 Site survey profile, site 403

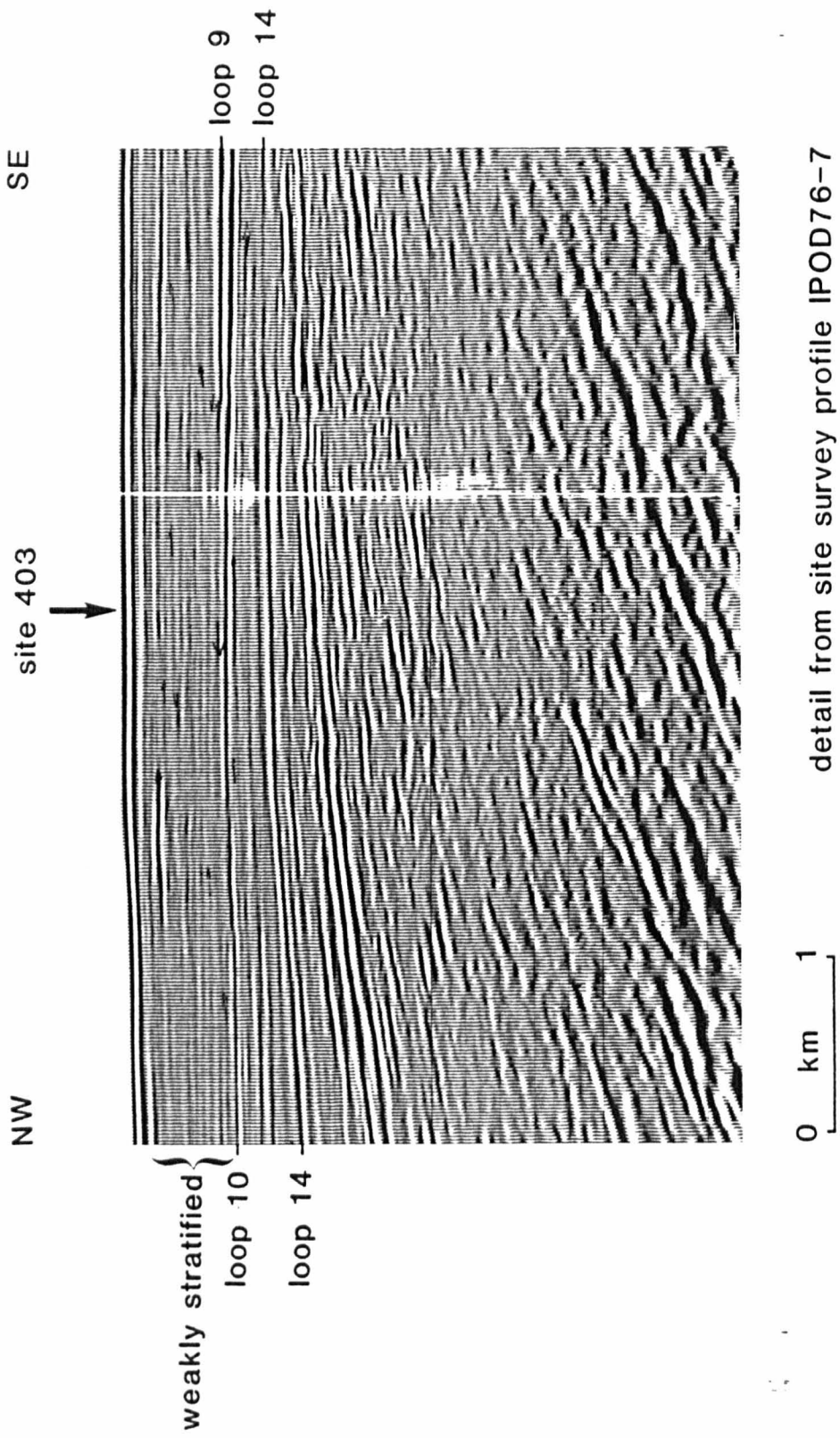

45-110 m foram-nanno ooze

110-190 m nanno ooze

190-220 m foram-nanno ooze.

Loops 2 through 9 belong to a weakly stratified unit (fig. 5.5). The shipboard sedimentologists did not notice any marked changes in this sequence. The only variation being in the proportion of foraminifera tests. There is no variation in the carbonate content.

Loop 8a is correlated with 226 m by my modelling which is the depth of the upper Oligocene/upper Miocene unconformity. There is not a strong reflection and there is no marked break in the physical properties data. This is the top of litho-unit 2.

Loop 9 correlates with 243 m by my modelling. It is the first occurrence (downwards) of siliceous sediments and although it is a weak reflection at the site and to the north-west, it becomes much stronger towards the south-west (fig 5.5). This amplitude variation is probably an interference effect related to bed thickness: the weakly stratified sequence exhibits downlap onto the loop 10 reflector (only poorly seen on fig. 5.5).

Loop 10 is the top of litho-unit 3A at 262 m which comprises interbedded mudstone and tuff. This is a very marked change in lithology and gives a large break in the physical properties. The horizon is labelled reflector 1A by the site chapter and is used for correlation with site 404.

Loop 12 is of low amplitude and consists of two minor loops, the lower of which becomes stronger to the north-west (fig. 5.5). It is more accurately modelled by model 5 which is based on physical property data. Model 5 correlates it to 333 m which is halfway down

Fig. 5.6 Site survey profile, site 404

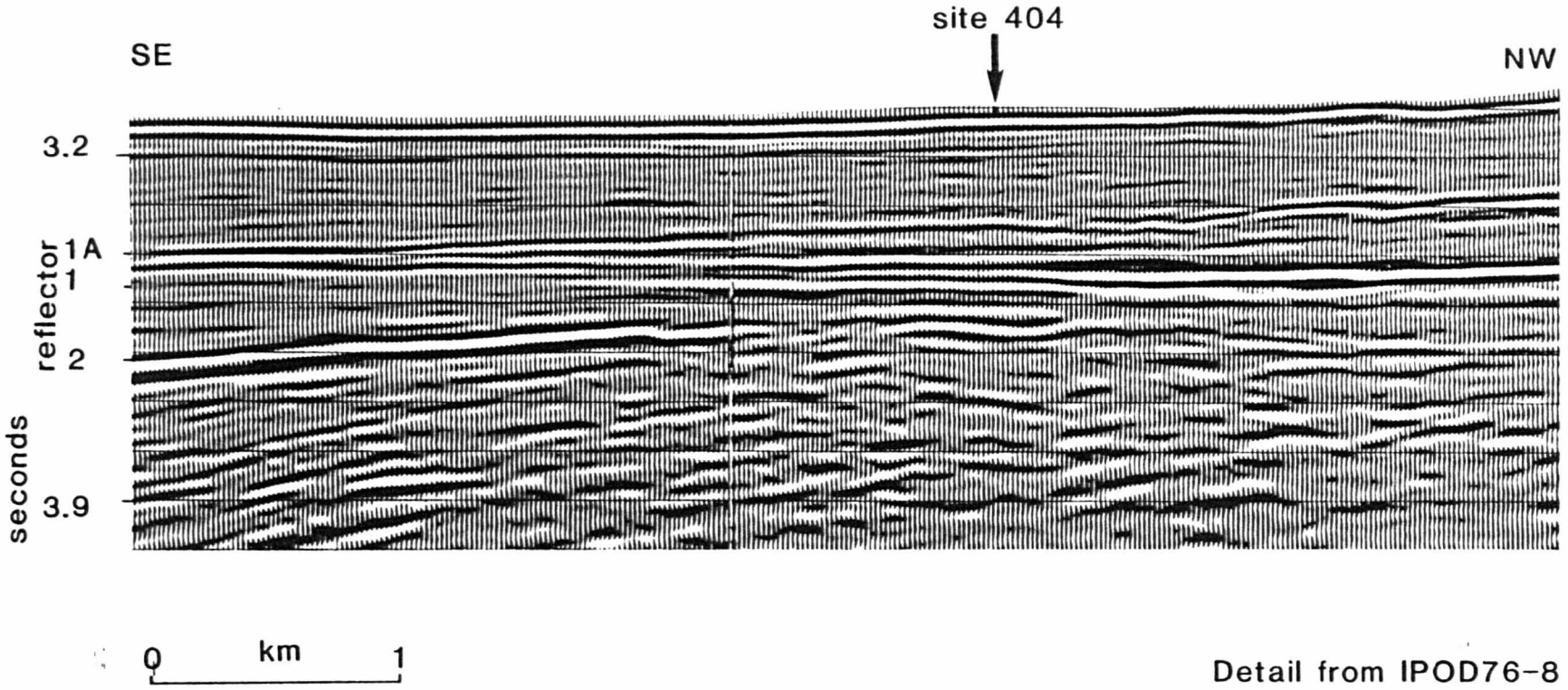

Detail from IPOD76-8

litho-unit 3A at a depth where the proportion of tuff layers within the mudstone and core recovery both increase.

Loop 13 is the interference pattern of reflection from 356 m and 374 m. Lithology changes from mudstone and tuff to lapelli tuff, marking the top of sub-unit 3B. The exact boundary is subjective: velocity shows a large increase at both depths. At 356 m the increase is due to the rise in grain density associated with the change in composition, while the increase at 374 m is due to a reduction in porosity and consequent increase in bulk density (fig 5.4). However, the reflection is caused by a number of tuff horizons of the order of 30 m thick interbedded in mudstone which is becoming more tuffaceous downwards. Consequently, impedance rises transitionally over an interval of 25 m (355 - 380 m).

Loop 15 is given a very high amplitude by both models 1 and 5. Model 5 has no data at this depth (what there is, is only trailing energy from the preceeding event.) Model 1 gives a strong reflection as a result of constructive interference with arrivals from a series of positive reflection coefficients at ca.367 m (loop 13) and a negative series at ca.385 m.

Site 404 was drilled 10 km SSE of site 403. It penetrated 389 m into Neogene calcareous oozes, Eocene porcellanites and limestones and bottomed in glauconitic sands and tuffaceous conglomerates of Paleocene age. One hiatus was found at 199 m between late Miocene and middle Eocene, (Montadert, Roberts, et al., 1979), (fig. 5.6).

The hole was spot cored to 170 m because the hole was expected to have identical stratigraphy to that found at site 403. Consequently, physical properties data are rather lean over this interval, so it is

Fig. 5.7 Direct physical property model, site 404

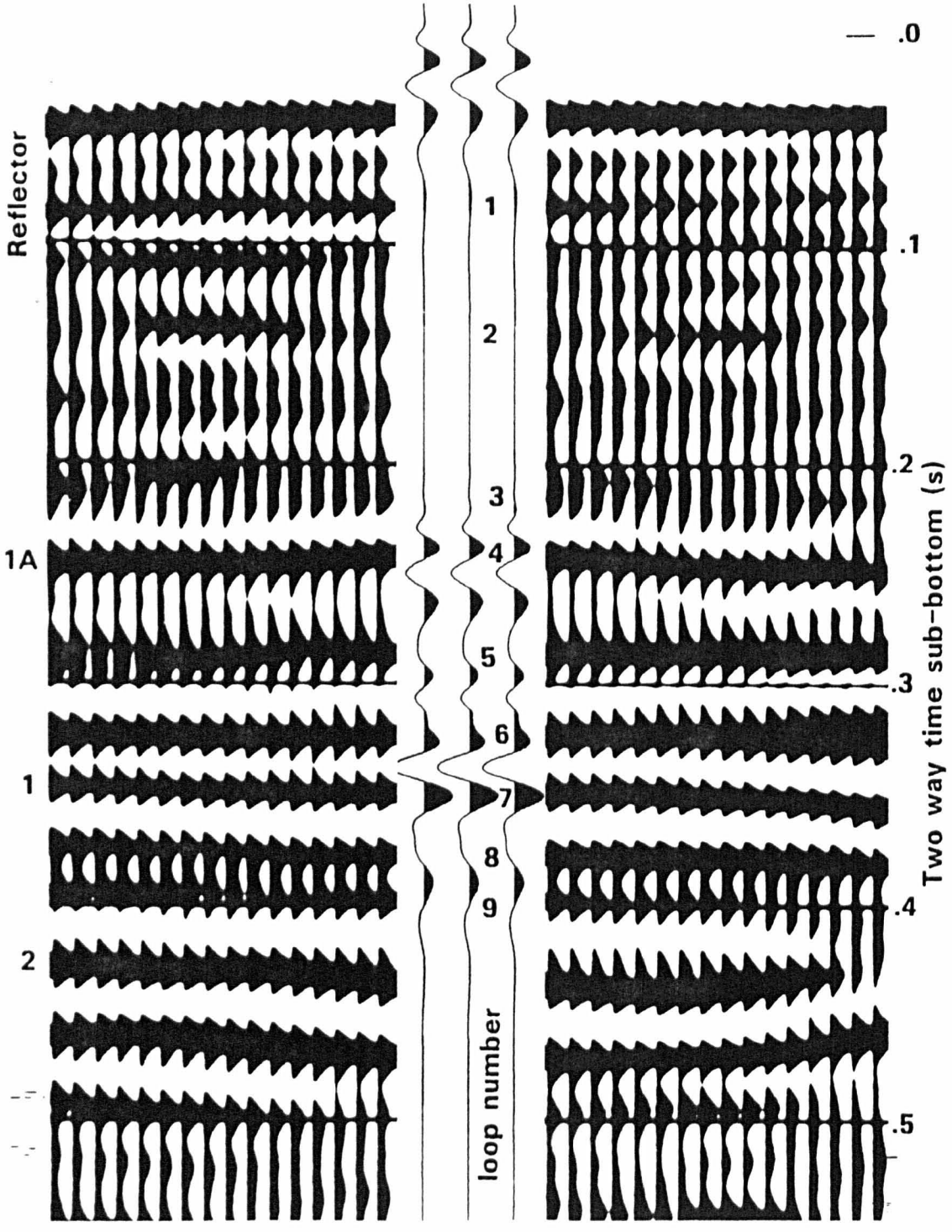

Table 5.2 Correlation of travel time to depth, site 404.

Reflector	Loop	Travel time (ms)	Depth	
			This study	Site chap*
1A	4	230	218	195
	5	273	284	
	6	311	310	290
1	7	335	340	
	8	363	ca.365	
	9	385		
2	10	410		360

* Montadert, Roberts, et al, 1979.

Fig. 5.8 Depth plot of physical properties, Site 404

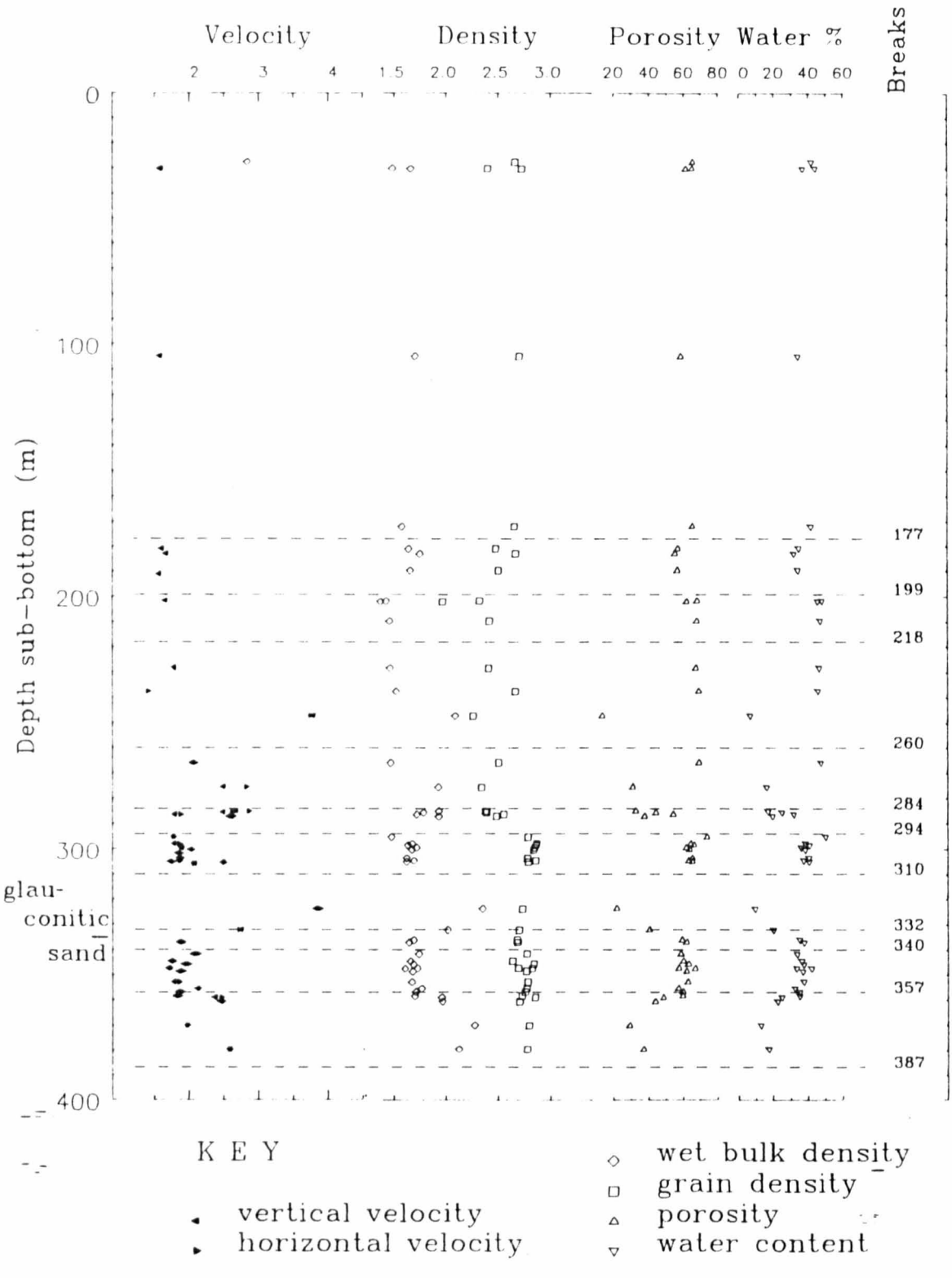

likely that the upper sediment velocity is inaccurately estimated. The direct model compares closely with the profile for the interval 170 - 389 m (fig. 5.7).

The site chapter (Montadert, Roberts, et al., 1979) recognises three reflectors that are correlated with site 403 (fig. 5.7). They are not easy to trace due to thinning of the stratigraphy which causes changes in the interference of reflections. The site chapter shows the results of velocity analysis performed on the multichannel data (see table 5.2). The values given are lower than both of the physical property models and are unreasonable compared with the velocity of sea water at this depth. In contrast the correlation between reflectors and lithology implies velocities that are greater than those of the models, although they have been based on the same physical properties data. If a correction for the 17 m discrepancy (see below) in the sea-bed depth is made, the interval velocities of the direct model agree with those of the site chapter.

Sites 403 and 404 illustrate the problem of seafloor identification described in section 3.3. Both sites show differences in the depth of the sea bed as measured by the echo-sounding PDR and by the 'bottom felt' criterion of the drill string. At site 404 this discrepancy is 17 m. The first reflector which can be interpreted using modelling is loop 5 at .311 s (TWT) and is correlated with 218 m. It is not particularly evident from the depth plot of physical properties (fig 5.8) but is clearly shown by a sudden reduction in the recovery of core from ca. 25% for the interval 199 - 218 m down to less than 1% for the interval 218 - 284 m.

Reflector 1A (loop 4) of the site chapter is more difficult to explain. This is partly due to a lack of data between 113 m and 170 m

and partly the small contrast in impedance across the unconformity at 199 m. This contrast is of negative polarity and correlates with loop 4a. This is a very weak event at site 404 but increases in amplitude to the north-west (fig. 5.6b). Traced south-west the same reflector again increases in amplitude. As at site 403, this may be explained by the interference pattern from sediment wedges, both above and below the unconformity and the variation in impedance contrast brought about by the juxtaposition of different lithologies across the unconformity.

Loop 6 is mostly tail end energy from 218 m, but also correlates with a minor positive break at 260 m. The lithology changes from calcareous chalk (above) to volcanic tuff (below). The latter has much higher velocity and lowered porosity as well as displaying the highest degree of anisotropy of any formation recovered at site 404 (fig 5.8). (Anisotropy is taken to be the difference between horizontal and vertical compressional velocity, and may be seen by the separation of velocity symbols on the physical properties depth plot.)

Loop 8 is correlated with 284 m. The interval velocity between 218 and 284 m is overestimated due to poor data resulting from low recovery. The direct model was corrected. This is similar to loop 6, being delineated by a change in the core recovery. The physical properties do not show any great change.

Loop 8a is not a strong white loop on the profile but according to my modelling it should be! It correlates with 294 m and is produced by the appearance (downwards) of tuffaceous glauconitic mudstone. The physical properties show it to be a strong negative break: velocity decreases compared to the overlying unit, porosity increases reducing wet bulk density and grain density rises abruptly. The character of

the physical properties depth plot (fig. 5.8) shows considerably less variation than the overlying units, although there is no anisotropy in the velocity data. The grain density is witness to a compositional change but the constancy of measurements suggests the sediment is more lithified.

Loop 9 does not correspond directly to a physical property break. Rather it is the interference of the negative break at 294 m and a positive break at 317 m. The latter is marked by a reduction in the grain density and variable measurements for the other parameters.

It is possible that there is a distinct lithological unit consisting of glauconitic sandstone between ca. 310 m and 332 m which gave very poor recovery. An earlier version of the physical properties' stratigraphy did not allow for this high velocity layer because no measurements allowed it to be delineated. The final model allows a velocity of 4 km/s for this bed. The mis-match of model and profile at loops 8 and 9 may be explained by such a layer.

Loop 10 (reflector 2 of the site chapter) is produced by the interference of a negative and a positive break at 332 m and 357 m respectively. The first of these is effectively the base of the glauconitic sandstone, where the lithology changes to tuffaceous mudstone. The velocity data displays a small degree of anisotropy indicating that this layer of mudstone is more lithified than the layer at 294 - 310 m (fig 5.8). Otherwise the two intervals have very similar physical properties. Below 357 m the lithology changes to sandstone, the coarseness of which increases downwards, ending in conglomerate at total depth. Porosity decreases elevating bulk density and velocity.

Fig. 5.9 Corrected model and reflection coefficient log, site 404

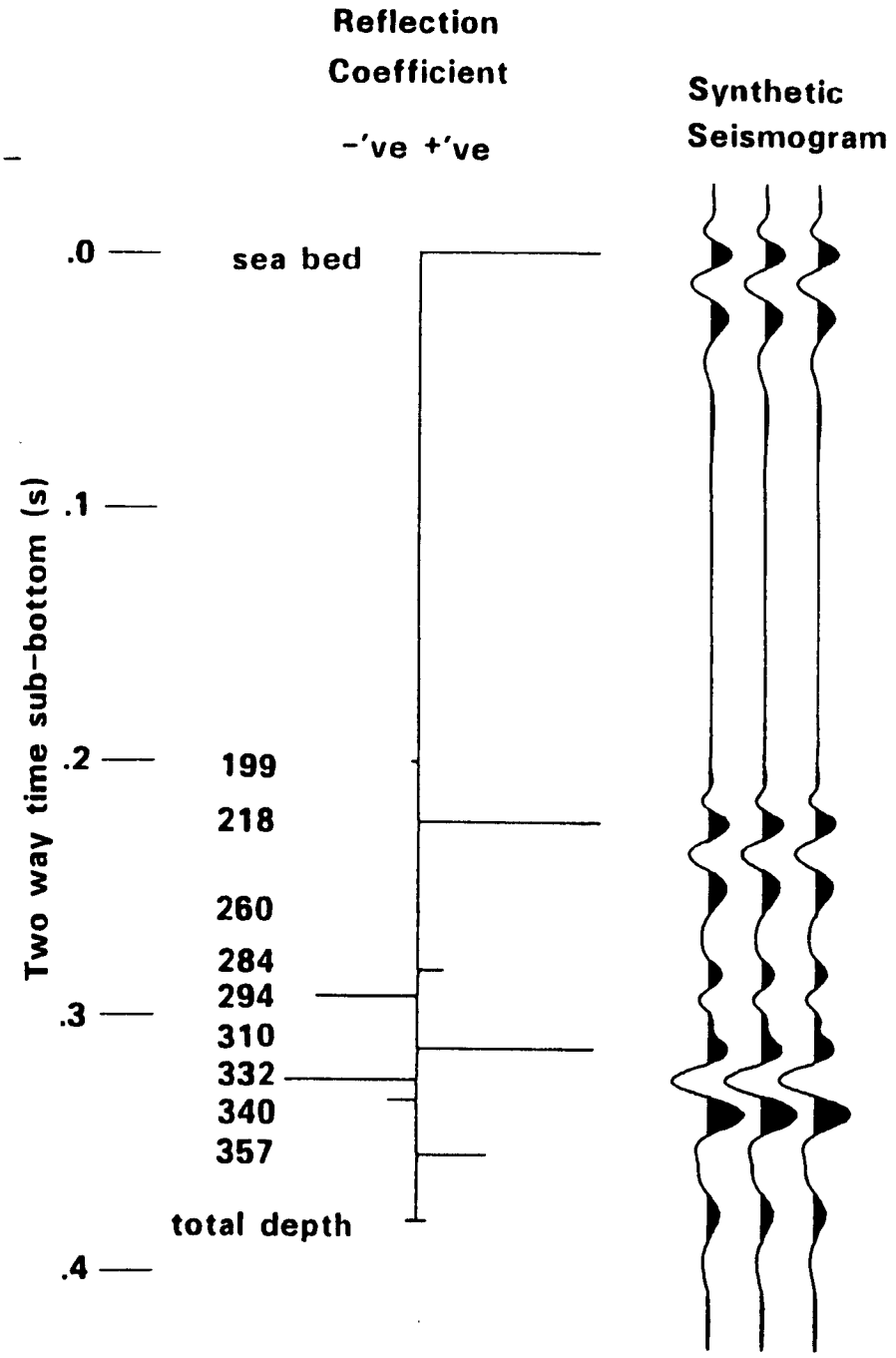

*Depths to boundaries in meters below sea bed

The site chapter correlations (see table 5.2) imply unlikely interval velocities. The similarity of our interpretations for reflector 2 shows my model to be plausible. The implication is that my original model (the direct model) is correct.

The modelling is made difficult by low recovery and a small number of measurements, so the correlations given must be considered tentative. They are made more difficult by the geometry of the layers which thin eastwards. The complex nature of the wavelet produces considerable interference between successive reflectors causing the pattern to change laterally. Normally, strong positive loops may be expected to match black loops on the profile. The last two horizons of the direct model interfere in such a way that positive events align with white loops (fig. 5.9). This underlines the need for seismogram synthesis as part of seismic interpretation. Simply matching lithological breaks with prominent reflectors causes errors. The reflectors used to correlate with site 403 suffer from the same thinning problem, so it must be considered doubtful whether they have been accurately traced. An error of one loop is approximately 30 m.

The unconformity at 199 m (top Eocene) and the appearance of porcellanite is expected to give a much bigger reflection or a change in seismic character. This is the most important lithological change and the easiest/surest way to tie the model to profile.

The widely differing lithologies make the use of a simple velocity/porosity function unsuitable. The changes in grain density clearly show the compositional variation and suggest this parameter may be useful in modifying the simple velocity/porosity function.

The contrasting lithologies show how lithological variation can be abrupt and produce large reflection coefficients.

The palaeo-history of site 404 is one of rifting followed by progressive subsidence of the passive margin. The most abrupt lithological changes occur in the near-shore, shallow marine facies and not the ooze dominated deep sea. Such a sequence is to be expected at sites near to the continental rise or over the transitional crust. No such clastic or volcanic influence is expected at mid-ocean-ridge-type spreading (Iceland being an exception).

5.2.2 Sites 406 and 405

Site 406 was drilled on the abyssal plain 8 km SW of the Rockall plateau. The hole was continuously cored between 410 m and total depth of 820 m and recovered pelagic carbonates of Pliocene through middle Eocene age. The site has already been discussed in section 3.5.2 so no detailed description of the correlation of reflectors will be given, but some general points bear repetition.

The site survey profile (figs. 3.9-10 and 3.12) may be divided at loop 11a into two acoustic units that may be described as weakly stratified (above) and strongly stratified (below). Loop 11a marks the top of lithological unit 3 which is lower Miocene to middle Oligocene in age. The sediments of Eocene age, which are commonly acoustically stratified correlate with loop 14 and below. The differential diagenesis of calcareous, siliceous and clastic sediments may be attributed with causing contrasts in impedance. These contrasts are then responsible for the stratified character of the lower acoustic unit. The conclusions drawn in section 3.5.2 note that the

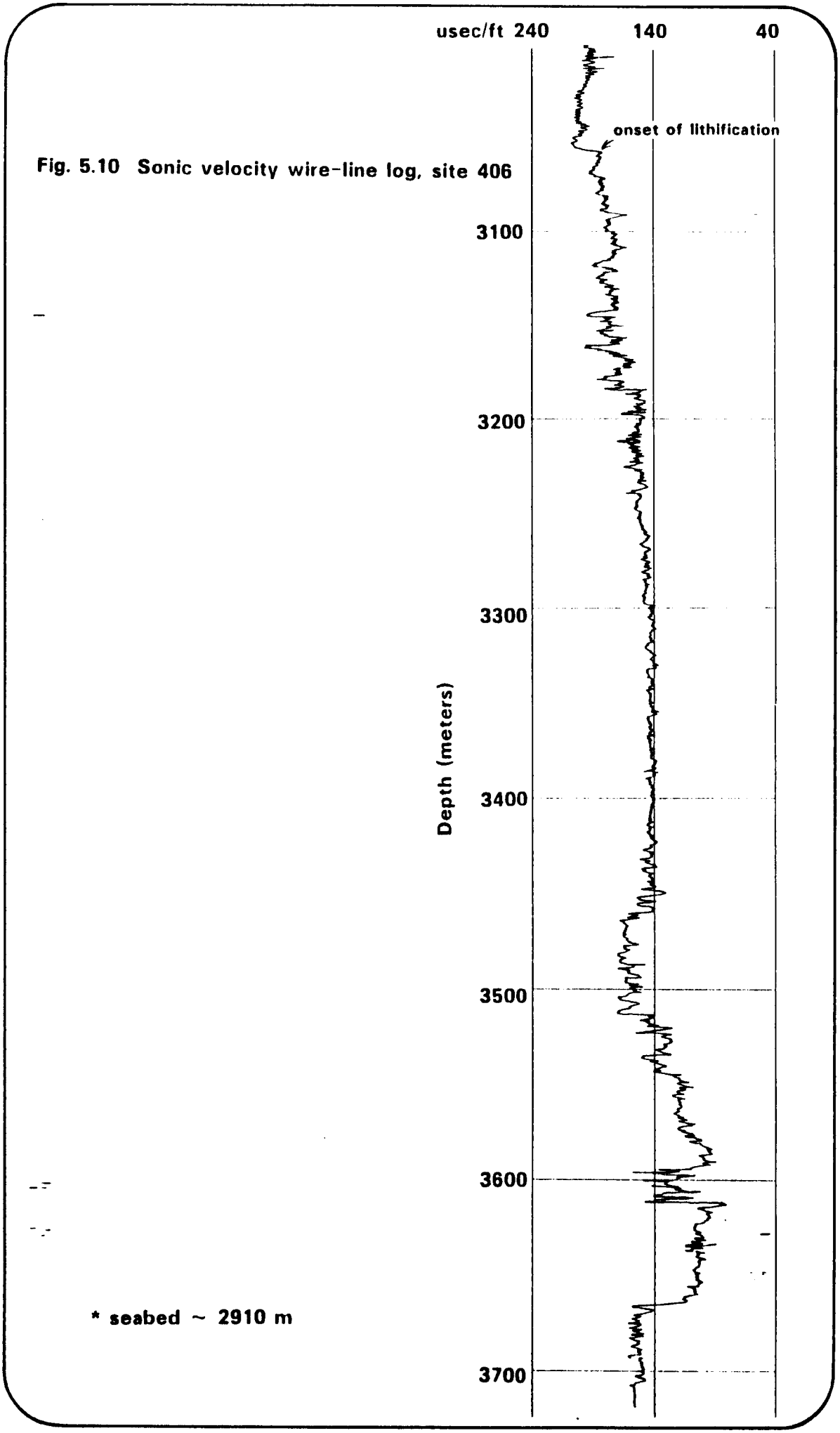

Fig. 5.10 Sonic velocity wire-line log, site 406

Fig. 5-11 Seismic profile IPOD76-2 between sites 405 and 406

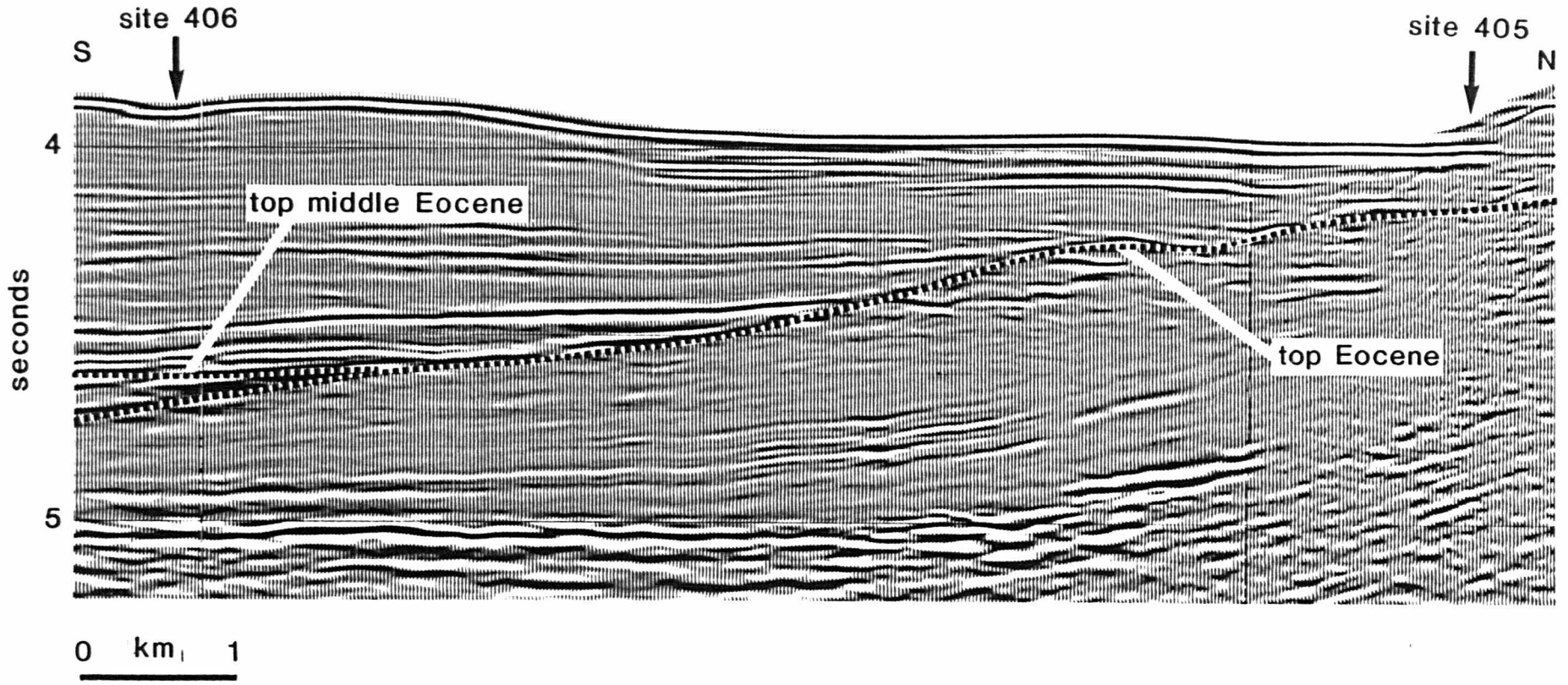

reflectors are caused by lithological variation, although the amount of such variation may be slight. The importance of diagenesis of siliceous sediments was shown to be foremost in causing the stratified nature of Eocene sediments. The presence of opal-CT shows a good correlation with the formation of reflectors; its downward appearance generally coinciding with a strong break in the physical properties. At site 406 such variation is also important in the Oligocene.

The upper acoustic unit correlates with pelagic oozes of upper Miocene to recent age. Variations in composition were noted in the lithological summary (Montadert, Roberts, et al., 1979) but coring is not sufficient for modelling of this interval. The wire-line logs show lithification starts at 3060 m (159 m) where velocity through sediment exceeds that of sea water (fig. 5.10). This depth correlates approximately with 0.21 s (TWT) and may correlate with loop 4. No great change is seen in density, which may indicate that this is some kind of compaction horizon. The mismatch between wireline model and profile at loop 4 is largely due to cyclicity in the density log caused by boat heave.

Site 405 is situated 10 km north of site 603 at the base of the continental rise (fig. 5.11). At this point the sea floor rises to the north producing high amplitude hyperbolae on the seismic profile which obscure reflectors and make interpretation difficult. The sediment wedges onlap to the north and cause ambiguity in the tracing of reflectors between sites 405 and 406.

Paleontology shows the overlap of reflectors is not very large (assuming reflections are roughly chronostratigraphic). The unconformity at the top of the Middle Eocene occurs at 765 m at site 406 only 24 m above total depth, while it is found at 100 m at site

Fig.5.12 Depth plot of physical properties, Site 405

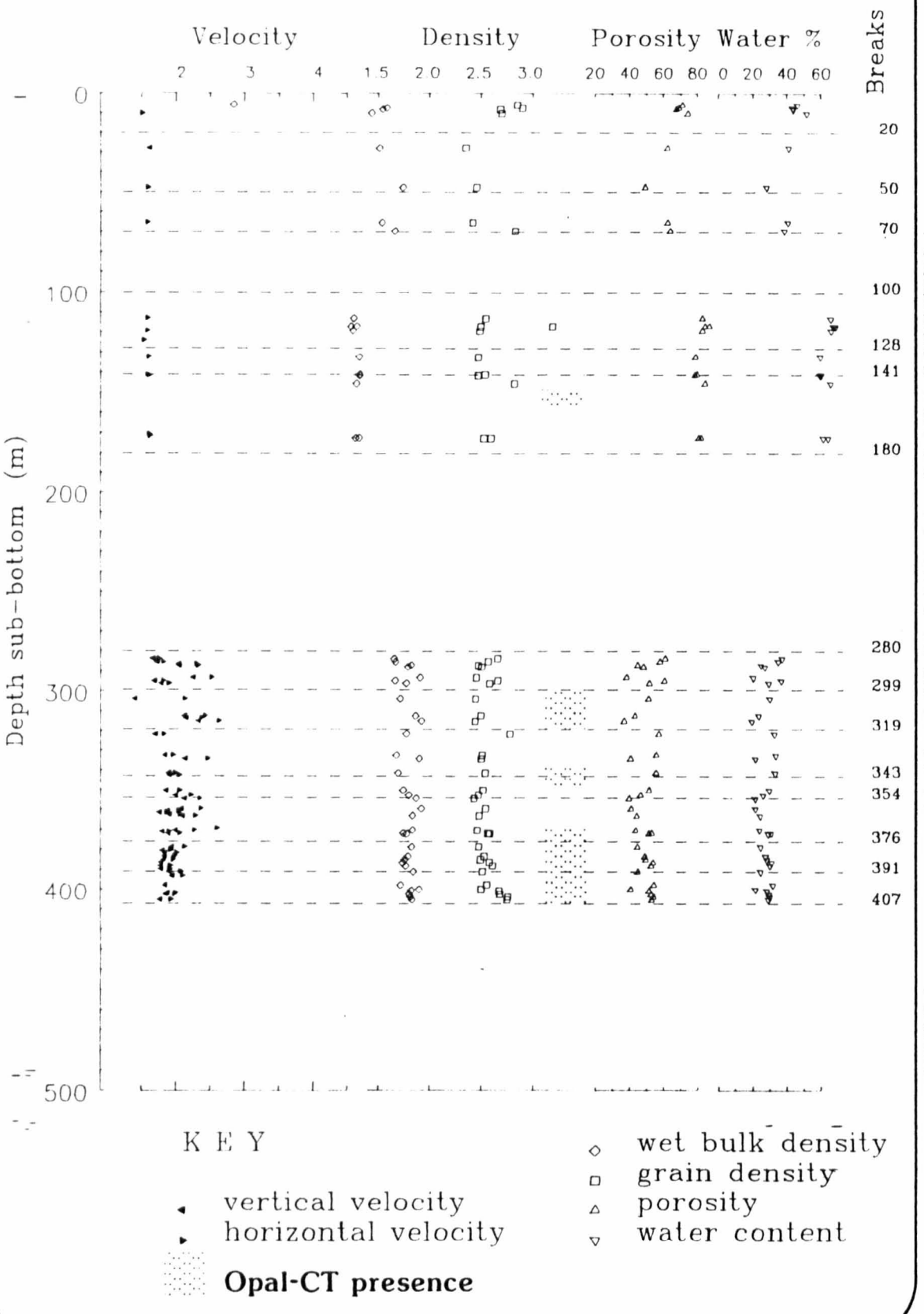

405 (fig. 5.11). A number of problems degraded modelling at site 405. The most acute of these is the quality of the profile. However, a number of useful points concerning the modelling can be made. The delineation of stratigraphy based on physical property measurements (fig. 5.12) not only coincides with the lithostratigraphy but affords further, more detailed sub-division.

The simple relationship between opal-CT and reflector formation is seen to be more complex. Apart from a shallow occurrence at 150 m (core 405-17-1) opal-CT is not seen until 300 m and then falters twice before becoming a constant constituent of the sediments. The first layer of opal-CT is between 302 m and 320 m, which matches closely the physical property unit defined by breaks at 299 m and 319 m (fig. 5.12). Porosity is lower than in adjacent beds (above and below) and velocity is 15% faster. The next layer with opal-CT is between 340 m and 350 m and does not show the same characteristics. although porosity shows its most marked decrease downwards at between 343 m and 354 m, yet higher velocities occur in a layer with amorphous silica between 354 m and 376 m. Opal-CT is present below 369 m, but velocity and porosity both indicate a more open framework and consequently lower impedance. (N.B. Amorphous silica is the primitive precursor from which opal-CT is formed).

The velocity functions of the direct and corrected physical property models fall either side of the in situ function measured by the sonic log. This implies that 60% of the unrecovered material was more argillaceous than the recovered lithology.

Fig. 5.13 Direct physical property model, site 400

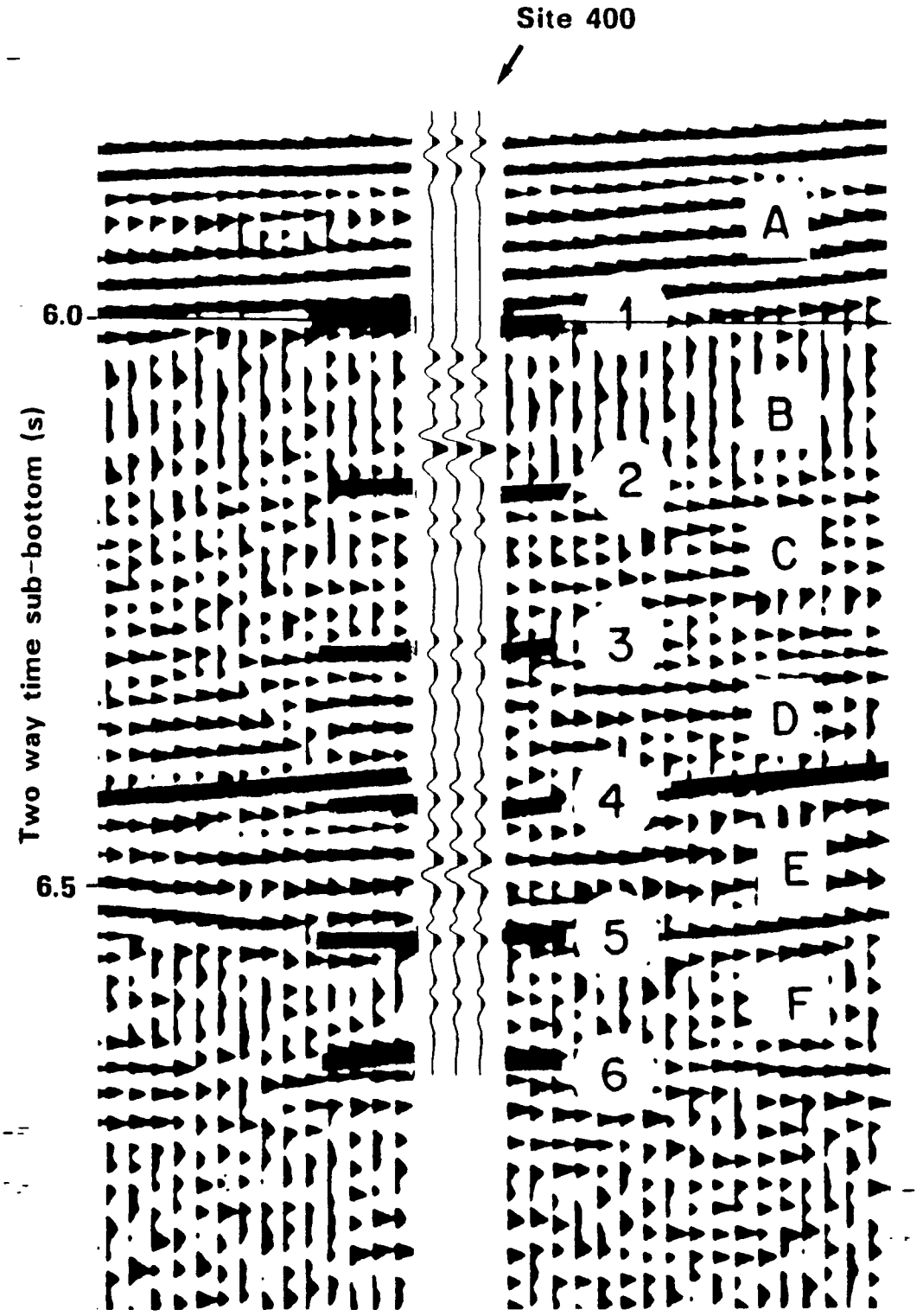

Fig.5.14 Depth plot of physical properties, Site 400

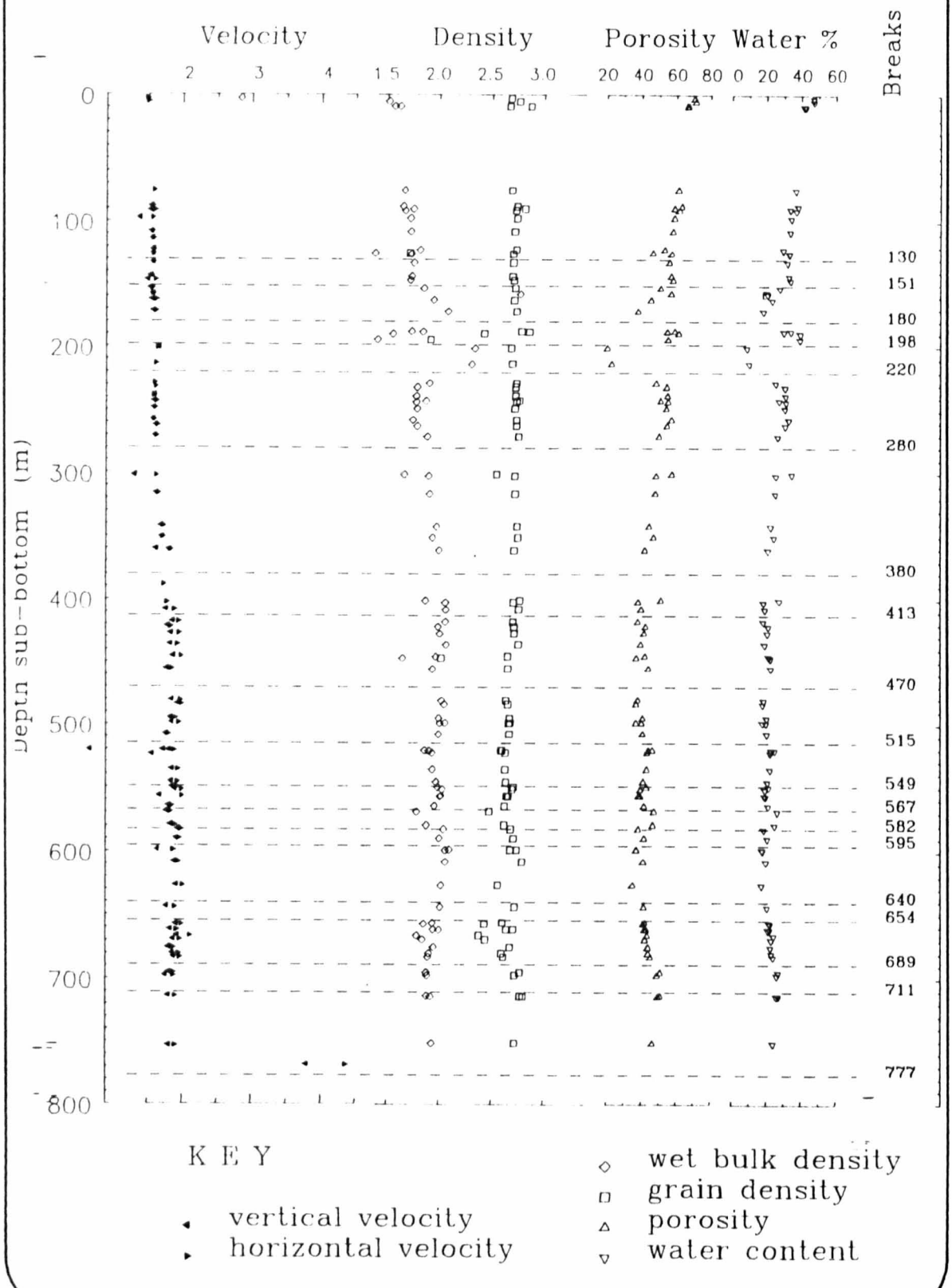

5.2.3 Site 400

Site 400 was drilled at the base of the Meriadzek Escarpment WSW of Brittany (fig. 5.1). The succession consists of 600 m of Paleocene to Recent nannofossil ooze which becomes more siliceous with depth. About 10 m of late Cretaceous chalk overlies 120+ m of middle Cretaceous carbonaceous claystones and calcareous mudstones. Hiatuses between Pliocene and Miocene, Oligocene and middle Eocene, Paleocene and Upper Cretaceous and between Campanian and Albian were found.

Physical properties data is sufficient to permit modelling, but the high dominant frequency of the seismic profile (40 Hz) means that greater resolution is required if a proper fit between model and profile is to be achieved. The direct model yields the closest fit and was used for interpretation,(see table 5.3 and fig. 5.13). The overall difference between my correlation and that of the site chapter (Montadert, Roberts, et al., 1979) is that I locate most horizons slightly shallower. The correlations of the site chapter were made with the aid of a synthetic seismogram study also based on the physical property data. Their model is not necessarily more accurate.

The site chapter recognises six acoustic units (A-F) delineated by six reflectors (1-6), (fig. 5.13). The most critical correlation is reflector 1 as there is no recovery between 10 m and 70 m. The lithology is mostly calcareous ooze with some marl. The even decrease in porosity and water content show it to be unconsolidated (fig. 5.14). It is somewhat surprising that it should have such a reverberant acoustic character. The correlation of the site chapter implies an interval velocity of 1.8 km/s which is too high. My modelling gives a velocity for the upper sediments of 1.63 km/s which is more reasonable. Therefore, I correlate reflector 1 with 130 m

which is the boundary between subunits 1A and 1B. The lithological difference between the two units is the appearance of nannofossil chalk in subunit 1B, which suggests the boundary is a consolidation horizon. Porosity and water content decrease throughout subunit 1A, but are more constant over subunit 1B (fig. 5.14).

The correlation at reflector 2 is not very good. It might be better drawn at 260 m, where the physical properties show a small increase in velocity and wet bulk density and a reduction in porosity and water content.

Reflector 3 is correlated with 380 m, 30 m above the base of unit 1. From the depth plot of physical properties (fig. 5.14) the delineation of the actual depth is seen to be subjective due to a gap in the data. Compaction proceeds throughout much of the acoustically transparent unit B, but porosity levels off below 380 m (approx.): cementation may be commencing or the minimum packing structure is reached.

Reflector 4 is the hiatus between early Oligocene and middle Eocene at 515 m. Acoustic unit D shows strong stratification which is not seen in my direct model. I have drawn only one physical property break within this unit, although the lithological log indicates greater variation, but more closely spaced data is needed to increase resolution. As at site 406 the Oligocene is found to have a high silica content, which coincides with greater lithification as witnessed by development of acoustic anisotropy (fig. 5.14). Once again the appearance of silica in the sediment correlates with strong reflectivity.

Reflector 5 is the product of two negative physical property breaks at 640 m and 654 m. These depths correlate with two unconformities

Fig. 5.15a High resolution profile GM402, site 402

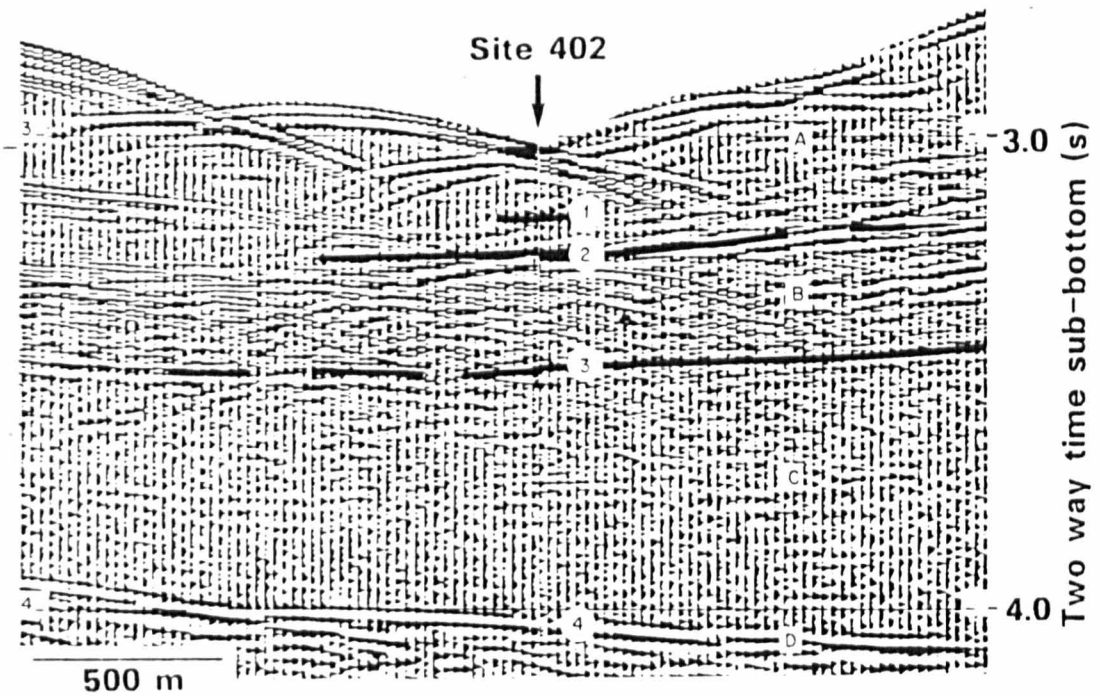

Fig. 5.15b Site survey profile OC301, site 402

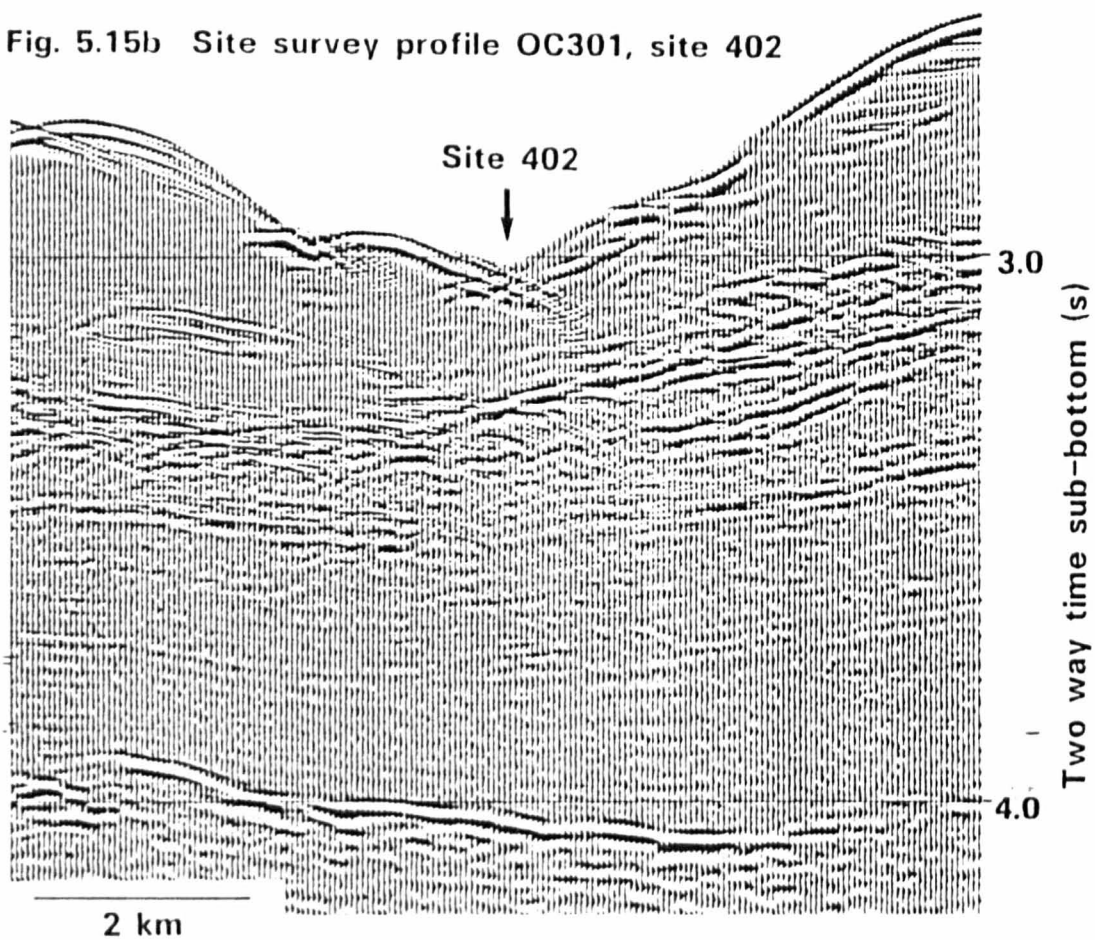

which bound litho-unit 3. Acoustic unit F is markedly quieter in character than the preceeding units and is typical of Aptian/Albian black claystone sequences elsewhere in the North Atlantic. However, there is a fairly high carbonate content, particularly in subunit 4A and the organic content is terrigenous rather than the product of stagnant bottom water (Montadert, Roberts, et al., 1979). The carbonate content decreases downwards from carbonaceous chalk at 654 m to calcareous mudstone with carbonaceous mudstone at 682 m. Such interbedding of distinct lithologies explains the scattered density measurements and the increase (downwards) of porosity (fig. 5.14), but the definite cause for the change in acoustic character is not obvious. The CCD does not show a sharp change in depth; the lithological variation is gradational. One explanation may be that the lower impedance of the claystones results in generally smaller impedance contrasts, which is the same as reduced reflectivity.

5.2.4 Site 402

Site 402 is situated in a canyon cut in the Amorican rise south-west of the Brest peninsula. The site survey was carried out using the high resolution flexotir method (fig. 5.15). Although the profile has been migrated it remains of poor quality, with many diffraction hyperbolae remaining. Interference from these hyperbolae is worse in the vicinity of the canyon where the sea-bed reflection is particularly obscure. The site chapter interprets the sea-floor at 3.06 s (TWT) and this has been used in modelling. Sedimentary reflectors are difficult to trace on the profile and are weaker at the location of the site, which may be due to the defocussing effect of bathymetry. The top acoustic unit thickens to either side of the site, which reduces the value of interpretation as it is more difficult to extend it away from the

Fig. 5.16 Depth plot of physical properties, Site 402

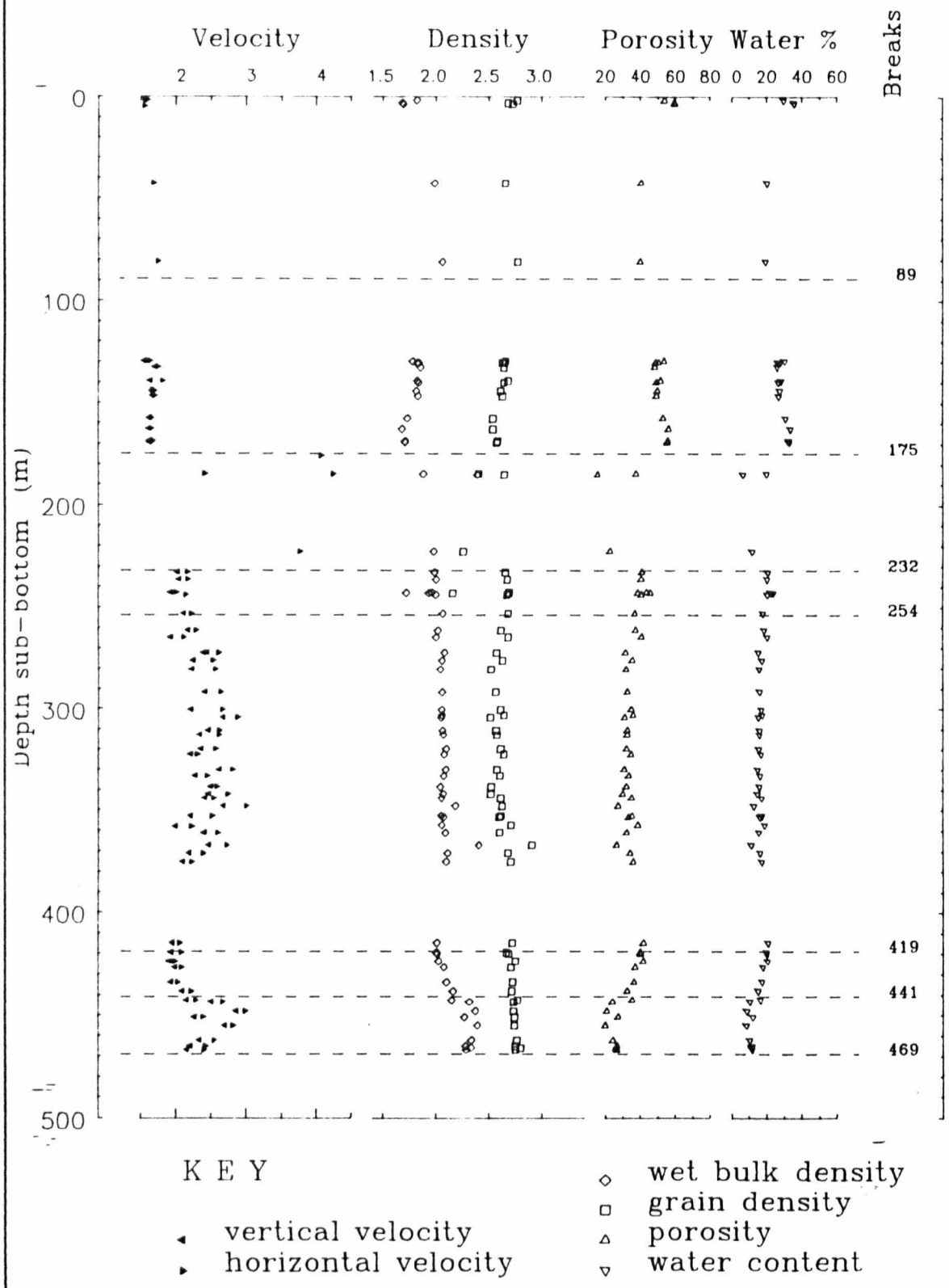

Fig. 5.17 Comparison of models, site 402

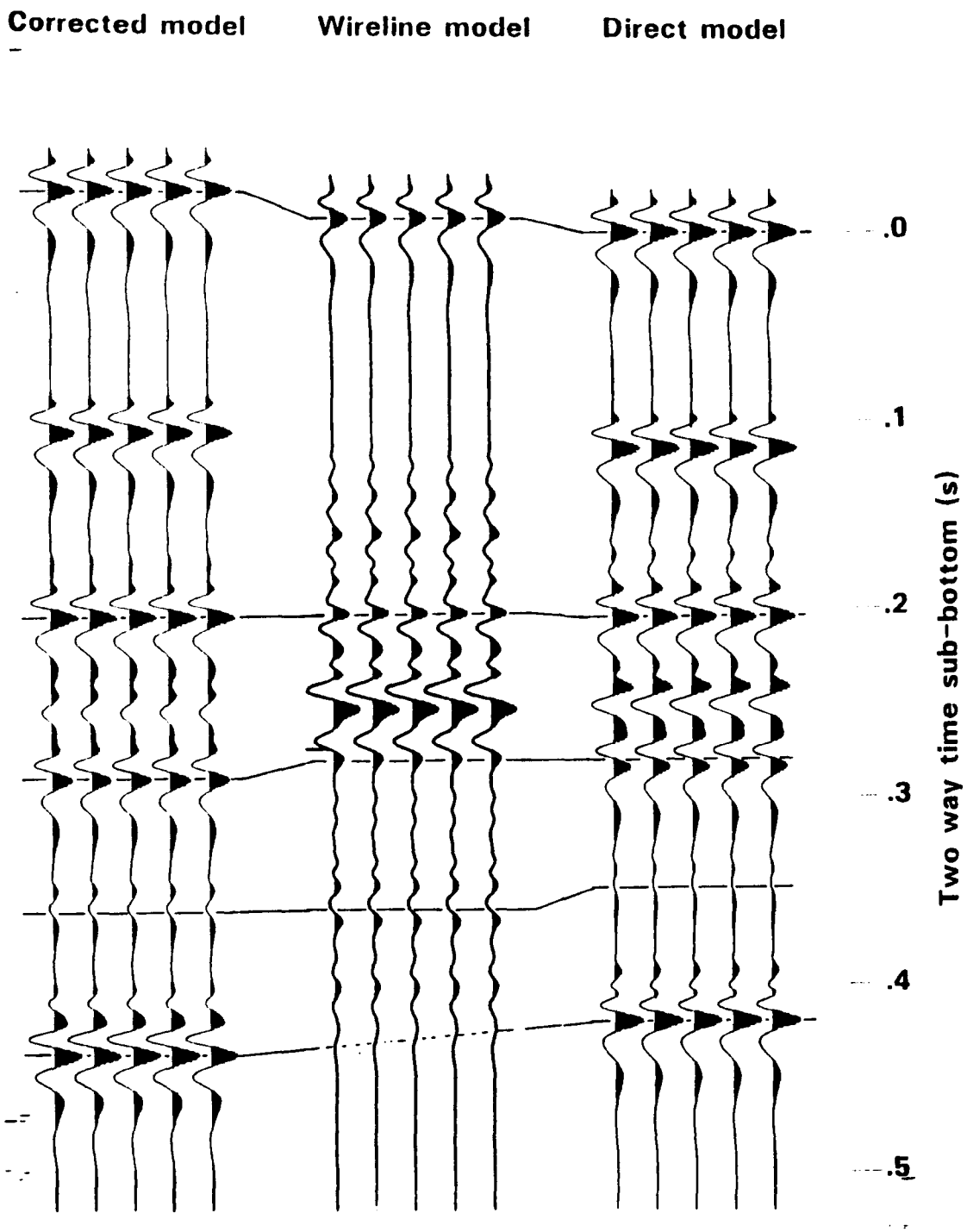

Fig. 5.18 Detail from sonic log, site 402

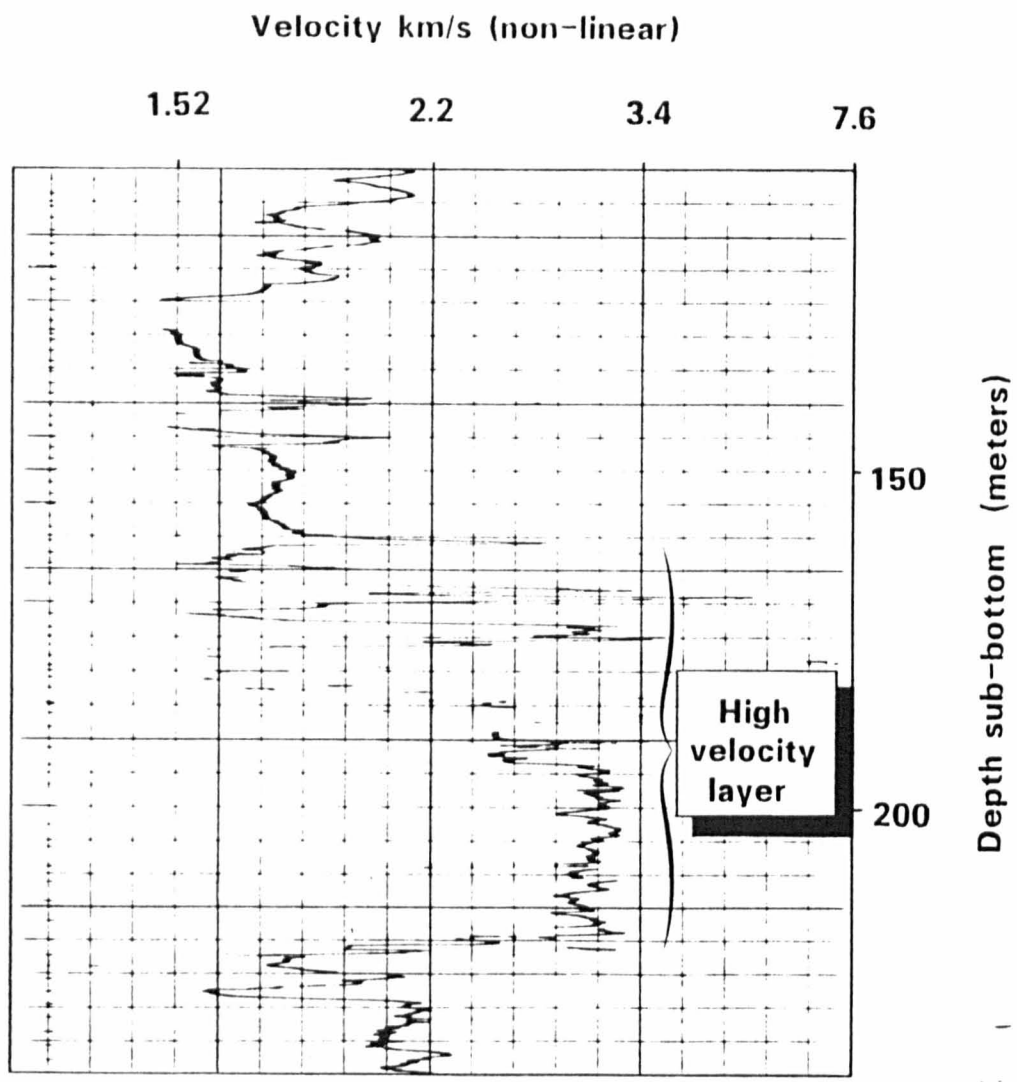

site.

The poor quality of data means that only the most abrupt breaks can be modelled and only the most prominent reflectors interpreted. Drilling found two unconformities:

1. at 89.5 m sub-bottom, between Pleistocene and Upper Eocene
2. at 175 m " , " Upper Eocene and Upper Albian

The most abrupt break in physical properties at 270 m does not coincide with any litho-unit boundary.

Basement was not reached, but a reflector, which occurs to either side of the site at about 3.5s TWT (fig. 5.15) appears to correlate with a very strong break in the physical properties seen at 440 m (fig. 5.16). Drilling time increased fourfold at the transition from chalk (and carbonaceous calcareous mudstone) to limestone (fig. 5.19). There is a corresponding sharp increase (downwards) in the carbonate content and a brief hiatus at this level may indicate that the reflector is an ancient hard-ground. The age designation changes from Upper to Lower Aptian. The character of this boundary is very similar to the boundary between the Blake-Bahama and Hatteras formations in the N.A.B. responsible for producing horizon Beta. The age is similar but younger at site 402. They are probably caused by the same mechanism of CCD shoaling. The shallower palaeodepth of site 402 meant that it did not sink below the CCD until much later (cf. horizon Beta is Hauterivan-Barremian in the N.A.B.). The interpretation of the reflector at the site is open to some debate. There are faults on either side and any continuation is weakened by de-focussing mentioned above. However, the interpretation shown in Figure 5.15 has been used and serves as an 'anchor' for modelling. Of the two physical property models (fig. 5.17) the direct model gives the best match between the two anchor points (the sea-bed and 440 m), implying that the

Fig. 5.19 Upper Aptian facies transition, site 402

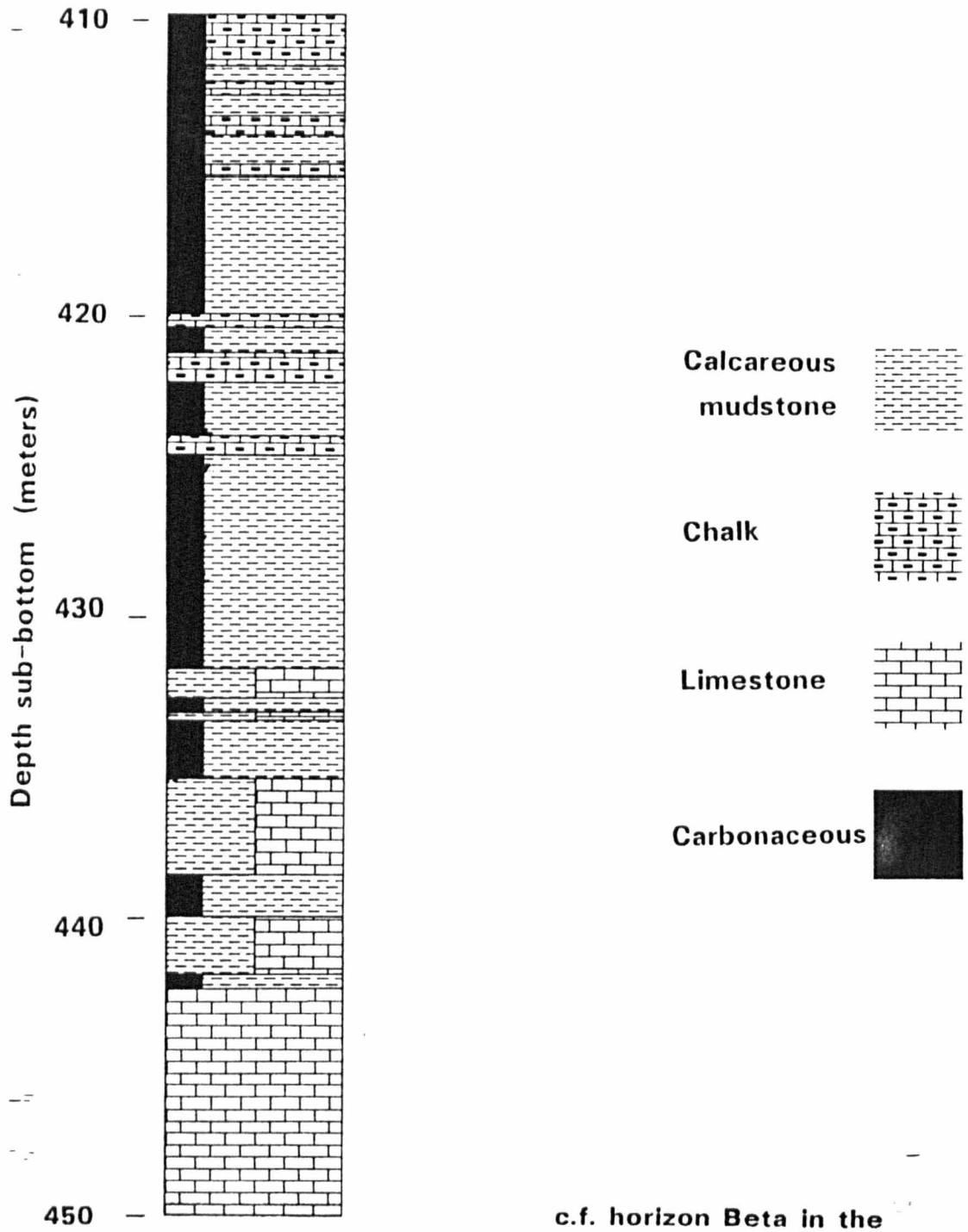

Table 5.3 - Correlation of seismic reflectors at site 400.

Reflections	Two-way travel time (ms)	Depth sub-bottom (m)	
		Site chapter*	This study
Sea bottom	0	0	0
1	160	150	130
2	330	300	ca.280
3	450	420	380
4	610	570	515
5	720	650	640/654

* Montadert, Roberts, et al, 1979

(N.B. The site chapter correlation of reflectors 4 and 5 with 570 m and 650 m respectively, results in an unrealistic interval velocity of 1.45 km/s.)

Table 5.4a - Velocity anisotropy, site 402

Depth	Anisotropy
0-230	none
230-270	slight
270-400	strong
400-440	slight
(440-469	medium)

Table 5.4b - Seismo-stratigraphic divisions at site 402

Unit	Character
I	very quiet, transparent
II	strongly layered
III	quiet, chaotic
IV	layered, quiet
V(basement)	quiet, chaotic to layered

unrecovered material is similar to the recovered core.

The physical properties shown in fig. 5.16 do not show great variation, but five layers are distinguished by the change in acoustic anisotropy.

The seismic stratigraphy is divisible into four units (table 5.4) but is less clear directly beneath the canyon in which the site is located. The comparison between seismic character and acoustic anisotropy will be discussed later (chapter seven).

The unconformity at 89.5 m does not match very well with the profile. However, this is to be expected in view of the low recovery and sparse data. The 10 m interval below the unconformity at 175 m is the most pronounced event on the wire-line logs (fig. 5.18). The site chapter notes a sharp increase in sonic velocity from 1.8 km/s to over 3.0 km/s. The break is also seen on the physical properties, but modelling yields an interval velocity of 2.5 km/s for the high velocity unit. The site chapter correlates this impedance with their reflector 2. They observed that the high velocity unit, of siliceous Albian limestones, continues to 222 m, amounting to a thickness of 47 m. The contrast at this depth is roughly equal to that at 175 m, but of reversed polarity. According to the site chapter this spacing is such that the lower reflector cannot be resolved. The site survey has a band-width of 20-80 Hz, which is quite sufficient to resolve this thickness. (Moreover, the stratigraphic interpretation has been done using a higher resolution survey shot after drilling, line GM402, which might be expected to have improved band-width.)

The site chapter attributes reflector generation to the controls of composition, in the form of carbonate content and cementation; silica

being particularly important in the latter. They note seven potential reflectors at 100, 175, 213, 270, 345, 365 and 440 m. Despite the construction of a synthetic seismogram in the site chapter, no precise correlation has been made. The events on the logs are assumed to cause the events on the profile. The controls cited to govern reflector formation have one factor in common: that of the grain-to-grain contact. It is hardly surprising that the Eocene sequence has silica controlling the reflector formation/development. One more observation concerning reflector control can be made: the numerous unconformities and hiatuses at the site dominate as the mechanism causing juxtaposition of contrasting lithologies, which rather obscure the more subtle types of reflector produced by minor compositional variation or progressive diagenesis. The comparison of horizon Beta is important and will be returned to later. The comparison of the two modelling schemes is not as clear as at site 406 but does show the value of being able to use physical properties data alone. The similarity of velocity function is encouraging.

5.2.5 Site 398

Site 398 is situated south of the Vigo Seamount on the continental rise to the west of northern Portugal. The site survey is a high quality multi-channel line shot by IFN/CNXO and enhanced by a special study which included seismogram synthesis and impedance recovery (Bouquigny & Willm, 1979). Their method of seismogram synthesis is to use velocity and density physical properties data to derive impedance. They state that "the depth to time conversion is very difficult and the result is not very accurate". They use a three layered linear velocity function based on detailed velocity analysis of the site survey profile, which they note to be very similar to the velocity

Fig. 5.20 Cross-plot of properties, site 398

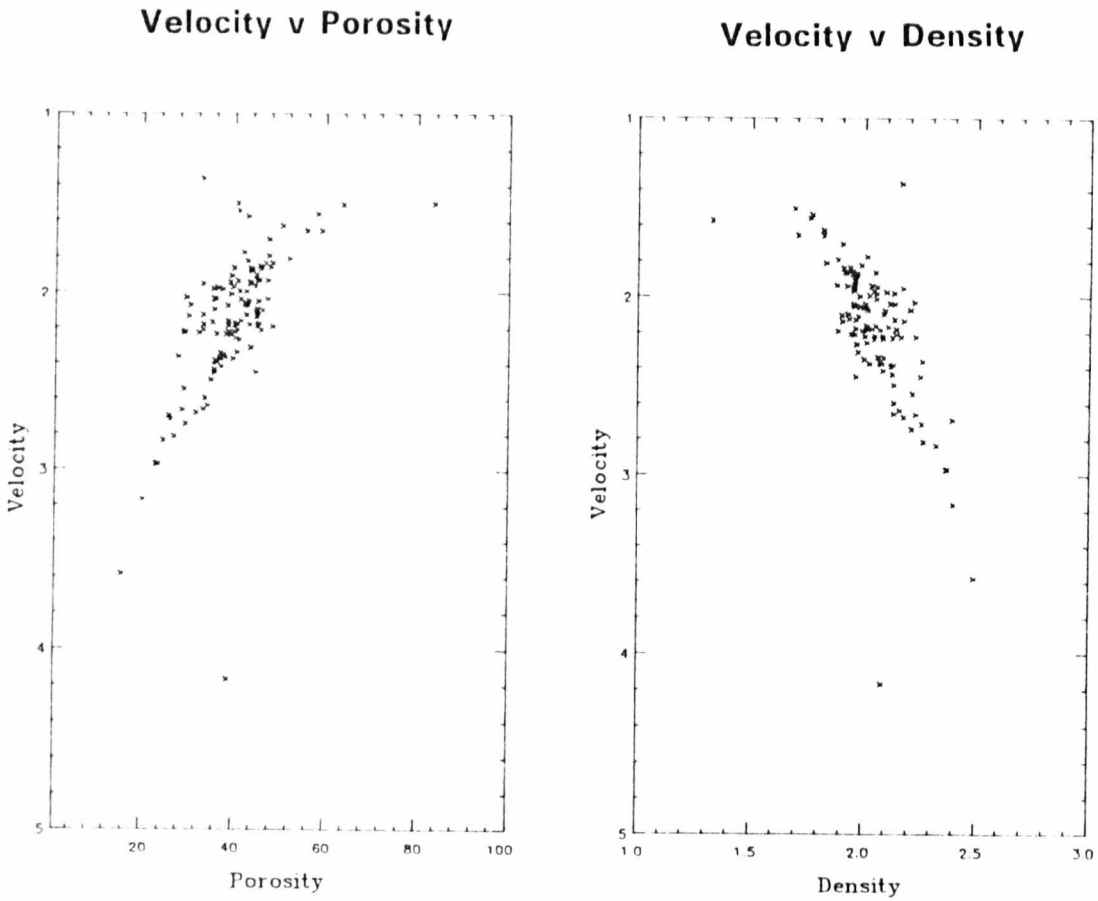

function used for correlation by C.A.Williams, physical properties specialist on board.

These latter velocities were derived in a very similar way to the physical properties scheme developed in this study (see section 3.2.3). "From the velocity-depth profile, different velocity groups were sub-divided visually and the individual values within each group averaged. ... A subjective choice was sometimes necessary to draw the velocity group boundaries; in these instances, guidance was taken from lithologic and other physical or geochemical features of the core" (Sibuet, Ryan, et al., 1979). The errors involved in using surface measurements to model **in situ** properties are also corrected by C.A.Williams. The velocities for the interval 0 - 373 m are increased by 10% and those for the interval 373 - 550 m are increased by 8%. This is similar to my correction for porosity rebound which extends over the interval 0 - 850 m and reaches a maximum at 640 m.
In contrast, my correction is applied to porosity data prior to the derivation of a velocity function. The reason for the 10% and 8% correction is not given; it seems they are needed to improve the fit.

The operations report details problems caused by poor weather which delayed the emplacement of the re-entry cone. As a result the hole (398D) was washed cored to ca.550 m and no physical properties data are available between the sea-floor and 580 m.

One of the observations of the physical properties summary is that the carbonate content appears to correlate with sediment reflectivity. The cross-plots for 398 show a small amount of bimodality for the higher porosity lithologies, which suggests there might be some benefit from using a more sophisticated model (ie. one that uses grain density to infer carbonate content) (fig. 5.20).

Fig. 5.21 Correlation of lithology, seismic profile and corrected model, site 398

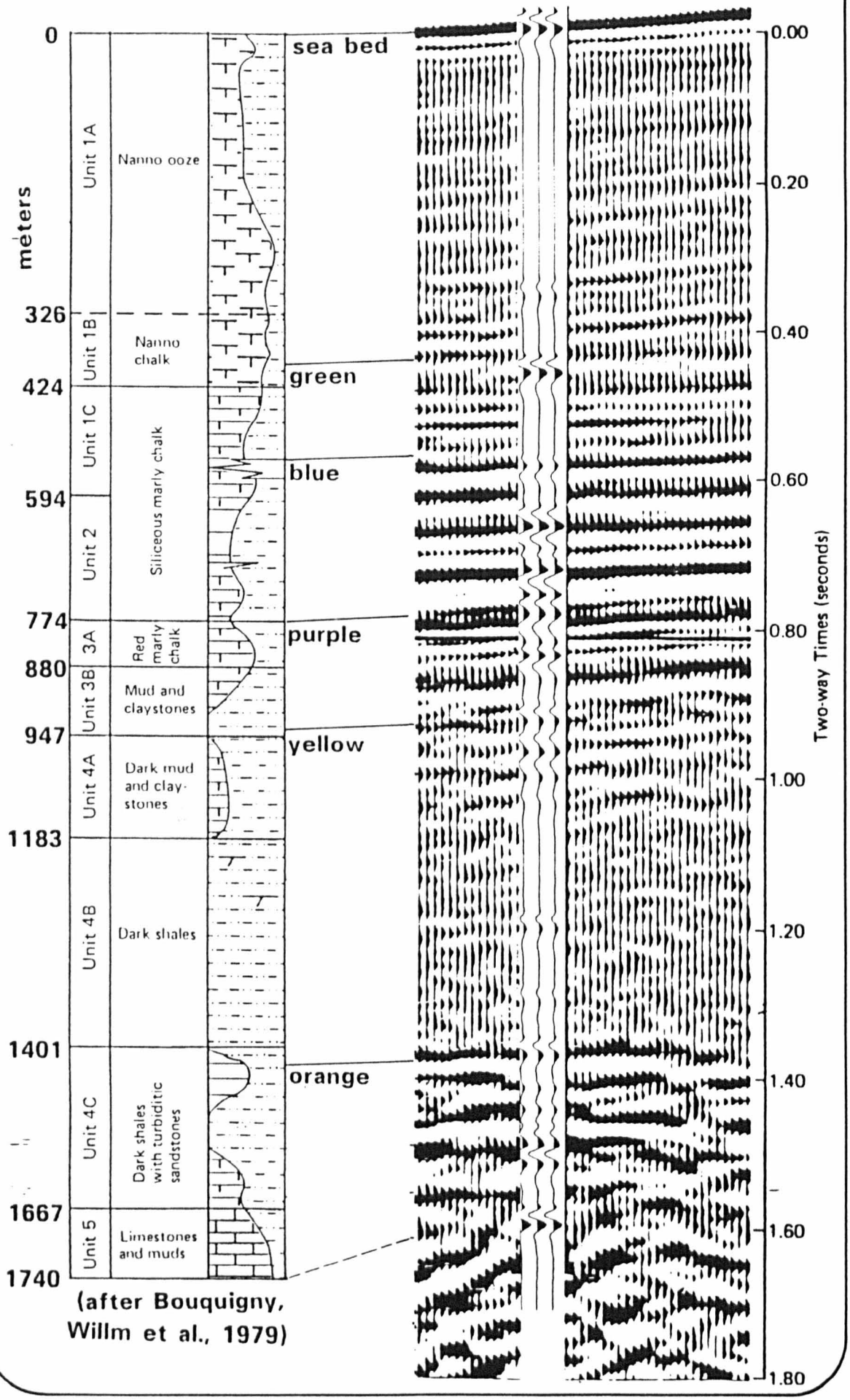

(after Bouquigny, Willm et al., 1979)

The corrected model correlates well with the reprocessed profile of Bouquigny and Willm (1979),(fig. 5.21). The interpretation given in the site chapter agrees with two minor exceptions:

1. The boundary between units 4A and 4B (1039 m) is slightly shallower
2. The boundary between units 4C and 5 (1667 m) is slightly deeper

No attempt was made by the shipboard party to correlate the seismic stratigraphy with other sites. Four acoustic units were identified and their bounding horizons assigned names of colours to "preclude correlation with other sites" (Sibuet, Ryan, et al., 1979).

The Green reflector delineates the base of acoustic unit I, but is not particularly strong. It has been interpreted as a middle to lower Miocene unconformity (Sibuet, Ryan, et al., 1979), which means that it is approximately coeval with horizon Au in the NAB. There is no physical properties data for this interval, but if the velocity function from my modelling is correct it correlates with ca. 376 m.

The same velocity function correlates the Blue reflector with 597 m and is roughly the top of the physical properties data. It has an age of late Eocene and marks the top of units IB and II, which together are described as (acoustically) strongly stratified. The lithology is described as 'siliceous marly chalk' (cf horizon Ac). It is interesting to note that if a seismic survey of less resolution were used, such as the seismic survey from the Glomar Challenger, this unit would appear acoustically opaque and might be considered as a single (although thick) reflector.

The Purple reflector marks the base of the strongly stratified unit. It is correlated with 774 m, which is 60 m above the boundary between subunits 3A and 3B, red marly chalk overlying mud and claystones. Such

Fig. 5.22 – Depth plot of physical properties, Site 398

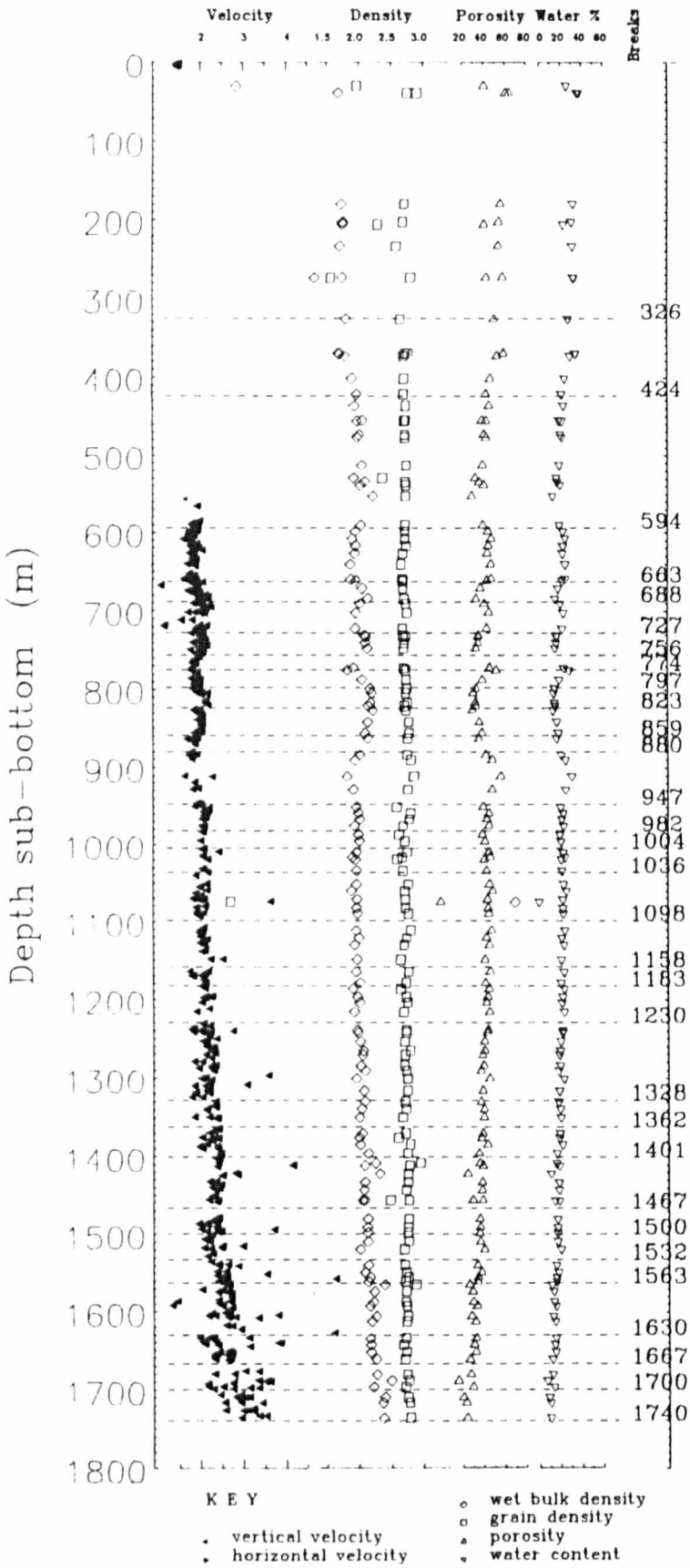

a change in sedimentation is characteristic of a shift in the level of the CCD; in this case a drop. The expected form of such a reflector is that it should be strongly negative and would therefore produce a white loop. Given the bandwidth and velocity the wavelength is calculated to be between 155 m and 46 m. The tendency to interpret only the black loops combined with the complex nature of the source wavelet mean that it is not surprising to find a 60 m gap between a strong reflector and marked break in the physical properties. On the depth plot of physical properties the break is shown as a marked rise in velocity over an interval of 20 m (fig. 5.22). My corrected model draws the correlation at 794 m, within subunit 3A (red marly chalk).

The Yellow reflector is not a strong event. I correlate it with 945 m where velocity shows a step increase that is responsible for the impedance contrast. It is also the depth of a tentative hiatus between Santonian and Cenomanian.

The Orange reflector defines the top of acoustic unit 4 which is strongly stratified. In terms of lithology it is the appearance downwards of turbidites within an otherwise uniform sequence of dark shales. I correlate it with 1401 m, which agrees with Sibuet, Ryan et al (1979). This is a lithostratigraphic boundary, the 'probable hiatus' between the Aptian and Albian (Sibuet, Ryan et al., 1979) but is not marked by an abrupt break in the physical properties (fig. 5.22). Lithologically, it is the contrast between dark shales which overly dark shales with turbiditic sandstones.

The number of named reflectors is less than at some N.A.B. sites and other loops are worth including. For example, the horizon at 0.326 s (TWT) may correlate with the ooze-to-chalk transition. Also a number of strong reflectors between the Blue and Yellow horizons can be

Table 5.5 - Correlation of reflectors, site 398.

Horizon	Depth (m)	Acoustic unit	Character
Sea-bed	0		
		IA	weakly stratified
Green	ca. 424		
		IB	strongly stratified
Blue	ca. 594		
		II	strongly stratified
Purple	794		
Yellow	947	III	homogeneous
Orange	1401	(u/c: Aptian/Albian)	
		IV	discontinuous or hatched
Basement	?		

Fig. 5.23 Acoustic stratigraphy, silica content and sediment rythms, site 398

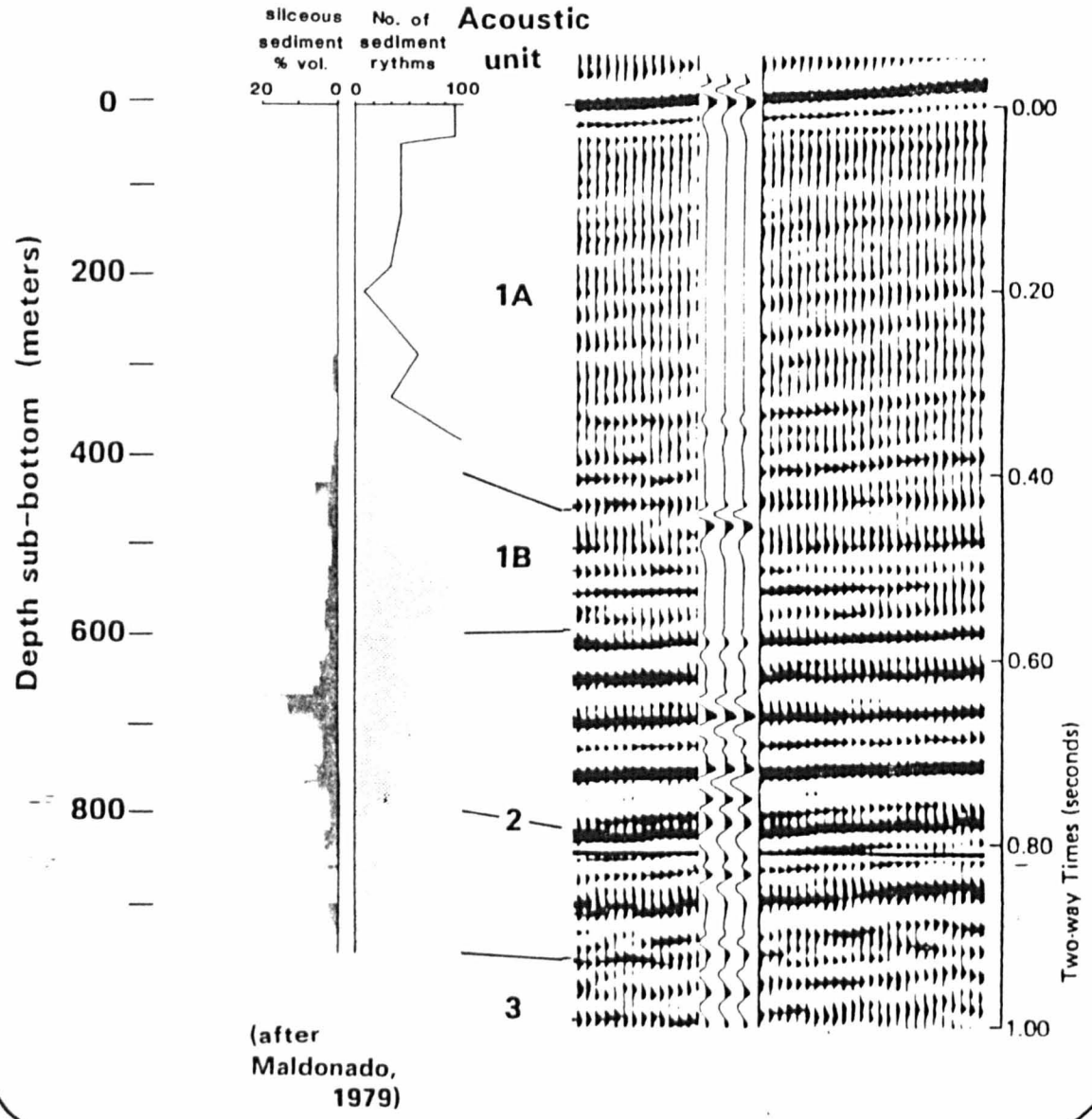

related to individual physical property breaks.

The seismic character of the siliceous marly chalk is markedly different from the dark shales below and from the nanno ooze/chalk above. The strongly stratified nature of the corresponding acoustic unit 2 (fig. 5.23) may be related to the degree of cementation and this in turn to the carbonate content, which increases steadily up section above the dark shales which were deposited beneath the CCD. The depth plot of physical properties shows there to be considerable variation in the porosity log which correlates with acoustic unit 2 and the number of sediment rhythms (fig. 5.23). Silica content is important at 650 - 700 m.

The accuracy of modelling is largely the result of the dense coverage of data and flat-lying reflectors which in turn make the derivation of the velocity function much more reliable and the interference pattern of reflectors less complex and, therefore, less ambiguous.

5.2.6 Site 416

Site 416 is situated off the Atlantic coast of Morocco at the base of the continental slope (fig. 5.1). The sedimentary succession consists of pelagic carbonates with variable amounts of turbidite deposits, which are dominant in the lower Cretaceous. Upper Eocene to lower Oligocene sediments are absent. The hole bottomed in Tithonian turbidites at a depth of 1624 m. Logging was attempted but was not fully successful and only the data from 100 - 690 m are sufficient to produce a model for the upper part of the hole.

The primary objective for the site was to reach basement, which had

Fig. 5.24 Composite model, site 416

Wire-line model ..... 5.5 s – 6.3 s

Direct model ..... 6.6 s – 7.1 s

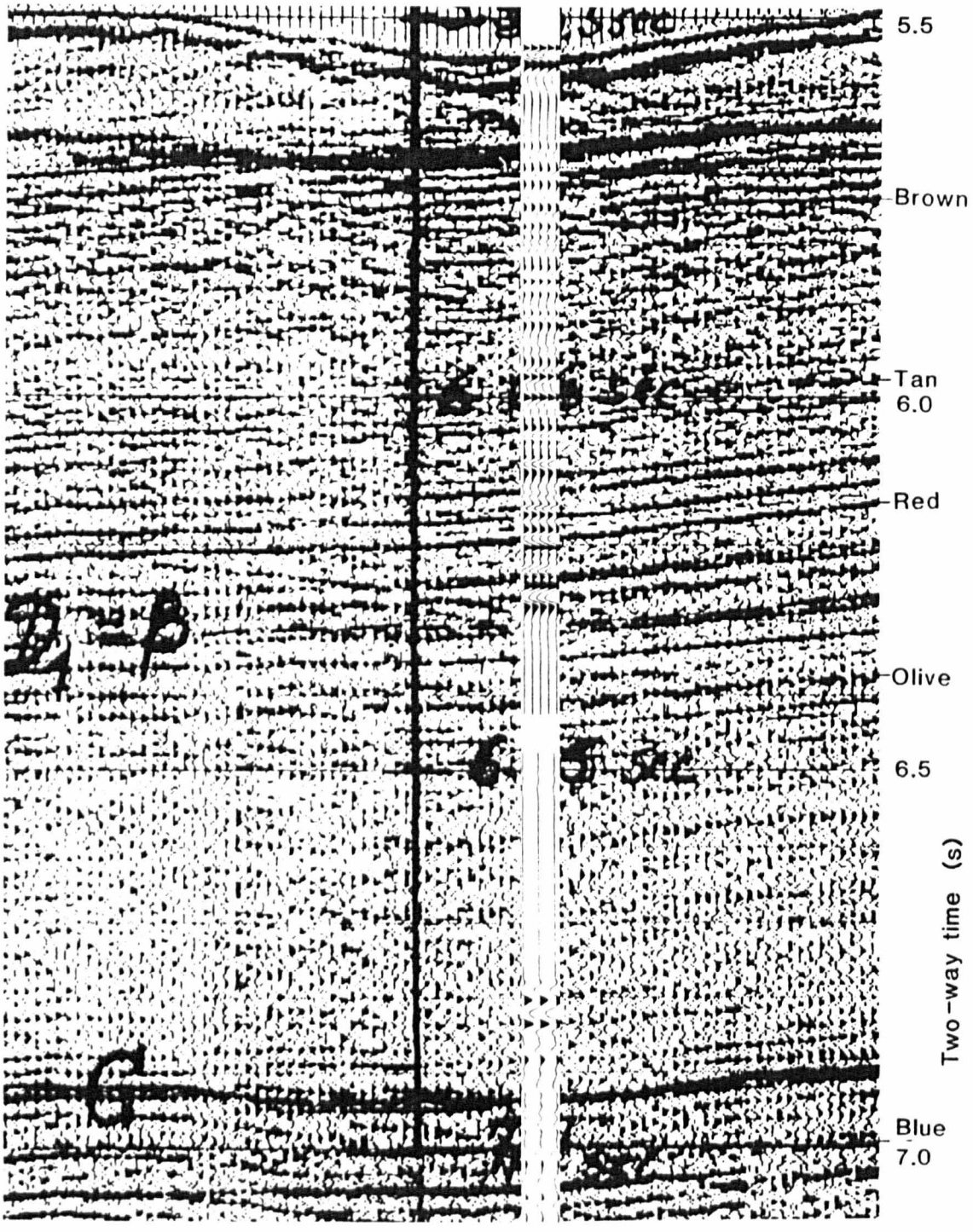

Fig. 5.25 Acoustic stratigraphy, site 416

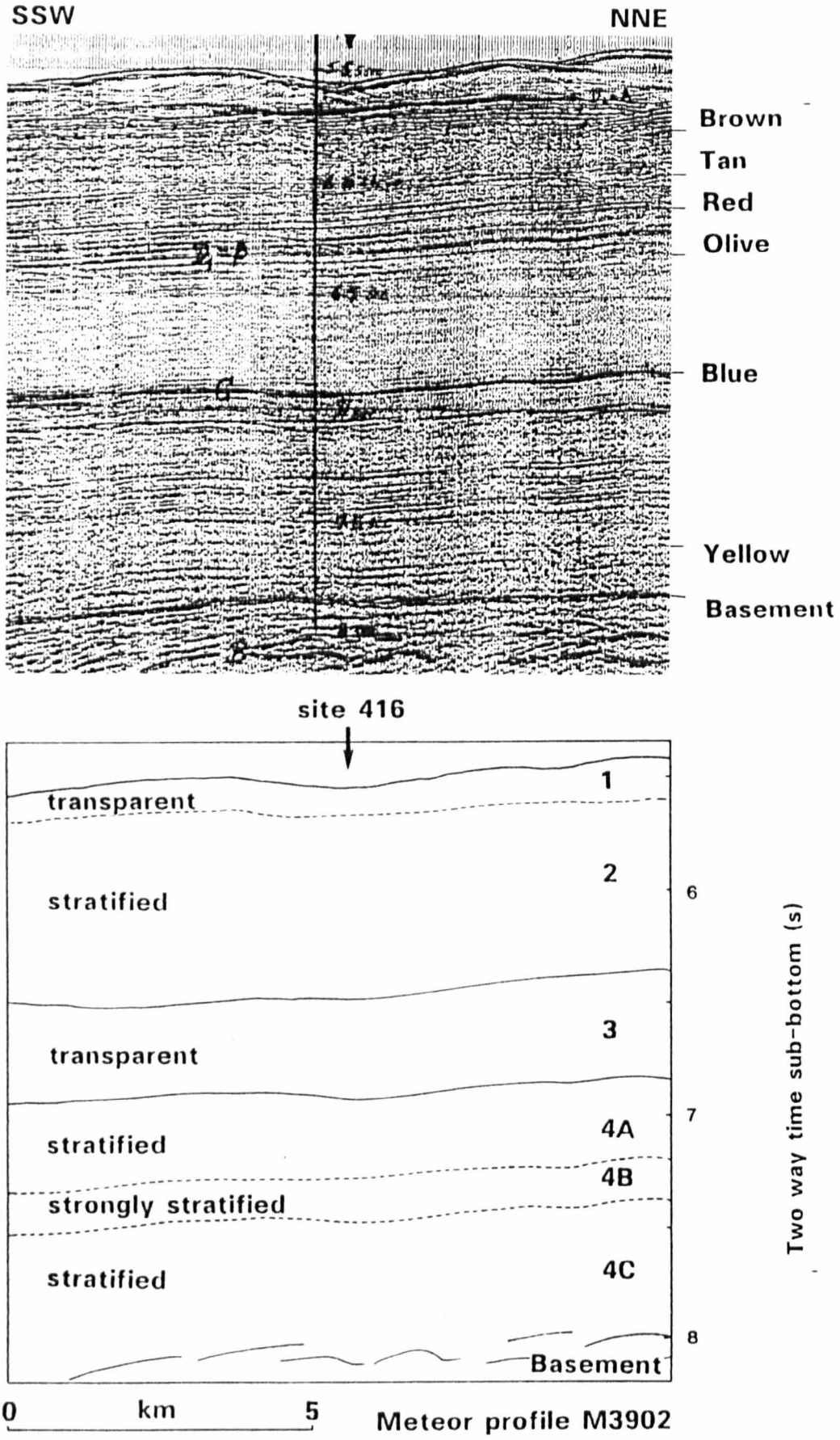

Fig. 5.26 Depth plot of physical properties, Site 416

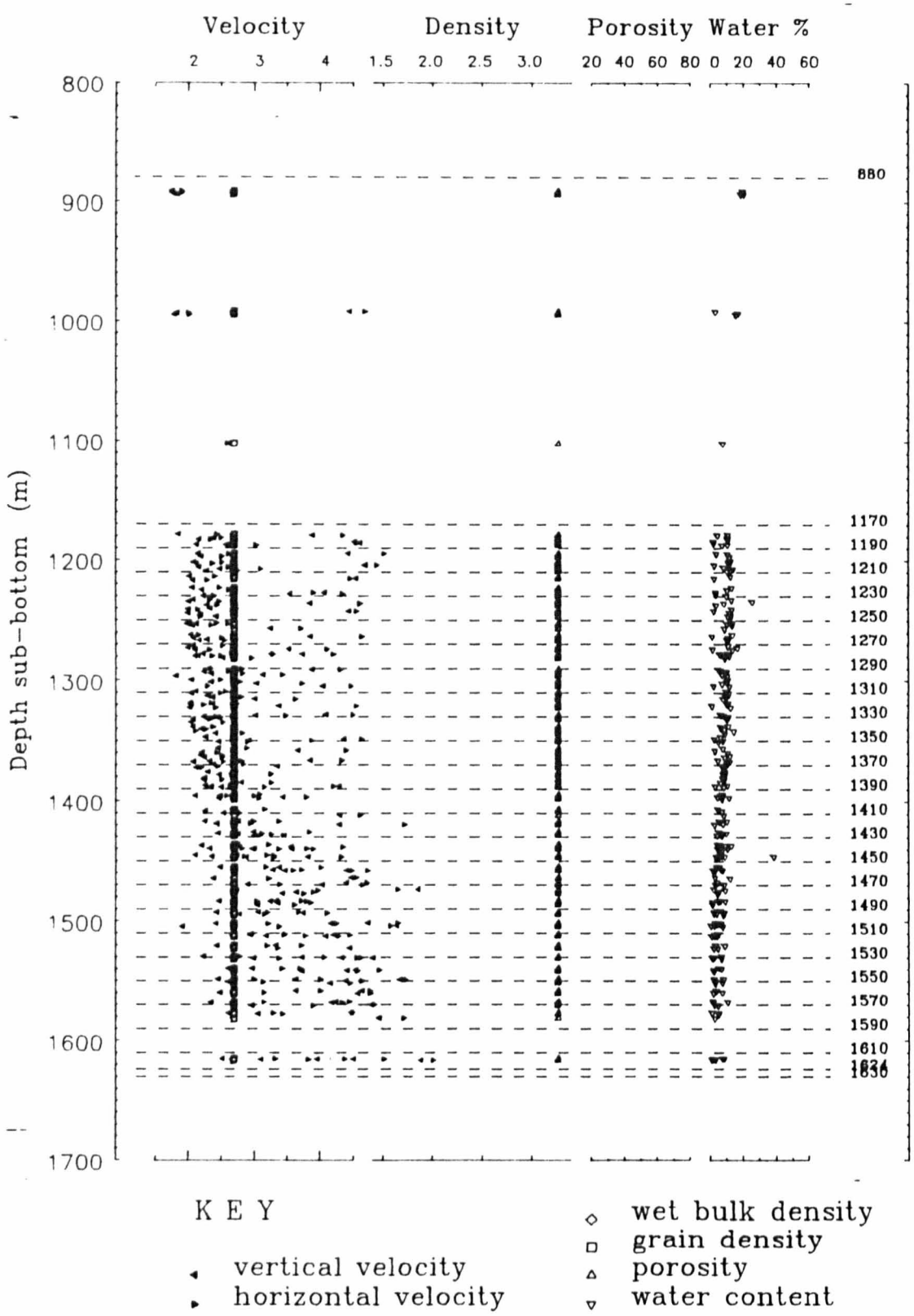

not been possible on Leg 41 at site 370, 3 km to the east. Site 370 had reached 1170 m, so site 416 was spot-cored to this depth before continuous recovery was commenced. In consequence, the physical properties data for the top 1170 m are very poor and only sparse data is available from site 370. Below 1170 m data are of good quality, but the delineation of a physical properties stratigraphy is not obvious (fig. 5.26). Water content data was used instead of porosity data for deriving the velocity function used in physical property modelling. Sonobuoy data from the Guinea-Sierra Leone basin (Houtz, 1974) is used to position the corrected model at the correct two-way travel time for comparison with the site survey profile. The velocity function used is: $V = 1.49 + 1.57\ t$

where t is one-way travel time V is instantaneous velocity.
Using this function 880 m is correlated with 0.946 s (TWT). It must be remembered that the data quality is not good. There are very many reflections and a narrow bandwidth, which together increase the error of interpretation. In particular, the sonobuoy data do not agree with velocity studies carried out on two multi-channel lines over the site (see table 5.6). From the table it is clear that there is considerable latitude in the interpretation of particular reflectors. Boyce (1984) correlates the Blue reflector with "roughly 1500 m", which is much shallower than might be expected from the semblance studies alone and close to the sonobuoy derived depth (1467 m).

The seismic stratigraphy can be divided into four acoustic units (fig. 5.25). The bottom part of the hole that was continuously cored is mostly within the acoustically transparent layer 3, which means that there are not many high amplitude reflections to model. The succession between 1170 m and 1610 m was divided into layers 20 m thick because no stratigraphy could be discerned from the plot of physical properties (fig. 5.26). This spacing gives high amplitude

Fig. 5.27 Lithological units and seismic stratigrapghy, site 416

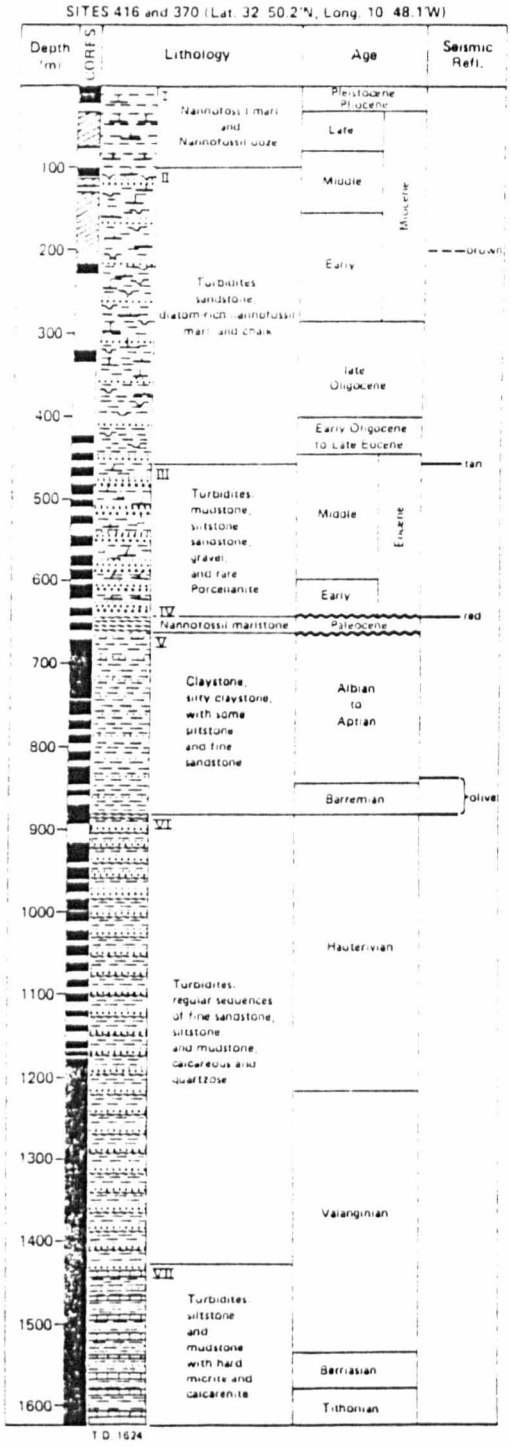

(after Lancelot, Winterer, et al., 1980)

Table 5.6 Comparison of velocity functions, site 416.

Reflector	Time to reflector (ms of TWT)	Estimated depth(m) Meteor	G.S.I.	S'buoy[1]	Drilling	Modelled depth
Brown	225	214	225	177	186-215	188
Tan	485	480	500	408	457	405
Red	660	670	700	577	642	565
	736					643
Olive	870	920	970	797	880	not modelled
Blue	1430	1660	1750	1467	1500[2]	1470
Yellow	2155	2780	3011	2516		
Basement	2625	3580	3867	3308		

[1] from Guinea-Sierra Leone basin, Houtz, 1974.

[2] The correlation of drilling results and the Blue reflector is after Boyce (1984).

Table 5.7 Correlation of lithostratigraphic units with travel time, site 416.

Unit	Depth (m)	Travel time (TWT/ms) wire-line	direct
1	0 - 100	122	
2	100 - 457	542	
3	457 - 642	704	
4	642 - 661	728	
5	661 - 880		946
6	880 - 1430		1429
7	1430 - 1624		1540

reflections for alternately positive and negative events but weaker returns for like polarity events due to destructive interference.

The broad matching of seismic units to lithological units is not obvious although attempted in the site chapter (fig. 5.27). Unit V is predominantly claystone and would be expected to be acoustically transparent. Yet it is interpreted to be above the Olive reflector, which implies it belongs to one of the most stratified parts of the column. Units I and II seem a more favourable match for my acoustic unit 2. Units VI and VII are sufficient for my unit 4, but seem unlikely to produce a transparent unit. The velocity-depth relationships suggest it is otherwise (unit VII may well belong in my acoustic unit 4a.)

The quality of the profile is poor and the major reflectors may have been mis-traced from site 415 where their interpretation is not certain (no data were available for modelling at site 415.)

Table 5.7 gives the depth to travel time correlations for the reflectors correlated from site 415 and the travel times to boundaries between the lithological units identified based on my modelling. These do not agree in detail with the site chapter (Lancelot, Winterer, et al, 1980).

In particular the Red reflector does not appear to have been accurately traced. The travel time (TWT) of 660 ms given in the site chapter correlates with 642 m. My modelling indicates that the travel time to 642 m is 736 ms indicating that the Red reflector should be picked lower if it is to mark the top of unit IV (consists of claystones and siltstones). One reason for the mis-correlation may be the nature of the unit III/V boundary (unit IV was not cored at site

416, but is inferred from results at site 370). The lower boundary of acoustic unit 2 can be seen to fade into unit 3 as it is traced SSW (fig. 5.25). If the stratified character of acoustic unit 2 is due to the turbidites of litho-unit 2 and 3 and the profile is along strike then the individual bed may well peter out laterally and with them their reflectivity. The acoustic stratigraphic boundary should be drawn, of course, at the envelope of the stratified layer.

(N.B. No comparison of the wireline and physical property model can be made as they cover different intervals.
The hole, site 416, is slightly off profile.)

(Conclusions drawn from this chapter are presented in chapter seven.)

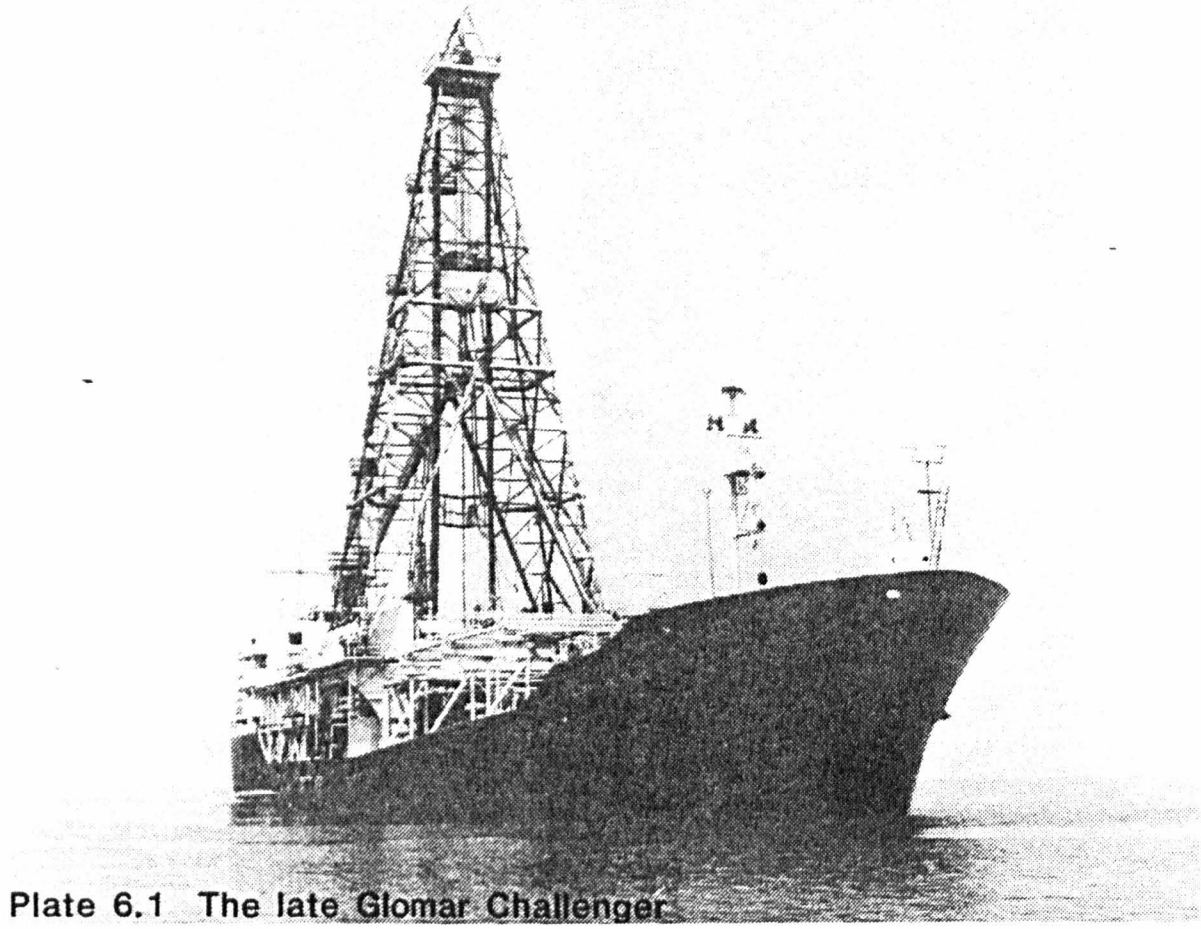

Plate 6.1 The late Glomar Challenger

Plate 6.2 Scientific crew, Leg 93

CHAPTER SIX

Case study: Physical properties modelling on Leg 93

6.1 Introduction

This chapter is presented as a case study on physical properties modelling of seismic reflectors within deep sea sediments. During May and June 1983 I was a member of the scientific crew aboard the late D.V. Glomar Challenger (Plate 6.1-2). Mark Johns and myself shared the task of collecting and measuring physical properties data, Mark being interested in the near surface gaseous sediments and myself in the impedance contrasts responsible for sediment reflectivity.

Three holes were drilled on the cruise, one in deep water in the Hatteras Abyssal Plain, site 603, and two in shallower water on the continental margin of North America as part of the New Jersey Transect, sites 604 and 605 (fig. 6.1). The holes were not logged.

6.2 Site studies

6.2.1 Site 603

Site 603 is situated in the Hatteras Abyssal Plain (fig. 6.1) as part of the New Jersey Transect study of the North American Continental Slope and Rise. Like site 534 it had primary objectives to reach basement and to investigate the (expected) Jurassic reflectors. The sediments above were also of interest so continuous recovery was

Fig 6.1 Location map for sites studied

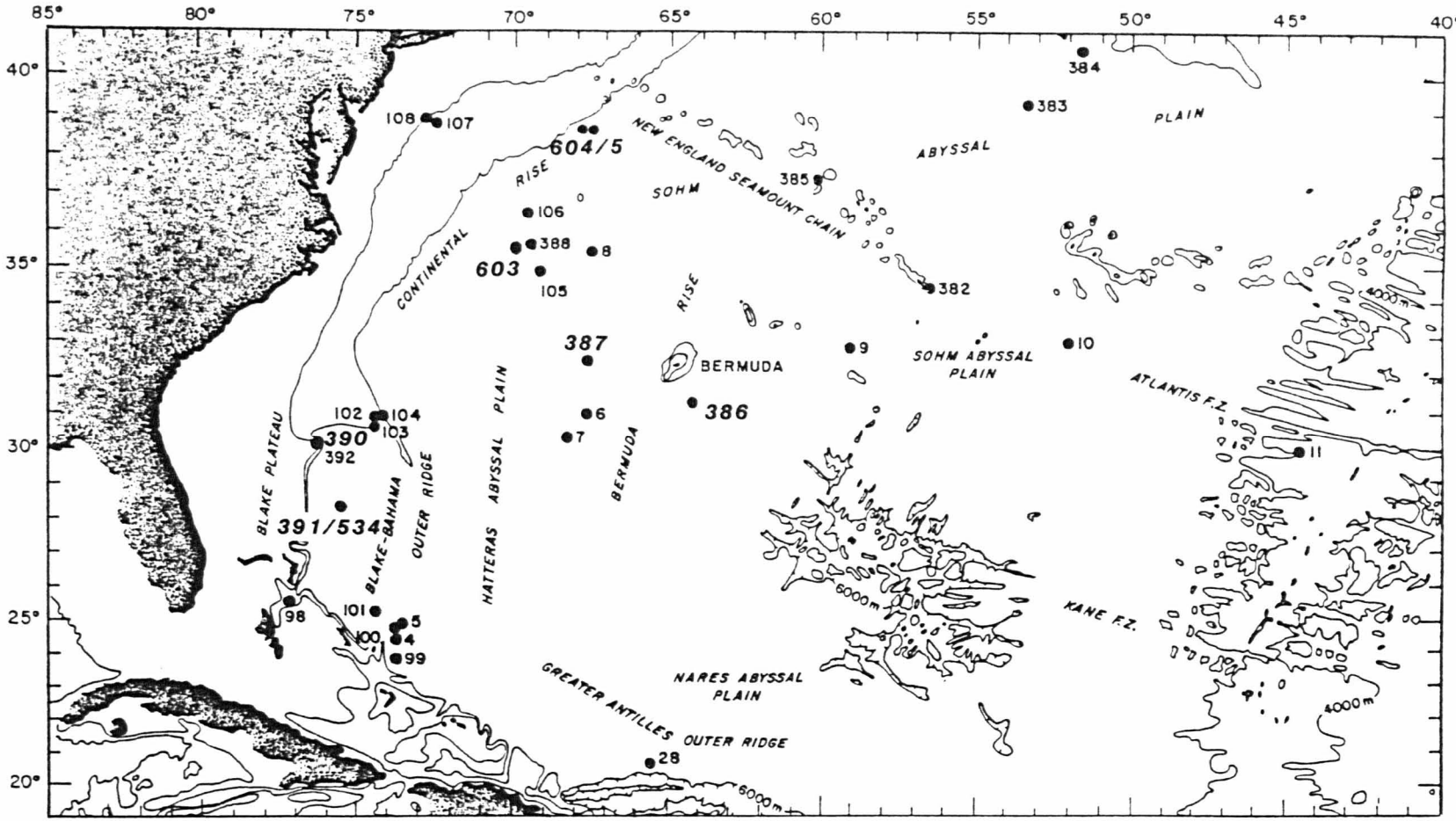

obtained which included use of the hydraulic piston corer (HPC) and extended core barrel (XCB) in the soft upper sediments (hole 603C). As a result site 603 has the fullest recovery of any DSDP site. Unfortunately, basement was not reached so modelling must proceed without the aid of an anchoring correlation.

'Breaks' in the physical properties were picked from the graphs of each parameter measured. Nine major and thirty-seven minor breaks can be picked, constituting a physical properties' stratigraphy of ten units and a total of forty-seven sub-units (fig. 6.3).

Unit 1 extends from the sea-floor to 110 m and represents an interval of unconsolidated sediment with low shear strength. It has one sub-division drawn where shear strength levels off following initial water loss.

Unit 2 has high shear strength and exhibits even trends in all properties. Carbonate content is very variable. It has eight sub-units defined by minor changes in velocity and bulk gravimetric properties.

Unit 3 is poorly sampled, measurements are all from core recovered from hole 603. It may be somewhat artificial. Porosity and water content show a faltering of their steep downward trend, again this is in part due to the difference between material recovered by HPC and that by rotary coring. Two sub-divisions are drawn at minor changes in gravimetric measurements.

Unit 4 is well sampled showing that the sediments have undergone sufficient diagenesis to withstand rotary coring. Five sub-divisions are defined, one by a slight elevation of carbonate content.

Fig. 6.2 Site survey profile and seismic stratigraphy, Site 603

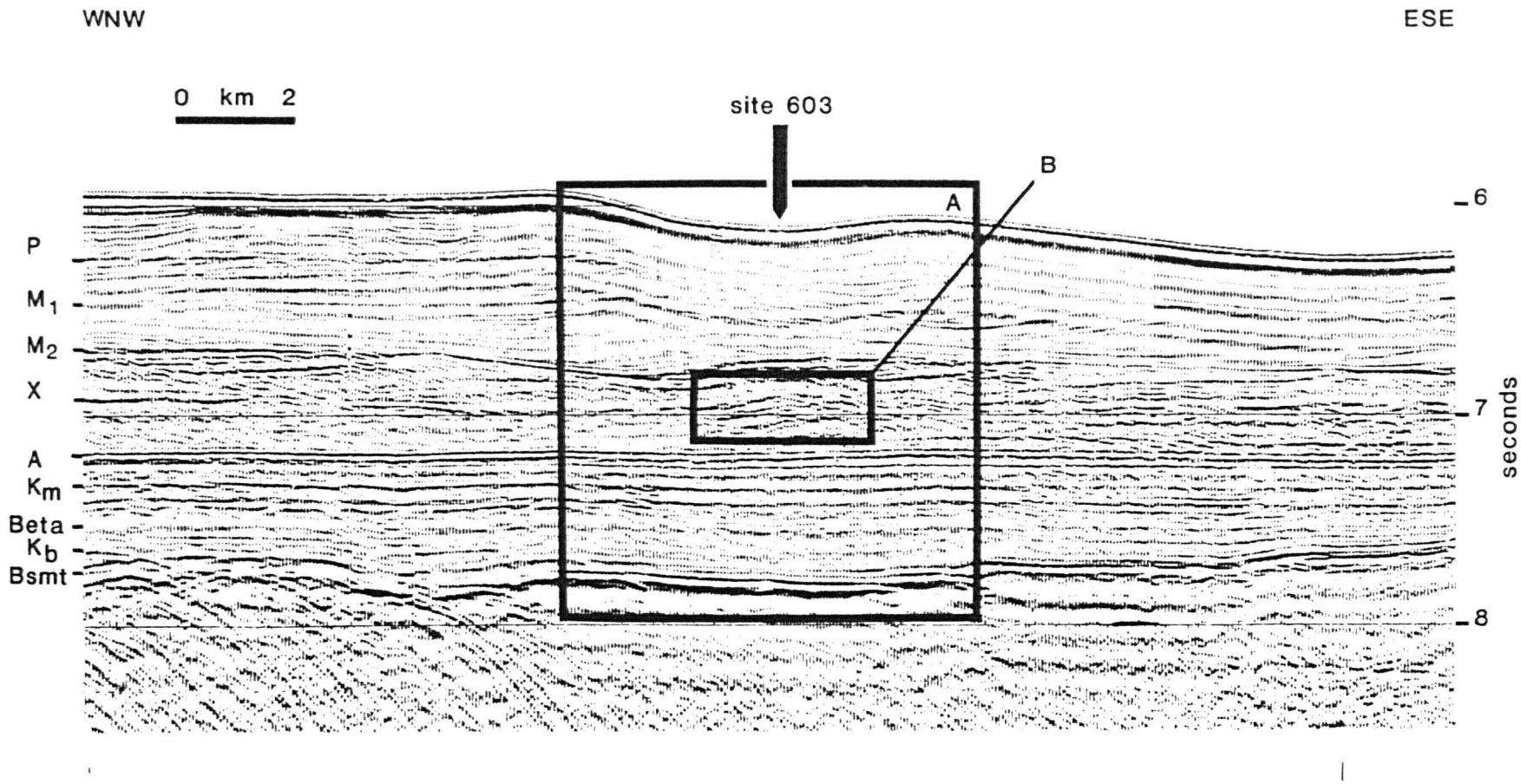

Unit 5 is distinguished by lower densities and increased porosity. Four minor divisions are drawn.

Unit 6, which coincides with the top of data from hole 603B, is drawn at a rise in velocity, and carbonate content. Only one sub-division is seen - the bottom 17 m approx. appear as transitional to the succeeding unit (unit 7).

Unit 7 has anomalously high velocities, and low densities. Porosity and water content are not particularly affected, while carbonate content is much reduced. There are no sub-divisions.

Unit 8 is a return to the otherwise even trend of units 1 through 6. Generally, it displays more variability making the definition of sub-unit boundaries much more definite, in particular sub-unit 8d.

Unit 9 is defined by a substantial increase in part of the carbonate content, whose distribution is strongly bimodal. Nine sub-divisions are recognised from minor changes of velocity, and gravimetric measurements. Low recovery from sub-unit 8h means that the unit 8/9 boundary is open to question - unit 9 may include sub-unit 8h.

Unit 10 shows steepened trends in velocity and wet bulk density. Carbonate content is reduced and no longer bimodal. Four sub-units are drawn.

The model (fig. 6.4) assumes that all boundaries are shown by porosity breaks. With increased lithification this is not so apparent and the correction to amplitude has been made based on the velocity log, although the velocity function remains dependent on the porosity derivation.

Fig. 6.3 Depth plot of physical properties, site 603

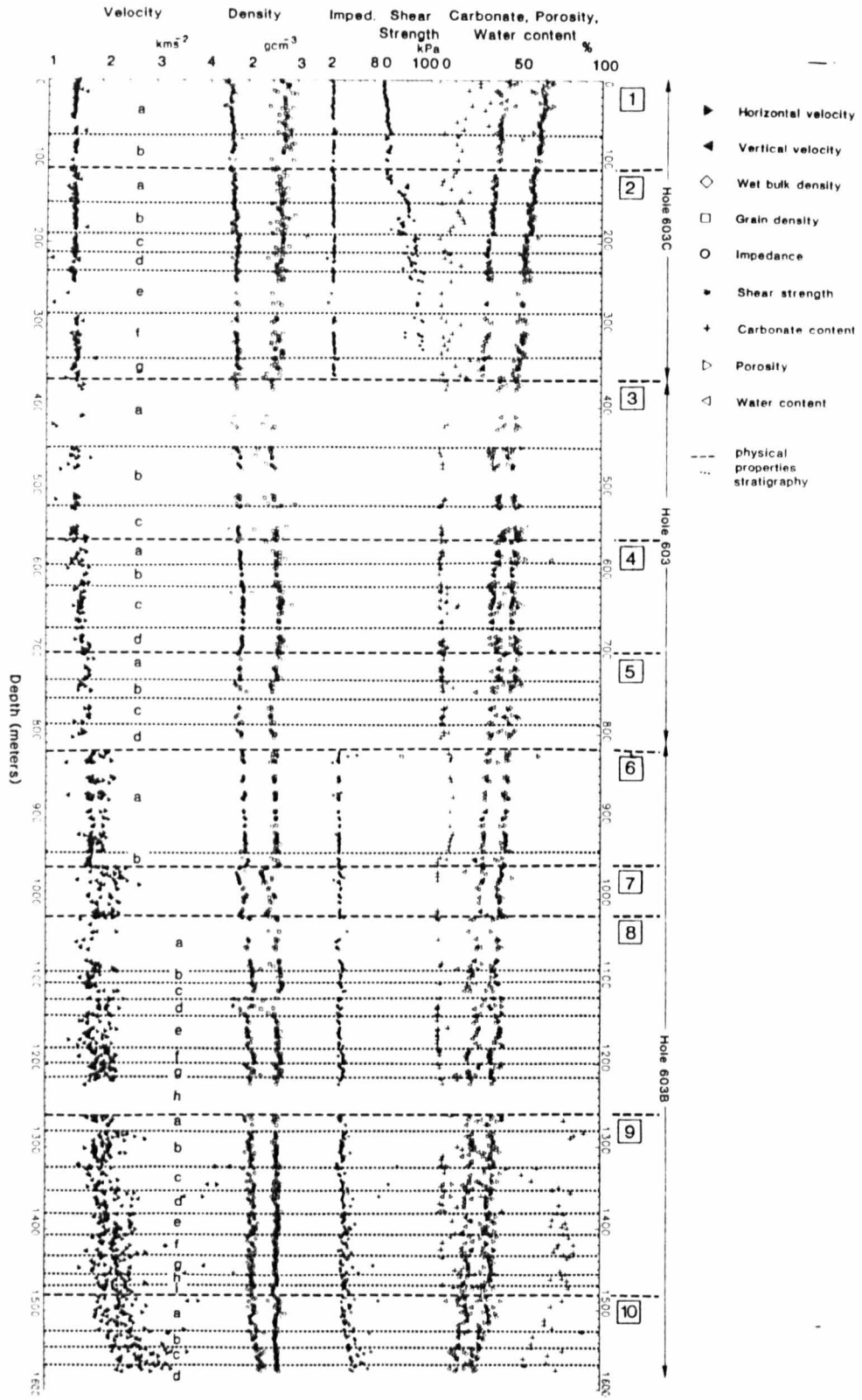

Fig. 6.4 Physical properties model, Site 603

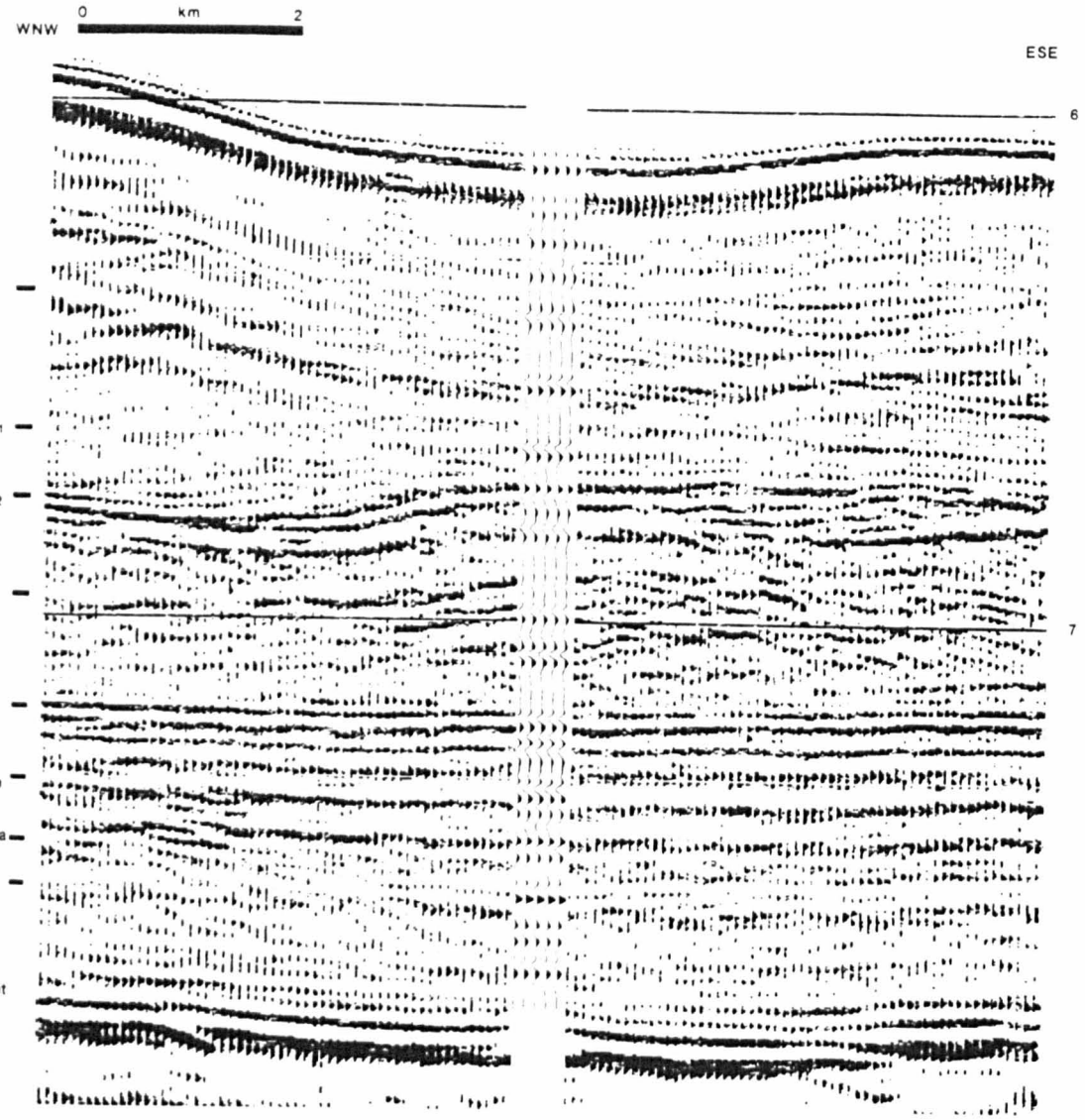

Based on this modelling the following correlations can be made (see table 6.1) depths used in description are drill string depths, correction to true vertical depths was made prior to modelling because the hole deviated from vertical.

Horizon K_b is drawn at 6.6s (TWT) and correlates with 1440m sub-bottom. This is the top of physical property unit 9h (fig. 6.3) which is characterised by variable lithology, in particular sedimentation starts to include turbidites which increase in importance upwards. It is a discontinuous reflector at site 603 and is not accurately modelled. The minor unit shows a change of porosity from relatively high (physical property unit 9g) to low (physical property unit 9i) and contains the deepest occurrence of low carbonate formations deposited below the CCD. Litho-unit 5, 1215m to total depth, is much more variable than units above which makes the assumption that the reflectivity can be accurately modelled by sampling at 1.5m or even more coarsely less valid. The horizon marks the approximate boundary between Barremian and Hauterivian sediments. The name 'horizon K_b' is inappropriate if it is meant to correlate with the basal Cretaceous. A better label might be K_L signifying intra Lower Cretaceous.

Horizon Beta is a very widespread reflector over much of the North American Basin. It is normally a strongly positive event produced by the impedance contrast between carbonate to non-carbonate dominated sediment. It is drawn at 7.42 s (TWT) at site 603 (fig. 6.2), which corresponds to the interference product of reflections from physical property breaks at 1216 m and 1264 m (fig. 6.3). The black loop at 7.42 s (TWT), (fig. 6.4), actually correlates with approximately 1240 m within the poorly recovered unit. These depths bound physical

Table 6.1 - Age range of sandy calc turbidites

Strat	603B	391C
Aptian		
Albian		
Barremian		
Hauterivian		
Valanginian		
Berriasian		

property unit 8h which comprised unlithified turbidites of which no measurements could be made (cores 603B-45-2 thro' 603B-48). The reflector picked is laterally continuous although it does develop a double-peaked character 3 km along section (SE), which, it may be argued, supports the interference origin. Correlations of horizon Beta at other sites in the North American Basin give a variety of ages (see table 6.2); it is accepted to result from a depth change in the carbonate compensation depth, and, in consequence is diachronous (Tucholke, 1983). Lithologically, horizon Beta is usually considered to be due to the impedance contrast between upper Lower Cretaceous black clays and lower Lower Cretaceous carbonates, that is, at the boundary between the Hatteras and Blake Bahama formations. At site 603 this boundary is confused by the deposition of sandy turbidites, which become more important throughout the Hauterivian and constitute over half of Barremian sediments. Thus, the juxtaposition of Aptian/Albian black carbonaceous claystone (litho-unit 4) with Neocomian carbonates is prevented by these clastics. It is possible to argue that horizon Beta should be drawn at 1264 m and tied to the white loop, which corresponds to the top of high carbonate content sediments. The negative polarity being produced by the boundary of the carbonates with the higher impedance sands above. This explains the character of horizon Beta at site 603, and the difficulty in tracing the reflector from other profiles. In one sense then, as a result of the extra formation, it is fair to say that this is not properly horizon Beta.

Horizon K_m is produced by the interference of three closely spaced impedance contrasts: a positive contrast at 1100 m and two of reversed polarity at 1085 m and 1120 m (fig. 6.3). They correspond to sections 603B-29-4, -31-1 and -32-2 and to the tops of physical property units 8b, c & d. Of these, the first two, which bound physical property unit 8b, are the more obtrusive on the velocity logs

Plates 6.3 – 6.7

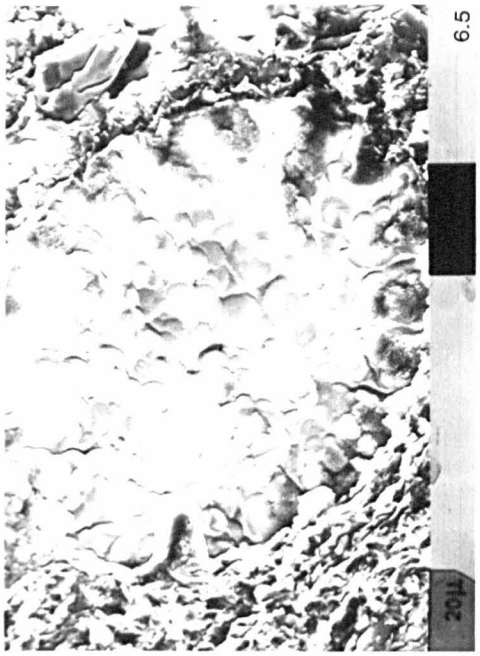

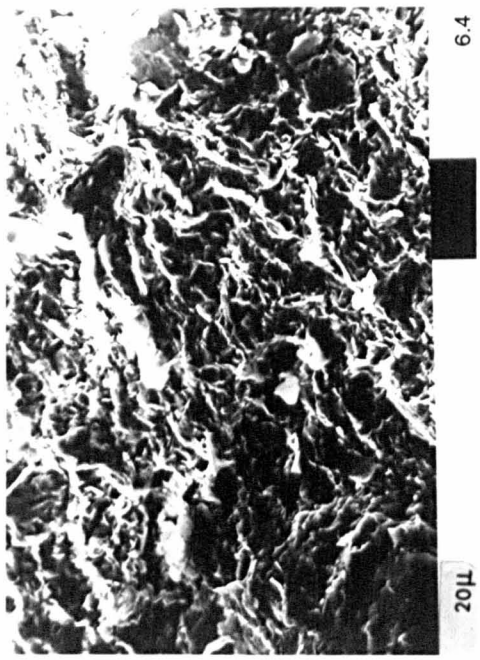

(particularly horizontal velocity), while the bulk gravimetric properties show a more marked break at the third depth (fig. 6.3). Lithologically, physical property units 8b and 8c are variegated claystone with a variable amount of coarser terrigenous input. Their red-brown colouration indicates deposition in an oxidising environment. The carbonate content is variable, but slightly higher than the units above. This is surprising as a high carbonate content is usually associated with high velocity, casting some doubt on the validity of the first two breaks. The last break is real: deposited in reducing conditions (grey colour), physical property unit 8d contains negligible carbonate, while black claystone is more common. Stratigraphically, this break (1120 m) equates with the top Aptian/Albian. Seen in this light horizon K_m is less important than the white loop that immediately succeeds it or, alternatively, horizon K_m should be drawn at the white loop. It is usually drawn between the Plantagenet and Hatteras Formations (1120 m).

The horizon A complex is produced by the interference of reflections from the top and bottom of physical property unit 7 (fig. 6.3). This corresponds closely with litho unit 2: a middle Eocene radiolarian claystone. The upper horizon correlates with a physical properties break at 953 m (603B-15-4). The study of physical properties over this interval is complicated by variable recovery. The preceeding interval shows little variation and in consequence contributes little to the reflected signal. The double peak is explicable in terms of the source wavelet, which has two black loops and one white (cf. the seabed reflection). The very strong lateral persistence of these reflections indicates strong lateral homogeneity. The physical properties of samples that were measured show no sign of more than one break, which is also consistent with the lateral persistence.

The upper horizon is characterised by a marked increase in both horizontal and vertical velocity and a decrease in the density; the latter being due to a higher proportion of biogenic silica. Together, these factors suggest an increase in the importance of the sedimentary framework to the transmission of sound. Lithologically, this break correlates with the boundary between litho-unit 1D and litho-unit 2 (silt-rich claystones above radiolarian claystone). I examined the ultra-fabric of these two units using a scanning electron microscope, which revealed a marked difference in their structure (Plates 6.3-6). Litho unit 1D is a monotonous claystone with silt-sized clasts such as feldspars, some of which show authigenic weathering (Plate 6.5). Litho unit 2 is similar but additionally exhibits abundant veins and cavities (Plate 6.3) possibly produced by dissolution of calcareous fossil debris. Each vugh is packed with lepispheres of opal-CT approximately 4 microns in diameter (Plate 6.6; Weaver and Wise, 1974; Oehler, 1975). Those lepispheres which seeded adjacent to the vugh walls coalesce to form a continuous radiaxial coating. The higher percentage of silica explains the reduced density, while early formation of a strong cement may have helped to preserve a greater proportion of the initial porosity and so explain the higher porosity. As explained in chapters four and five, opal-CT is intermediate in the diagenesis of biogenic silica (porcelanite) to chert (quartz). Reprecipitation of silica as cement would explain the increased strength of the sedimentary frame as indicated by the increase in sonic velocity.

The lower reflector appears to be the interference of a negative impedance contrast at 1020 m (603B-21-6/603B-22-1) and of the tail of the reflection from the upper reflector. The top of physical property unit 8a, 1020 m, is characterised by a sharp rise in grain density and a fall in porosity. The increase in grain density is more than offset

by the porosity change, as the polarity of reflection is governed by the fact that velocity falls due to the lower porosity (fig. 6.3). It should be noted that the low velocities recorded were partly due to (i) the friable state of samples which hindered measurement because only a poor acoustic couple could be achieved and (ii) that core 603B-22, containing green claystone, exsolved large amounts of gas, increasing the liklihood of damage to the sedimentary fabric. The negative impedance break at 1020 m coincides with the boundary between litho unit 2 and litho unit 3 (radiolarian claystone above variegated claystone). The decrease in biogenic silica correlates with a decrease in the sonic velocity as a result of the comparatively retarded diagenesis.

Lack of data for two sections within physical property unit 7 is unfortunate, but it seems unlikely that any significant boundaries have been missed. Cores 603B-15 through 603B-29 are unfossiliferous making any chronostratigraphy unreliable. A study of sedimentation rate indicates the presence of at least one unconformity within the interval and a significantly lower sedimentation rate. The upper horizon may equate with horizon A^u, which is widespread along the continental margin of the North American Basin. It is attributed to increased contour-current activity during late Eocene to early Miocene times (Tucholke, 1983). The lower horizon poses greater problems of correlation. It marks a raising of the calcite compensation depth (CCD), causing biogenic silica to dominate which is consistent with the lower sedimentation rate. Elsewhere, a similar event is thought to be responsible for the production of a chert-rich horizon of middle Eocene age, which is accepted to be the lithological correlation of horizon A^C. Strictly speaking horizon A^C is the top of this chert-rich layer, suggesting it coincides with the upper horizon and therefore the lower horizon has no seismostratigraphic name. The

Fig. 6.5 Interpretation of horizon X, site 603

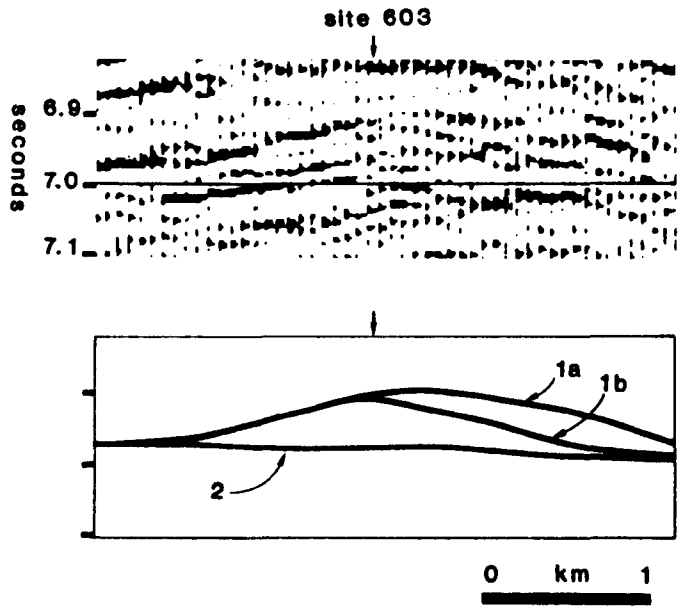

Interpretations:

1. a & b this study
2. van Hinte (pers. comm.)

Detail of site survey profile for site 603 (box B of fig. 6.2) showing the ambiguity of interpretation of Horizon X in the vicinity of the site

absence of cherts makes the name 'horizon A^c' inappropriate, though whether their absence is because they never formed as a result of insufficient diagenesis or were removed by bottom-currents during erosion of horizon A^u is not known. Similarly, the names horizons A^t and A* are unsuitable due to the lack of significant turbidites or lithified limestones respectively (the upper and lower horizons are labelled A^u/A^t and A^c/A^* in the site chapter (van Hinte, Wise, et al., in prep). They have not been used here for the above reasons.)

Horizon X correlates with 700 m (core 603-42-2). There is some uncertainty with the interpretation of horizon X on the profile in the vicinity of site 603 (fig. 6.5) and other correlations would obviously yield different interpretations. Horizon X is the top of physical property unit 5a, which is defined by an increase (downwards) in velocity and a low carbonate content (fig. 6.3). This corresponds to the top of litho-unit 1C, which is characterised by the appearence of biogenic silica. The lower bulk density is a combination of a lowering of the grain density and an increase in porosity. Higher velocity and low porosity indicate that for some reason the sedimentary framework is better cemented and more important for sound transmission.

Horizon M_2 correlates with 563 m (core 603-27). This is the largest of a number of physical property breaks between 510m and 617m, all of low amplitude. Velocity increases markedly, while grain density and porosity both contribute to a local lowering of bulk density. Horizon M_2 is correlated with horizon X of site 388 which was attributed to an increase in the stiffness of hemipelagic clays (Benson, Sheridan et al., 1978; van Hinte, pers. comm.). The change in grain density suggests that compositional change is also a factor: site 388 shows no comparable change in grain density. The higher

carbonate content is attributed to siderite nodules, burrows and layers: the greater velocity of siderite only contributes a small amount to the overall velocity rise, the balance being due to variation in the degree of diagenesis. The density break is more gradual suggesting energy is returned from a slightly broader depth of sediments between 547 m and 575 m.

Horizon M_1 does not correlate well with the direct model. It is difficult to trace on the profile and is particularly weak at site 603. However, the broad reflector immediately preceeding horizon M_1 does match closely. This correlates with 366 m (core 603-16-3) the top of physical property unit 3a. Both sonic velocity and bulk density increase at this depth. Similarly, the immediately succeeding white loop matches (fig. 6.4) and correlates with the base of litho unit 1A at 448 m (core 603-19-CC) the top of physical property unit 3b. Here, nannofossil-bearing clay/claystone overlie quartz-mica-bearing claystone, and sonic velocity decreases, while no clear trend is visible in other properties ,(fig. 6.3).

Horizon P does not give a good match (fig. 6.4). Again, it is low amplitude and difficult to trace locally. It appears to correlate with 190m (core 603 C-22-4) the top of physical property unit 2c, which is defined by a rise in shear strength. No abrupt variation is shown by other properties (fig. 6.4).

Horizon M_2 marks the top of a sequence of strong reflectors (seismic subunit 2D of site chapter). The seismic units above horizon M_1 (seismic subunit 2A and 2B) are characterised by a migrating wave pattern which 'appear to be formed by current action in deep water' (Benson,Sheridan, et al., 1978). They were large scale features on the order of 3 km wavelength and 75 m amplitude. Their sub-surface

seismic expression, although of low acoustic amplitude, clearly shows them to be laterally and vertically persistent. It can be assumed that this expression is due to small systematic changes in the physical properties of the sediments and, therefore, should be discernable from the measurements taken. The seismic unit is entirely within litho unit 1, hemipelagic claystone. Recovery is much disturbed by drilling in hole 603; hole 603B washed through this interval. Hole 603C, which was hydraulic piston cored, provided the best chance to gain reasonable recovery of the upper 360 m. None of the breaks picked from the data are particularly striking, as might be expected from the low amplitude of reflections from the unit. Porosity, water content and bulk density show a very even trend that is controlled by dewatering. Variation in the measured velocity may be explained in terms of the disturbance of the sample and poor signal propagation due to high attenuation and the presence of gas. Shear strength and carbonate content are the most reliable properties. Composition is unlikely to be affected and shear strength may be expected to show the breaks, being directly related to the ability of a sediment to resist deformation (grain size analysis would also be relevant but no data was available). On the basis of these two parameters seven minor breaks can be identified (fig. 6.3). The comparison between synthetic seismogram and the profile is nowhere near as good as for the lower formations (fig. 6.4) but in such a sequence of dipping reflectors any errors in the positioning of the hole to one side of the seismic profile will obviously degrade the correlation (also, if the absolute error remains the same, then as the amplitude decreases, the percentage error must increase.) The precise velocity function over this interval, 0-554 m, is a further source of error. So, while precision in the timing of breaks and their relative amplitude is poor, the causes for the breaks remain real and bear witness to minor changes in the depositional process. The number of breaks identified

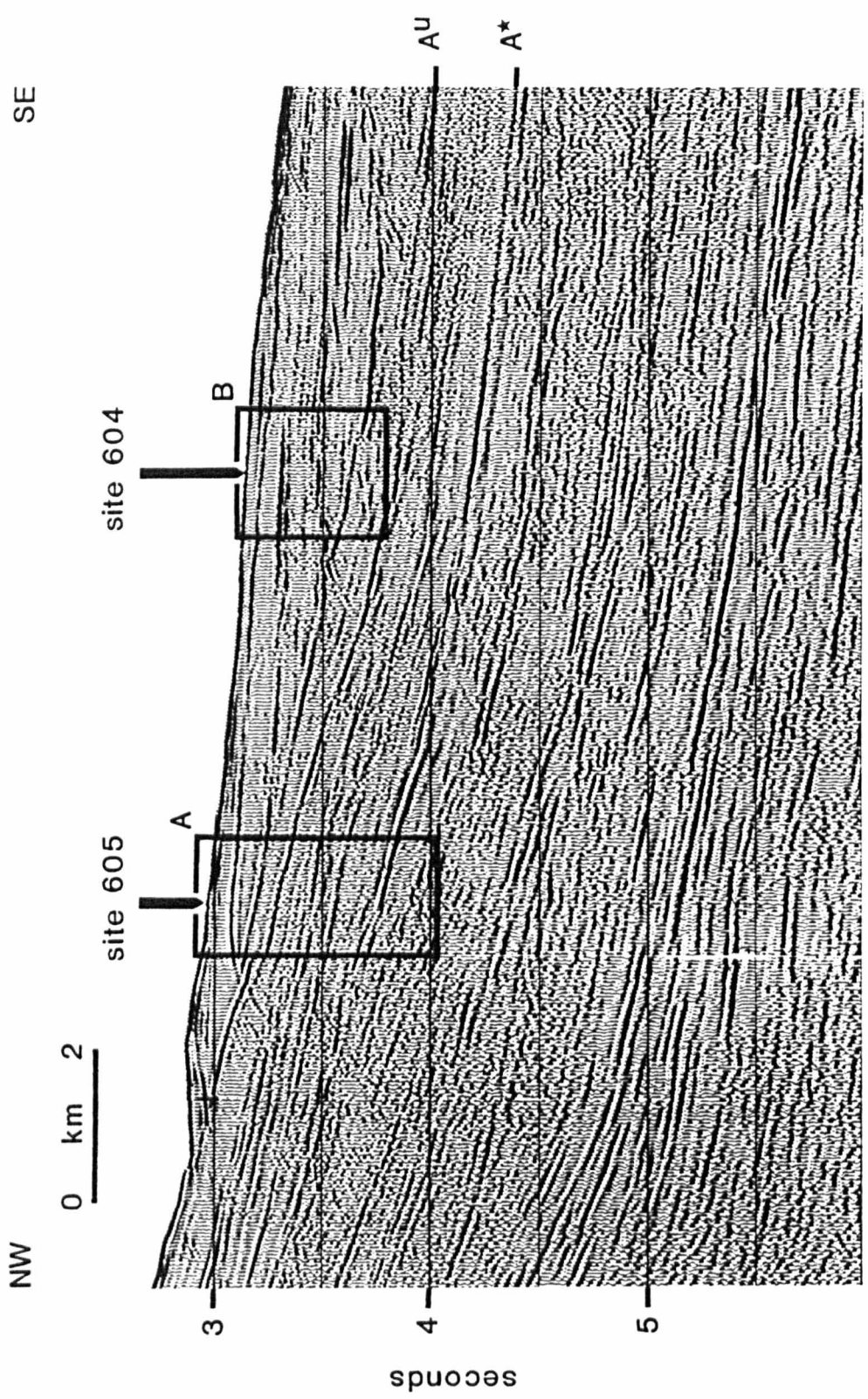

Fig. 6.6 Seismic profile USGS #25 between Sites 604 and 605

is sufficient to produce all the reflections at the frequencies used.

The percentage of carbonate has been related to palaeoclimate (Mayer,1979a) and changes in shear strength may be related to changes in the depositional rate, itself related to the intensity of bottom current activity (palaeoclimate has been related to this, Jones et al, 1970). The high terrestrial content will tend to degrade the climatic signal, but in as much as processes affect physical properties, so reflectors of this type may still be attributed to climatic factors. If climate is an important factor, then it seems likely that the variation is of a spatial frequency considerably higher than either that of the site survey seismic profiling or the measurements taken from the recovered core. More detailed work is needed to confirm this hypothesis.

At site 603 there is a noticeable difference in the character of the main reflectors below the horizon A complex and those above (including horizon A). The more advanced state of diagenesis of the lower sediments produce significantly higher transmission velocities. On a time section, this has the effect of squeezing each unit so that interference between individual reflections is much more important. The homogeneity of the upper sediments at the site increases this contrast.

6.2.2 Site 604

Site 604 drilled approximately 290 m into Quaternary and Neogene sediments. No significant regional reflectors were penetrated at site 604. Accurate correlation with the seismic profile (USGS line 25, fig. 6.6) is hindered by the absence of wireline logs and the precise

Fig. 6.7 Depth plot of physical properties, site 604

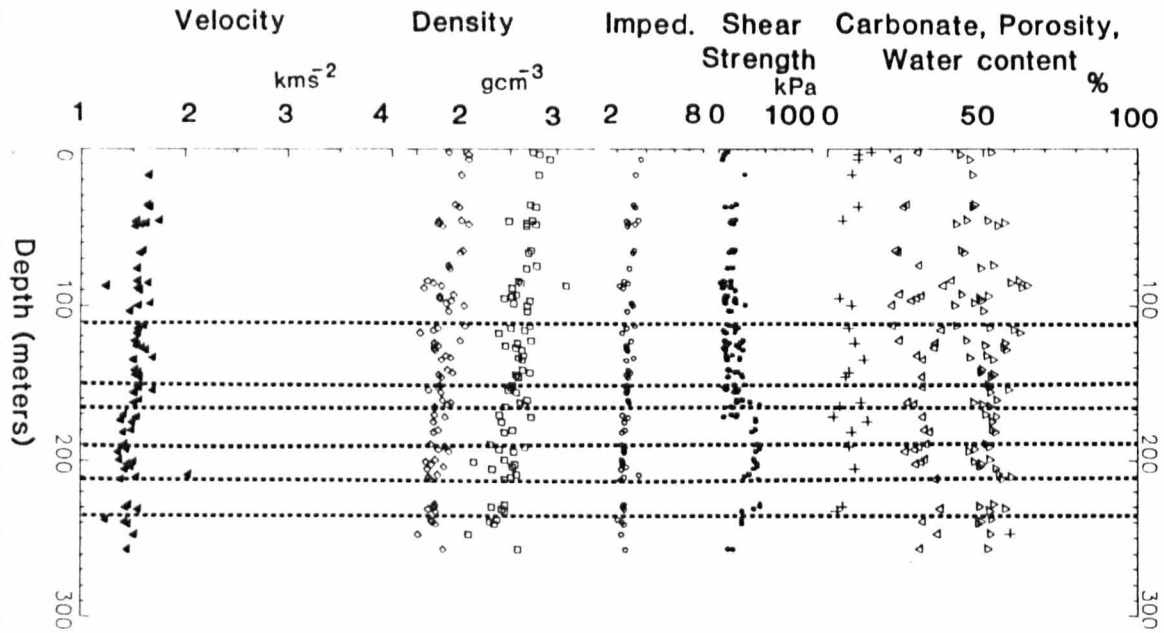

Fig. 6.8 Physical properties' model, site 604

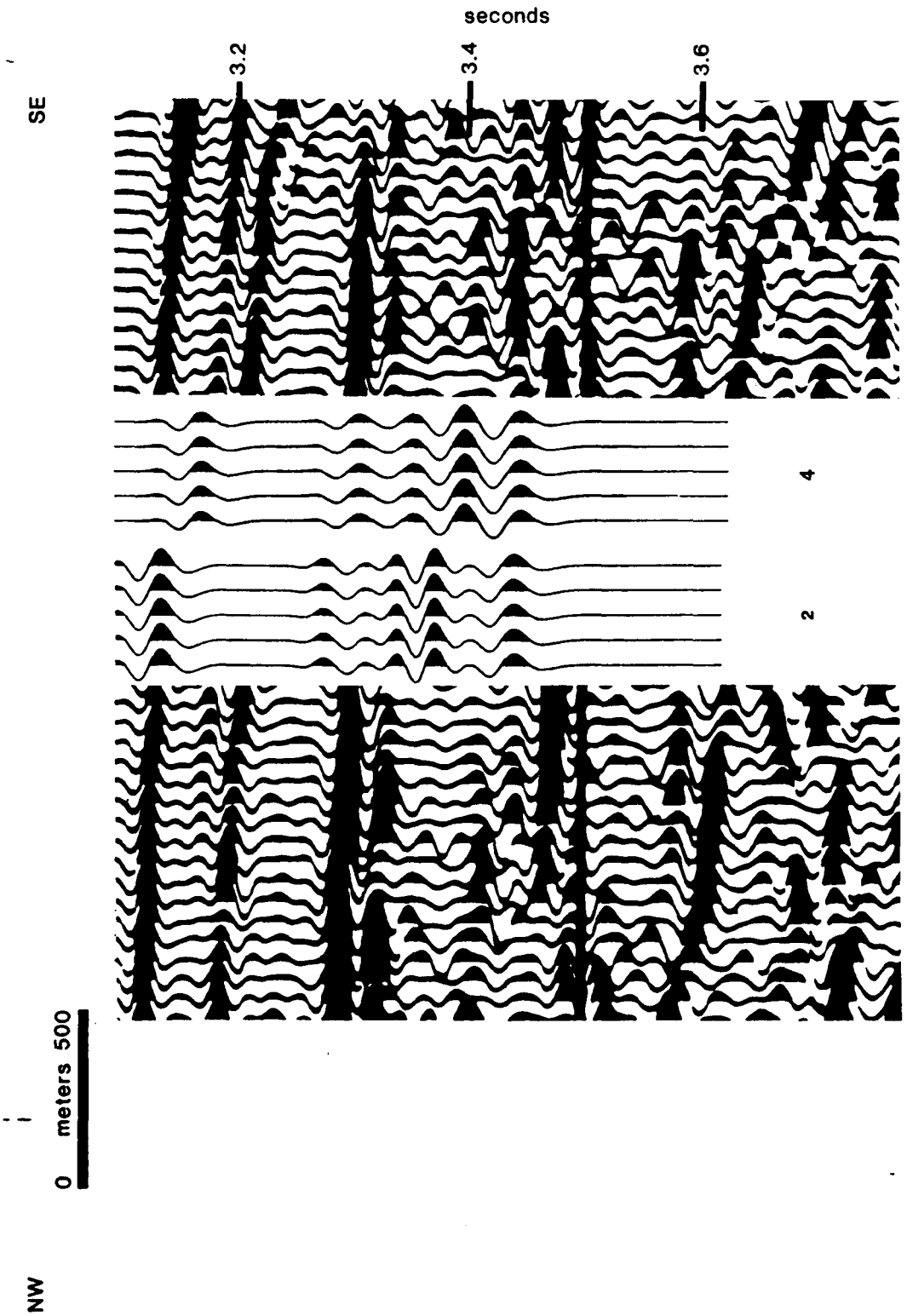

offset from the line of section. Four velocity functions have been examined: the first is from sonobuoy data (Houtz, 1973), the second is from the semblance data determined from stacking of the seismic line, while the third and fourth are determined from correction of the physical proprties of recovered core measured in the shipboard laboratory, with and without mud correction for unrecovered material. Again a physical properties stratigraphy was used (fig. 6.7). All models give transit times (two-way) between events which match to within two milliseconds for events below 151 m (see table 6.3) but there is a large disparity in the initial transit time to this depth. In particular, the mud corrected physical property model and the semblance analysis model (models 2 and 4, fig. 6.8) compare very closely over the interval 151 m to total depth, even for the interval of low recovery (212-235 m). The top interval velocity is over-estimated (due to an absence of data for the uppermost sediments which were not recovered (fig. 6.8, table 6.4)).

When interpreting the seismic section at site 604 care is needed in assessing which reflectors are the most important. The problem of modelling the velocity of sediments immediately below the sea-bed suggests that the site location is out of the plane of the section. Therefore, only those reflectors which are laterally continuous are likely to be seen at the site and these are not necessarily the highest amplitude events. The scale of figure 6.8 is insufficient to show lateral continuity and careful comparison with the more complete section is advisable prior to interpretation (fig. 6.6). In particular, the events at 3.34 s, 3.41 s and 3.45 s are more important than the higher amplitude events at 3.30 s and 3.48 s (TWT).

The hole bottomed in a Miocene debris flow which appears to have a top seismic expression at 3.45 s (TWT). This would then correlate with

the litho-unit 3/4 boundary at 238 m (sub-bottom).

The models can be given a static correction to compensate for the lack of modelling data at the top of the hole and aligned at 3.45 s (TWT). Model 2 now gives the best fit (fig. 6.8). If the misfit at the sea-bed is accepted, the high amplitude reflector at 3.30 s (TWT) is close to the boundary between sub-units 3A and 3B, 122 m. The reflector at 3.34 s (TWT) correlates with 151 m (sub-bottom) within sub-unit 3B. If other models are used, these interpretations will obviously differ. The fact that stacking velocity is equal to the **in situ** velocity indicates a near constant velocity function for the surficial sediments (see table 7.4).

Again, we are making an assumption about the correlation ahead of modelling, implying, in this case, that we know where the top of litho-unit 4 is in order to make a correlation at other depths. With the available data any amount of modelling is going to be imprecise, primarily because all the physical property breaks are of particularly low amplitude. This study at site 604 is a good illustration of the difficulties of modelling and interpretation. The velocity function need be varied only slightly in order to alter the exact correlation. The fact that we are working on dipping strata increases the need for accurate positioning. For example, the problem of a misfit at the sea-bed is removed by picking the site location 1 km south east of the present position. In such a case, while modelling supplies useful constraints, reasoned judgement by an experienced interpreter is probably superior.

6.2.3 Site 605

At site 605, I constructed five models in an attempt to determine the

Fig. 6.9 Depth plot of physical properties, site 605

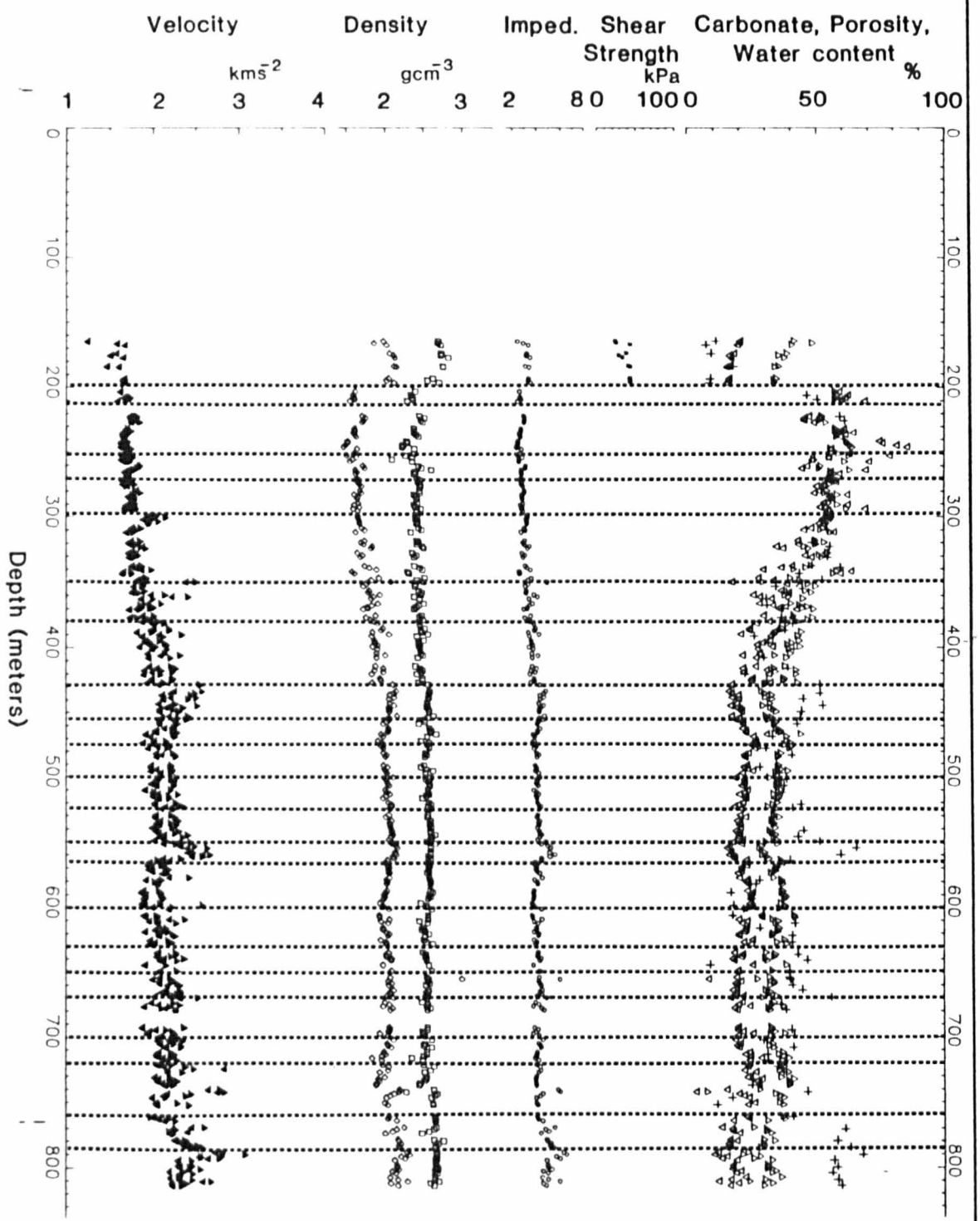

Fig. 6.10 Physical properties' model, site 605

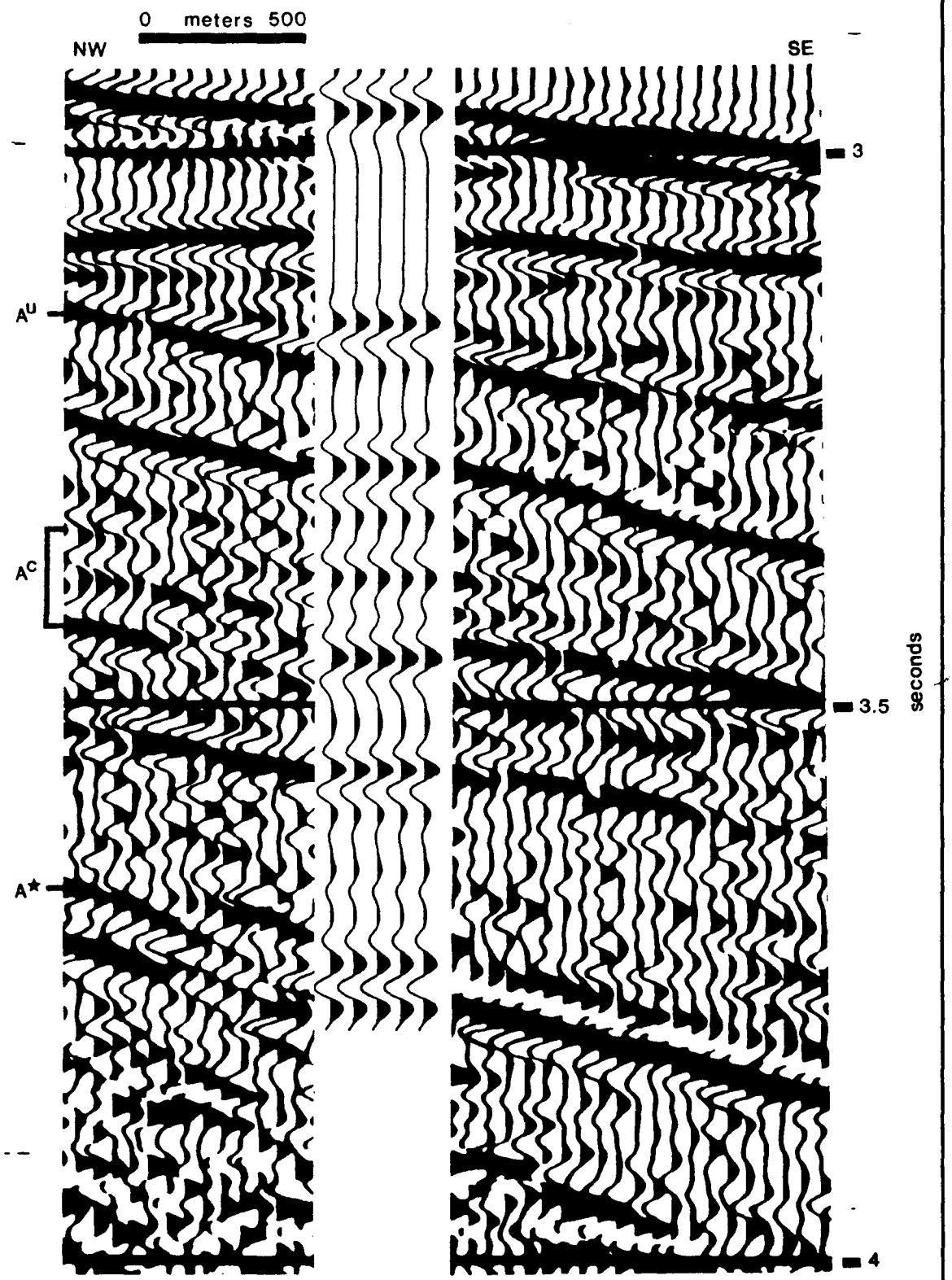

velocity function. The same stratigraphy has been used in each model and is based on discontinuities in the physical properties of samples as measured aboard ship (fig. 6.9). The first is based on Houtz' (1973) velocity function deduced from sonobuoy data. A second uses the semblance data obtained from stacking of USGS line 25. Models 3 and 4 use averaged corrected physical property data as described above, model 4 includes the mud correction for unrecovered material. Various shortcomings of the latter modelling scheme are apparent from this study and their correction yields a fifth model. The inadequacy of the semblance data, which should be accurate, suggests the positioning of the hole is wrong - either along section and/or off section. Model 4/5 has been used for interpretation of lithology (fig. 6.10).

The first problem is to interpret the section and even the tracing of horizon A^u is not trivial (fig. 6.6). The high amplitude reflection at 0.17 s at site 604 onlaps onto the erosional surface that is horizon A^u just downslope of site 605 causing polarity reversal, horizon A^u is faulted upslope from site 605. My preferred interpretation is shown which correlates a strong black loop with the unconformity (fig. 6.10). There seems little doubt that an unconformity of the correct age and stature was encountered at 203 m sub-bottom at site 605 at the boundary between litho-unit 1 and -unit 2. These are strongly contrasting lithologies of grey silt-rich clay (unit 1) and greenish-grey biogenic silica-rich nannofossil chalk (unit 2). There is no data for the interval 198 m - 203 m; the thickness of subunit 1B is insignificant with respect to the resolution of seismic imaging. Therefore, it is valid to model the horizon A^u unconformity as one strong reflection coefficient. The polarity is negative although the break is marked by a rise in velocity, there is an even greater drop in bulk density. The change in

lithology is most pronounced on the porosity log (and density log) (fig. 6.9) and in consequence gives a strong reflection in models 3-5 (the physical properties modelling scheme is based on porosity data).

The upper sediment velocities of sites 604 and 605 as calculated from semblance study of multi-channel data are very different (see table 6.4). It seems likely that the top interval velocity of site 605 is overestimated and should be closer to that of site 604. It should be remembered that the most difficult interval to model is the uppermost one that extends down from the sea-floor because the velocity is so variable and the sediments difficult to measure. A further source of modelling error at site 604/605 results from the empirical velocity/porosity relationship used to correct to **in situ** values, which was based on data recovered at site 603. This was necessary as the accurate determination of the functions relating parameters require a larger dataset than is available at sites 604 and 605. The function determined at 603 was used instead, although the lithology at site 603 is considerably more clastic than the chalks, etc. found at the New Jersey Transect sites.

The interval, 203-270 m, corresponding to the uppermost chalk, is distinguished by negligible separation of vertical and horizontal velocities. This low acoustic anisotropy shows the sediments have undergone minimal diagenesis. Lack of cementation make them more prone to drilling disturbance and the effects of pressure reduction. Porosity rebound has been corrected, but in view of the very high porosity of this formation there may still be a significant error. This will be compounded when the value is used for velocity and density correction. The break at 250 m appears to be more important than the measured values indicate. It correlates with a very strong event at 3.28 s (TWT).

The physical property break at 260/250 m is defined by an increase in velocity and wet bulk density, which only lasts for two sections. Grain density does not change, suggesting the packing/cementation is responsible for the change. Porosity is lower for these two sections, which contrasts with the scattered values from the interval immediately above.

If the assumptions concerning the upper part of the model are correct then the fit between model and profile from 270 m down to total depth (815 m) is very reasonable (fig. 6.10).

The break at 270 m is swamped by the bright reflection at 250/260 m and thus shows as a white loop at 3.30 s (TWT) (fig. 6.10). It occurs within litho unit 2 and is defined by a slight reduction (downwards) in impedance following the sharp rise at 250 m. It corresponds to core 605-14, which was lithologically indistinguishable from adjacent cores, suggesting the delineation of a break may not be appropriate at this depth.

The break at 293 m is very marked on the velocity log, but is not seen in any other properties. The bulk density measurements for the interval 299 m-308 m (core 17) display a consistency that is not repeated until measurements from below 428 m are compared (top of physical property unit 6, fig. 6.9), which have undergone considerable diagenesis. The lack of expression in the porosity log means that no significant reflection will be produced by the modelling scheme (see above). There is little doubt that there exists a layer of about 10m thickness which exhibits an advanced state of diagenesis compared to adjacent strata. The presence of opal-A in unit 2 indicates that diagenesis is not very advanced which may be explained by the shallow

depth of burial.

The next break in the physical properties is seen at 350 m. It is marked by increases in horizontal and vertical velocity and the depth at which the sediments become acoustically anisotropic, which indicates the development of a frame-work structure. This contrasts with the bulk density values (below 350 m) (fig. 6.9), which exhibit considerable scatter. This might be due to compositional variation, but the grain density shows less variation than might be expected were this the case. Generally, the bulk gravimetric measurements for this interval (350-380 m) are variable although it is not clear why. This break is responsible for a medium amplitude event, which matches well with a discontinuous reflector at 3.32 s (TWT).

Horizon A^C was encountered at site 612 (Leg 95) some 16 km upslope from site 605. Wilkens (in press) has demonstrated a clear diagenetic boundary, which is characterised by a large reduction in porosity (of the order of 60% down to 40%). This is caused by the mobilisation of silica, which reprecipitates replacing carbonate clasts such as foraminifer tests and as lepispheres of opal-CT (Weaver and Wise, 1974). Thus horizon A^C is well defined at site 612 as occurring at 324 m sub-bottom (Wilkens, pers comm).

I traced this horizon on the site survey profile to site 605. The correlation crosses several faults and is further complicated by the dipwise thinning of reflectors down-slope mid-way between the two sites; here, correlation is drawn at a tenuous surface of truncation and onlap. This horizon correlates with 350 m sub-bottom at site 605. The same depth is identified to be horizon A^C by the Leg 93 shipboard sedimentologists, their interpretation being based on the presence of opal-CT. This diagenetic horizon is coincident with a

minor compositional change at site 605, which is demonstrated by the change in carbonate content from approximately 50% above 350 m to around 33% below. It should be emphasised that this is by no means a major reflector at site 605 and its correlation with horizon A^C at site 612 is far from certain. If erosion has occurred at the site then horizon A^C proper may have been removed - or possibly the components necessary for its diagenetic formation never deposited. Nevertheless, the fact that a reflection was traced, and, accurately matched by the subsequently developed model is a strong indication that the interpretation given is accurate. This depth (350 m) is the top of litho unit 3 which is upper Early Eocene in age.

At 380 m velocity increases and bulk density becomes less variable (fig. 6.9). No change is seen in grain density, which suggests that the change is due to further cementation of the framework. The reflection produced is low amplitude and appears to be truncated a few kilometers down slope by the surface identified to be horizon A^C.

The next break in the physical properties is at 428 m and is one of the three strongest breaks at the site (fig. 6.9). It is clearly seen as a change in grain density (increase downwards) and a reduction in porosity. Bulk density and velocity also increase. The scatter of bulk gravimetric measurements is much reduced and indicates a significant increase in the stage of diagenesis. The rise in grain density indicates compositional change, which is in agreement with the carbonate log, which shows a significant jump from approximately 30% to 50%. No break is seen on the lithology log - the break lies roughly in the middle of unit 3, but interestingly there is a change in age assignation between core 29 (lower Middle Eocene) and core 30 (lower Eocene) at this level. There is no evidence of onlap/ truncation on the profile (indeed this surface is truncated downslope

by the surface termed horizon A^C). The change in biostratigraphic assignation may be interpreted as a change in palaeo-ecology (different fossils have different age ranges) rather than as an actual hiatus or other chronostratigraphically significant horizon.

With regard to horizon A^C at site 612, it is worth noting that the sedimentological horizon was coincident with a physical properties break defined by porosity reduction from approximately 60% to approximately 40% in responce to silica mobilisation (Wilkens, pers comm). A very similar signature is seen on the porosity log from site 605 at 428 m, and correlates with a reflector of similarly high amplitude. Thus on the basis of physical properties alone the correlation of horizon A^C would be made at this depth, some 78m lower. The age at site 612 (for cores 35 and 36; 309-338 m) is middle Eocene, which compares more favourably with the lower-middle Eocene age of core 605-22 (346-356 m). Thus, the reflector as traced appears chronostratigraphic (given the resolution of palaeontological zonation, and providing that the different teams of sedimentologists have picked the same horizon). In contrast the high amplitude event, which would have been traced with a profiling system of lower quality than the 12-fold USGS line corresponding to the physical properties unit boundary is <u>not</u> chronostratigraphic in form. Whether a wireline log interpretation would follow the porosity break is not known, but it seems likely. Unfortunately, problems of resolution and sedimentological consistency cannot be ignored and could equally reverse the argument if wrong. More precision is required in dating and the similarity of sedimentological interpretation must be established. (Leg 93 used smear slide analysis to identify opal-CT, while Leg 95 base their delineation on routine XRF study).

Problems of detailed seismic correlation in the deep sea have been

incurred by previous site surveys: 'Reflector intensity can vary greatly along the profiles. The top of the M sequence mentioned above is an obvious example. A strong reflector sometimes fades out completely and another reflector at a slightly different depth appears and grows in intensity until it becomes the dominant event. Where the two overlap there is no thinning of the intervening layer and no evidence of the interference effects such as those discussed by Vail et al. (1977). The effect is more consistent with a variation in acoustic impedance in the intervening layer which simultaneously decreases the impedance contrast at the first interface and increases it at the second. This behaviour, together with the limited vertical resolution, makes it difficult to correlate reflection events from one profile to another across a data gap.' (Bryan et al.,1979).

The velocity data show anisotropy to increase strongly at 428 m coinciding with an increase in the value of velocity. The values decrease (downwards) slightly over the next 30 m (approximately) and then show a further negative break at about 455 m. This trend is also seen on the porosity log and in consequence produces a medium amplitude coefficient (negative) on the physical properties model. This is a broad white loop immediately succeeding the strong (black) reflection from 428 m and matches the profile well (Fig. 6.10). Again this is entirely within litho-unit 3.

A series of low amplitude events at 475 m, 500 m and 525 m interfere to produce the acoustically quiet interval between .564 s and .615 s sub-bottom. These breaks are arbitrarily chosen to permit more (apparent) continuous modelling - they do not correspond to breaks (in the strict meaning) in the physical properties and are effectively ignored by the modelling scheme. Lithologically this is within unit 3, which is a monotonous sequence of nannofossil limestones and chalks.

Evidence for cyclicity seen in the cores is not discernible from the physical properties although it may explain the acoustic character of the interval, which tends towards random/chaotic downslope (thickening cycles interfering differently).

High amplitude physical property breaks at 552 m and 565 m, which bound physical property unit 8, together are responsible for the next strong reflector. This has no name, although it has been suggested to correlate with the 52 Ma hiatus of Vail et al. (1980)(van Hinte, pers comm). The evidence of onlap above this horizon is ambiguous. The break is produced by an abrupt decrease (downwards) in sonic velocity and wet bulk density. Porosity is reduced and carbonate content is elevated to around 60%. The top of unit 4, 565 m, represents the 'sharp contact between the light greenish nannofossil limestone and the underlying dark clayey nannofossil limestone (marl)' (van Hinte, Wise, et al., in prep.). Considered as a pair of reflections emanating from the top and bottom of physical property unit 8, their separation is close to the optimum for constructive interference between the individual reflections (at 45 Hz). The lower, negative reflection is the stronger, which explains the negative polarity of their combined strong reflection at .608 s sub-bottom. The model does not compare particularly well in the timing to this horizon and suggests the interval velocity between 428 m and 565 m is overestimated. The direct model gives .109 s (2.514 km/s), while the profile indicates a transit time of .135 s (2.030 km/s) and suggests the actual interval velocity lies somewhere between these two values. Model 5 has been corrected at this level. Lithologically, this is the top of unit 4 which is a clay-rich nannofossil limestone of Ynezian age.

Between 600 m and 720 m there are a number of low amplitude reflections, which correspond to the acoustically quiet interval

between 3.57 s and 3.75 s (TWT). Below 663 m carbonate diagenesis is advanced enough to have caused recrystallisation of most biogenic fragments.

Important breaks in the bulk density and velocity data occur at 760 m and 785 m. The modelling scheme fails to give high values to the coefficients at these depths, simply because the porosity log does not show an equivalent variation. This demonstrates a lower limit to the applicability of the modelling scheme based primarily on porosity. Once porosity is much reduced, variation is less sensitive and no reflections can be modelled. Model 5 has been corrected using velocity data to adjust amplitude - the timing has not been altered.

The top of unit 5, 740 m, is characterised by an abundance of foraminifers and terrigenous silt. 'The uppermost six meters of subunit 5A is a unique interval in which the silt and clay content decreases rapidly upward, distinct dark filled burrows vanish, and the lithology becomes a very dense light greenish grey limestone of almost 99% carbonate' (van Hinte, Wise, et al., in prep.). The uppermost 7 cm of this limestone is noted as an unconformity in the sedimentology report. This group of reflectors (roughly) correlates with horizon A^C of Klitgord and Grow (1980). Van Hinte (pers. comm.) correctly positions horizon A^C somewhat higher and names this strong reflector 'horizon A*'. Horizon A* is a regional reflector in the North American Basin and, generally, is accepted to be a particularly well lithified limestone of Maestrichtian age (Tucholke, 1977). Vail et al. (1980) consider horizon A* to be Thanetian in age which has been equated with horizon A^{52} (see above).

The bulk density change is more noticeable at 740 m and is particularly variable throughout unit 5. The uppermost 6 m of subunit

Fig. 6.11 Physical properties' model, site 612

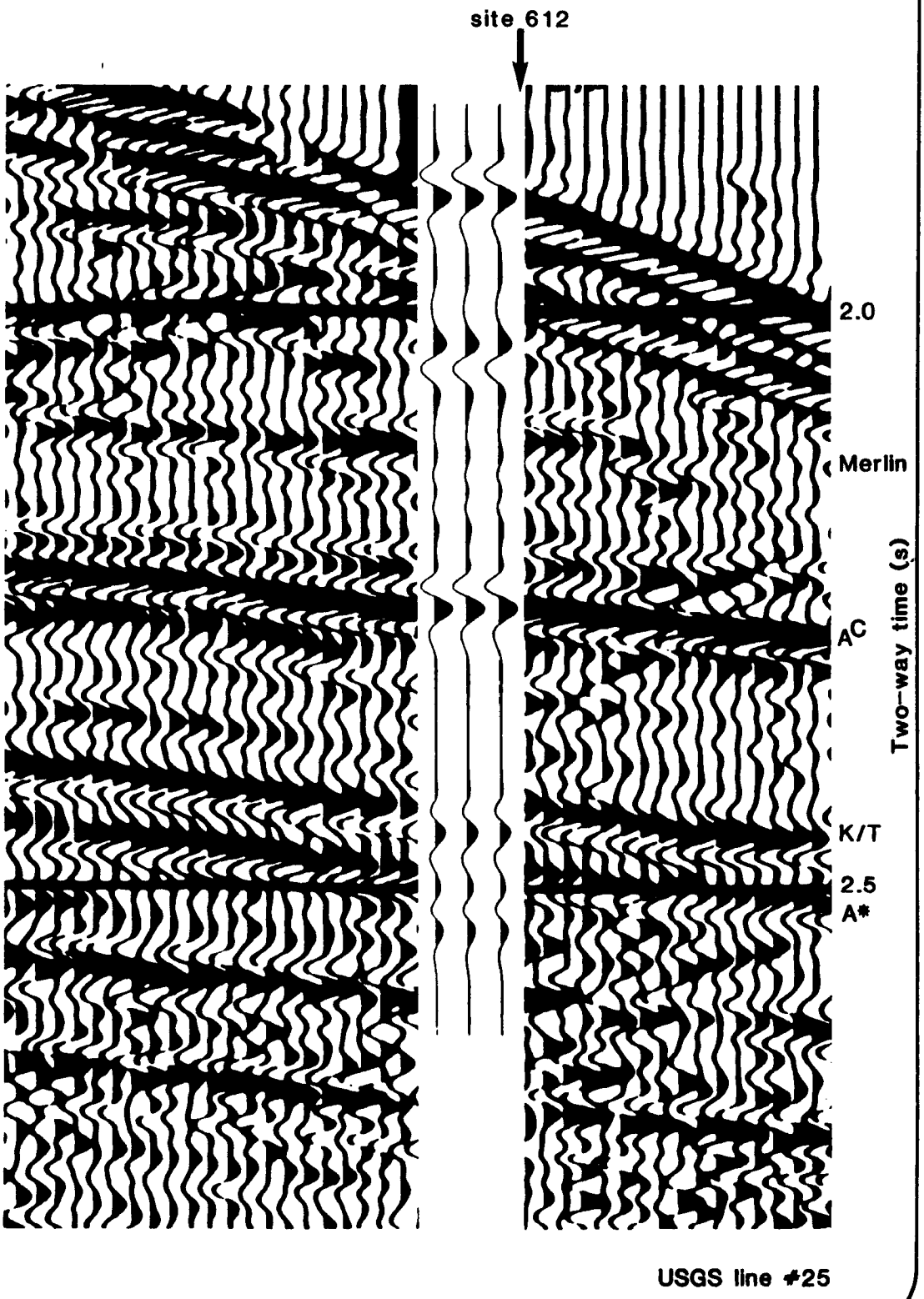

5A exhibits high velocity, but the main rise in velocity does not occur until 760 m, coinciding with the rise in carbonate content. Another thin high velocity stratum at 786-791 m (core 605-69-1/2; fig. 6.9) further complicates the pattern of interfering reflections.

The strong reflectors at .775 s (white loop) and .792 s (black loop) on the profile are the product of these closely spaced impedance contrasts. The suggestion that 740 m may be an unconformity is not supported by the seismic profile: only the very vaguest onlap is discernible and there is no sign of truncation. If the modelling is accurate then the boundary between unit 4 and unit 5 can be drawn at 3.72 s (TWT): this is the Cretaceous/Tertiary boundary.

Exactly where horizon A* is picked must depend upon the definition of this horizon. It is debateable whether it is the top of subunit 5A or the top of subunit 5B.

6.2.9 Site 612

Physical property modelling was performed at site 612 to permit correlation with site 605 - both sites are located on USGS line 25. The site will not be discussed in detail as it was not part of the same cruise. Wire-line data was collected at the site, but was not available for this study.

The reflectors seen at site 612 are Ac, A* and a more (recently named) horizon Merlin, which is top-middle Eocene (similar reflectors are seen at site 613 - no modelling available.)

CHAPTER SEVEN

Summary of modelling results

7.1 Introduction

There are a number of questions that have been posed throughout the body of this thesis. These include the general nature of reflectors in the deep sea, their chronostratigraphic relevance and, in a more, philosophical way, how correlation should be approached. I have attempted to solve these problems by computer modelling of reflections using data that describe the physical variations of the sedimentary column. The performance of this modelling has shown deficiencies in the algorithm, as well as high-lighting some relationships that were not previously realised.

7.2 Summary of modelling

The modelling schemes described in chapter three and used thereafter allow many of the reflectors found on site survey profiles to be modelled, that is, for them to be placed in terms of TWT below seafloor and with appropriate amplitude.

However, a number of problems were encountered. The most reliable form of modelling was shown to be that using wire-line data as the primary data input. The scheme might be improved if exact travel-time-to-depth correlations were known, such as might be the case if velocity survey information were available but this has never been the case in the deep sea. The absolute value of density

measurements relies on assumptions of the lithology, but as described in section 3.5.1, it is only the relative value that is important for the purposes of modelling. The close match between model and profile obtained at site 406 (fig. 3.8) is a strong indication that the in situ measurements obtained by wire-line logging are accurate. Most important is the accuracy of the velocity function.

The subjectivity involved in delineating litho- or physical property boundaries within gradational facies is clear. The results at site 398 show that the grouping of the interbedded unit as a whole and using averaged properties to calculate reflectivity is valid.

It is worth remembering the relationship between the velocity of compressional wave and the bulk density (equation 1, chapter 2). From the dependency of velocity on density it is quite clear that density remains important. The same two parameters are used for the calculations of reflectivity. However, to consider only two parameters when considering the formation of reflectors is unwise, especially in view of their interdependence. The variation in velocity can be seen to be independent of density across some horizons and it is this 'degree of freedom' between these two parameters that is the most important single factor in the generation of seismic reflectors within apparently homogenous formations. This 'factor' is difficult to define (and measure) but may be considered similar to the sedimentary fabric.

The modelling scheme based on physical properties was attempted in order to allow modelling at many more sites than those at which wire-line logging had been performed. While it has proved useful at a number of localities it does not allow as reliable a method as wire-line logging. A number of refinements may be possible, but two

factors implicit to its function always make its performance questionable. The first of these concerns the data. The availability and quality of data are very variable and on many cruises, particularly data from the earliest Legs, are insufficient for modelling. My modelling relies on closely spaced measurement of as many properties as possible in order that, through redundancy of data, the breaks are correctly identified and erroneous values eliminated. The density of this coverage must be sufficient for the delineation of a physical properties stratigraphy of sufficiently fine scale to allow the discrete model to approximate the continuous site survey profile.

This leads to the second factor limiting the performance of modelling. The physical properties stratigraphy is limited to a resolution of about 10 m. If modelling is intended for comparison with high resolution surveys with a wavelength less than this then clearly no good fit can be expected. The majority of site surveys have a dominant frequency below 60 Hz, which at 2000 m/s is equivalent to 33 m wavelength and well within the resolution of modelling.

With regard to sampling theory, the data need not satisfy the Nyquist criterion of 'two samples per wavelength' if the individual measurements can be relied upon for their accuracy and known, with reasonable certainty, to be representative of a thicker lithological unit. On the face of it this may seem to be a rather dangerous assumption. However, it should be remembered that the physical properties measurements are taken from samples that are selected to be representative and while actual physical measurement is sadly discrete, visual examination is limited only by primary core recovery. Physical variation between samples that is not directly visible will be missed, but is probably not significant for reflector generation.

Nevertheless, the idea that the in situ velocity function may be approximated by correction of surface measurements is important. Equally, the assumption that reflectivity may be modelled as the difference between the averaged impedance of adjacent layers, rather than the bed-by-bed calculation used in wire-line modelling is important. The modelling scheme serves as a useful independent means of interpretation and correlation. It is not the answer and it does not give greater accuracy. Its value lies in aiding a more thorough understanding of the possibilities and a more objective interpretation.

7.3 Sedimentology of reflectors

Overall the existing interpretations have been supported, and, dubious areas where interpretation is doubtful have been highlighted. Modelling affords a more quantitative method of interpretation and allows the error in the velocity function to be examined.

Although the number of models is not large, several reflectors have been sampled at more than one locality. It is possible to draw some generalisations about individual reflectors and in particular note distictions in the character of different reflectors. Those to be discussed are:

7.3.1 Clay-to-claystone compaction horizon

7.3.2 Cementation reflectors

7.3.3 Calcite compensation depth reflectors

7.3.4 Lower Cretaceous and Jurassic reflectors.

7.3.1 Clay-to-claystone compaction horizon

Sedimentation in the deep sea environment has been shown to be more

Fig. 7.1 Idealised physical properties variation over a clay-to-claystone transition horizon

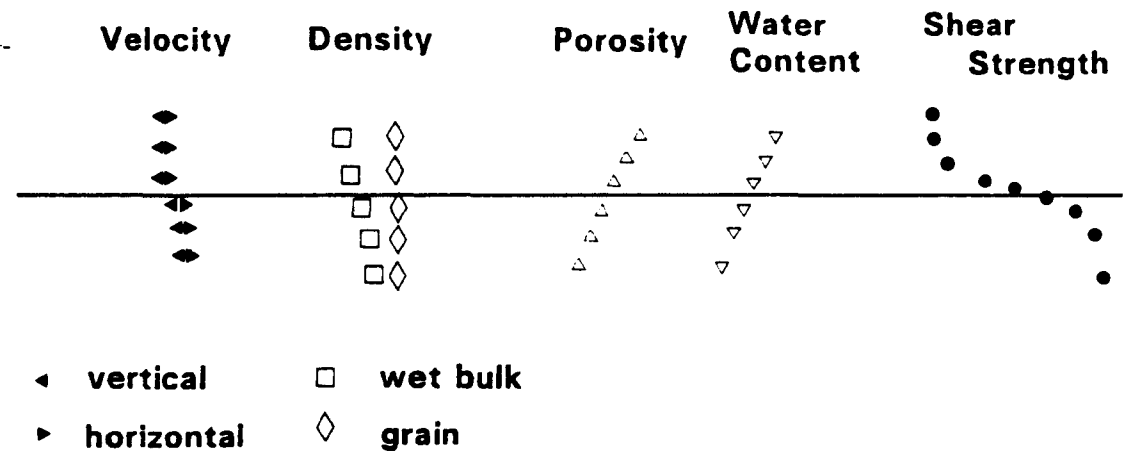

Fig. 7.3 Idealised physical properties variation over a cementation horizon

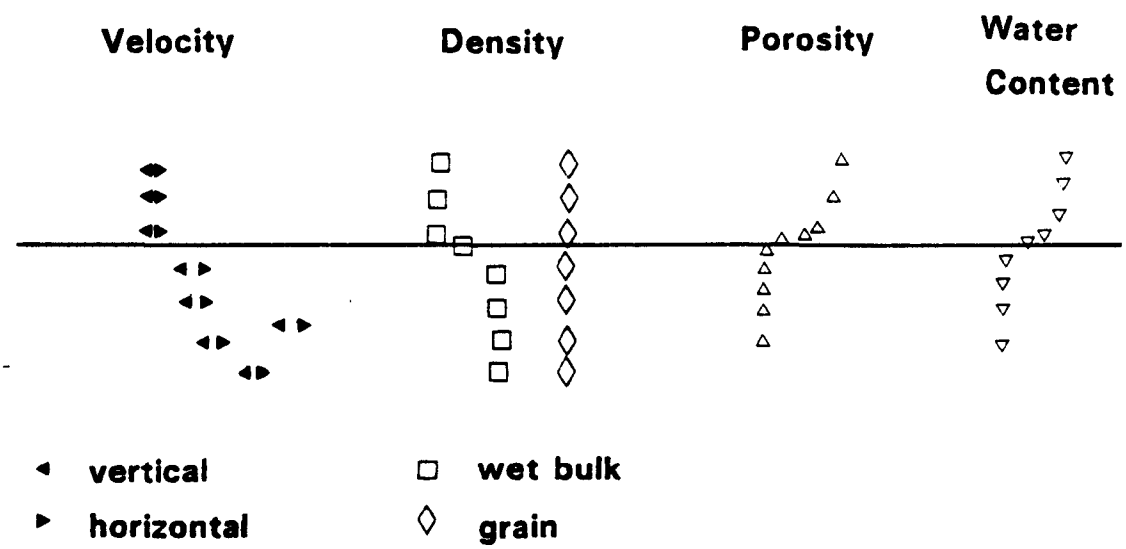

complicated with the recognition of turbidites and gravity flows (Kuenen & Migliorini, 1950) and contourites (Heezen, Hollister & Ruddiman, 1966). Nevertheless, the idea that the floor of the deep sea is a quiet environment remains a reasonable one. Sedimentation may not be continuous but it is more gentle when compared to shallow water and sub-aerial environments. The initial form of many deep sea sediments is as highly unconsolidated aggregates with water contents that may exceed 90% (indeed, nephloid layers may preclude the definition of a sea-floor, where turbid bottom water grades into soupy sediment.) The processes involved in turning such an aggregate into a 'hard' sediment are both chemical and physical and appear to operate more or less continuously up to the completion of lithification. The processes involved are divisible into those of compaction and cementation. The force for compaction is overburden pressure and is calculated as the non-buoyant weight of overlying sediment. Although the sediment may de-water evenly with increasing overburden, the effects of such progressive change are not so even. In particular, the sediment shear strength increases suddenly as the particles reach a minimal packing structure. In this way, a small decrease in the water content of a sediment can bring about a large rise in the shear strength. Acoustic transmission is enhanced, and as a consequence impedance rises. Density may be expected to show no particular sharp break. We may construct a physical property model of such a horizon (fig. 7.1).

The clarity of such a signature in the physical properties will depend on the constancy of sedimentation rate and sediment supply. Therefore, it shows a tendancy to be strata-parallel (and not bottom simulating). Fine grained clastic sediments are expected to show this transition most clearly. In them this represents the clay-to-claystone transition. It occurs at about 180 m sub-bottom, or at an overburden pressure of 12 kPa (site 603).

At site 603 the reflector is labelled horizon P and occurs at a depth of 190 m sub-bottom. Horizon X at site 388 was attributed to an increase in stiffness of hemi-pelagic clays (Benson, Sheridan et al., 1978). This horizon occurs at 285 m sub-bottom which is somewhat deeper than might be expected. Indeed, horizon X is correlated with horizon M2 at site 603, which occurs at a depth of about 560 m (van Hinte, pers. comm.). Correlation by process of reflector generation would draw the line between P and X.

Horizon Av at site 386 is reported to correspond to the occurrence of coarse, high-velocity sands recovered from 170 m sub-bottom. This is rather shallow, and the lithological variation is probably more important. At site 387, horizon At is identified to be at 175 m sub-bottom. It is not characterised by any abrupt change in lithology or physical properties (shear strength was not measured). The only observable change is that the physical properties become more clustered, indicative of more indurated sediment.

Elsewhere, this horizon may be the ooze-chalk-limestone transition. The difference is obviously dependent on the accumulation of carbonate dominated sediment and no interference from other diagenetic processes. This may be more relevant in studies of Pacific sites where terrigenous influence is at a minimum.

7.3.2 Cementation reflectors

The second process responsible for diagenesis is cementation. This is a complex process and may be affected by many factors. These need not be described in detail, but those relevent to the formation of particular reflectors will be highlighted.

Reflectors sampled at sites 603 and 605 demonstrate the sensitivity of acoustic reflection to very small changes in the degree of diagenesis. Slight compositional changes permit different stages of diagenesis to be reached as different constituent minerals become mobile at different depths and/or ages of burial. Perhaps the most important physical characteristic is the nature of the grain-to-grain contact, which is affected by consolidation and the development of a cement. Horizon A and horizon X at site 603 and horizon A^c at site 605 all result from increased silica content: elevated velocity and low porosity indicating an increase in the strength of the sediment framework as a result of the early formation of a cement.

Horizon Ac is an important member of the horizon A complex. As mentioned (section 1.3) the early drilling results suggested that chert-rich layers of Eocene age were responsible for the reflector. The Eocene is a special time in the history of North Atlantic sedimentation. The exact causes are not fully understood, but for some reason the sediments of the Eocene are anomalously rich in silica. This may be due to a Maestrichtian/Paleocene rise in the CCD, or due to anomalous productivity of siliceous organisms. The result is that without a great deal of lithological contrast, the composition of Eocene sediments, particularly those of the middle and lower Eocene, was subtly different from that of earlier and later deposits. This difference is responsible for altering the course of diagenesis. The end form of the sediment and the time taken for such changes to occur are altered. Both of these are important for the impedance contrast that causes horizon Ac. The importance of the middle and lower Eocene as a time of distinct sedimentation is underlined by the direct correlation between the thickness of silicified layers and in the sedimentation rate (von Rad et al., 1978). Chert horizons are

Fig. 7.2 Silica diagenesis

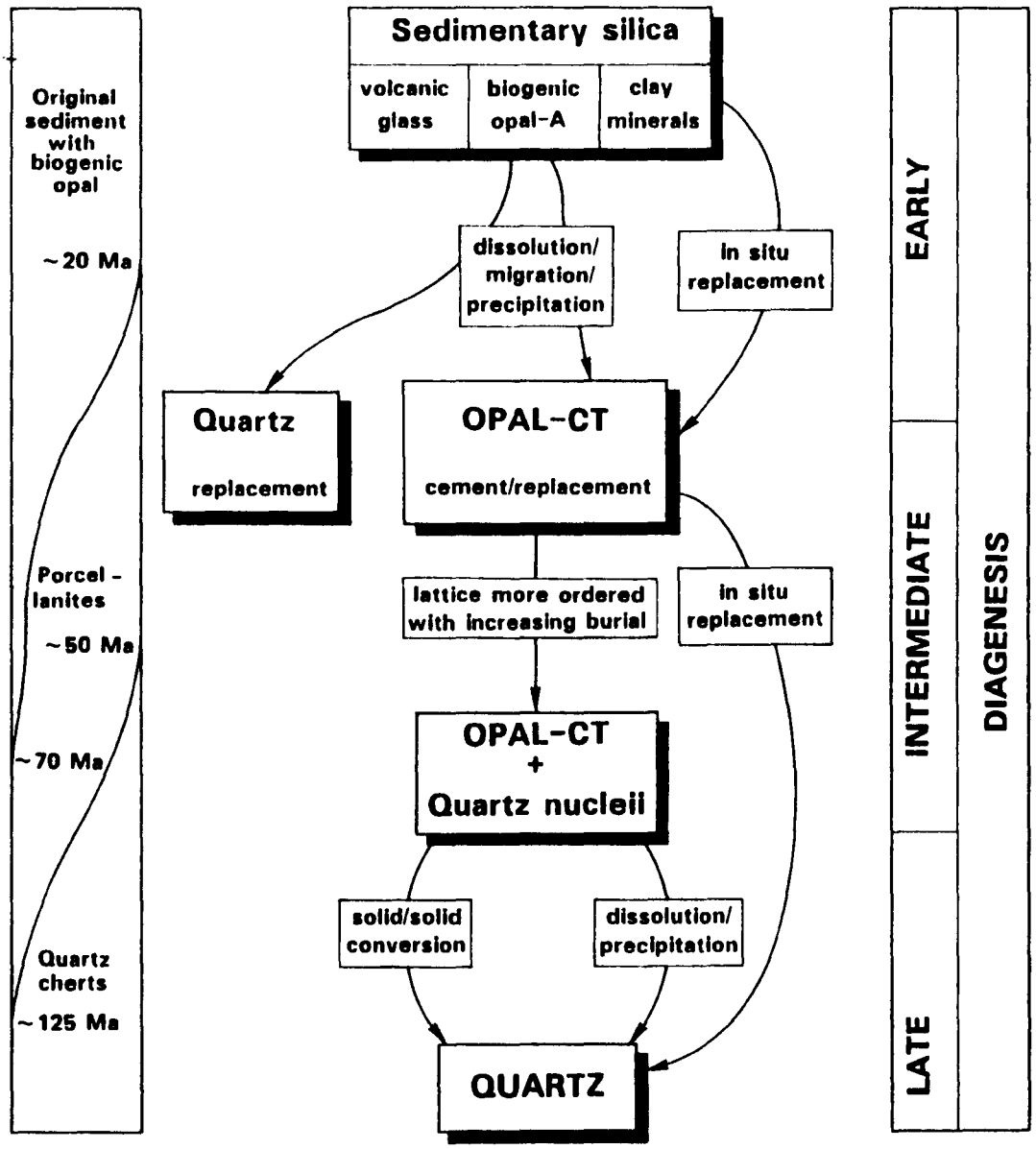

(after von Rad, et al., 1977)

individually too thin to be resolved by seismic reflection. It is the anomalous nature of the sediment in which they form that is responsible for reflection.

In the case of horizon Ac the important factor appears to be the early formation of opal-CT from amorphous silica. It is the nature of this process - its time-scale and its early intermediate product, porcellanite, that is most important for the existence of the impedance contrast.

The Eocene porcelanites form in a wide variety of lithofacies ranging from clayey abyssal sediments deposited below the CCD to calcareous oozes. There is no tendency for preferred silicification of a given lithofacies type. However, the product of silicification does vary with lithofacies and allows opal-CT porcelanites to be subdivided (Reich & von Rad, 1979):

1. bedded porcelanites associated with clayey sediments
2. silicified turbidites with opal-CT replaced matrix
3. calcareous (nodular) porcelanites

Opal-CT is always the first silica phase during silicification (fig. 7.2). In carbonates early opal-CT forms on the first calcite cement. Thus, this initial silicification is already a second phase during diagenesis. The maximum opal-CT content appears to occur in high porosity zones of the associated oozes and chalks. Nodular porcelanites may result from patchy or diffuse silicification within sediments possibly caused by the higher permeability and concomitantly less restricted conditions of crystallisation. In silicified turbidites the opal-CT has a dense or lepisphere character (chapter 6). Because of a high nucleation rate, abundant lepispheres fill the pore space before most of the micritic sediment is replaced.

In terms of the reflector formation the important factor is the abruptness (in depth) with which porosity is reduced. This abruptness appears to be due to the palaeoceanographic event which caused a sharp reduction in the silica supply or the degree of preservation of silica. It is not just a front that is advancing with time. As such it may be a time-line (i.e. isochronous) and its regional character may well be recognisable on a much wider scale, although the same event may be manifested in a different way.

The physical property signature appears to be of a sharp porosity reduction from 60% to 40%. This increases wet bulk density, velocity increases sharply, but may be somewhat scattered and anisotropy is increased. Grain density is also slightly reduced as a result of the higher silica content (fig. 7.3).

The fact that two reflectors at site 603 are caused by anomalous silica content shows that the widespread Eocene event which is unique should be distinguished from the process that resulted from it. A process that through repetition generated two separate horizons.

Site 406 appears to show a very simple relationship between silica diagenesis and the formation of reflecting horizons. A number of the sites studied show a broad correlation between sediments with high silica content and strongly stratified acoustic units, for example sites 398, 403 and 400 (chapter 5). The occurrence of opal-CT at site 405 does not show such a good correlation with reflectors: siliceous sediments have a lower impedance than adjacent formations. One idea (of mine) is that early diagenesis of amorphous silica to opal-CT increases rigidity of the sediment framework and produces impedance

Fig. 7.4 Diagram to show the variation of impedance through time for two sediments of similar initial structure but different composition

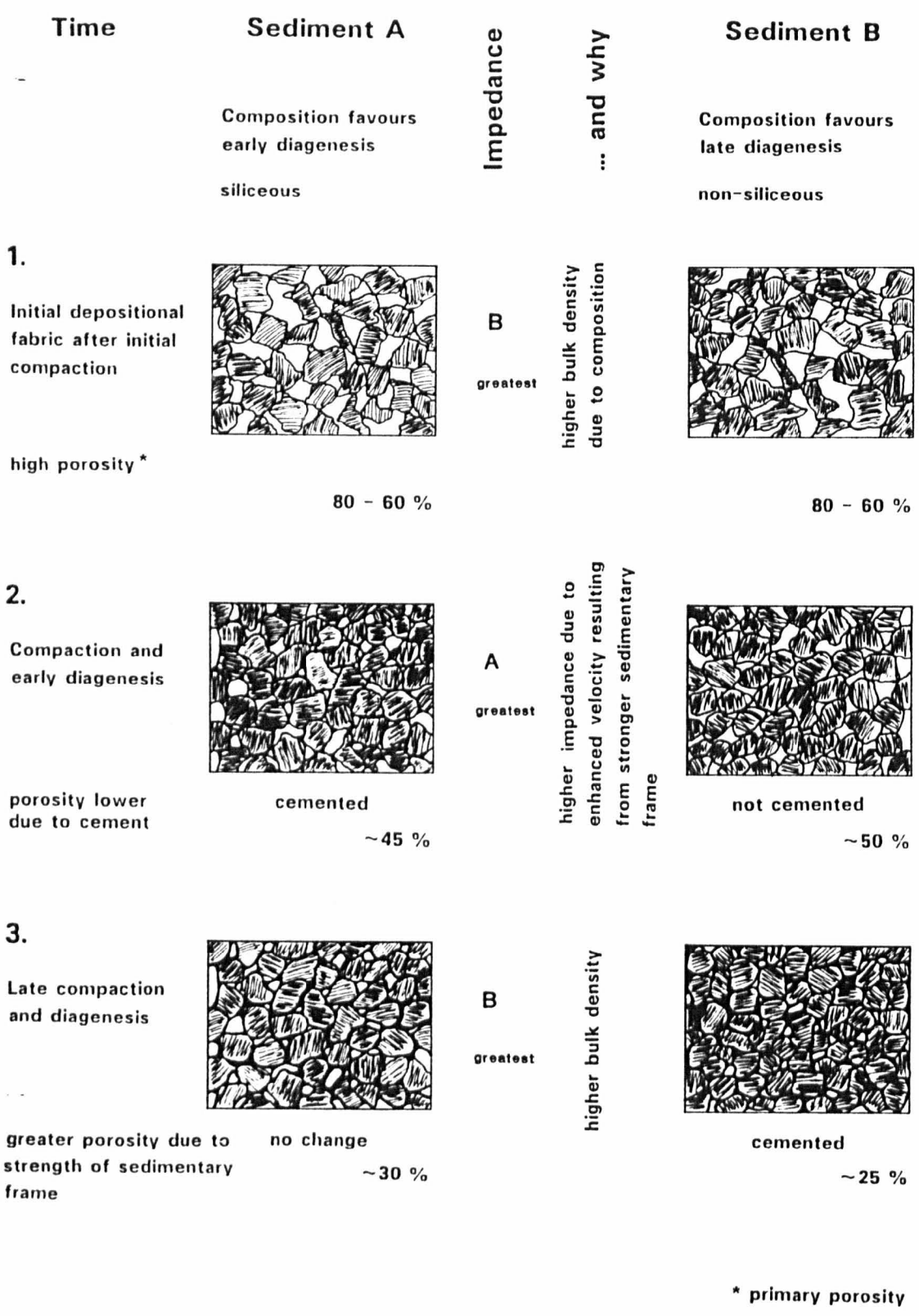

contrasts. Later, the adjacent strata undergo diagenesis and suffer greater porosity loss (either because of higher overburden pressures prior to cementation or the way carbonate diagensis proceeds). Eventually these non-siliceous sediments attain a higher impedance than those formations that were lithified early and gained sufficient strength to retain the porosity extant following their lithification. This is only an idea, but it does explain the form of reflectors found towards the bottom of site 405 and why reflectors within older sediments do not have the same dependence on silica content (fig. 7.4).

7.3.3 Carbonate compensation depth reflectors

The idea that horizon Ac resulted from a rising of the Maestrichtian/Paleogene CCD is subtly different from similar events considered to cause reflectors such as horizon Beta and horizon A*. In the case of horizon Ac, it is the absence of carbonate that allows minor variations in silica to play a more dominant role in reflector formation. The recognition of horizon Ac within calcareous sediments shows that a CCD rise is not the most important factor.

In contrast the abrupt decrease in carbonate content across horizons Beta and A* results directly in changes in the physical properties and so can be attributed with causing the reflector.

The impedance contrast is more noticeable where it is strongly positive, such as may be produced where claystones overly limestones or limestone/shale sequences. The horizon as defined by carbonate variation remains even if the overlying sediment has the greater impedance, such as is the case at site 603, where sandstone turbidites succeed the limestones. The polarity is reversed but the horizon

remains. The name of the horizon must therefore be related to the event causing it and not to a particular seismic character; it is incorrect to say that horizon Beta is a strong positive reflector. Instead, horizon Beta is a reflector which results from a particular palaeo-oceanographic event.

This distinction is more important when we compare the seismic stratigraphies of adjacent basins. In the eastern North Atlantic the same process of CCD shoaling is responsible for the production of reflectors at site 402. As mentioned in section 5.2.4 the diachronous effect of such an event leads to the production of a wide range in reflector ages.

Loop 13 at site 403 (section 5.2.1) is produced by a gradational change in facies from volcani-clastic to pelagic mudstone. This is manifested by interbedding over 65 m (310 - 375 m) in which the ratio of contrasting lithologies changes 'slowly, but surely' which is comparable to the Beta-type reflector modelled in section 3.6.

A similar facies change is found at site 416 (section 5.2.6). The lithologies are turbidites with mudstone which change to mudstone only. The reflector is the Orange reflector.

The similarity of succession despite their separation of ca. 2000 miles and 15 Ma remains a striking example of both the lateral persistence of such reflectors and, in a more cautionary tone, the care needed when making long range seismic correlations.

The latter is perhaps more important if , as Tucholke (1979) observes 'seismic reflection aims at prediction of stratigraphy'. However, this class of reflectors produced by changes of the relative depth of

Fig. 7.5 Early shape of the North Atlantic Ocean

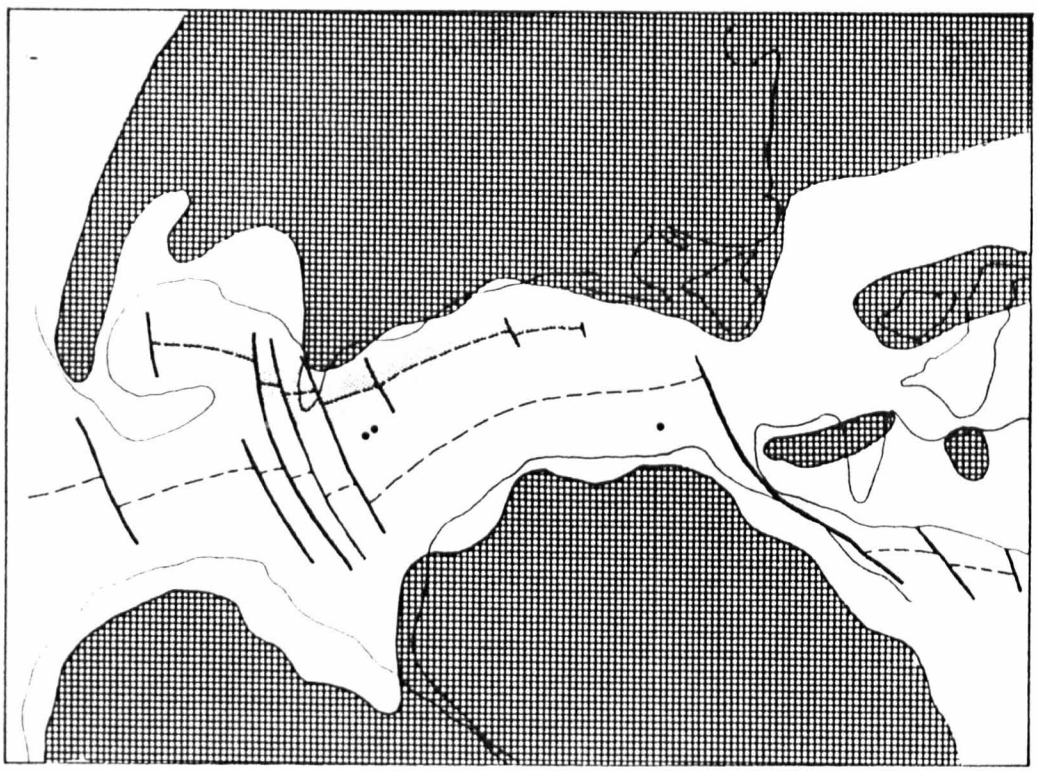

M24 Anomaly time

Palaeogeography

Geography

Spreading axis

Abandoned axis

(after Tucholke, 1981)

the CCD and seafloor should be carefully divided between those produced by the absolute shoaling or depression of the CCD and those produced by subsidence of the sea-floor below the CCD. Such subsidence is characteristic of passive margin evolution (see section 1.4) and reflectors produced in this way may be expected at all times of the basins history. Those reflectors resulting from active CCD movement will be more limited in time, which is important when considering the chronostratigraphic importance of reflectors in the deep sea.

7.3.4 Lower Cretaceous and Jurassic reflectors

The accurate interpretation of these deeper reflections relies on correct correlation of the overlying sequence, which is commonly in excess of 1000 m in thickness. Any errors are cumulative with depth and, when combined with the squeezing effect of high interval velocities, the problem of accurate interpretation is made more difficult. The study of the deeper reflections at site 534 illustrates this point. Miscorrelation causes the additional confusion of whether the name of a reflector remains with the line on the profile or with the stratigraphic position to which it has mistakenly been tied.

The shape of the North Atlantic Ocean was considerably different prior to horizon Beta (fig. 7.5). The exact age of opening of the Atlantic is not known, but was probably shortly before the Callovian (ca. 160 Ma), (Robertson et al., 1983). Horizon Beta has an age of roughly 125 Ma. Therefore, the pre-Beta reflectors document about 35 Ma of sedimentation in a narrow, elongate basin in which circulation was restricted by comparison to recent times. These factors reduce the areal distribution and the constancy of lithology needed if reflectors are to be identified regionally.

The correlation of horizon C between sites 391 and 534 has already been described (see section 4.2.5). The lithological contrast between grey limestone turbidites overlying bioturbated white limestone is similar to that found at site 603 within litho-unit 5. The age is also Lower Cretaceous but Barremian-Hauterivian. There is no strong reflector at site 603 although horizon Kb would provide a close match (see table 7.1).

7.4 Correlation and deep sea reflectors

Returning to the statement of section 1.4 concerning the method of stratigraphic prediction of Vail et al. (1977). Their method hinges on the chronostratigraphic significance of seismic reflections and the validity involved in assuming that an unconformity always divides units of strictly differing age and that these unconformities may be equated with their correlative conformities.

The assumption that strata below an unconformity predate those above is largely true with the exception of those unconformities formed by bottom currents. From my work it is not possible to comment further as all studies presented are largely one dimensional examples of reflector generation. Only the case study of sites 604 and 605 (see chapter 6) allows two dimensional interpretation and here no one unconformity is common to the two sites. On the scale of a basin-wide study large unconformities are very useful as witnessed by the use of horizon Au in the study of sedimentation history in the N.A.B.

However, this example also illustrates one of the problems inherent in the method. By no means are all reflectors caused by unconformities

nor are reflector terminations necessarily due to truncation/ downlap.

Important exceptions include the common occurrence of interference of adjacent horizons, which are more important in these formations with high transmission velocities. Also, transitional facies, whether smoothly graded (e.g. chalk to limestone) or consisting of a change in the ratio of interbedding of adjacent facies. These are more acute in formations of slow sedimentation.

But perhaps the most important cause of reflector generation which breaks the Vail et al. assumption is that of the diagenetic horizon. Quite simply this is not necessarily time-stratigraphic if it can be considered to obey any controls then they are more related to facies than any thing else.

The conclusion must be drawn that while the method is applicable (with some reservations, e.g. Thorne & Watts, 1982) to continental margins it is not sufficiently reliable to be trusted in the deep sea environment. The example of horizon Ac between sites 604 and 605 is witness to this.

References

Adelseck C.G., Geeham G.W. & Roth P.H.
Experimental evidence for the selective dissolution and overgrowth of calcareous nannofossils during diagenesis, Geological Society of America Bullitin 84 p 2755, 1973.

Aoyagi K. & Kazama T.
Transformational changes of clay minerals, zeolites and silica minerals during diagenesis., Sedimentology 27 pp 179-188, 1980.

Attenborough K.
Acoustical characteristics of porous materials, Physics Reports, 82/3, 179-227, 1982.

Bachman,R.T.
Acoustic anisotropy in marine sediments and sedimentary rocks., Journal of Geophysical Research 84(B13) pp 7661-7663, 1979.

Bader R.G., Gerard R.O., et al.
On the nature of reflecting horizons, Initial Reports of the Deep Sea Drilling Project 4 pp 670-672 Washington (USGPO), 1970.

Banthia B.S., King M.S. & Fatt I.
Ultrasonic shear wave velocity in rocks subjected to simulated overburden pressure and internal pore pressure., Geophysics 30 pp 117-121, 1965.

Becking L.G.M. & Moore D.
Density distributions in sediments, Journal of Sedimentary Petrology 29 p 47-55, 1959.

Benson W.E., Sheridan R.E. et al.
Initial Reports of the Deep Sea Drilling Project 44 Washington (USGPO), 1978.

Berger W.H. & Mayer L.A.
Deep-sea carbonates : acoustic reflectors and lysocline fluctuations., Geophysics 6 pp 11-15, 1978.

Biart B.N.M.
Computer programs for seismogram synthesis and associated software, Department of Earth Sciences, The Open University, Internal report, 1985.

Physical properties modelling and seismic stratigraphy at Leg 93 sites of the DSDP, in van Hinte J., Wise S., et al., Initial Reports of the Deep Sea Drilling Project 93 in prep. Washington (USGPO), 19in review.

Biot M.A.
Theory of propagation of elastic waves in a fluid-saturated porous solid 1.Low frquency 2.High frequency, Journal of the Acoustical Society of America 28 pp 168-191, 1956.

Birch F.
Compressibility : elastic constants, in Handbook of Physical Constants (ed)Clark S.P.Jr Geological Society of America Memoir 97 pp 98-174, 1966.

Bouquigny R. & Willm C.
Tentative calibration of site 398 and special processing of parts of lines GP-19 and GP-23, Initial Reports of the Deep Sea Drilling Project 47 pt 2 pp 623-629 Washington (USGPO), 1979.

Boyce R.E.
Sound velocity-density parameters of sediment and rock from DSDP drill sites 315-318 on the Line Islands Chain, Manihiki Plateau, and Tuamotu Ridge in the Pacific Ocean, Initial Reports of the Deep Sea Drilling Project 33 p 695-728, 1976.

Laboratory-determined sound velocity, porosity, wet-bulk density, acoustic impedance, acoustic anisotropy and reflection coefficients for Cretaceous-Jurassic turbidite sequences at DSDP sites 370 and 416 off the coast of Morocco., in Hay W.W., Sibuet J-.C., et al., Initial Reports of the Deep Sea Drilling Project 75 1229-1244 Washington (USGPO), 1984.

Brandt H.P.
A study of the speed of sound in porous granular media., Journal of Applied Mechanics 22 pp 479-486, 1955.

Brandt H.P.,Whitney & Keir
Factors affecting compressional wave velocity in unconsolidated marine sand sediments, Journal of the Acoustical Society of America 32 pp 171-179, 1960.

Bryan G.M.
Hydrodynamic model of the Blake Outer Ridge, Journal of Geophysical Research 75 pp 4530-4537, 1970.

Bryan G.M.,Markl R.G. & Sheridan R.E.
IPOD site surveys in the Blake-Bahama basin, Marine Geology 35 pp 43-63, 1980.

Buchan S. et al.
Relations between the acoustic and geotechnical properties of marine sediments, Quarterly Journal of Engineering Geology 5 pp 265-284, 1972.

Casand J., Fail J.P. & Montadert L.
Sismique reflexion en eau profonde, Geophysical Prospecting 18 pp 600-614, 1968.

Chapman N.R., Zelt C.A. & Busch A.E.
Geoacoustic modelling of deep ocean abyssal plains, in Acoustics and the Sea-bed, Pergamon, London, 297-305, 1983.

Chersky N. & Makogon Y.
Solid Gas - world reserves are enormous, Oil & Gas International 10/8 82-84, 1970.

Clarke S.P. (ed)
Handbook of physical constants, Geol. Soc. Amer. Memoir 97, 1966.

Davies T.A. & Edgar N.T.
Some geophysical aspects of deep-sea drilling, Geophysical Surveys 1 pp 391-407, 1974.

Dillon W.P., Grow J.A. & Paull C.K.
Unconventional gas hydrate seals may trap gas off southeast U.S., Oil & gas Journal 78/1 124-130, 1980.

Dillon W.P.,Sheridan R.E. & Fail J.P.
Structure of the western Blake-Bahama basin as shown by 24 channel CDP profiling, Geology 4 pp 459-462, 1976.

Domenico S.N.
Effect of brine-gas mixture on velocity in an unconsolidated sand reservoir, Geophysics 41 pp 882-894, 1976.

Embley R.W. & Johnson D.A.
Acoustic stratigraphy and biostratigraphy of Neogene carbonate horizons in the north equatorial Pacific, Journal of Geophysical Research 85/B10 pp 5423-5437, 1980.

Ewing J. & Ewing M.
Seismic refraction measurements in the Atlantic Ocean basins, in the Mediterranean Sea, on the Mid-Atlantic Ridge and in the Norwegian Sea, Geological Society of America Bulletin, 70 291-318, 1959.

Reflection profiling in and around the Puerto Rico Trench, Journal of Geophysical Research 67/12 4729-4739, 1962.

Ewing J., Worzel J.L. & Ewing M.
Sediments and oceanic structural history of the Gulf of Mexico, Journal of Geophysical Research 67 pp 2059, 1962.

Ewing J., Worzel J.L., Ewing M. & Windisch C.
Ages of Horizon A and the oldest Atlantic sediments, Science 154/3753 1125-1132, 1966.

Ewing J.I. & Hollister C.D.
Regional aspects of drilling in the western North Atlantic, in Hollister C.D., Ewing J.I. et al., Initial Reports of the Deep Sea Drilling Project 11 951-973 Washington (USGPO), 1972.

Ewing J.I. & Tirey G.B.
Seismic profiler (for use in the deep-sea), Journal of Geophysical Research 66 2917-2927, 1961.

Ewing J.I., Ewing M., Aitken T. & Ludwig W.J.
North Pacific sediment layers measured by profiling., in Knopoff L., Drake C.L., & Hart P.J. (eds), The crust and upper mantle of the Pacific area, A.G.U. Monograph 12 pp 147-173, 1968.

Ewing J.I., Windisch C. & Ewing M.
Correlation of Horizon A with JOIDES borehole results, Journal of Geophysical Research 75 pp 5645-5653, 1970.

Ewing M. & Ewing J.I.
Sediments at proposed LOCO drilling sites, Journal of Geophysical Research 68/1 251-256, 1963.

Ewing M. & Ewing J.I.
Distribution of oceanic sediments, in Studies on Oceanography, Kozo Yoshida (ed) 568 pp University of Washington Press., 1965a.

The sediments of the Argentine Basin, Ann. Brazilian Acad. Sci. 37 (supplement) pp 1-61, 1965b.

Ewing M., Ludwig W.J. & Ewing J.
Sediment distribution in the oceans : the Argentine Basin, Journal of Geophysical Research 69/10 2003-2032, 1964.

Ewing M., Saito T., Ewing J.I. & Burckle L.H.
Lower Cretaceous sediments from the north-west Pacific, Science 152 pp 751-755, 1966.

Ewing M., Talwani M., Ewing J.I. & Edgar N.T.
Proc. Intern. Conf. Trop. Oceanog., pp 101-129, 1965.

Fatt I.
Compressibility of sandstones iat low to moderate pressures, Bulletin of the Association of American Petroleum Geologists 42 pp 1924-1957, 1958.

Fitch A.A
Seismic reflection interpretation, Geopublication associates pub. Gebruder Borntraeger Berlin/Stuttgart, 1976.

Frazer L.N. & Phinney R.A.
The theory of finite frequency body wave syntheteic seismograms in inhomogeneous elastic media. Geophys. J. R. astr. Soc. 63 691-717, 198

Gaskell T., Hill M. & Swallow J.
Seismic measurements made by H.M.S. Challenger in the Atlantic, Pacific and Indian Oceans , and in the Mediterranean Sea, 1950-53, Philosophical Transactions of the Royal Society 251 23-83, 1958.

Gassman F.
Uber die Elastizitat Poroser Median, Vierteljahrsschr. Naturforsch. Ges. Zurich 96 pp 1-23, 1951a.

Elastic waves through a packing of spheres, Geophysics 16 pp 673-685, 1951b.

Gregory A.R.
Aspects of rock physics from laboratory and log data that are important to seismic interpretation, in Seismic Stratigraphy - applications to hydrocarbon exploration C.E.Payton(ed), AAPG, Tulsa, 1977.

Grim R.
Applied clay mineralogy, pub McGraw-Hill, New York, 1962.

Hamilton E.L.
Low sound velocity in high porosity sediments, Journal of the Acoustical Society of America 28 pp 16-19, 1956.

Sound velocity and related properties of marine sediments in the north Pacific, Journal of Geophysical Research 75 pp 4423-4446, 1970.

Hamilton E.L.
Elastic properties of marine sediments, Journal of Geophysical Research 76 pp 579-604, 1971a.

Prediction of in situ acoustic and elastic properties of marine sediments, Geophysics 36 pp 266-284, 1971b.

Variations of density and porosity with depth in deep-sea sediments., Journal of Sedimentary Petrology 46 280-300, 1976.

Hamilton E.L. et al.
Acoustic and other physical properties of shallow water sediments off San Diego, Journal of the Acoustical Society of America 28 pp 1-15, 1956.

Hardin B.O. & Richart F.E.Jr
Elastic wave velocities in granular soils, J. Soil Mech. Found. Div. ASCE 89, SM1,33-65, 1963.

Heezen B.C., Hollister C.D. & Ruddiman W.F.
Shaping of the continental rise by geostrophic contour currents, Science 152(3721) p 502, 1966.

Heezen B.C., MacGregor I.D., Foreman H.P. and others
A kinematic interpretation of the post-Jurassic sedimentary sequence on the Pacific plate, Nature 241 pp 25-32, 1973.

Hein J.R.,Scholl D.W.,Barron J.A.,Jones M.G. & Miller J.
Diagenesis of late Cenozoic diatomaceous deposits and formation of the bottom simulating reflector in the southern Bering Sea, Sedimentology 25 pp 155-181, 1978.

Hersey J.B. & Ewing M.
Seismic reflections from beneath the ocean floor, Transactions , AGU 30/1 5-14, 1949.

Hill R.
Elastic properties of reinforced solids : some theoretical principles, Journal of Mech. Phys. Solids 11 pp 357-372, 1963.

Hinz K.,Siebold E. & Wissman G.
Continental slope anticline and unconformities off W.Africa, 'Meteor' Forsch.-Ergebnisse C/17 pp67-73, 1974.

Horn A.D. et al.
Correlation between acoustical & other physical properties of deep-sea cores, Journal of Geophysical Research 73 pp 1939-1957, 1968.

Houtz R.E.
Preliminary study of global sediment sound velocity from sonobuoy data, in Hampton L., The physics of sound in marine sediments, New York Plenum Press, pp519-535, 1973.

south Tasman Basin and borderlands: a geophysical summary, in Kennet J.P. & Houtz R.E., 1974, Initial Reports of the Deep Sea Drilling Project 29 pp 1135-1146 Washington (USGPO), 1974.

Preliminary sonobuoy study of rapidly accumulating shelf sediments, Journal of Geophysical Research 83 pp 5397-5404, 1978.

Ide J.M.
Comparison of statistically and dynamically determined Young's Modulus of rocks, Nat. Acad. Sci. Proc. 22 pp 577-593, 1976.

Jansa L.F., Enos P., Tucholke B.E., Gradstien F.M. & Sheridan R.E.
Mesozoic and cenozoic sedimentary formations of the North American Basin; western North Atlantic, in Talwani, Hay & Ryan, Deep Drilling Results in the Atlantic Ocean: continental margins and palaeoenvironment, pub AGU, 1979.

Johnson D.L., Plona T.J., Scale C., Pasiers F. & Kojima H.
Tortuosity and acoustic slow waves, Phys. Rev. Letters, 1982.

Johnson T.C.,Hamilton E.L. & Berger
Physical properties of calcareous ooze : control by dissolution at depth, Marine Geology 24 pp 259-277, 1977.

Jones E.J.W.
Continuous reflection profiles from the European continental margin in the Bay of Biscay, Earth and Planetary Science Letters 5 pp 127-134, 1968.

Jones E.J.W. & Funnell B.M.
Association of a seismic reflector and upper Cretaceous sediment in the Bay of Biscay, Deep-Sea Research 15 pp 701-709, 1968.

Jones E.J.W., Ewing M., Ewing J.I. & Eittreim S.L.
Influences of Norwegian Sea overflow water on sedimentation in the northern North Atlantic and Labrador Sea, Journal of Geophysical Research 75/9 pp 1655-1680, 1970.

Kagami H.
Transformation of opaline silica in sediments from Bay of Biscay and Rockall Bank, Initial Reports of the Deep Sea Drilling Project 48 757-764 Washington (USGPO), 1979.

Katz H.-R.
Probable gas hydrate south east of North island, New Zealand, Journal of Petroleum Geology 3/3 pp 315-324, 1981.

Kidd R. et al.
Initial Reports of the Deep Sea Drilling Project 95 Washington (USGPO), 19in prep.

Kidd R.B. & Hill P.R.
Drilling north-eastern Atlantic sediment drifts (abs), Palaeoenvironments meeting, Geological Society of London, Nov. 1984, 1984.

Klitgord K.D. & Grow J.A.
Jurassic seismic stratigraphy and basement structure of the western Atlantic magnetic quiet zone, Bulletin of the Association of American Petroleum Geologists 64/10 pp 1658-1680, 1980.

Kuenen P.H. & Migliorini C.I.
Turbidity currents as a cause of graded bedding, Journal of Geology 58 pp 91-127, 1950.

Kuster G.T. & Toksoz M.N.
Velocity and attenuation of seismic waves in two-phase media : Part 1 Theoretical formulations Part 2 Experimental results, Geophysics 39/5 pp 587-606, 607-618, 1974.

Kvenden K.A. & McMenamin M.A.
Hydrates of natural gas: a review of their geologic occurence, USGS circular 825, 1981.

Lancelot Y. & Siebold E. et al.
Initial Reports of the Deep Sea Drilling Project 41 Washington (USGPO), 1977.

Lancelot Y. & Winterer E.L.
Eution of the Morroco oceanic basin and adjacent continental margin - a synthesis, in Lancelot Y., Winterer E.L., et al., 1980,, Initial Reports of the Deep Sea Drilling Project 50 Washington (USGPO), 1980.

Latouche C. & Maillet N.
X-ray mineralogy studies, Leg 48 - Rockall region (sites 403, 404, 405 and 406), Initial Reports of the Deep Sea Drilling Project 48 pp 665-676 Washington (USGPO), 1979.

Laughton A.S.
Sound propagation in compacted ocean sediments, Geophysics 22 pp 233-260, 1957.

South Labrador Sea and the eution of the North Atlantic, Nature 232 Aug 27 p 612, 1971.

Laughton A.S., Berggren W.A., et al.
Initial Reports of the Deep Sea Drilling Project 12 Washington (USGPO), 1972.

Levin F.K.
Seismic velocities in transversely isotropic media, Geophysics 44 pp 918-936, 1979.

Markl R.G.,Bryan G.M. & Ewing J.I.
Structure of the Blake-Bahama Outer Ridge., Journal of Geophysical Research 75/24 4539-4555, 1970.

Mattson P.H. & Pessagno E.A.
Caribbean eocene canism and the extent of Horizon A, Science 174 pp 138-139, 1971.

Mayer L.A.
The origin of fine scale acoustic stratigraphy in deep-sea carbonates, Journal of Geophysical Research 84 pp 6177-6184, 1979a.

Deep sea carbonates: acoustic, physical and stratigraphic properties, Journal of Sedimentary Petrology 49/3 pp 819-836, 1979b.

A depositional-process-orientated impedance model for marine sediments, in Acoustics and the Sea-bed 61-, 1983.

McCave I.N.
Diagnosis of turbidites at sites 386 and 387 by particle-counter size analysis of the silt (2-40 microns) fraction, in Hollister, Ewing, et al., 1979, Initial Reports of the Deep Sea Drilling Project 43 pp 395-406 Washington (USGPO), 1979.

McKenzie D.P.
Some remarks on the development of sedimentary basins, Earth and Planetary Science Letters 40/1 pp 25-32, 1978.

The Earth's Mantle, Sci Am Sept. 51-62, 1983.

Montadert L., de Charpal O., Roberts D.G., Guennoc P. & Sibuet J-.C.
Northeast Atlantic passive continental margins: rifting and subsidence processes, in Talwani, Hay & Ryan, 1979 pp 154-186, 1979.

Moore D.G.
Shear strength and other related properties of sediments from Experiment Mohole (Guadelupe Site), Journal of Geophysical Research 69 pp 4271-91, 1964.

Morner N.-A.
Eustacy and geoid changes, Journal of Geology 84 123-151, 1976.

Eustacy and Geoid changes as a function of core/mantle changes., in Morner N.-A.(ed) Earth rheology, isostacy and eustacy : New York, John Wiley & Sons p535-553, 1980.

Reution in Cretaceous sea-level analysis, Geophysics 9 344-346, 1981.

Morton R.W.
Sound velocity in carbonate sediments from Whiting Basin, Puerto Rico., Marine Geology 19 pp 1-17, 1975.

Sound velocity in carbonates sediments from Whiting Basin, Puerto Rico, Marine Geology 19 pp 1-17, 1975.

Nafe J.E. & Drake C.L.
Variation with depth in shallow and deep water marine sediments of porosity, density and the velocity of compressional and shear waves, Geophysics 22 pp 523-552, 1957.

Oehler J.H.
Origin and distribution of silica lepispheres in porcelanite from the Monterey Formation of California., Journal of Sedimentary Petrology 45/1 252-257, 1975.

Officer C.B.
A deep-sea seismic reflection profile, Geophysics 20/2 pp 270-282, 1955.

Packham & van der Lingen
Progressive carbonate diagenesis at deep sea drilling sites 206, 207, 208 & 210 in the SW Pacific and its relationship to sediment physical properties and seismic reflectors, in Burns R.E., Andrews J.E., et al., 1973, Initial Reports of the Deep Sea Drilling Project 21 pp 495-507 Washington (USGPO), 1972.

Paull C.K. & Dillon W.P.
Erosional origin of the Blake Escarpment : an alternative hypothesis, Geophysics 8 pp 538-542, 1980.

Raitt R.W.
Seismic refraction studies of the Pacific Ocean basin. 1, Crustal thickness of equatorial Pacific, Geological Society of America Bullitin 67 pp 1623-1640, 1956.

Reyment R.A. & Morner N.-A.
Cretaceous transgressions and regressions exemplified by the South Atlantic, Palaeontological Society of Japan Special Papers, 21 247-261, 1977.

Riech V. & von Rad U.
Silica diagenesis in the Atlantic Ocean : diagenic potential and transformations, in Maurice Ewing Series 3 by Talwani,Hay & Ryan, 1979.

Roberts D.G.
Marine geology of the Rockall Plateau and Trough, Philosophical Transactions of the Royal Society ser A 278 pp 447-509, 1975.

Roberts D.G.,Masson D.G. & Miles P.R.
Age and structure of the southern Rockall Trough : new evidence, Earth and Planetary Science Letters 52 pp 115-128, 1981.

Robertson A.H.F.
Latest Cretaceous and Eocene palaeoenvirnoments in the Blake-Bahama Basin, western North Atlantic, in Sheridan, Gradstein, et al., Initial Reports of the Deep Sea Drilling Project 76 pp 763-780 Washington (USGPO), 1984.

Rona P.A.
Worldwide unconformities in marine sediments related to eustatic changes of sea level, Nature Physical Science 244 pp 25-26, 1973.

Rona P.A. & Clay C.S.
Stratigraphy and structure along a continuous seismic reflection profile from Cape Hatteras, North Carolina, to the Bermuda Rise, Journal of Geophysical Research 72/8 pp 2107-2130, 1967.

Savit C.H., Knox W.A., Blue D.M. & Paitson L.
Reflection and velocity profiles at the Outer Ridge, Puerto Rico., Journal of Geophysical Research 69/4 pp 701-719, 1964.

Schlanger S.O.& Douglas R.G.
The pelagic ooze - chalk - limestone transition and its implication for marine stratigraphy, Spec. pub of Int. Assoc. Sedimentologists 1 pp 177-148, 1974.

Scholl D.W. & Creager J.S.
Geological synthesis of Leg 19 (DSDP); far north Pacific, and Aleutian Ridge and Bering Sea, Initial Reports of the Deep Sea Drilling Project 19 pp 897-913 Washington (USGPO), 1973.

Schreiber B.C.
Sound velocity in deep sea sediments, Journal of Geophysical Research 73 pp 1259-1268, 1968.

Scrutton R.A. & Roberts D.G.
Structure of Rockall Plateau and Trough, northeast Atlantic, ICSU/SCOR Working party 31 Symposium, Cambridge 1970: The geology of the east Atlantic continental margin, F.M.Delaney (ed) IGS report 70/14 pp77-78 HMSO, 1971.

Sheridan R.E. & Gradstein F.M. and others
Early history of the Atlantic Ocean and gas hydrates on the Blake Outer Ridge: results of the Deep Sea Drilling Project Leg 76, Geological Society of America Bulletin 93 876-885, 1982.

Sheridan R.E., Bates L.G., Shipley T.H. & Crosby J.T.
Seismic stratigraphy in the Blake-Bahama basin and the origin of Horizon D, Initial Reports of the Deep Sea Drilling Project 89 Washington (USGPO), 1983.

Sheridan R.E., Golovchenko X. & Ewing J.I.
Late Miocene turbidite horizon in the Blake-Bahama basin, Bulletin of the Association of American Petroleum Geologists 58 pp 1797-1805, 1974.

Sheridan R.E., Pastouret L. & Mosditchian G.
Seismic stratigraphy and related lithofacies of the Blake-Bahama Basin, Initial Reports of the Deep Sea Drilling Project 44 529-546 Washington (USGPO), 1978.

Shipley T.H.
Physical properties, synthetic seismograms and seismic reflections: correlations at DSDP site 534, Blake-Bahama basin, in Sheridan R.E., Gradstein F.M. et al., Initial Reports of the Deep Sea Drilling Project 76 pp 653-666 Washington (USGPO), 1983.

Shipley T.H. & Watkins J.S.
Fine-scale seismic stratigraphy in the western North Atlantic, Geophysics 6 pp 635-639, 1978.

Shumway G.
Sound speed and absorbtion studies of marine sediments by a resonance method (parts 1 & 2), Geophysics 25 pp 451-467 and 659-682, 1960.

Sibuet J.-C., Ryan W.B.F., et al.
Initial Reports of the Deep Sea Drilling Project 47 part 2 Washington (USGPO), 1979.

Silva M.T. & Robinson E.A.
Deconution of geophysical time series in the exploration for oil and natural gas, pub. Elsevier, Amsterdam - Oxford - New York, 1979.

Smythe D.K.,Chalmers J.A.,Skuse A.G.,Dobinson A. & Mould A.S.
Early opening history of the North Atlantic - 1. Structure and origin of the Faeroe-Shetland escarpment., Geophysicl Journal of the Royal Astrnomical Society 72 pp 373-398, 1983.

Stoll R.D. & Bryan G.M.
Physical properties of sediments containing gas hydrates, Journal of Geophysical Research 84/B2 pp 1629-1634, 1979.

Stoll R.D.,Ewing J.,& Bryan G.M.
Anomalous wave velocities in sediments containing gas hydrates, Journal of Geophysical Research 76 pp 2090, 1971.

Sutton G.H.,Berckhemer H. & Nafe J.E.
Physical analysis of deep sea sediments, Geophysics 22 pp 779-812, 1957.

Talwani M., Mutter J.C., Eldholm O. & Stoffa P.L.
Comments on paper by Smythe et al. 'Early opening history of the North Atlantic - 1. Structure and origin of the Faeroe-Shetland Escarpment'., Geophysicl Journal of the Royal Astrnomical Society 78 pp 627-637, 1984.

Talwani, Udintsev et al.
Initial Reports of the Deep Sea Drilling Project 38 Washington (USGPO), 1976.

Thorne & Watts
Seismic stratigraphy related to thermal subsidence of passive margins, Science, 78, 187-190, 1984.

Tucholke B.E.
Relationships between acoustic stratigraphy and lithostratigraphy in the western North Atlantic Basin, in Tucholke B.E., Vogt, et al., Initial Reports of the Deep Sea Drilling Project 43 pp 827-846 Washington (USGPO), 1979.

Geologic significance of seismic reflectors in the deep western North Atlantic basin, in Warmes J.E., Douglas R.G. & Winterer E.L. (eds), The Deep Sea Drilling Project: a decade of progress. Soc. Econ. Palaeont. Mineral. Spec. Pub. 32 pp 23-37, 1981.

Tucholke B.E. & Mountain G.S.
Seismic stratigraphy, lithostratigraphy and palaeosedimentation patterns in the North American Basin, in Deep Drilling Results in the Atlantic Ocean: continental margins and palaeoenvironment, AGU, Washington, 1979.

Tucholke B.E. & Vogt P.R.
Western North Atlantic : sedimentary eution and aspects of tectonic history, in Tucholke B.E., Vogt P.R. et al., Initial Reports of the Deep Sea Drilling Project 43 pp 791-825 Washington (USGPO), 1979.

Tucholke B.E., Bryan G.M. & Ewing J.I.
Gas hydrate horizons detected in seismic profiler data from the western North Atlantic, Bulletin of the Association of American Petroleum Geologists 61/5 pp 698-707, 1977.

Urick R.J.
A sound velocity method for determining the compressibility of finely divided substances, Journal of Applied Physics 18 pp 983-987, 1947.

Vail P.R., Mitchum R.M., Shipley T.H. & Buffler R.T.
Unconformities in the eution of the North Atlantic, Philosophical Transactions of the Royal Society 294(1409) pp 137-155, 1980.

Vail P.R., Mitchum R.M., Todd R.G., Widmier J.M., Thompson S., Sangree J.B., Bubb J.N. & Hatelid W.G.
Seismic stratigraphy and global changes of sea level, in Payton C.E. (ed) Seismic Stratigraphy - applications to hydrocarbon exploration,, Bulletin of the Association of American Petroleum Geologists Memoir 26 pp 49-211, 1977.

von Rad U. & Rosch H.
Petrography and diagenesis of deep sea cherts from the central Atlantic, International Association of Sedimentologists Spec Pub no.1 pp 327-347, 1974.

von Rad U., Reich V. & Rosch H.
Silica diagenesis in continental margin sediments off north-west Africa, in Lancelot Y., Siebold E., et al., 1977, Initial Reports of the Deep Sea Drilling Project 41 pp 879-905 Washington (USGPO), 1977.

Watkins J.S., Moore J.C. et al.
Initial Reports of the Deep Sea Drilling Project 66 Washington (USGPO), 1981.

Watts A.B.
Tectonic subsidence, flexure and global changes of sea level, Nature 297 (June) pp 469-474, 1982.

Weaver F.M. & Wise S.W.
Opaline sediments of the southeastern coastal plain and Horizon A: biogenic origin, Science 184 pp 899-901, 1974.

Windisch C.C., Leyden R.J., Worzel J.L., Saito T. & Ewing J.
Investigation of Horizon Beta, Science 1473-79 , 1968.

Wood
A textbook of sound, pub. Bell (London)., 1941.

Wyllie M.R.J.,Gregory A.R. & Gardiner L.W.
Elastic wave velocities in heterogenous and porous media, Geophysics 21 pp 41-70, 1956.